UNIVERSITY OF CAPE TOWN

Synthesis, Characterisation and Reactivity Studies of $\mu(\alpha,\omega)$-Alkanediyl Complexes of Ruthenium, Iron and Cobalt

A thesis submitted for the degree

of Master of Science

by

KAROL PAULA FINCH
BSc (Hons)

MARCH 1988

ACKNOWLEDGEMENTS

I would like to extend my sincere thanks and appreciation to the following persons:

Associate Professor John Moss, for his invaluable guidance and support throughout this project;
Dr Graham Jackson who was my acting supervisor during the sabbatical leave of Assoc. Prof Moss;
My good friends Selwyn Mapolie, Holger Friedrich and Philip Hall who acted as informal " supervisors ";
Professor Graham Hutchings and Dr. Neil Coville, of the University of the Witwatersrand, who supervised the catalysis part of this thesis; special thanks also to Peter Johnston and Mark van der Riet for their cooperation and assistance during my research at the University of the Witwatersrand;
Mr. William Hendricks for maintaining a clean and tidy laboratory;
Mr. Noel Hendricks and Mr. Zayed Brown for the numerous NMR spectra;
Mr. W.T. Hemsted and Mr. G.P. Benin-Casa, who performed the microanalyses;
Miss B. Williamson and Mrs. H. von der Stratten for running the mass spectra; also Sir Jack Lewis and R. McQueen of the University of Cambridge, England, for performing the FAB mass spectrometry;
Dr. M. Niven, who solved the crystal structure of $[CpRu(CO)_2]_2[\mu\text{-}(CH_2)_5]$;
Johnson Matthey (Pty) Ltd. for the loan of Ruthenium Trichloride Hydrate;

The Council for Scientific and Industrial Research, the University of Cape Town and the University of the Witwatersrand for financial assistance;

Mrs. Y. Loots for typing the tables;

Alan Lathwood and Holger Friedrich for proof-reading this thesis;

And last, but by no means least, my family and friends for their unfailing support and encouragement throughout.

SUMMARY

The new series of μ(α,ω)-alkanediyl compounds of ruthenium, $[CpRu(CO)_2]_2[\mu\text{-}(CH_2)_n]$, where n=5-10, have been prepared from $Na[CpRu(CO)_2]$ and the corresponding diiodoalkane. These compounds, which are stable crystalline solids at ambient temperature, have been fully characterised by microanalysis, infrared, ^1H and ^{13}C NMR spectroscopy, melting point and mass spectrometry. The new heterodinuclear complex $[Cp(CO)_2Fe(CH_2)_4Ru(CO)_2Cp]$ has been synthesised by the reaction of $[CpFe(CO)_2(CH_2)_4I]$ with $Na[CpRu(CO)_2]$ and characterised by all the above mentioned techniques.

The fragmentation pathways exhibited in the mass spectra of the compounds $[CpRu(CO)_2]_2[\mu\text{-}(CH_2)_n]$ (n=5-10) are discussed in comparison to those reported previously for the iron analogues $[CpFe(CO)_2]_2[\mu\text{-}(CH_2)_n]$. In addition, the crystal structure of the compound $[CpRu(CO)_2]_2[\mu\text{-}(CH_2)_5]$ is reported and discussed.

The monohaloalkyl complexes $[CpRu(CO)_2(CH_2)_nX]$, (where X=Cl, n=3 and X=Br, n=4) have been synthesised from $Na[CpRu(CO)_2]$ and the corresponding dihaloalkane. Both compounds exist as oils at room temperature and have been partially characterised by infrared and ^1H NMR spectroscopy.

The carbonyl insertion reactions of $[CpRu(CO)_2]_2[\mu\text{-}(CH_2)_5]$ have also been investigated by the reaction of the latter with tertiary phosphines and with t-BuNC. These ruthenium polymethylene bridged compounds undergo CO migratory insertion reactions only at high temperature. Thus, no reaction of $[CpRu(CO)_2]_2[\mu\text{-}(CH_2)_5]$ with PPh_3

was observed in refluxing THF or toluene, even in the presence of catalysts (PdO and $[CpRu(CO)_2]_2$) or Me_3NO. In refluxing acetonitrile, the CO insertion reaction proceeds extremely slowly to yield the monoacyl, monosubstituted product, $[Cp(CO)_2Ru(CH_2)_5C(O)Ru(CO)(PPh_3)Cp]$. The diacyl, disubstituted products $[CpRu(CO)(PR_3)]_2[\mu\text{-}C(O)(CH_2)_5C(O)]$ (PR_3 = PPh_3, PPh_2Me and $PPhMe_2$) have subsequently been isolated from the reactions of $[CpRu(CO)_2]_2[\mu\text{-}(CH_2)_5]$ with PR_3 after prolonged refluxing in xylene (140°C) and characterised by infrared, ^1H and ^{13}C NMR spectroscopy and microanalysis. These reactions are compared to the CO insertion reactions of the mononuclear ruthenium alkyls, $[CpRu(CO)_2R]$ (R = alkyl) and the di-iron complexes, $[CpFe(CO)_2]_2[\mu\text{-}(CH_2)_n]$ which have been reported elsewhere.

Possible mechanisms for the CO alkyl migratory insertion reaction are postulated and the effects of chirality of the disubstituted, diacyl species, $[CpRu(CO)(PR_3)]_2[\mu\text{-}C(O)(CH_2)_5C(O)]$ on ^1H and ^{13}C NMR chemical shifts are examined.

The reactions of $[CpM(CO)_2]_2[\mu\text{-}(CH_2)_n]$ (M = Fe or Ru) with tertiary butylisocyanide, in refluxing THF or xylene respectively, were also investigated. $[CpFe(CO)(t\text{-}BuNC)]_2[\mu\text{-}C(O)(CH_2)_5C(O)]$ was isolated as a yellow oil at room temperature and fully characterised by the usual techniques. Only the decarbonylated product, $[CpRu(CO)(t\text{-}BuNC)]_2[\mu\text{-}(CH_2)_5]$, was isolated in the case of ruthenium.

The reactions of $[CpRu(CO)_2]_2[\mu\text{-}(CH_2)_5]$ with electrophiles have been studied. $[CpRu(CO)_2]_2[\mu\text{-}(CH_2)_5]$ reacted rapidly with I_2 and Br_2 at room temperature in THF to afford the expected cleavage

products, $[CpRu(CO)_2X]$ and $X(CH_2)_5X$, in high yield. No reaction of $[CpRu(CO)_2]_2[\mu\text{-}(CH_2)_5]$ with $Ph_3C^+PF_6^-$ was observed in CH_2Cl_2 at room temperature after 24 hours.

The three binuclear cyclopentadienyl iron compounds, $[CpFe(CO)_2]_2[\mu\text{-}(CH_2)_n]$ (where n=0, 3 and 5) were supported on γ-alumina and decomposed at 250°C. The resulting materials were subsequently investigated in a pilot reactor for CO hydrogenation activity.

In order to ascertain the decomposition temperatures and thermal behaviour of the samples, the three compounds were studied using Differential Scanning Calorimetry in air and under hydrogen. In appropriate cases the volatile products of some of the thermal decompositions have been analysed by G.C. and G.C.-M.S. techniques. The behaviour of the three samples supported on γ-alumina was also investigated by Diffuse Reflectance FT-IR Spectroscopy. The results of these preliminary studies are reported and discussed.

In a separate study, the mononuclear bromoalkyl cobaloximes of type $[Co(DH)_2py(CH_2)_nX]$, where X=Br (n=3-7) or X=I (n=3) have been prepared by the reaction of the chloro(pyridine)cobaloxime, $[Co(DH)_2pyCl]$ with 1.5 moles of dihaloalkane in the presence of sodium borohydride (where DH = monoanion of dimethylglyoxime). The dinuclear polymethylene bridged cobaloximes of type $[Co(DH)_2py]_2[\mu\text{-}(CH_2)_n]$, where n=4-6, can be synthesised by reaction of the mononuclear haloalkyl cobaloximes $[Co(DH)_2py(CH_2)_nX]$, with an equimolar quantity of the chloro(pyridine)cobaloxime in the presence of the reducing agent,

$NaBH_4$. The dinuclear complexes where n=4-8 have also been prepared from $[Co(DH)_2pyCl]$ and the corresponding dihaloalkane in a 2:1 molar ratio in the presence of $NaBH_4$. All the cobaloximes have been fully characterised by microanalysis, NMR and IR spectroscopic techniques. In addition, the molecular weights of some representative samples of both the mono- and dinuclear cobaloximes have been determined. These data are reported and discussed.

TABLE OF CONTENTS

LIST OF FIGURES

LIST OF TABLES

TABLE

LIST OF SYMBOLS AND ABBREVIATIONS

Å	: Angstroms
t-BuNC	: Tertiary butylisocyanide, $(CH_3)_3CCN$
B	: Axial base
^{13}C NMR	: Carbon-13 Nuclear Magnetic Resonance Spectroscopy
[Co]	: Vitamin B_{12s} residue
(DH)	: Monoanion of dimethylglyoxime
DSC	: Differential Scanning Calorimetry
FAB-MS	: Fast Atom Bombardment Mass Spectrometry
FT-IR	: Fourier Transform Infrared Spectroscopy
GC-MS	: Gas Chromatography - Mass Spectrometry
GHSV	: Gas hourly space velocity - defined as the gas flow rate (mls) per gram of catalyst per hour
^{1}H NMR	: Proton Nuclear Magnetic Resonance Spectroscopy
IR	: Infrared Spectroscopy
J	: Nuclear Magnetic Resonance coupling constant (in Hertz)
L	: A coordinating ligand
LxM, LyM	: Transition metal, M, with associated ligand system, Lx or Ly

M^+	: Molecular ion peak (Mass Spectrometry)
m/e	: Mass to charge ratio (Mass Spectrometry)
Me	: Methyl group, CH_3
OTs	: Tosyl group, p-toluenesulphonyl
Ph	: Phenyl group, C_6H_5
ppm	: Parts per million
PR_3	: Tertiary phosphine
py	: Pyridine, C_5H_5N
R	: An alkyl group, eg. CH_3, CH_3CH_2
RT	: Room temperature
T	: Temperature
THF	: Tetrahydrofuran, C_4H_8O
TMS	: Tetramethysilane
δ	: NMR Chemical shift in ppm
η^5-C_5H_5 (Cp)	: Pentahapto-cyclopentadienyl
μ-$(CH_2)_n$	: An alkyl chain bridging two metal atoms in which the terminal carbons are each σ- bonded to one metal atom

1. INTRODUCTION

1.1 Definition of μ(α,ω)-Alkanediyl Compounds and General Motivation for Study.

The dramatic escalation of crude oil prices in the early seventies, led scientists to investigate alternate sources for the production of liquid fuels. Furthermore, it is estimated that existing crude oil supplies are only sufficient to last into the early twenty-first century. On the other hand, vast reserves of coal as an alternate source of carbon are available for exploitation. Although the conversion of coal into fuel is economically unviable in most parts of the world at present, the dwindling reserves of crude oil will ultimately reverse this situation.
Thus, it is imperative that we seek alternate sources and processes for the production of liquid hydrocarbons.

An alternate process for the production of fuels is based on the direct gasification of coal at elevated temperatures to carbon monoxide and hydrogen, called "syngas". After purification of the syngas mixture, it is passed over a suitable heterogeneous catalyst where the two components, CO and H_2, react to produce a range of hydrocarbons. This synthesis, known as the Fischer-Tropsch process [1], is employed at the SASOL plants in South Africa. (Equation 1).

$$n\,CO + m\,H_2 \xrightarrow{\text{CATALYST}} C_x H_y O_z \qquad 1$$

Amongst the catalysts that are used in the Fischer-Tropsch process, iron, nickel, cobalt and ruthenium are the most important. A variety of hydrocarbons are produced, depending on the reaction conditions and the catalysts chosen. Renewed interest in the Fischer-Tropsch reaction, which was employed commercially in nine plants in Germany during World War II, has led to considerable research in an attempt to ellucidate the reaction mechanism and so develop more selective and efficient catalyst systems.

Fischer and Tropsch originally proposed that CO hydrogenation could be regarded as a "polymerisation of methylene groups", where surface carbide species were thought to be the key precursors of such methylene units, [1]. (Scheme 1a and b). Chain propagation is initiated by the reaction of surface methyl with surface methylene groups (Scheme 1c). Finally, β-elimination results in the termination of chain growth and an olefinic product is desorbed from the catalyst surface (Scheme 1d).

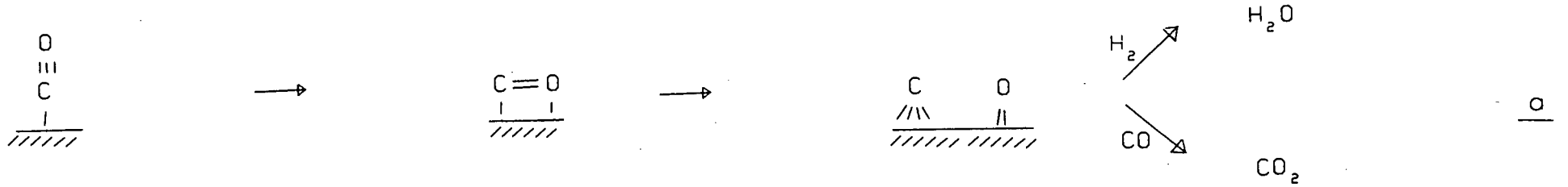

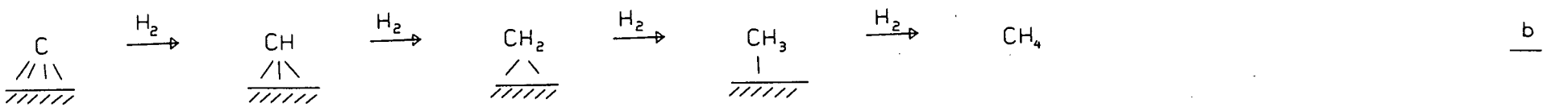

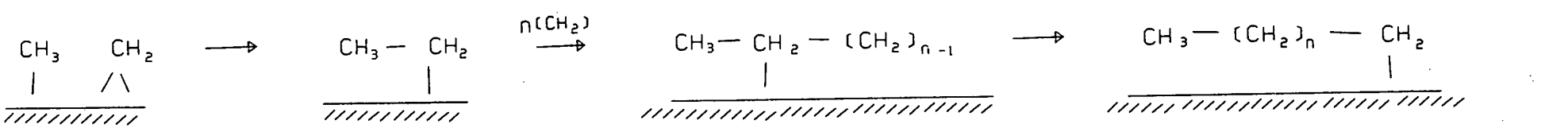

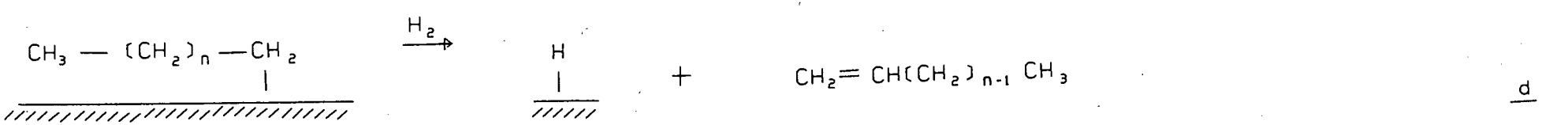

SCHEME 1

The relatively recent discovery of stable transition metal methylene compounds containing either a terminal (1) or bridging (2) $-(CH_2)-$ function, has lent fresh support to the above mechanistic proposal, [2-5].

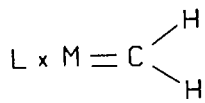

(1)

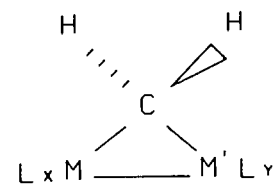

(2)

The insertion of a methylene group into a metal-methyl bond has been verified by a model reaction as shown in Scheme 2, [6].

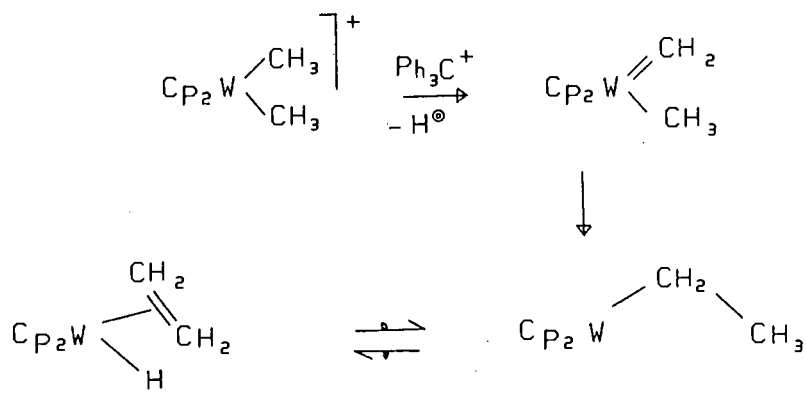

SCHEME 2

Transition metal-methylene complexes, such as those represented by (1) and (2), are now widely accepted as models for the intermediates occurring in the Fischer-Tropsch reaction (Scheme

1). The formal extension of the μ-methylene bridge in (2) is the "polymethylene" bridge, $-(CH_2)_n-$. Two types of complexes containing this bridging structural feature are known; those containing metal-metal bonds (3), called "dimetallocycloalkanes" and those without metal-metal bonds (4), called "polymethylene bridged" compounds.

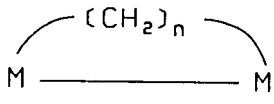

(3)

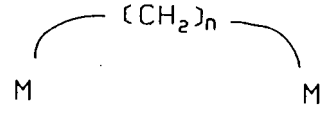

(4)

Complexes of this type, where two metal centres are bonded to the two terminal carbons of an alkyl chain are termed μ(α,ω)-alkanediyl compounds, and can be represented by the general formula, $LxM-(CH_2)_n-M'Ly$, where $n \geq 2$.

Since the original mechanistic proposal for the Fischer-Tropsch reaction involved the growth of a hydrocarbon chain on a metal surface, dimetallocyclic (3) and polymethylene bridged (4) complexes are of interest as models for the surface intermediates in this and other catalytic reactions. For example, in the Ziegler-Natta process, the polymerisation of ethylene is thought to proceed by insertion of an alkene (C_2H_4 or C_3H_6) into a titanium-alkyl bond to produce intermediates of the type $Ti-CH_2-CH_2-CH_2R$. This insertion of an alkene into a transition metal-

alkyl bond was only recently observed for a cobalt trimethylphosphine-methyl complex, [7]. Dimetallocyclic intermediates have also been implicated in olefin metathesis [8] and alkene dimerization [9] processes.

In the light of the preceding discussion, it is clear that the study of $\mu(\alpha,\omega)$-alkanediyl complexes could provide much valuable information, especially regarding the mechanisms of such catalytic reactions, and indeed serve as models for the intermediates involved. Ultimately, it is hoped that such investigations will lead to the development of more selective and efficient catalysts.

In addition, relatively little research has been carried out on the reactivity of such hydrocarbon bridged binuclear compounds. In this respect, the elucidation of structures and the study of the reactivity (eg. insertion reactions, decarbonylation, β-hydride eliminations etc.) of these $\mu(\alpha,\omega)$-alkanediyls are of great interest.

1.2 Summary of the Known μ-(α,ω)-Alkanediyl Complexes of the Iron Group (Fe, Ru and Os).

Dinuclear transition metal compounds, in which hydrocarbon fragments bridge the two metal atoms, have been the subject of several recent extensive reviews, [10-14].

In particular, μ-methylene complexes in which a single $-CH_2-$ fragment bridges two metal atoms, either with or without metal-metal bonds, have been covered by Herrmann [10] and to a lesser

extent by Casey and Audett [13]. Moss and Scott [12], and more recently Casey and Audett [13] have reviewed the known μ(α,ω)-alkanediyl complexes, comprising both dimetallocycloalkanes (3) and polymethylene bridged compounds (4), while Lappert et.al. have covered (in detail) a broad spectrum of hydrocarbyl bridged compounds, [14]. For this reason, a summary only of pertinent μ(α,ω)-alkanediyl complexes is discussed here. Further elaboration on the chemistry of the complexes of $[CpM(CO)_2]_2[\mu\text{-}(CH_2)_n]$ (M = Fe, Ru) is covered in subsequent chapters.

King [15] reported the synthesis of the first μ(α,ω)-alkanediyl compounds, $[CpFe(CO)_2]_2[\mu\text{-}(CH_2)_n]$ (5) where n=3-6, in 1963. (Equation 2).

$$2Na[CpFe(CO)_2] + Br(CH_2)_nBr \xrightarrow[R.T.]{THF} [Cp(CO)_2Fe(CH_2)_nFe(CO)_2Cp] \quad (5a\text{-}d),\ n = 3\text{-}6 \qquad 2$$

These dinuclear iron compounds (5) were also produced when $[Cp(CO)_3M(CH_2)_nBr]$ (M = Mo, W; n=3, 4) [16] or $[Cp(CO)_2Fe(CH_2)_nBr]$ (n=3-5) [17] were reacted with $Na[CpFe(CO)_2]$. Pettit et.al. [18] have also synthesised $[CpFe(CO)_2]_2[\mu\text{-}(CH_2)_n]$ by photolysis of $[CpFe(CO)_2]_2[\mu\text{-}C(O)(CH_2)_nC(O)]$.

The series of di-iron complexes (5) has since been extended by Moss and Scott [19], who prepared the new compounds of $[CpFe(CO)_2]_2[\mu\text{-}(CH_2)_n]$ where n=7-12 (5e-j). A detailed study of the mass spectrometry and thermal behaviour of complexes of type

(5) (where n=3-12) was also reported, [19]. These mass spectral fragmentation patterns are discussed in Section 2.2.3 and compared with those observed for the diruthenium complexes, $[CpRu(CO)_2]_2[\mu\text{-}(CH_2)_n]$ where n=5-10 (7e-j), prepared in this present study.

X-ray crystal structure determinations of the complexes (5a, n=3) and (5b, n=4) have confirmed that the iron atoms are σ-bonded to the α-carbon atoms of a linear alkyl chain, [20]. These structures are discussed further in Section 2.2.5.

Attempts to prepare the μ(1,2)-ethanediyl complex, $[CpFe(CO)_2]_2[\mu\text{-}(CH_2)_2]$, have resulted only in the isolation of the iron dimer, $[CpFe(CO)_2]_2$, [16,18]. However, the evolution of ethylene during the photochemical decarbonylation of $[CpFe(CO)_2]_2[\mu\text{-}C(O)(CH_2)_2C(O)]$ provides evidence for the formation of the desired decarbonylated ethanediyl di-iron complex as a reaction intermediate, [18]. The perfluoroethanediyl compounds, $[Fe(CO)_3]_2[\mu\text{-}(CF_2)_2][\mu\text{-}(SCH_3)_2]$ and $[Fe(CO)_2(PMe_3)]_2[\mu\text{-}(CF_2)_2][\mu\text{-}(SCH_3)_2]$ [21] represent the only known two-carbon bridged di-iron complexes. Even so, these contain additional bridging ligands to stabilise them, and rearrange in solution to form the carbene species, $>CFCF_3$.

The reactions of the compounds $[CpFe(CO)_2]_2[\mu\text{-}(CH_2)_n]$ (5a-j, n=3-12) have been well studied, [18,22,23]. In the presence of excess donor ligands, L (where L = PR_3 or CO), the complexes undergo the familiar carbonyl insertion (or alkyl migration) reaction under photochemical or thermochemical conditions. (Equation 3). These reactions are discussed in detail in Section 3.

$$[Cp(CO)_2Fe(CH_2)_nFe(CO)_2Cp] \xrightarrow[\Delta \text{ OR } h\nu]{\text{EXCESS L}} [Cp(CO)LFeC(=O)(CH_2)_nC(=O)FeL(CO)Cp] \qquad 3$$

Thermal and photochemical decomposition of compounds (5a-5d) (n=3-6), both in solution and in the solid state, results in elimination of the alkyl bridge as alkanes, alk-1-enes and cis and trans- alk-2-enes, [18,19,24-26]. The formation of these decomposition products has been rationalised in terms of a dimetallocyclic intermediate of type (6), [18, 24,25].

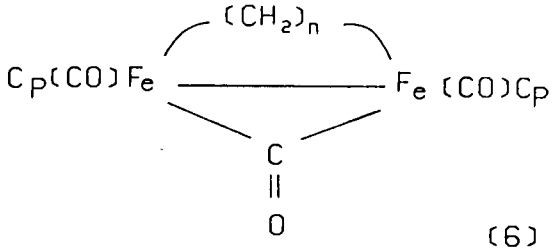

(6)

The increase in the ratio of alkane to alkene decomposition products as n increases, is possibly due to decreasing stability of large ring dimetallocyclic intermediates. An alternate pathway involving homolytic Fe-C bond fission, followed by hydride abstraction has been proposed to account for the formation of alkanes in the longer chain alkanediyl complexes, [12,18,24,25].

Such a dimetallocyclic product has been isolated on photolysis of $[CpRu(CO)_2]_2[\mu\text{-}(CH_2)]$, [27]. This product, $[CpRu(CO)_2]_2[\mu\text{-}CO][\mu\text{-}CH_2]$ was also prepared from $[CpRu(CO)_2]_2[\mu\text{-}CO][\mu\text{-}C(O)C_2(Ph)_2]$ and $Ph_3P{=}CH_2$ by Knox et.al., [28]. Other known ruthenium

dimetallocycloalkanes include $[CpRu(CO)_2]_2[\mu\text{-}CO][\mu\text{-}CHCH_3]$ and $[CpRu(CO)_2]_2[\mu\text{-}C(CH_3)_2][\mu\text{-}C(CH_3)_2]$ in which the Ru-Ru distance of 2.7 A and the Ru-C-Ru angle of 80° are indicative of the metal-metal bond, [29].

The polymerisation of ethylene is believed to proceed by insertion of an alkene into a metal-alkyl bond. Evidence for such insertion mechanisms is provided by the reactions of $[(CO)_3Fe]_2[\mu\text{-}(CO)]_2[\mu\text{-}(CH_2)]$ and $[Cp(CO)Fe]_2[\mu\text{-}(CO)][\mu\text{-}(CH_2)]$ with ethylene to yield propene. The mechanism (Scheme 3) is thought to involve insertion of C_2H_4 into the iron alkyl bond to form a dimetallocyclopentane, followed by β- elimination, [18,30].

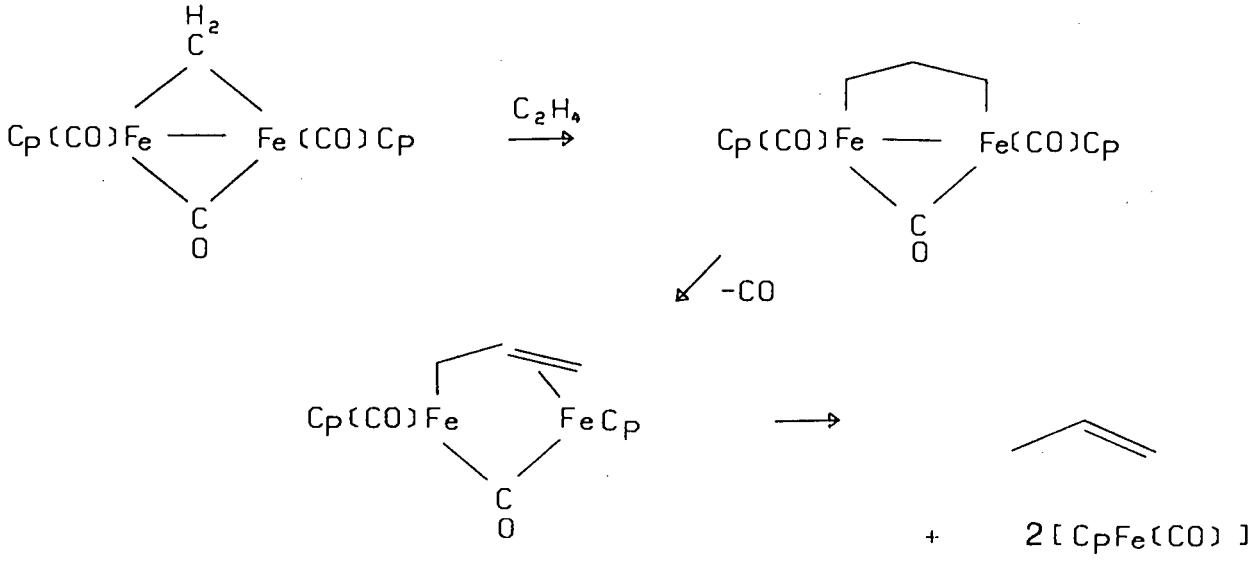

SCHEME 3

The analogous methylcyclopentadienyl derivatives of (5) $[(\eta^5\text{-}C_5R_4Me)Fe(CO)_2]_2[\mu\text{-}(CH_2)_n]$ (R=H, n=3-10; R=Me, n=3-6) have recently been reported by Mapolie and Moss, [31]. The complex $[(\eta^5\text{-}C_5Me_5)Fe(CO)_2]_2[\mu\text{-}(CH_2)_5]$ was also reported by Hsu, [32]. These compounds are prepared by reaction of $Na[(C_5R_4Me)Fe(CO)_2]$ with $Br(CH_2)_nBr$ using essentially the same procedure as for the preparation of the cyclopentadienyl analogues (5). The pentamethylcyclopentadienyl complexes, $[(\eta^5\text{-}C_5Me_5)Fe(CO)_2]_2[\mu\text{-}(CH_2)_n]$ were obtained as stable, yellow , crystalline solids. However, the mono-methylcyclopentadienyl complexes $[(\eta^5\text{-}C_5H_4Me)Fe(CO)_2]_2[\mu\text{-}(CH_2)_n]$ were isolated as yellow crystalline solids for n_{even} and as yellow-brown oils for n_{odd}. Studies of the reactivities of the $[C_5Me_5]$, $[C_5H_4Me]$ and $[C_5H_5]$ complexes will enable ligand effects to be evaluated. All the complexes of $[(\eta^5\text{-}C_5R_4Me)Fe(CO)_2]_2[\mu\text{-}(CH_2)_n]$ show similar fragmentation in their mass spectra to that exhibited by the compounds of $[CpFe(CO)_2]_2[\mu\text{-}(CH_2)_n]$ reported in [19].

In 1968, Stone et.al. [33] reported the synthesis of $[Cp(CO)_2Ru(C_6F_4)C(O)Ru(CO)_2Cp]$ from $Na[CpRu(CO)_2]$ and C_6F_5COCl. This compound is thermally stable to 178°C (melting point). The corresponding iron analogue can be prepared following a similar route, [33].

The synthesis of the first ruthenium analogues of (5) viz. $[CpRu(CO)_2]_2[\mu\text{-}(CH_2)_n]$ (7), where n=3 and 4, was carried out by Knox and co-workers [24,25] by the reaction of $Na[CpRu(CO)_2]$ and $I(CH_2)_nI$. (Equation 4).

$$2Na[CpRu(CO)_2] + I(CH_2)_nI \xrightarrow[R.T]{THF} [Cp(CO)_2Ru(CH_2)_nRu(CO)_2Cp]$$

(7c), n = 3

(7d), n = 4 . 4

Knox et.al. also investigated the thermal and photochemical decomposition of complexes of type $[CpM(CO)_2]_2[\mu\text{-}(CH_2)_n]$ (M = Fe, Ru; n=3,4), [24,25]. Comparison of the decomposition products revealed that iron favoured the formation of cyclopropane more strongly than ruthenium, while propene formation was favoured by photolysis rather than thermolysis. The mixed-metal compound, $[Cp(CO)_2Fe(CH_2)_3Ru(CO)_2Cp]$ (8a), prepared by the addition of $Na[CpRu(CO)_2]$ to $[Cp(CO)_2Fe(CH_2)_3I]$, showed a decomposition product ratio intermediate between that of $[CpFe(CO)_2]_2[\mu\text{-}(CH_2)_3]$ and $[CpRu(CO)_2]_2[\mu\text{-}(CH_2)_3]$, [24,25]. The formation of these products was again explained in terms of decomposition via a dimetallocyclic intermediate.

In 1983, Wreford and co-workers [36] reported the first μ-methylene complex without either metal-metal bonds or other bridging ligands to stabilise it. This compound $[CpRu(CO)_2]_2[\mu\text{-}(CH_2)]$ (7a), was prepared from $Na[CpRu(CO)_2]$ and CH_2Cl_2 at -35°C in THF. All other known μ-methylene complexes contain either additional bridging ligands or metal-metal bonds to stabilise them. Reviews of such compounds have appeared elsewhere, [10,12,14].

The complex (7a), although stable indefinitely at low temperature (-35°C), decomposes rapidly on warming to room temperature. $[CpRu(CO)_2]_2[\mu\text{-}(CH_2)]$, which shows unusual reactivity, undergoes CO insertion to afford $[CpRu(CO)_2]_2[\mu\text{-}C(O)CH_2]$ (9) in 80% yield. The latter complex has also been prepared in low yield from $Na[CpRu(CO)_2]$ and $ClCH_2C(O)Cl$, (Scheme 4), [27]. Similarly, rapid reaction of (7a) with excess PMe_3 yields the substituted derivative of (9) viz. $[Cp(CO)_2Ru(CH_2)C(O)Ru(CO)(PMe_3)Cp]$, [27].

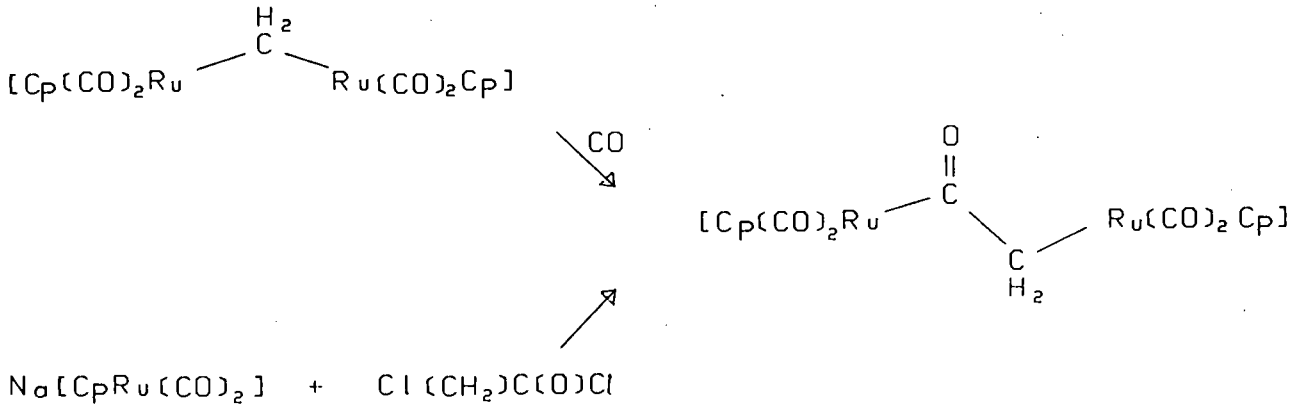

SCHEME 4

Wreford et.al. also reported the preparation of the $\mu(1,2)$-ethanediyl compound, $[CpRu(CO)_2]_2[\mu\text{-}(CH_2)_2]$ (7b), which eliminates ethylene on photolysis or when heated above 70°C, [27]. The isolation of the complexes (7a) and (7b) suggests that the ruthenium polymethylene bridged compounds are more stable than their iron counterparts and hence differences in reactivity are to be expected.

In addition to the previously described polymethylene bridged complexes (without metal-metal bonds), numerous other iron and ruthenium complexes containing hydrocarbon bridges and bridging CO ligands are also known, [12-14]. However, these compounds although related, are not directly relevant to this study and will therefore not be discussed further.

At present no polymethylene bridged complexes of osmium without Os-Os bonds are known. On the other hand, several examples of dimetallocyclic compounds of osmium have been prepared. The diosmacycloalkanes (10), (11) and (12) shown in Scheme 5 were reported by Norton and co-workers, [38]. These products were obtained from the reaction of $Na_2[Os_2(CO)_8]$ with $CH_2(OTs)_2$, $TsOCH_2CH_2OTs$ (where OTs = p-toluenesulphonyl) and $I(CH_2)_3I$ respectively.

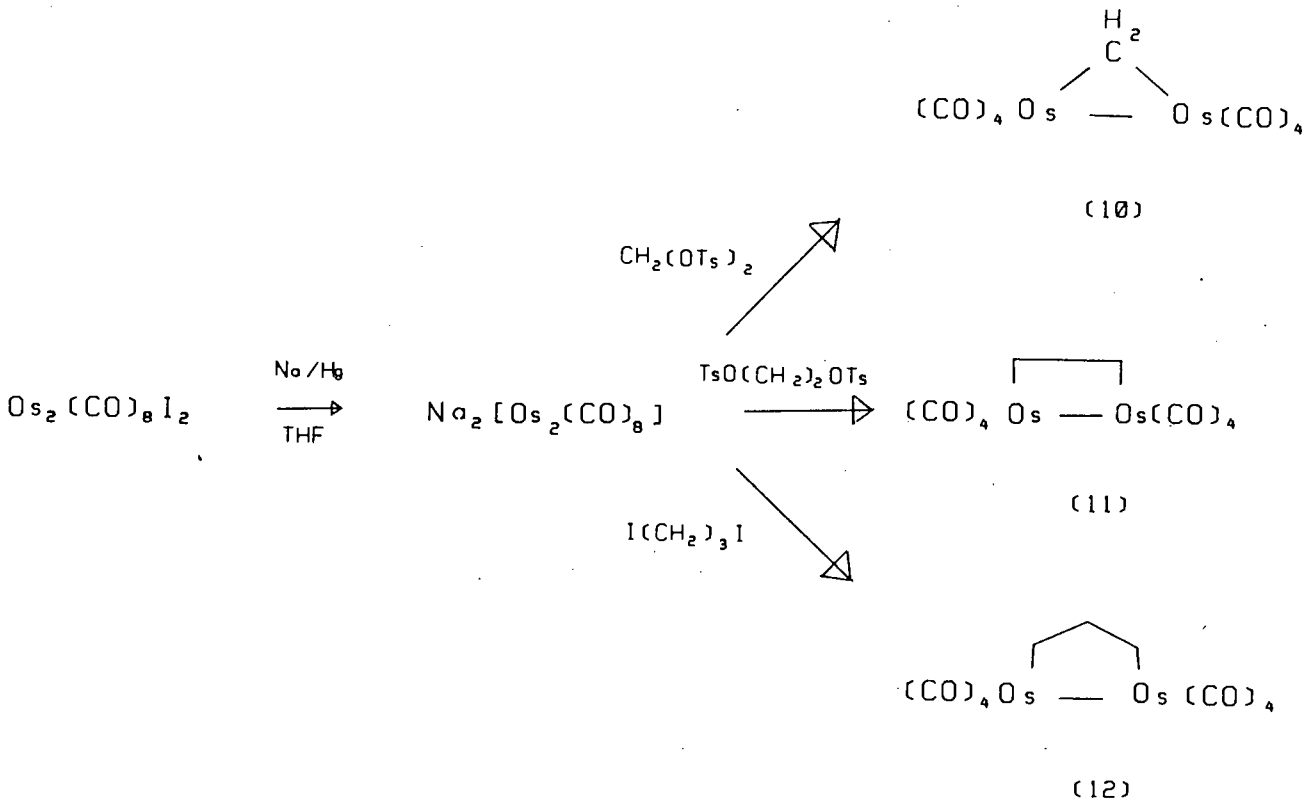

SCHEME 5

The diosmacyclopentane (12) has also been isolated from the reaction of the diosmacyclopropane (10) with ethylene at 100°C [38], thus providing further evidence for the insertion mechanism proposed in Scheme 3. The reaction is reversible in toluene at 130°C to give the diosmacyclopropane (10) and ethylene as the major products, together with some propene (21%) and methane (32%).

The diosmacyclobutane (13) was isolated by Takats et.al. [39] on photolysis of $Os_3(CO)_{12}$ in the presence of methyl acrylate. A mononuclear alkene adduct was also recovered from this reaction. (Equation 5).

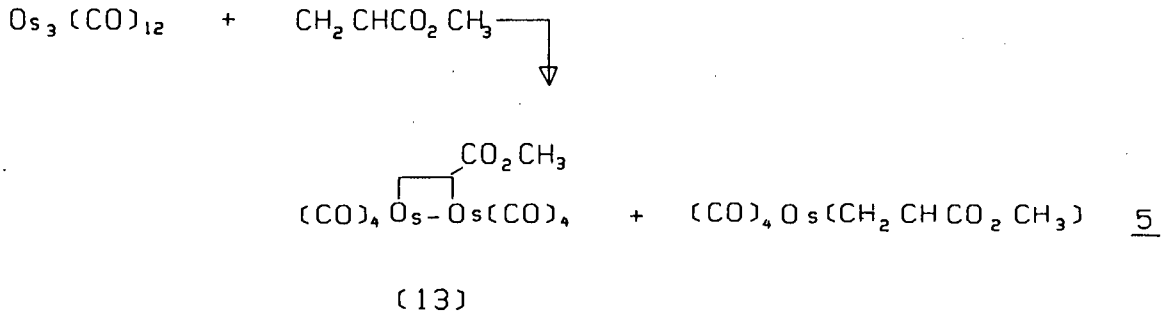

$$Os_3(CO)_{12} + CH_2CHCO_2CH_3 \longrightarrow (CO)_4Os(CO_2CH_3)Os(CO)_4 + (CO)_4Os(CH_2CHCO_2CH_3) \quad 5$$

(13)

Attempts to prepare the analogous diruthenacyclobutane from $Ru_3(CO)_{12}$ under similar conditions resulted only in the isolation of mononuclear alkene adducts. This was explained in terms of a weaker Ru-Ru bond in $Ru_2(CO)_8$, resulting in cleavage of this intermediate before trapping by an alkene could occur. The photochemical reaction of $Os_3(CO)_{12}$ with ethylene also produces the diosmacyclobutane (11) (see Scheme 5), [39].

In this study, the synthesis, characterisation and reactivity of some new ruthenium alkanediyl complexes of the type $[CpRu(CO)_2]_2[\mu\text{-}(CH_2)_n]$ (7e-j, n=5-10) are reported and discussed. In addition, the X-ray crystal structure of $[CpRu(CO)_2]_2[\mu\text{-}(CH_2)_5]$ has been determined.

1.3 Heterogeneous Compounds of Iron, Ruthenium and Osmium as CO Hydrogenation Catalysts.

In the early development of catalysts for CO hydrogenation, emphasis was placed on maximising the C_{5+} product yields for use as liquid fuels. The only metals of commercial importance as Fischer-Tropsch catalysts were cobalt and iron. However, these iron and cobalt-based catalysts gave a broad product distribution (C_1-C_{25} hydrocarbons). With the increases in the oil price in the 1970's, the attention was focused on developing catalysts that would yield a narrow product distribution of hydrocarbons and alcohols in the C_2-C_4 range, for use as feedstocks for the petrochemical industry, [40].

The use of partially reducible oxides, such as MnO_2, TiO_2 and V_2O_5, as catalyst supports is reported to be one method by which significant changes in the product distribution can be achieved, [41]. Of particular interest are the manganese oxide-iron catalysts which have been demonstrated to give extremely low methane yields and increased olefin selectivity, [40,45]. However, these catalysts have been found to exhibit relatively short lifetimes under industrial-type conditions. Furthermore, as the pressure is increased the time periods for which C_2-C_4 hydrocarbons are observed decrease, [40]. This catalyst deactivation has been ascribed to the formation of iron-carbides, [46]. Similarly, MnO has been used to modify cobalt catalysts to produce high yields of C_2-C_4 hydrocarbons, [47].

The preceding discussion has described only iron and cobalt-based catalysts. However, supported ruthenium catalysts are reported to have a higher Fischer-Tropsch specific activity than any other supported Group VIII metal catalyst, [48]. In addition, studies have shown that ruthenium catalysts afford a product spectrum with the highest average molecular weight and the largest C_{5+} fraction even at atmospheric pressure, [40]. These higher molecular weight, straight chain paraffins are ideal for use as jet and diesel fuels.

Typical products of CO hydrogenation over a supported ruthenium catalyst are demonstrated by the results of Everson et.al., [49]. Mainly straight chain, saturated hydrocarbons with a C_5-C_{10} selectivity were produced over a 0.5% Ru on γ-Al_2O_3 catalyst. As in the iron catalysts supported on manganese oxide, Ru supported on TiO_2 demonstrates decreased methane and higher molecular weight fractions (C_{6+}) and increased yields of C_2-C_5 hydrocarbons, particularly alkenes, in comparison to Ru on γ-alumina, [40].

Of the iron, ruthenium and osmium systems available for study as CO hydrogenation catalysts, the metal carbonyl cluster compounds, $[M_3(CO)_{12}]$, supported on inert oxides such as Al_2O_3 and SiO_2 are relevant to this work and have been well studied by various groups, [50-54].

In particular, Commereuc et.al. [51,53] demonstrated that $[Fe_3(CO)_{12}]$ and $[HFe_3(CO)_{11}]^-$ supported on Al_2O_3, SiO_2, La_2O_3 or MgO showed high selectivity for low molecular weight (C_2-C_3) olefins in the Fischer-Tropsch synthesis. Alumina or silica supported $[Ru_3(CO)_{12}]$ or $[Os_3(CO)_{12}]$ also exhibited a product

distribution favouring low molecular weight hydrocarbons, however, most of these were saturated, [55]. Baird et.al. [52] also reported that Al_2O_3 supported $[Ru_3(CO)_{12}]$ is a very efficient catalyst for the hydrogenation of carbon dioxide. Carbon dioxide is potentially a very important feedstock for the production of hydrocarbons since CO_2 is more readily available than CO.

A recent study [56] has provided vibrational and X-ray absorption spectroscopic evidence for the nature of these metal carbonyl Al_2O_3 or SiO_2 supported catalyst precursors. Such data strongly support the presence of hydride ligands with the involvement of two surface oxygens in cluster binding as shown in (14).

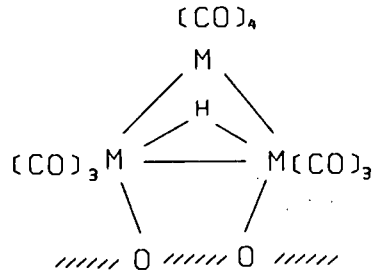

(14)

A sodium-anionic triruthenium cluster, $Na[Ru_3H(CO)_{11}]$, supported on TiO_2 or MgO has been shown to selectively yield light C_2-C_5 olefins at 270°C, with high catalytic activity in the Fischer-Tropsch synthesis, [54].

The lack of control of product selectivity has been the major area of concern in the Fischer-Tropsch process. Relatively recently, supported bimetallic catalysts have become important as a means of controlling catalytic activity and selectivity, [57-61]. Supported alloy catalysts significantly alter product selectivities,

especially with respect to olefin / paraffin ratios and oxygenate formation. Vannice and Garten [57] demonstrated such effects in a supported Fe-Pt catalyst.

Supported bimetallic systems of iron and ruthenium show unique catalytic activity, which is thought to be due to the change in the electronic nature of the alloyed catalyst, [58,59]. Such bimetallic catalysts are readily obtained from organometallic mixed-metal carbonyl clusters as the catalyst precursors, [60-62].

Vannice et.al. [61] reported that the Fe-Ru bimetallic catalysts, prepared from the mixed-metal carbonyl precursors, showed a steady increase in CO hydrogenation and methanation specific activities with increasing ruthenium content. These trends are consistent with Ru being a more active CO hydrogenation catalyst than Fe. The higher activity of the Fe-Ru catalysts in comparison to the Fe-only catalysts is probably due to a strong Fe-Ru contact in which Ru catalyses the reduction of the iron component, [58].

Several other bimetallic catalyst systems exist. For example, ruthenium-cobalt catalysts have been found to be effective for the homologation of various compounds, [63-65]. In particular, a Ru-Co system showed enhanced activity and improved selectivity towards ethanol formation in the hydrocarbonylation of methanol, [66-67]. Similarly, a novel ruthenium-rhenium bimetallic catalyst has been observed to enhance the formation of ethylene glycol from CO / H_2, [68].

Although by no means comprehensive, this short introduction is intended to give some insight as to the rôle of the metals within the iron group (and especially Fe and Ru) as catalysts in the hydrogenation of carbon monoxide. In this present study, the three complexes of type $[CpFe(CO)_2]_2[\mu\text{-}(CH_2)_n]$, (where n=0, 3 and 5) have been supported on γ-alumina and studied as catalyst precursors for the hydrogenation of CO.

1.4 Scope of this Thesis.

In this thesis, the synthesis and characterisation of the new ruthenium alkanediyl complexes, $[CpRu(CO)_2]_2[\mu\text{-}(CH_2)_n]$ (7e-j, n=5-10) are reported. The mass spectral results are compared to those for the analogous iron compounds $[CpFe(CO)_2]_2[\mu\text{-}(CH_2)_n]$. In addition, the X-ray crystal structure of the compound $[CpRu(CO)_2]_2[\mu\text{-}(CH_2)_5]$ has been determined and is reported and discussed. Two new mononuclear haloalkyl compounds, $[CpRu(CO)_2(CH_2)_nX]$ (X=Cl, n=3; X=Br, n=4), as well as the new mixed-metal complex $[Cp(CO)_2Fe(CH_2)_4Ru(CO)_2Cp]$, have also been prepared.

The reactions of $[CpRu(CO)_2]_2[\mu\text{-}(CH_2)_5]$ with tertiary phosphines, tertiary butylisocyanide and with various electrophiles (I_2, Br_2 and $Ph_3C^+PF_6^-$) have been investigated and the results contrasted to those obtained for the analogous reactions of $[CpFe(CO)_2]_2[\mu\text{-}(CH_2)_n]$.

The catalyst precursors, $[CpFe(CO)_2]_2[\mu\text{-}(CH_2)_n]$ (where n=0, 3 and 5) have been supported on γ-alumina, decomposed and subsequently investigated for CO hydrogenation activity under Fischer-Tropsch conditions.

In a separate study, the new mononuclear cobaloximes $[Co(DH)_2py(CH_2)_nX]$ (X=Br, n=3-7; X=I, n=3), as well as the dinuclear $\mu(\alpha,\omega)$-alkanediyl cobaloximes $[Co(DH)_2py]_2[\mu\text{-}(CH_2)_n]$ (n=4-8), have been synthesised and fully characterised.

2. SYNTHESIS AND CHARACTERISATION OF μ(α,ω)-ALKANEDIYL COMPLEXES OF RUTHENIUM AND THEIR MONONUCLEAR HALOALKYL PRECURSORS.

2.1 Introduction

The first μ(α,ω)-alkanediyl complexes of type $L_xM-(CH_2)_n-M'L_y$ to be prepared were the iron complexes $[CpFe(CO)_2]_2[\mu-(CH_2)_n]$ (5a-d, n=3-6), reported by King [15], following the method shown in Equation 2. This series was subsequently extended by Moss and Scott [19] to include the compounds where n=7-12 (5e-j). (Figure 2.1).

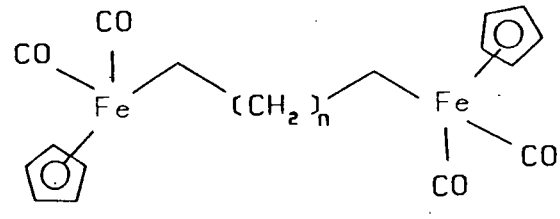

FIGURE 2.1 Structure of the first polymethylene bridged complexes, $[CpFe(CO)_2]_2[\mu-(CH_2)_n]$ (n=3-12)

Moss has also shown that these dinuclear polymethylene bridged complexes (5a-c) can be synthesised from their mononuclear haloalkyl precursors, $[CpFe(CO)_2(CH_2)_nX]$ (X=Br, n=3-5; X=Cl, n=3), [17].

The analogous dinuclear ruthenium compounds, $[CpRu(CO)_2]_2[\mu-(CH_2)_n]$ (where n=1-4) [25,27], as well as the mixed-metal complex $[Cp(CO)_2Fe(CH_2)_3Ru(CO)_2Cp]$ [25], have since been prepared. Knox

et. al. reported that the reaction of $Na[CpRu(CO)_2]$ with the dibromoalkanes, $Br(CH_2)_nBr$ (n=3,4), gave the desired dinuclear compounds in only 10 % yield as an inseparable mixture with $\{Hg[Ru(CO)_2Cp]\}$. However, using the di-iodoalkanes the products $[CpRu(CO)_2]_2[\mu(CH_2)_n]$ where n=3 and 4 (7c and 7d) were isolated in good yield, [25]. (Equation 4). The methylene bridged complex $[CpRu(CO)_2]_2[\mu\text{-}(CH_2)]$ (7a) was prepared from $Na[CpRu(CO)_2]$ and dichloromethane by Lin et. al., who also mentioned the synthesis of the ethylene bridged complex (7b) although no details of the preparation appeared, [27]. This methylene bridged compound (7a) was the first μ-methylene complex without other bridging ligands to stabilise it.

The mixed metal complex, $[Cp(CO)_2Fe(CH_2)_3Ru(CO)_2Cp]$ (8a), was also prepared previously from $[CpFe(CO)_2(CH_2)_3Br]$ and $Na[CpRu(CO)_2]$, [25].

In this study, a series of new diruthenium polymethylene bridged complexes has been synthesised (where n=5-10, 7e-j) using essentially the same route as that of Knox et. al. (Equation 4), [25]. The new mixed metal complex, $[Cp(CO)_2Fe(CH_2)_4Ru(CO)_2Cp]$ (8b) has also been prepared by an adaptation of the method proposed by Knox et. al., [25]. In addition, the mononuclear haloalkyl complexes of ruthenium $[CpRu(CO)_2(CH_2)_nX]$, (where n=3, X=Cl; n=4, X=Br) have been prepared by a route similar to that of Moss [17] for the preparation of $[CpFe(CO)_2(CH_2)_nX]$.

2.2 Results and Discussion

2.2.1 Synthesis of $[CpRu(CO)_2]_2[\mu\text{-}(CH_2)_n]$, n=5-10 (7e-j).

The starting material, $[CpRu(CO)_2]_2$ was prepared by adaptations of reported literature methods either from $Ru_3(CO)_{12}$ [69,70] or from $RuCl_3.nH_2O$, [71]. The ruthenium dimer, $[CpRu(CO)_2]_2$, was reduced over sodium mercury amalgam in THF for approximately three hours to produce the rich red-brown anionic solution, $Na[CpRu(CO)_2]$ / THF.

The reaction of $Na[CpRu(CO)_2]$ with $I(CH_2)_nI$ (n=5-10) in a 2:1 molar ratio, in THF at ambient temperature, produced the new dinuclear polymethylene bridged complexes (7e-j) where n=5-10 in generally good yields (55-75%). (Equation 6).

$$2Na[CpRu(CO)_2] + I(CH_2)_nI \xrightarrow{THF\ /\ R.T.} [CpRu(CO)_2]_2[\mu\text{-}(CH_2)_n] \qquad 6$$

(7e), n=5 (7h), n=8
(7f), n=6 (7i), n=9
(7g), n=7 (7j), n=10

The compounds of type (7) were isolated by extraction with hexane followed by chromatography on Florisil. Elution with hexane gave the compounds in fairly pure crystalline form, which could be recrystallised from hexane to produce cream coloured crystals. The only other products of the reaction were $[CpRu(CO)_2]_2$ and a very small amount of $[CpRu(CO)_2I]$ which were identified by their IR spectra in the $\nu(CO)$ region.

Complexes (7e-j) all exist as air stable, cream coloured crystalline solids at room temperature. However, solutions of these compounds in hydrocarbon solvents decompose within a few hours in air, as do the iron complexes (5). Under nitrogen, however, the ruthenium compounds exhibit unusually high stability in solution, even at elevated temperatures and for prolonged periods of time (ca. 140^{o}C for several days - see Chapter 3).

All these compounds (7e-j) have been characterised by infrared, ^{1}H and ^{13}C NMR spectroscopy, mass spectrometry and elemental analysis. The mass spectra have been compared to those of the di-iron complexes (5) [19] and are discussed in Section 2.2.3. The thermal decomposition of compounds (7d) and (7e) has been studied by Differential Scanning Calorimetry, which is covered in Section 2.2.4.
The structure of the compound $[CpRu(CO)_2]_2[\mu\text{-}(CH_2)_5]$ has been determined by X-ray crystallography and is discussed later in Section 2.2.5.

The infrared spectra (see Table 2.1) of complexes (7e-j) all show two very strong terminal carbonyl absorption bands at 2019 and 1959 cm^{-1} compared to 2008 and 1954 cm^{-1} for the iron complexes

(5a-j). This is indicative of a weaker ruthenium-carbon synergic interaction resulting in a stronger C≡O bond in the compounds of $[CpRu(CO)_2]_2[\mu\text{-}(CH_2)_n]$. This is surprising since, being a second row transition element, one would expect the ruthenium-carbon orbital overlap to be greater resulting in a stronger Ru-C bond in comparison to the Fe-C bond. The fact that a weaker Ru-C bond is observed is probably due to a lower electron density on the ruthenium atom arising from the lower nucleophilicity of the ruthenium anion precursor $[CpRu(CO)_2]^-$ relative to the iron anion $[CpFe(CO)_2]^-$, [72].

TABLE 2.1 Melting point and IR data for the compounds $[CpRu(CO)_2]_2[\mu\text{-}(CH_2)_n]$, n=5-10 (7e-j)

COMPOUND No.	n	Melting Point Range (°C)	ν(CO) (cm^{-1}) [a]
7e	5	77 - 84	2018 vs , 1959 vs
7f	6	106 - 109	2019 vs , 1959 vs
7g	7	65 - 70	2019 vs , 1959 vs
7h	8	73 - 77	2019 vs , 1959 vs
7i	9	34 - 37	2019 vs , 1959 vs
7j	10	45 - 51	2019 vs , 1959 vs

a Hexane solution, vs = very strong

The lower electron density on the ruthenium atoms in these complexes (7e-j) is also reflected in the ^1H NMR resonance of the cyclopentadienyl protons. A singlet at ca. δ 5.2 ppm for the five equivalent protons on the C_5H_5 ring is observed in the diruthenium compounds. This signal occurs at ca. δ 4.8 ppm in the ^1H HMR spectra of the di-iron analogues. [19]. The protons of the polymethylene chain in compounds (7e-j) give rise to three complex signals at ca. δ 1.67 ppm (4H), δ 1.53 ppm (4H) and δ 1.27 ppm { (2n-8)H }, which do not differ significantly with changes in the chain length, (Table 2.2). These signals correspond closely to the two broad resonances at ca. δ 1.5 and δ 1.3 ppm observed in the ^1H NMR spectra of the di-iron complexes (5), [19].

The melting points of the compounds $[CpRu(CO)_2]_2[\mu\text{-}(CH_2)_n]$ (n=5-10) decrease with increasing chain length. In addition to this, the compounds with n = even number (7f,h,j) have generally higher melting points than those with n = odd number (7e,g,i), (Table 2.1).

This trend has also been observed for the dinuclear iron complexes [19], and could be due to different crystalline forms for n_{even} and n_{odd} as a result of steric interactions of the CO ligands. This possibility is discussed in detail in Section 2.2.5 (see Figure 2.21) containing the X-ray crystal structure of the compound $[CpRu(CO)_2]_2[\mu\text{-}(CH_2)_5]$.

TABLE 2.2 ^{1}H NMR Data for the compounds $[CpRu(CO)_2]_2[\mu\text{-}(CH_2)_n]$ n=4-10 (7d-j) in $CDCl_3$

COMPOUND No	n	δ (ppm) C_5H_5	Ru-CH_2	β-CH_2-	-CH_2-
7d	4	5.23(s,10H)	1.68(m,4H)	1.55(m,4H)	
7e	5	5.22(s,10H)	1.66(m,4H)	1.53(m,4H)	1.28(m,2H)
7f	6	5.22(s,10H)	1.67(m,4H)	1.53(m,4H)	1.28(m,4H)
7g	7	5.23(s,10H)	1.67(m,4H)	1.53(m,4H)	1.27(bs,6H)
7h	8	5.22(s,10H)	1.67(m,4H)	1.53(m,4H)	1.27(bs,8H)
7i	9	5.22(s,10H)	1.67(m,4H)	1.54(m,4H)	1.27(bs,10H)
7j	10	5.23(s,10H)	1.67(m,4H)	1.53(m,4H)	1.26(bs,12H)

s - singlet
m - multiplet
bs- broad singlet

2.2.2 ^{13}C NMR Spectroscopy of $[CpRu(CO)_2]_2[\mu\text{-}(CH_2)_n]$.

The proton-decoupled ^{13}C NMR spectra of the diruthenium alkanediyls, $[CpRu(CO)_2]_2[\mu\text{-}(CH_2)_n]$ (7d-j, n=4-10), were recorded in $CDCl_3$ and externally referenced to tetramethylsilane (δ 0.00 ppm). These ^{13}C NMR chemical shifts, together with their assignments, are presented in Table 2.3.

The resonance due to the terminal carbonyl ligands at δ 202.5 ppm was readily observed even in the absence of paramagnetic relaxation agents such as $[Cr(acac)_3]$ (acac = acetylacetonate). A single sharp resonance at δ 88.55 ppm was assigned to the cyclopentadienyl carbon atoms. These values agree well with previous ^{13}C NMR data for the compounds $[CpRu(CO)_2]_2[\mu\text{-}(CH_2)_n]$ where n=3 and 4, [25]. No shift in either the C_5H_5 or the CO ^{13}C resonance was observed on increasing the alkyl chain length.

In previous studies [25], Knox and co-workers assigned the ^{13}C signals at δ 45.2 ppm and δ -3.3 ppm respectively to the α and β carbons of the alkyl chain in the compound $[CpRu(CO)_2]_2[\mu\text{-}(CH_2)_4]$, (7d). In the propylene bridged dinuclear compound, $[CpRu(CO)_2]_2[\mu\text{-}(CH_2)_3]$ (7c), these resonances were reported to occur at δ 49.1 ppm (α-CH_2) and δ 28.7 ppm (β-CH_2) respectively. However, on the basis of the present work, this assignment of the highest field chemical shift to the β-carbon atoms of the alkyl chain is believed to be incorrect. Thus, in this study, the high field, slightly broadened and less intense ^{13}C signals at ca. δ -3.2 ppm observed for the series of compounds (7d-j) are assigned to the α-carbons of the alkyl chain. This assignment has been made after careful examination of the ^{13}C NMR spectra for the

TABLE 2.3 ^{13}C NMR (decoupled) data for the compounds $[CpRu(CO)_2]_2[\mu\text{-}(CH_2)_n]$, n=4-10 (7d-j) in $CDCl_3$

COMPOUND No.	n	δ (ppm) CO	C_5H_5	α-CH_2	β-CH_2	γ-CH_2	δ-CH_2	ϵ-CH_2
7d	4	202.54	88.56	-3.30	45.18	-	-	-
7e	5	202.52	88.54	-2.99	39.65	40.08	-	-
7f	6	202.52	88.56	-3.15	34.42	39.86	-	-
7g	7	202.52	88.55	-3.12	34.93	39.88	29.05	-
7h	8	202.50	88.54	-3.16	34.88	39.84	29.44	-
7i	9	202.50	88.54	-3.18	34.85	39.85	29.38	29.83
7j	10	202.50	88.54	-3.18	34.87	39.85	29.37	29.79

diacyl, disubstituted derivatives of (7) ie. $[CpRu(CO)(PR_3)]_2[\mu\text{-}C(O)(CH_2)_5C(O)]$ (see Table 3.2). In the spectra of the latter compounds, the high field signal at δ -3.2 ppm (observed in the spectra of compounds (7)) is replaced by a new signal at ca. δ 65 ppm due to the deshielded methylene carbon in $Ru\text{-}C(O)\text{-}CH_2$. This would suggest that the signals at δ -3.2 ppm in the spectra of compounds (7) are correctly assigned to the α-carbons of the alkyl chain.

Further confirmation of this assignment was derived from the ^{13}C NMR spectra of the mixed-metal compounds $[Fp(CH_2)_4Ru(CO)_2Cp]$, $[Fp(CH_2)_4M(CO)_3Cp]$ (M = Mo,W) and $[Fp(CH_2)_4Re(CO)_5]$ (Fp = $CpFe(CO)_2$), [73]. A common resonance, occurring between ca. δ 3.0 and δ 3.9 ppm, was observed in the ^{13}C NMR spectra of all these compounds. In addition, one other high field signal was also observed which was found to vary with the nature of the second metal (eg δ -3.2 ppm (M = Ru); δ 2.59 ppm (M = Mo); δ -9.12 ppm (M = W) or δ -9.44 ppm (M = Re)). This common chemical shift in all the mixed-metal compounds must therefore be due to the carbon atoms adjacent to the Fe atom in each case. The $\beta\text{-}CH_2$ carbon resonance would be expected to fluctuate more with changes in the nature of the second metal atom.

Having assigned the high field ^{13}C signals to the α carbons of the alkyl chain, the remaining lower field signals in the region of δ. 29-40 ppm are easily assigned to the β, γ, δ carbon atoms etc. by comparison of the peak intensities. Thus, in compound (7e) the γ-carbon signal at δ 40.08 ppm was half the intensity of the β-carbon signal at δ 39.65 ppm and so on.

A fairly large shift in the β-carbon signal was observed as n increased from 3-6 in the complexes of $[CpRu(CO)_2]_2[\mu\text{-}(CH_2)_n]$ (7). (See Table 2.3). If one re-assigns the α- and β-CH_2 resonances in the compound where n=3 on the basis of the above observations (ie. δ 49.1 ppm (β-CH_2) and δ 28.7 ppm (α-CH_2)) the β-carbon resonance shifts from δ 49.1 ppm in (7c, n=3) to δ 34.4 ppm in (7f, n=6). A possible explanation for this large β-carbon shift in the shorter chain compounds lies in the close proximity of the β-CH_2 groups to the cyclopentadienyl ring (see Section 2.2.5, Figure 2.19 showing the X-Ray crystal structure of $[CpRu(CO)_2]_2[\mu\text{-}(CH_2)_5]$).

This interaction of the β-methylene group (particularly the protons) is reflected in the larger Ru-C_α-C_β bond angles of 113.5°/116.5° compared to the C_α-C_β-C_γ bond angles of 112.1°/110.9° (see Section 2.2.5). A similar interaction in the di-iron complexes, $[CpFe(CO)_2]_2[\mu\text{-}(CH_2)_n]$ (n=3,4) has also been reported to result in an enlarged Fe-C_α-C_β bond angle, [20]. The decrease in the β-carbon shift can thus be explained as follows. In the complex (7c, n=3), the β-CH_2 group is highly deshielded by the close proximity of two cyclopentadienyl ligands due to steric crowding. Slight relief of this steric interaction is brought about by an increase of one -CH_2- unit to the chain length. As the chain length becomes progressively longer, each β-CH_2 group will be decreasingly affected by the cyclopentadienyl ligand on the more distant metal atom resulting in a decrease in the chemical shift of the β-carbon atom. It would therefore appear that for n>6, the β-CH_2 groups are only affected by the cyclopentadienyl ligand on the nearest metal atom and no further decrease in chemical shift is observed on increasing the chain length.

However, this trend may also be due to the decreasing influence of the second metal atom as n increases.

The shorter C_α-C_β single bonds in comparison to the other C-C single bonds in the alkyl chain (determined by X-Ray crystallography - Section 2.2.5), suggested that some agostic interaction may be present between the metal and one of the β hydrogen atoms. Agostic interactions, in which a carbon-hydrogen group interacts with a transition metal centre to form a two-electron-three centre bond, have been recognised and found to have a marked effect on the molecular and electronic structure and hence the reactivity of the molecule, [74]. Such agostic M←H-C interactions are readily detectable by NMR. The most reliable indication of the presence of such a bridged system is the significantly reduced value of the coupling constant $J(^{13}C^b\text{-}H^b)$ of 75-100 Hz due to the reduced bond order of the C-H bond in C-H→M. This is much lower than the values of $J(^{13}C\text{-}H)$ of 120-130 Hz for normal saturated sp^3 C-H bonds. Furthermore, like metal-hydrides, the agostic hydrogen exhibits a high field chemical shift ($\delta<0$), [74].

In order to investigate the possibility of an agostic M←H-C interaction in the ruthenium complexes, $[CpRu(CO)_2]_2[\mu\text{-}(CH_2)_n]$, the proton-coupled ^{13}C NMR spectra for the compounds (7d, n=4) and (7e, n=5) were recorded and the $J(^{13}C\text{-}H)$ coupling constants measured. These are reported in Table 2.4.

TABLE 2.4 J(^{13}C-H) data for the compounds $[CpRu(CO)_2]_2[\mu-(CH_2)_n]$, n=4, 5

COMPOUND No	n	C_5H_5[a]	J (^{13}C - H) Hz C_α - H[b]	C_β - H[b]	C_γ - H[b]
7d	4	177.8(d), 6.8(q)	133.8	127.0	-
7e	5	177.9(d), 6.8(q)	134.6	130.4	125.3

a. Signal occurs as a doublet of quintets; values represent the coupling constants of the doublet (d) and quintet (q) respectively.

b. Signals occur as triplets.

The values of $J(^{13}C\text{-}H)$ for the C-H bonds of the β- and γ-(CH_2) groups of the alkyl chain all lie within the range characteristic of normal saturated sp^3 C-H bonds. The $J(^{13}C\text{-}H)$ for the C-H bonds of the α-(CH_2) groups lie marginally higher than the predicted range for sp^3 C-H bonds and thus provide no evidence for agostic C-H→M interactions. Furthermore, no high field proton resonance ($\delta<0$) was observed in either of the ^1H NMR spectra for (7d) or (7e) (spectra were recorded from δ -20 ppm). In addition, the cyclopentadienyl carbon signal was observed as a doublet of quintets in the proton coupled ^{13}C NMR spectrum of both (7d) and (7e), instead of the expected doublet. Initially it was thought that the further splitting could be due to coupling of a Cp carbon with four rapidly exchanging protons on C_α and C_β in a diene type system, M-(η^2-CH_2CH_2). This would agree with the shorter C_α-C_β bond distance observed in the crystal structure of (7e). However, this would necessitate a single broad proton resonance in the ^1H NMR spectrum for the four "equivalent" α and β-CH_2 protons. Since two distinct chemical shifts for the α and β-CH_2 protons are observed (Table 2.2) this possibility is ruled out.

In order to check whether or not this splitting was peculiar only to the dinuclear alkanediyl complexes, a proton-coupled ^{13}C NMR spectrum of $[CpRu(CO)_2]_2$ was recorded in $CDCl_3$. This revealed the same doublet of quintets for the Cp carbons as before. The observed splitting of the doublet (due to coupling between bonded carbon and hydrogen) could be explained by further (through space) coupling of each carbon atom in the Cp ring to the other four cyclopentadienyl protons on the remaining carbon atoms.

2.2.3 Mass spectrometry of $[CpRu(CO)_2]_2[\mu\text{-}(CH_2)_n]$ - A comparison with the mass spectral results of $[CpFe(CO)_2]_2[\mu\text{-}(CH_2)_n]$.

A comprehensive study of the mass spectra for the compounds $[CpFe(CO)_2]_2[\mu\text{-}(CH_2)_n]$ (5a-j, n=3-12) was reported by Moss et. al., [19]. Molecular ion peaks of low intensity were observed in the mass spectra for all these complexes. Extensive fragmentation pathways were also proposed on the basis of metastable peaks and high resolution mass spectrometry which facilitated differentiation between losses of CO (27.995 mass units) and C_2H_4 (28.031 mass units) respectively. The mass spectra of compounds of (5) (where n=3-12) exhibited several peaks characteristic of compounds containing the $[(C_5H_5)Fe(CO)_2]$ fragment, [75,76]. These peaks have been assigned to the ions $[(C_5H_5)Fe(CO)_2]^+$ (m/e 177), $[(C_5H_5)Fe(CO)]^+$ (m/e 149), $[(C_5H_5)Fe]^+$ (m/e 121), $[(C_3H_3)Fe]^+$ (m/e 95), $[(C_5H_5)]^+$ (m/e 65) and $[Fe]^+$ (m/e 56), [75,76]. An intense peak at (m/e 186) due to the ferrocinium ion, $[(C_5H_5)_2Fe]^+$ was also observed in all the spectra, [19].

In this study the low resolution mass spectra of the compounds $[CpRu(CO)_2]_2[\mu\text{-}(CH_2)_n]$ (7e-j, n=5-10), and of the mixed-metal compound $[Cp(CO)_2Fe(CH_2)_4Ru(CO)_2Cp]$ (8b) (shown in Figures 2.2-2.8) are reported. Possible fragmentation routes are discussed (Figures 2.10-2.16) in comparison to the fragmentation patterns for the iron analogues. The intensities and probable assignments of the high mass peaks in the spectra of compounds (7e-j) are presented in Table 2.5. However, it must be borne in mind that these fragmentation patterns and assignments are only tentative as

TABLE 2.5 Peak intensities and assignment of common peaks in the mass spectra of $[CpRu(CO)_2]_2[\mu\text{-}(CH_2)_n]$, n=5-10 (7e-j)

Ion[a]	m/e	Relative Peak Intensity (%)[b]					
		7e	7f	7g	7h	7i	7j
$[M]^+$	-	-	5	2	2	2	3
$[M - CO]^+$	-	1	6	6	6	6	11
$[M - CO\text{-}C_nH_{2n}]^+$	418	3	5	5	3	4	6
$[M - 2CO - C_nH_{2n}]^+$	390	6	19	24	23	16	24
$[M - 3CO - C_nH_{2n}]^+$	362	3	6	5	5	4	6
$[M - 4CO - C_nH_{2n}]^+$	334	9	16	7	9	6	25
$[CpRu(CO)_3]^+$	251	22	52	21	23	20	21
$[CpRu(CO)_2]^+$	223	77	98	64	63	61	79
$[CpRu(CO)]^+$	195	52	63	55	55	56	70
$[Cp_2Ru]^+$	232	45	18	16	13	14	15
$[CpRu]^+$	167	100	100	100	100	100	100
$[CpRu(CO)_3(C_nH_{2n})]^+$	-	29	80	37	35	23	25
$[C_3H_3Ru]^+$	141	14	14	13	15	15	14
$[Ru]^+$	102	3	3	4	3	3	5
$[C_nH_{2n}]^+$	-	2	-	2	2	2	10

a M is the molecular ion $Cp_2Ru_2(CO)_4(C_nH_{2n})$

b percentage of the base peak m/e 167 in the low resolution mass spectra.

high resolution mass spectrometry is necessary to distinguish between losses of CO and C_2H_4 respectively (as in the case of the iron complexes). A mass spectrum of $[CpRu(CO)_2]_2$ is included for comparison, (Figure 2.9).

For the iron polymethylene bridged compounds, $[CpFe(CO)_2]_2[\mu\text{-}(CH_2)_n]$ (n=3-12) four decomposition pathways were proposed, [19]. The major fragmentation route involved stepwise loss of CO from the molecular ion to give $[(C_5H_5)_2Fe_2(C_nH_{2n})]^+$, followed by elimination of the hydrocarbon chain to give $[(C_5H_5)_2Fe_2]^+$. The other three routes involved a common initial loss of one CO group from the molecular ion to form $[(C_5H_5)_2Fe_2(CO)_3(C_nH_{2n})]^+$ which could then fragment via three different routes:

i) By elimination of the hydrocarbon bridge to form $[(C_5H_5)_2Fe_2(CO)_3]^+$ followed by successive loss of CO to give $[(C_5H_5)_2Fe_2]^+$ and $[(C_5H_5)_2Fe]^+$ - the latter being the most abundant ion in the mass spectra of all the compounds.

ii) By elimination of $[(C_5H_5)Fe(CO)_2]$ in a single step resulting in $[(C_5H_5)Fe(CO)(C_nH_{2n})]^+$. This could subsequently lose CO to form $[(C_5H_5)Fe(C_nH_{2n})]^+$ and break down by elimination of the hydrocarbon chain as H_2, C_2H_4 and C_3H_6 to give $[(C_5H_5)Fe]^+$.

iii) By elimination of C_5H_6 to give an alkenyl species $[(C_5H_5)Fe_2(CO)_3(C_nH_{2n-1})]^+$ which fragments via stepwise loss of CO to $[(C_5H_5)Fe_2(C_nH_{2n-1})]^+$. The latter ion then decomposes by loss of H_2 and hydrocarbon fragments to the $[(C_5H_5)Fe_2]^+$ ion, [19].

As in the case of the iron compounds, the ruthenium polymethylene bridged compounds $[CpRu(CO)_2]_2[\mu\text{-}(CH_2)_n]$, (n=6-10) also exhibit a molecular ion, M^+, as well as $(M^+{+}1)$ and $(M^+{+}2)$ ions, all of low intensity in their mass spectra. For the compound where n=5, the molecular ion was not observed probably because of low intensity. However, a peak at m/e 488 corresponds to M^+-CO indicating that a CO ligand is dissociated very easily from the compound under the existing conditions.

A study of these low resolution mass spectra for $[CpRu(CO)_2]_2[\mu\text{-}(CH_2)_n]$ reveals only two important fragmentation pathways, although two other minor routes are also possible. Unlike their iron analogues, stepwise loss of CO from the molecular ion, $[Cp_2Ru_2(CO)_4(CH_2)_n]^+$, to form $[(C_5H_5)_2Ru_2(C_nH_{2n})]^+$ is not observed. Instead, the major decomposition route (Route A in Figures 2.10-2.16) appears to be the initial loss of one CO ligand to give $[(C_5H_5)_2Ru_2(CO)_3(C_nH_{2n})]^+$ followed by the elimination of $[(C_5H_5)Ru(CO)_2]$ in a single step to form $[(C_5H_5)Ru(CO)(C_nH_{2n})]^+$. This ion fragments further by loss of CO / H_2 followed by elimination of the alkyl chain as C_2H_4 and H_2 units. This fragmentation pathway gives rise to the most abundant

ion $[(C_5H_5)Ru]^+$ (m/e 167), which decomposes to $[(C_3H_3)Ru]^+$ (m/e 141) and finally $[Ru]^+$ (m/e 102). This decomposition route has also been observed for the iron complexes [19] and has already been discussed above.

In a second, less significant pathway, loss of CO from the molecular ion, followed by elimination of the whole alkyl chain, gives a low intensity peak at m/e 418 for $[(C_5H_5)_2Ru_2(CO)_3]^+$. This ion can decompose via one of two competing routes:

i) By successive loss of CO to produce the ions $[(C_5H_5)_2Ru_2(CO)_2]^+$ (m/e 390), $[(C_5H_5)_2Ru_2(CO)]^+$ (m/e 362) and $[(C_5H_5)_2Ru_2]^+$ (m/e 334). $[(C_5H_5)_2Ru_2]^+$ can then fragment further to give $[(C_5H_5)_2Ru]^+$ (m/e 232), of low intensity, and the most abundant ion $[(C_5H_5)Ru]^+$ (m/e 167). The very low intensity of the peaks arising from this fragmentation pattern suggests it is a very minor decomposition route. (Route C, Figures 2.10-2.16).

ii) Loss of $[(C_5H_5)Ru]^+$ from $[(C_5H_5)_2Ru_2(CO)_3]^+$ (m/e 418) giving rise to $[(C_5H_5)Ru(CO)_3]^+$ (m/e 251), followed by successive loss of the CO groups to give $[(C_5H_5)Ru(CO)_2]^+$ (m/e 223), $[(C_5H_5)Ru(CO)]^+$ (m/e 195) and $[(C_5H_5)Ru]^+$ (m/e 167) respectively. The higher relative intensity of these peaks in comparison to those for the route described in (i) above, implies that this is the more favourable pathway for the fragmentation of $[(C_5H_5)_2Ru_2(CO)_3]^+$. (Route B, Figures 2.10-2.16).

In addition to the three fragmentation routes already described, the compounds (7g-j, n=7-10) show loss of a second CO group from $[Cp_2Ru_2(CO)_3(C_nH_{2n})]^+$ giving rise to a peak of very low intensity for $[(C_5H_5)_2Ru_2(CO)_2(C_nH_{2n})]^+$. The latter ion subsequently loses the alkyl chain in one step to give the ion $[(C_5H_5)_2Ru_2(CO)_2]^+$ (m/e 390). However, this would appear to be the least significant of all the fragmentation pathways. (Route D, Figures 2.10-2.16).

In contrast to the iron complexes, no elimination of C_5H_6 to form an alkenyl species of type $[(C_5H_5)Ru_2(CO)_3(C_nH_{2n-1})]^+$ was observed.

It is interesting to note that while $[CpRu]^+$ (m/e 167) is the most abundant ion in the mass spectra of $[CpRu(CO)_2]_2[\mu\text{-}(CH_2)_n]$, the most abundant ion in the spectrum of $[CpRu(CO)_2]_2$ is $[Cp_2Ru_2]^+$ (m/e 334). In the case of $[CpRu(CO)_2]_2$, the molecular ion (m/e 446) fragments by stepwise loss of four CO groups producing the ions at (m/e 418) $[Cp_2Ru_2(CO)_3]^+$, (m/e 390) $[Cp_2Ru_2(CO)_2]^+$, (m/e 362) $[Cp_2Ru_2(CO)]^+$ and (m/e 334) $[Cp_2Ru_2]^+$. A second competitive fragmentation pathway appears to involve initial elimination of CpRu from the molecular ion to give $[CpRu(CO)_4]^+$ (m/e 279), which also fragments by sequential loss of CO giving rise to $[CpRu(CO)_3]^+$ (m/e 251), $[CpRu(CO)_2]^+$ (m/e 223), $[CpRu(CO)]^+$ (m/e 195) and $[CpRu]^+$ (m/e 167). In addition, a peak of low intensity is observed at (m/e 232) and is assigned to $[Cp_2Ru]^+$ on the basis of the analogous peak at (m/e 186) for $[Cp_2Fe]^+$ in the mass spectrum of $[CpFe(CO)_2]_2$, [75,76].

A study of the mass spectrum (Figure 2.8) of the heterodinuclear alkanediyl complex $[Cp(CO)_2Fe(CH_2)_4Ru(CO)_2Cp]$ (8b) shows three major fragmentation pathways (Figure 2.16, Routes A-C) and a fourth less important route (Figure 2.16, Route D). Three of these fragmentation routes (Routes A,C and D) give rise to the most abundant ion $[CpFe]^+$ at m/e 121.

The major fragmentation route (Route A) appears to involve stepwise loss of CO from the molecular ion (M^+=456), followed by loss of the alkyl chain as C_2H_4 units to give $[Cp_2FeRu]^+$, which can fragment to $[Cp_2Fe]^+$ (m/e 186) or $[Cp_2Ru]^+$ (m/e 232). However, high resolution mass spectrometry is necessary to distinguish between these losses of CO and C_2H_4. The loss of (C_5H_6) (m/e 66) (Route B) from $[Cp_2FeRu(CO)(C_4H_8)]^+$ (m/e 372) to give an ion at m/e 306 corresponding to $[CpFeRu(CO)(C_4H_7)]^+$ (Route B), followed by the loss of CO, C_2H_3 and C_2H_4 to give the ions $[CpFeRu(C_4H_7)]^+$ (m/e 278), $[CpFeRu(C_2H_4)]^+$ (m/e 251) and $[Cp_2FeRu]^+$ (m/e 278) supports the initial loss of three CO ligands.

However, a third major competitive fragmentation pathway (Route C) could also account for these peaks at m/e 306, 278, 251 and 223. Initial elimination of [CpFe(CO)H] as a whole from the molecular ion could give rise to the ion $[CpRu(CO)_3(C_4H_7)]^+$ (m/e 306). Successive loss of CO, C_2H_3, C_2H_4 and CO gives rise to the ions $[CpRu(CO)_2(C_4H_7)]^+$ (m/e 278), $[CpRu(CO)_2(C_2H_4)]^+$ (m/e 251), $[CpRu(CO)_2]^+$ (m/e 223) and $[CpRu(CO)]^+$ (m/e 195) respectively.

In a minor fragmentation path (Route D), loss of $[CpRu(CO)_2]$ from $[Cp_2FeRu(CO)_3(C_4H_8)]^+$ (m/e 428) produces the low intensity ion $[CpFe(CO)(C_4H_8)]^+$ (m/e 205). Elimination of CO, and two C_2H_4 units gives rise to the ions at m/e 177 ($[CpFe(CO)(C_2H_4)]^+$ or $[CpFe(C_4H_8)]^+$), m/e 149 ($[CpFe(CO)]^+$ or $[CpFe(C_2H_4)]^+$) and m/e 121 $[CpFe]^+$.

Thus, the fragmentation pathways for the heterodinuclear complex $[Cp(CO)_2Fe(CH_2)_4Ru(CO)_2Cp]$ (8b) show similarities to those of both the di-iron (5) and the diruthenium (7) alkanediyls. However, the fact that $[CpFe]^+$ (m/e 121) is the most abundant peak in the mass spectrum of (8b) suggests that the decomposition of $[Cp(CO)_2Fe(CH_2)_4Ru(CO)_2Cp]$ more closely resembles that of $[CpFe(CO)_2]_2[\mu\text{-}(CH_2)_n]$ than that of $[CpRu(CO)_2]_2[\mu\text{-}(CH_2)_n]$. The elimination of a C_5H_6 fragment in Route B to form an alkenyl species - observed only in the mass spectra of $[CpFe(CO)_2]_2[\mu\text{-}(CH_2)_n]$ - supports this assumption.

In order to establish these fragmentation routes conclusively, high resolution mass spectrometry is essential to differentiate between losses of CO and C_2H_4.

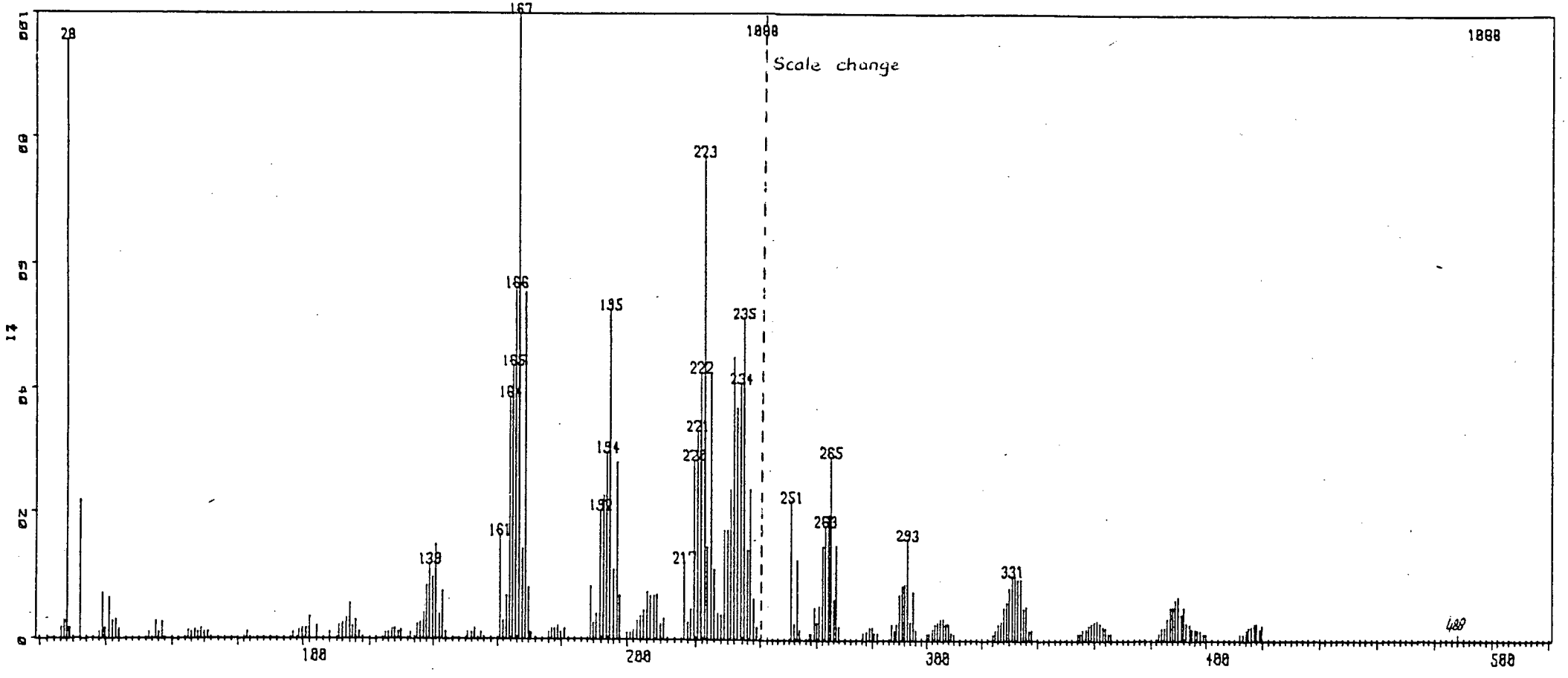

FIGURE 2.2 Mass spectrum of $[CpRu(CO)_2]_2[\mu\text{-}(CH_2)_5]$

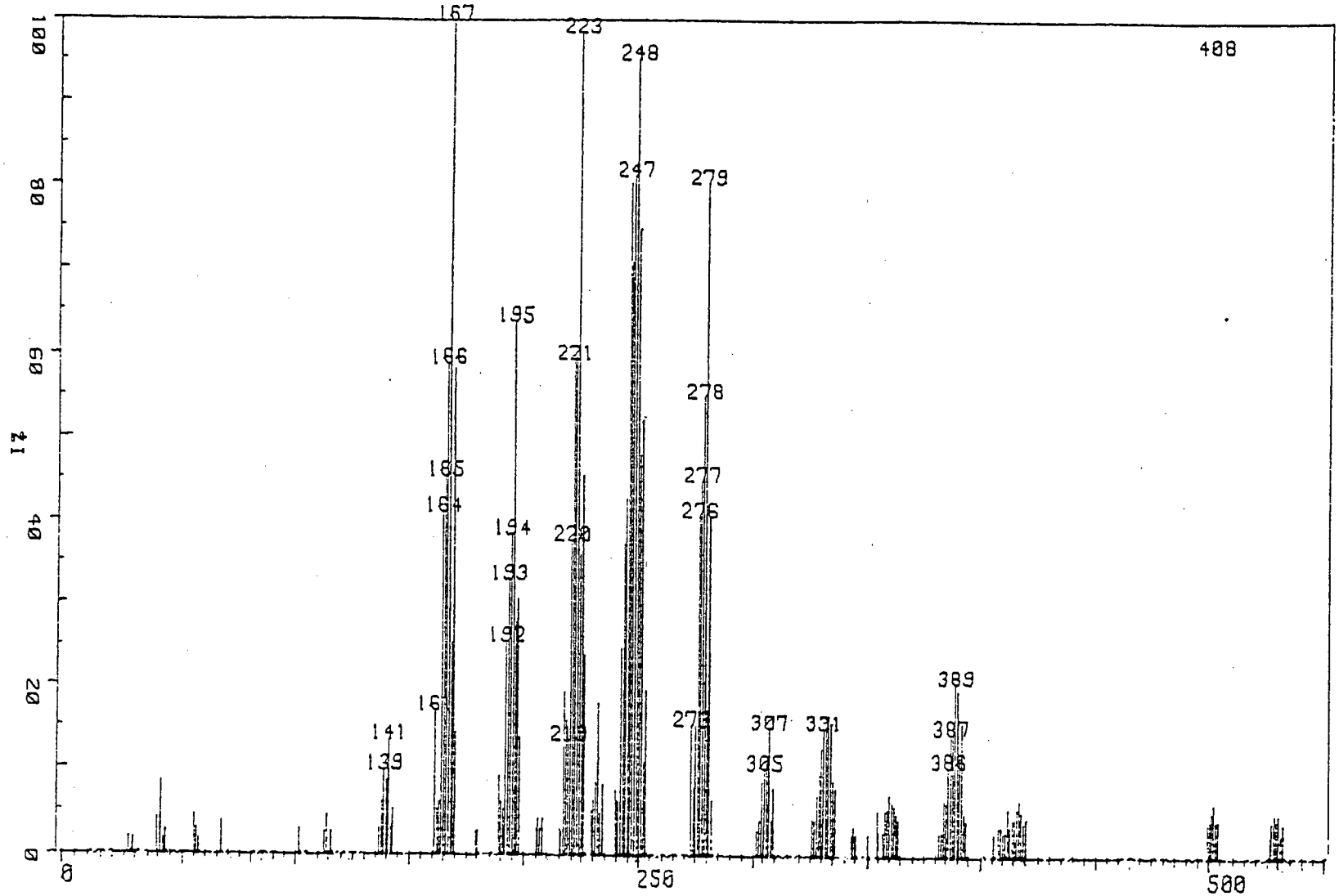

FIGURE 2.3 Mass spectrum of $[CpRu(CO)_2]_2[\mu\text{-}(CH_2)_6]$

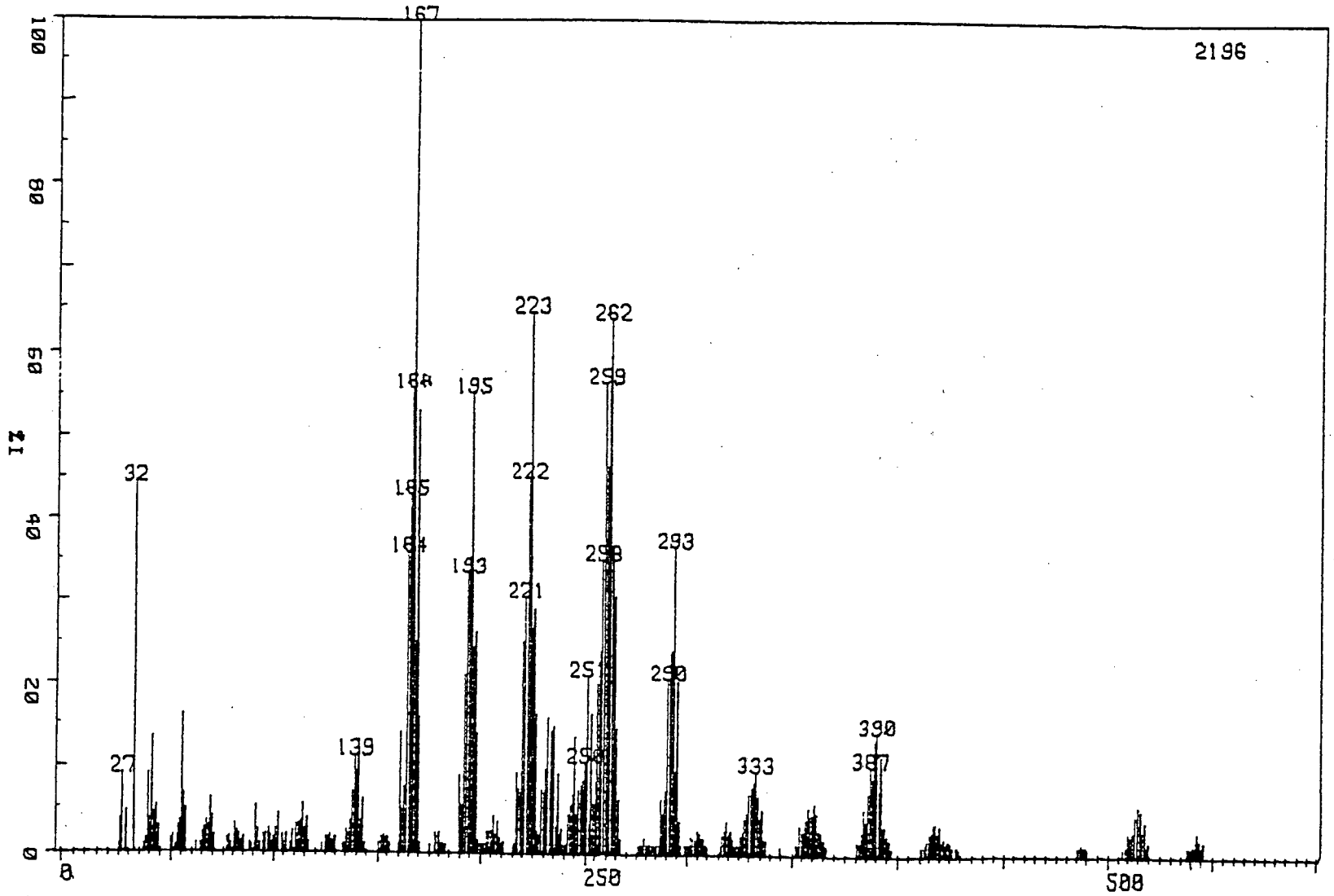

FIGURE 2.4 Mass spectrum of $[CpRu(CO)_2]_2[\mu\text{-}(CH_2)_7]$

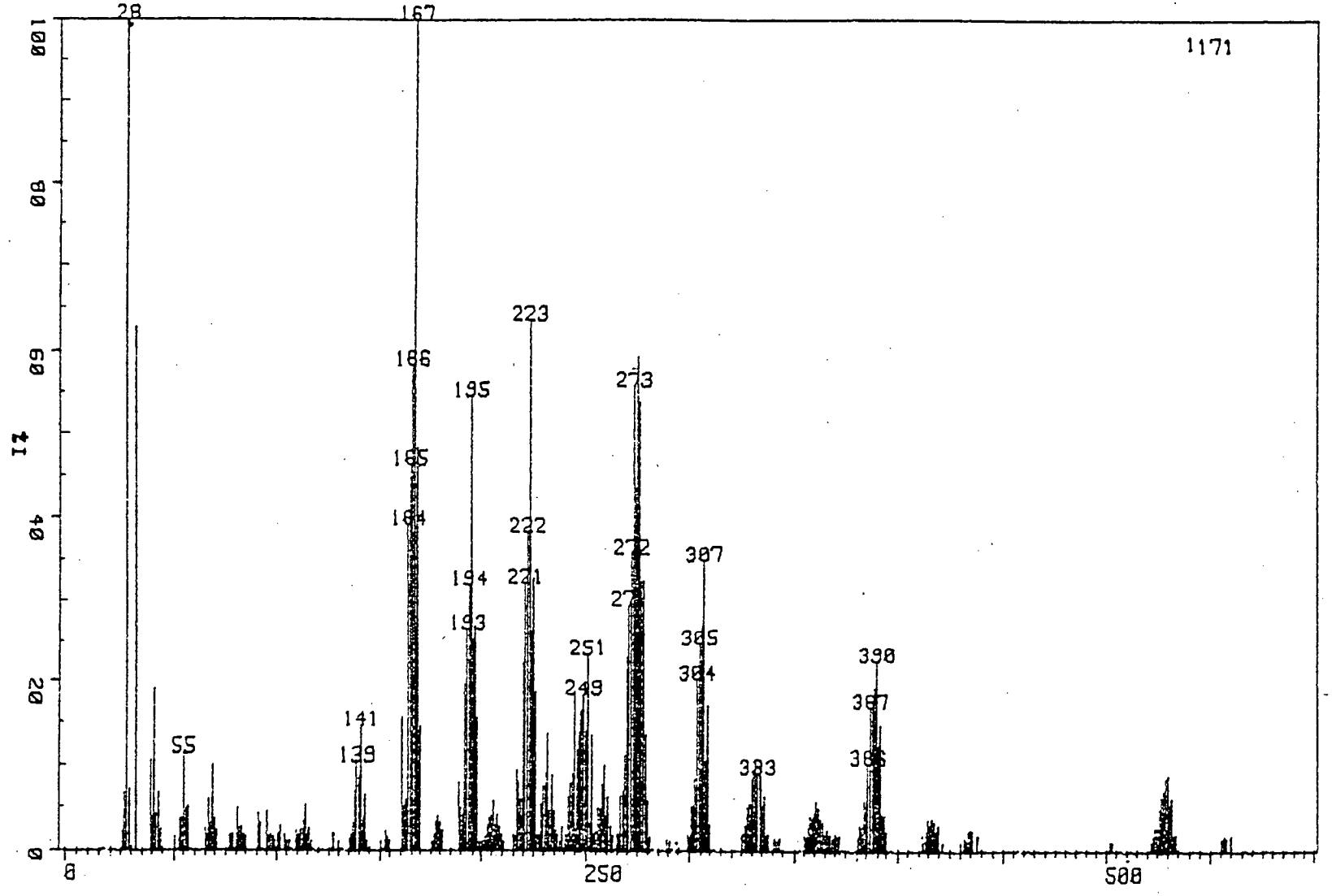

FIGURE 2.5 Mass spectrum of $[CpRu(CO)_2]_2[\mu\text{-}(CH_2)_8]$

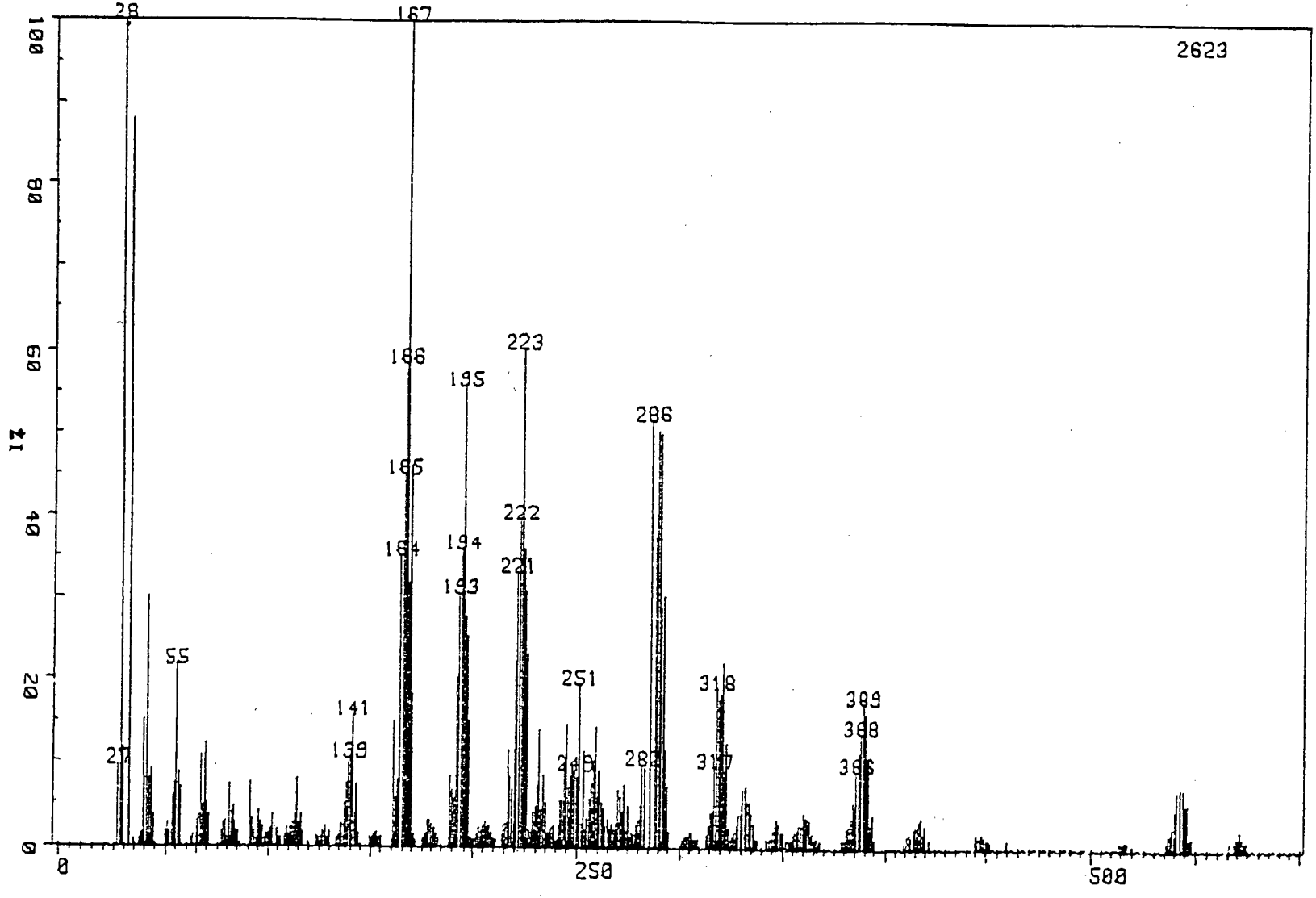

FIGURE 2.6 Mass spectrum of $[CpRu(CO)_2]_2[\mu\text{-}(CH_2)_9]$

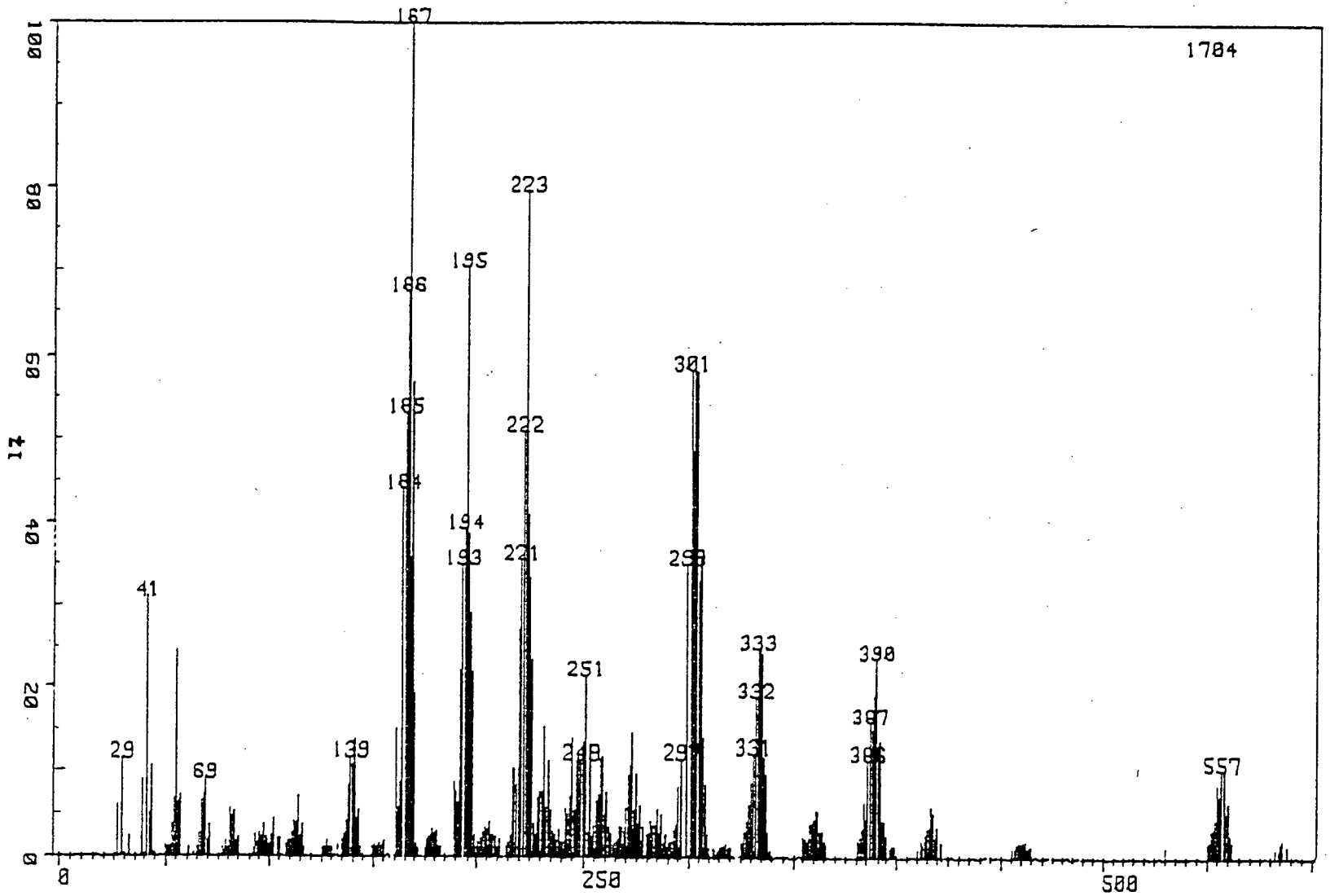

FIGURE 2.7 Mass spectrum of $[CpRu(CO)_2]_2[\mu\text{-}(CH_2)_{10}]$

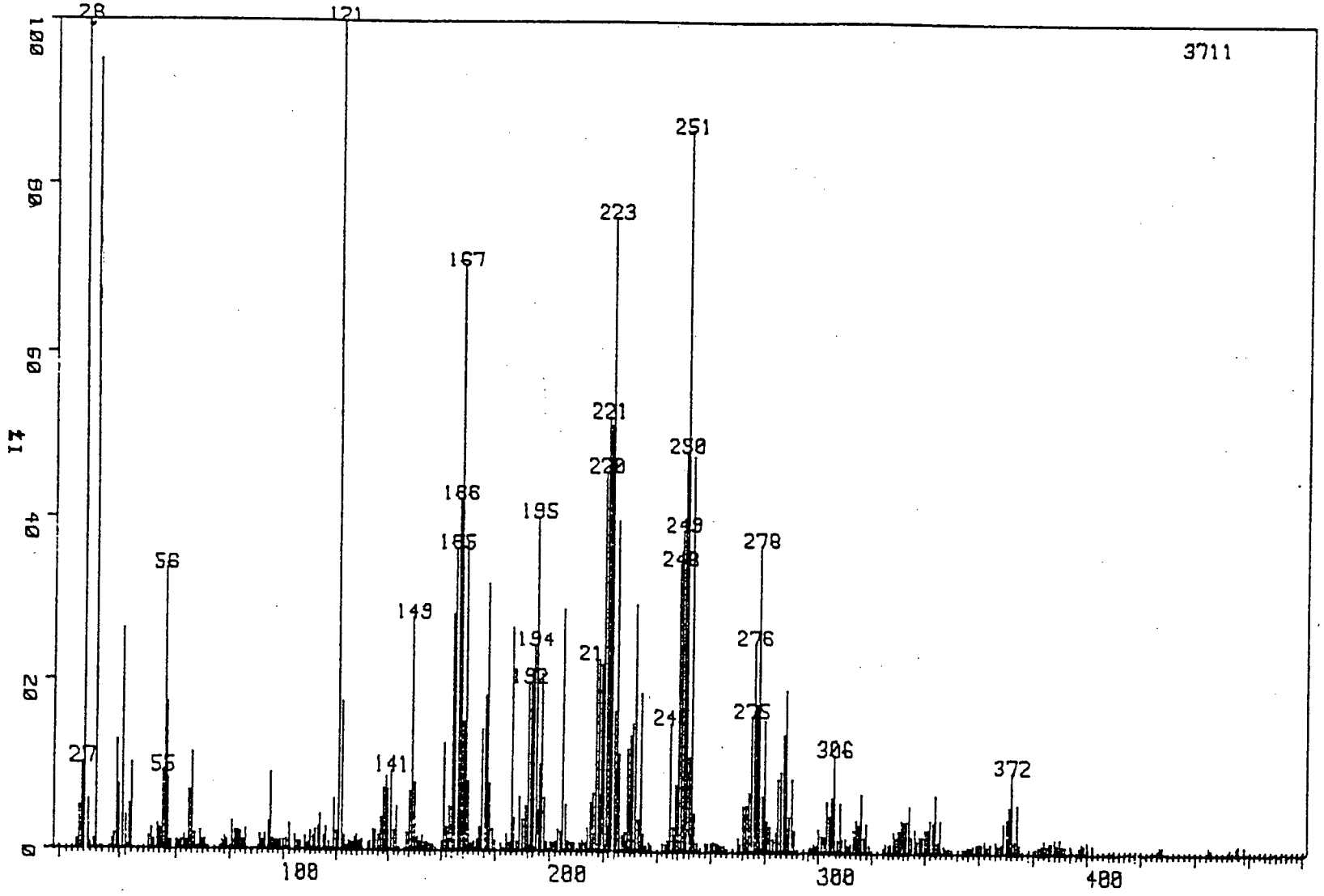

FIGURE 2.8 Mass spectrum of $[Cp(CO)_2Fe(CH_2)_4Ru(CO)_2Cp]$

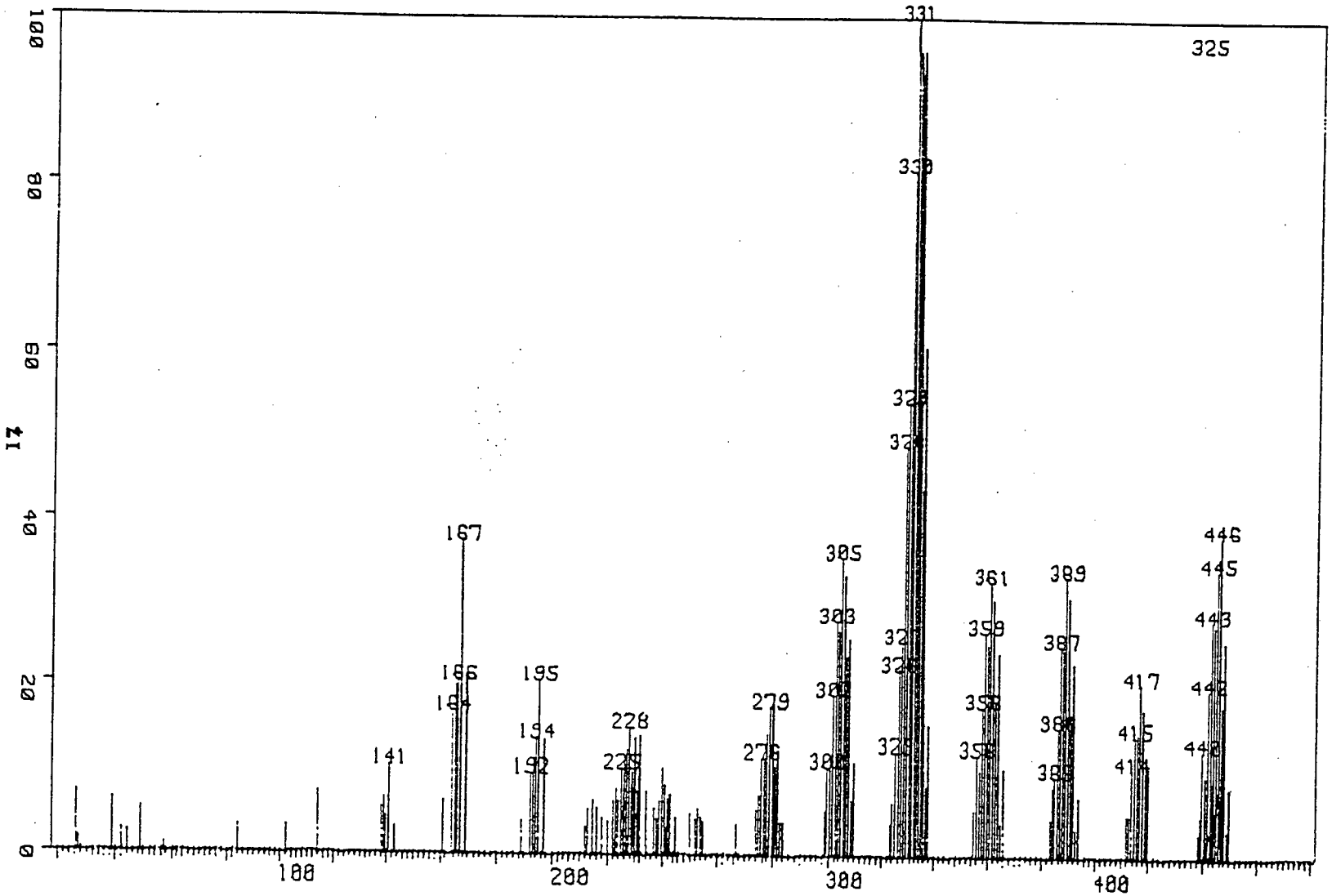

FIGURE 2.9 Mass spectrum of $[CpRu(CO)_2]_2$

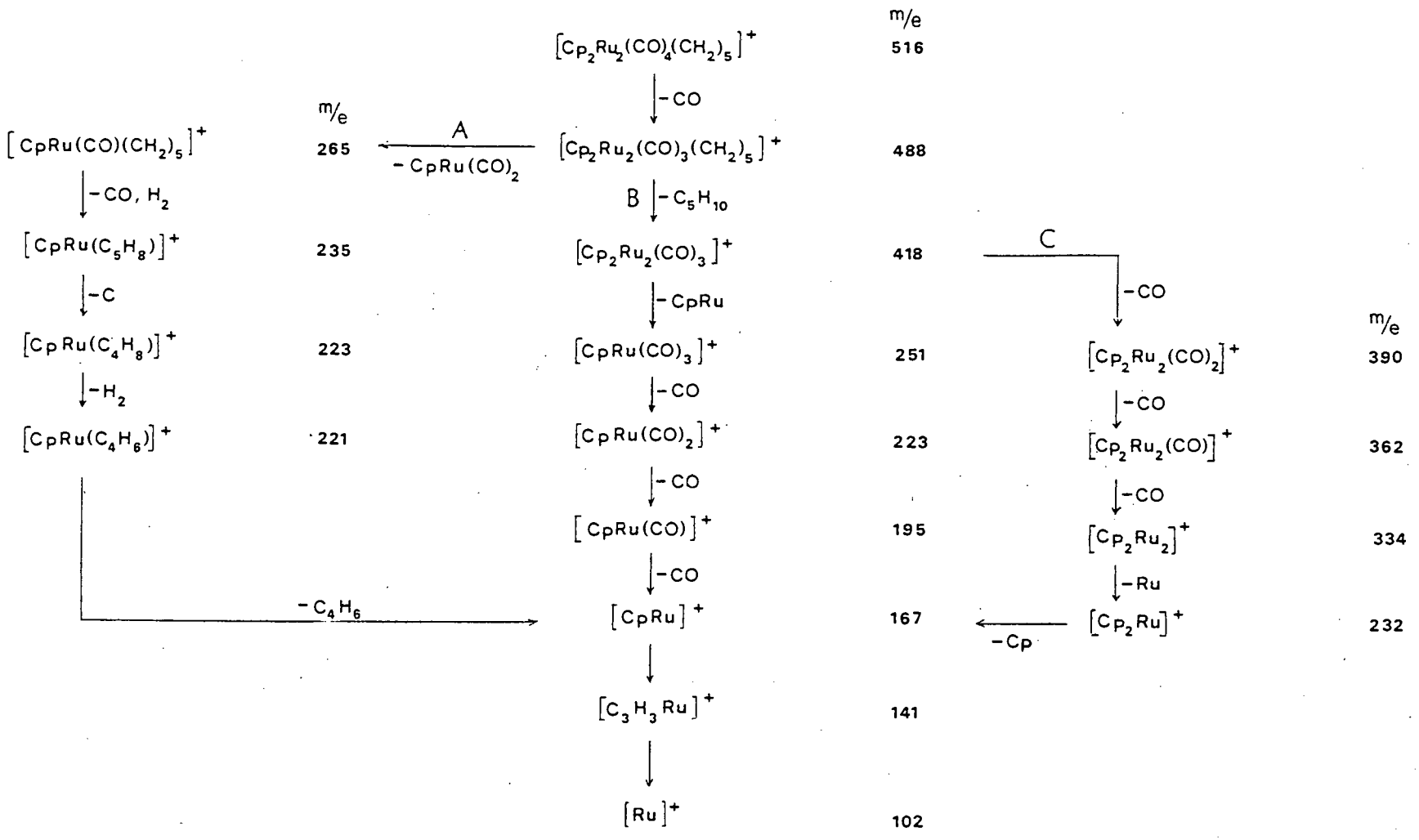

FIGURE 2.10 Fragmentation scheme for $[CpRu(CO)_2]_2[\mu\text{-}(CH_2)_5]$

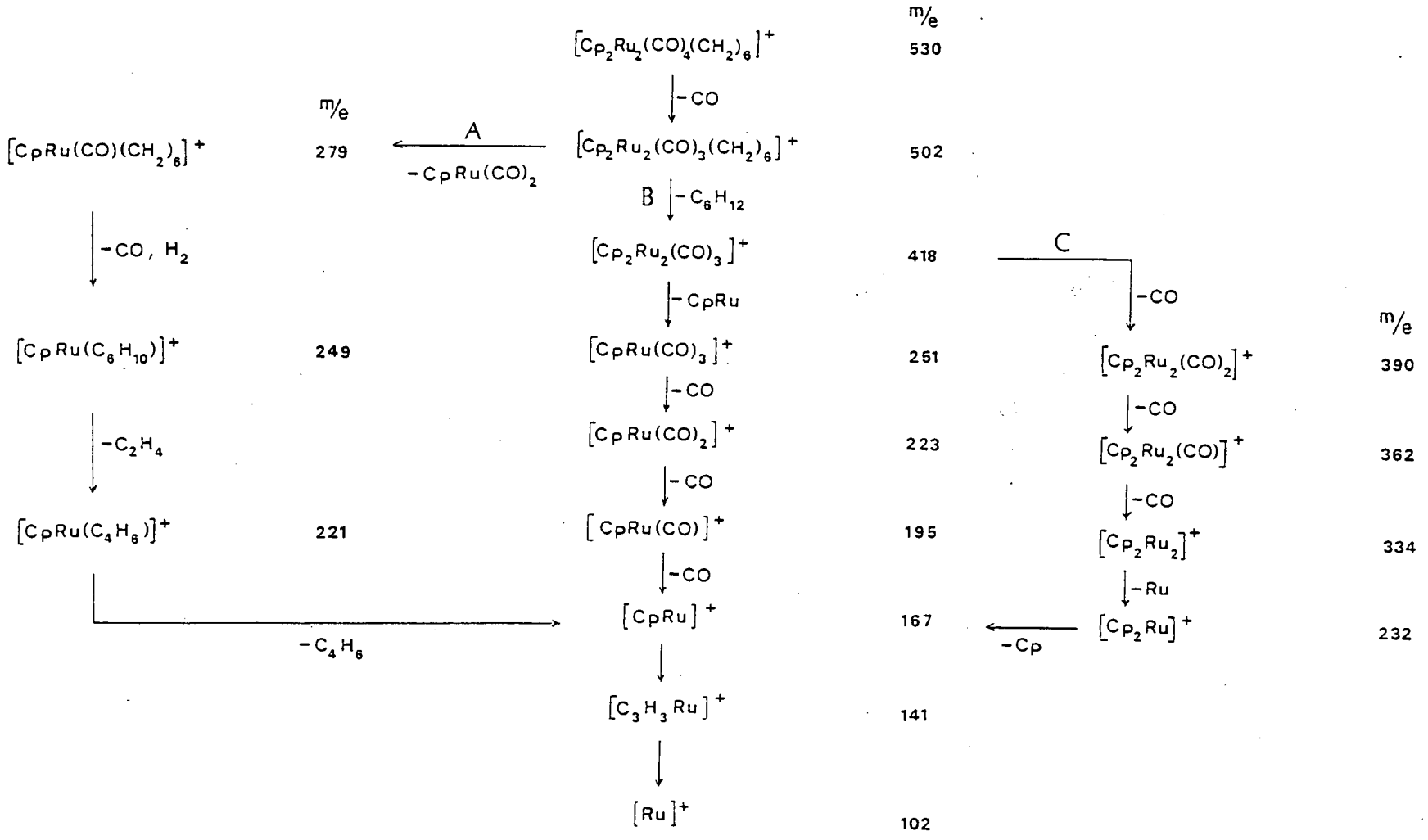

FIGURE 2.11 Fragmentation scheme for $[CpRu(CO)_2]_2[\mu\text{-}(CH_2)_6]$

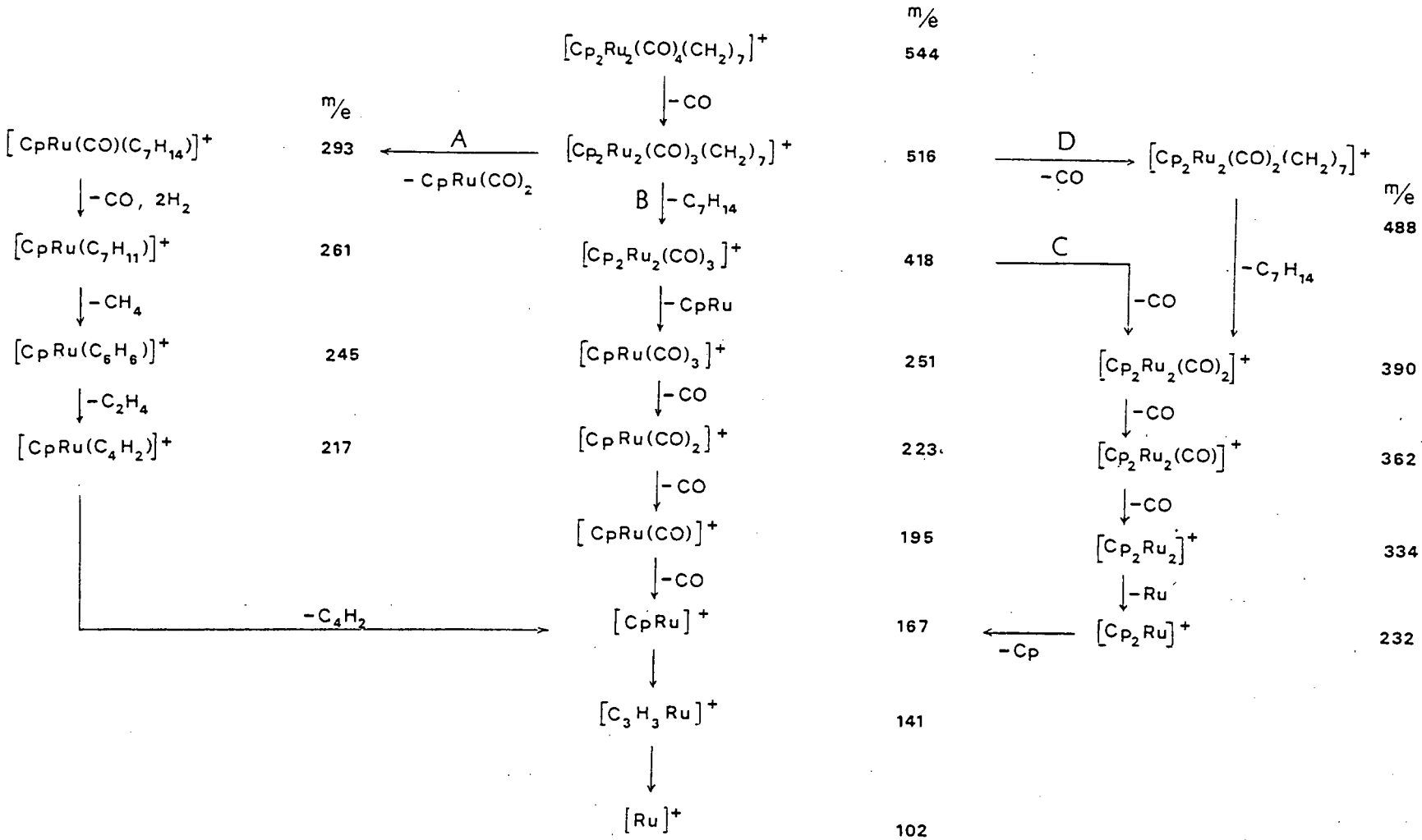

FIGURE 2.12 Fragmentation scheme for $[CpRu(CO)_2]_2[\mu\text{-}(CH_2)_7]$

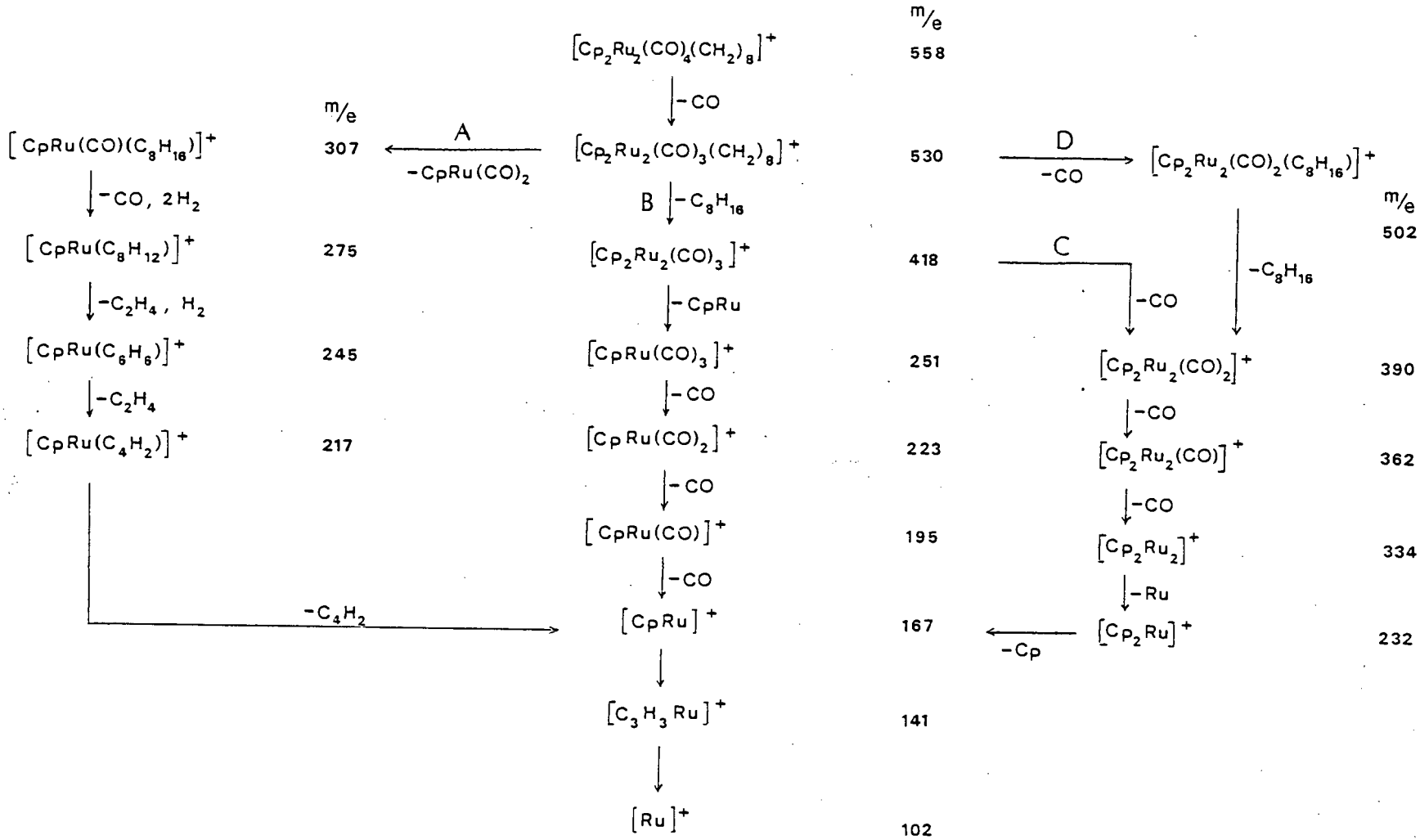

FIGURE 2.13 Fragmentation scheme for $[CpRu(CO)_2]_2[\mu\text{-}(CH_2)_8]$

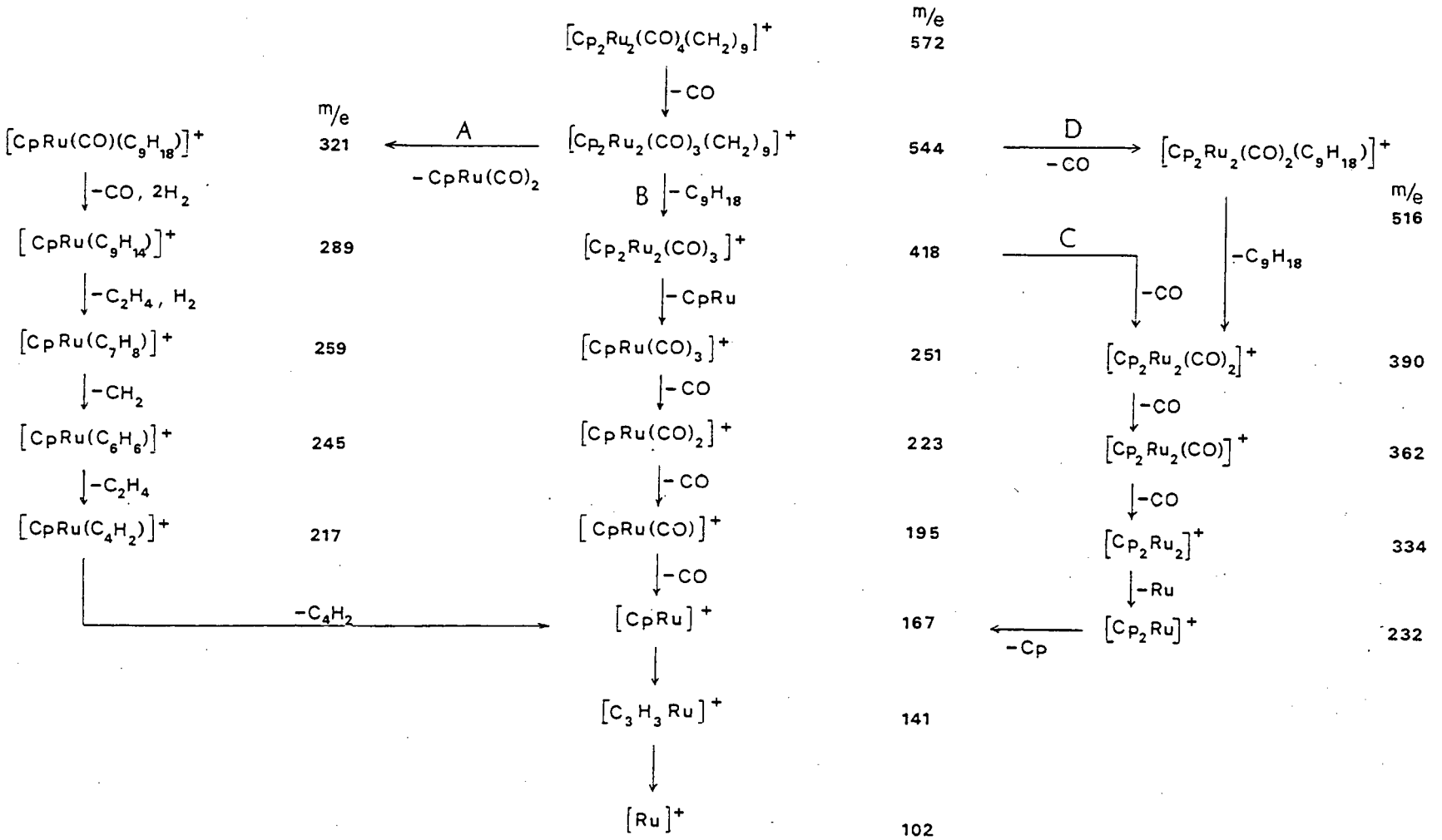

FIGURE 2.14 Fragmentation scheme for $[CpRu(CO)_2]_2[\mu\text{-}(CH_2)_9]$

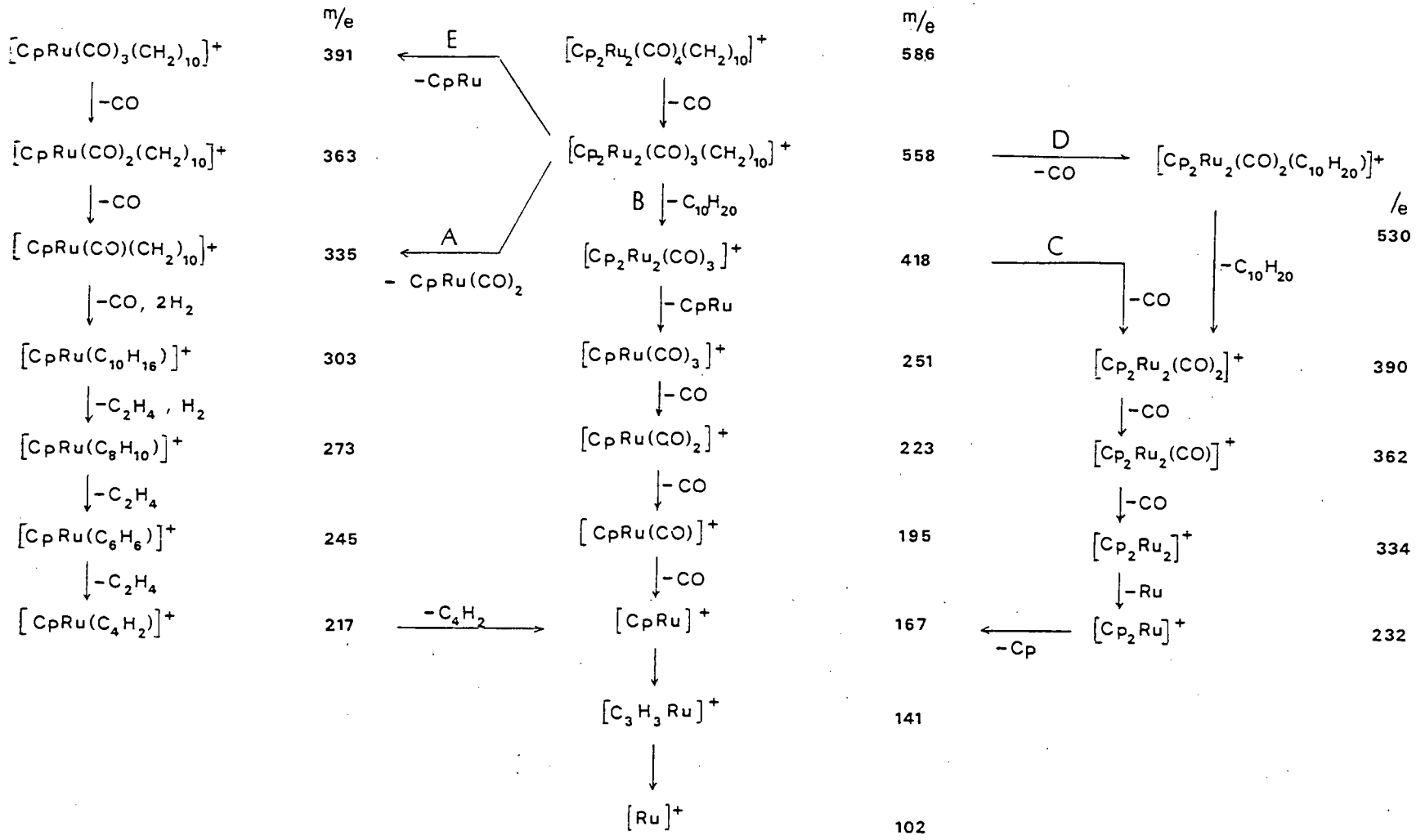

FIGURE 2.15 Fragmentation scheme for $[CpRu(CO)_2]_2[\mu\text{-}(CH_2)_{10}]$

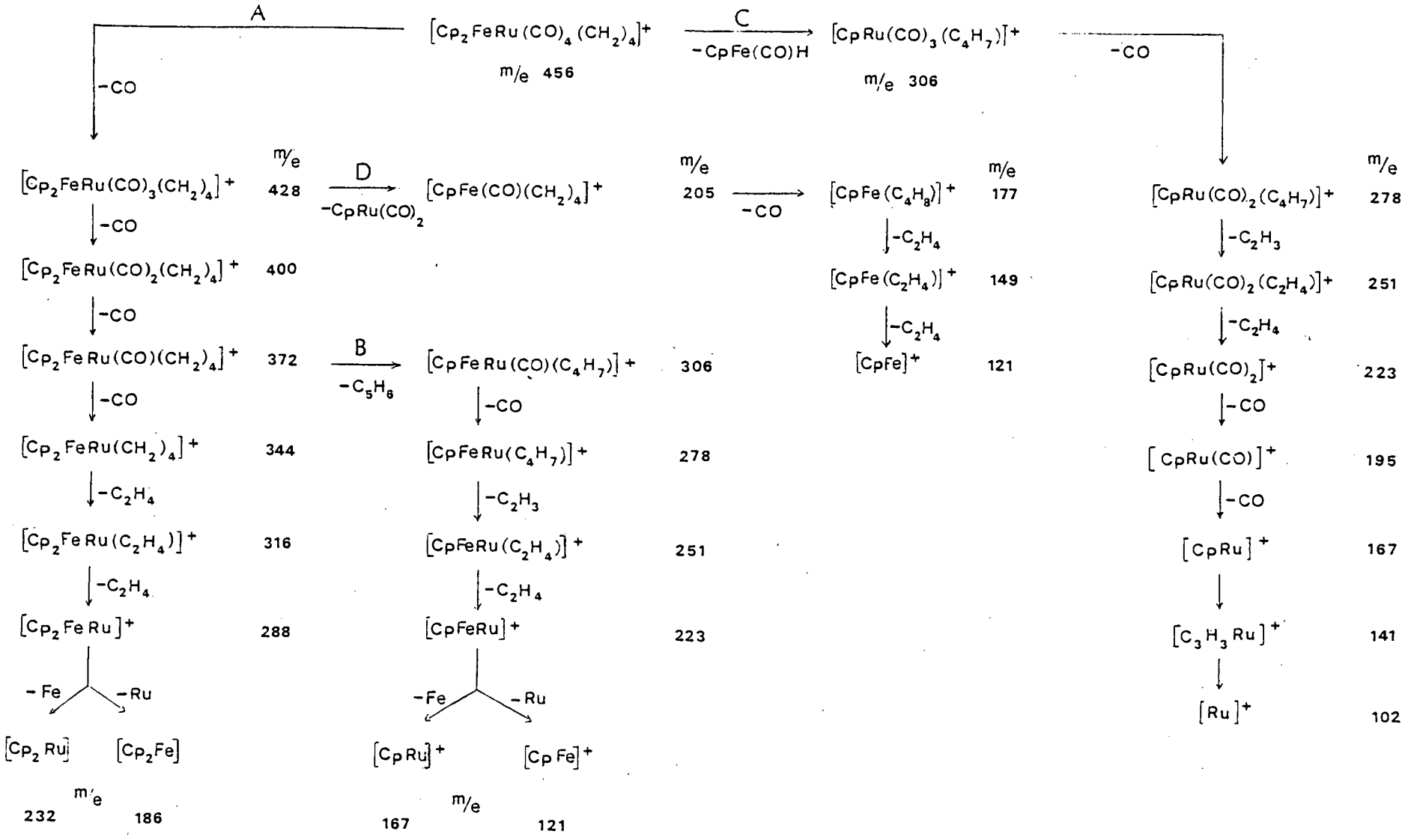

FIGURE 2.16 Fragmentation scheme for $[Cp(CO)_2Fe(CH_2)_4Ru(CO)_2Cp]$

2.2.4 Thermal Analysis of $[CpRu(CO)_2]_2[\mu-(CH_2)_n]$ (n=4,5) by Differential Scanning Calorimetry (DSC).

Thermal analysis of the bridged compounds, $[CpRu(CO)_2]_2[\mu-(CH_2)_n]$ (where n=4 and 5) was carried out using Differential Scanning Calorimetry. In this technique, a sample and reference are heated simultaneously at the same rate and the temperatures of the two maintained the same by adjustment of the heat input to the sample. A signal, proportional to the difference between the heat input to the sample and that to the reference, dH/dt, is fed into a recorder which plots the differential heat input against temperature, T, or time, t. Whenever a material undergoes any change in physical state, such as melting or transition from one crystalline form to another, heat is either absorbed or released, thus producing a peak in the DSC thermogram.

Calibration of a DSC instrument is usually carried out using high purity metals (eg. indium) with accurately known enthalpies of fusion, H_c , as the calibration standards. A DSC trace of a known mass of the calibrant, m_c , is recorded and the area of the melting peak, A_c , used to calculate a calibration constant, k. (Equation 7).

$$k = \frac{\Delta H_c \times m_c}{A_s} \qquad 7$$

The value of k is then used to find enthalpy values, H_s , for other samples from the relationship shown in Equation 8, where M is the molar mass of the sample, A_s is the area of the sample peak recorded under the same conditions as the calibrant, and m_s is the known mass of the sample.

$$\Delta H = k \frac{M \times A_s}{m_s} \qquad 8$$

Samples of $[CpRu(CO)_2]_2[\mu\text{-}(CH_2)_n]$ (n=4 and 5) were thermally decomposed under a hydrogen atmosphere in open pans and in pans sealed hermetically in air. The DSC traces were recorded over the range 50°C to 300°/350°C. All the traces showed a sharp endothermic peak , T_1, corresponding to the melting point range of the particular sample. (Tables 2.6 and 2.7)

The samples heated in hermetically sealed pans in air (Table 2.7) revealed a broad exothermic peak, T_2, with T_{max} at 171°C (n=4) and 156°C (n=5) respectively. This is believed to be due to decomposition of the compounds of $[CpRu(CO)_2]_2[\mu\text{-}(CH_2)_n]$ by loss of the alkyl chain and / or CO ligands, as was observed for the iron complexes $[CpFe(CO)_2]_2[\mu\text{-}(CH_2)_n]$. (Section 4.2.2) The weak endotherms at 248°C (n=4) and 284°C (n=5) are probably due to slight impurities in the samples.

The DSC traces for the compounds of $[CpRu(CO)_2]_2[\mu\text{-}(CH_2)_n]$ decomposed in open pans under hydrogen (Table 2.6) revealed significant differences to those for the di-iron complexes $[CpFe(CO)_2]_2[\mu\text{-}(CH_2)_n]$ decomposed under hydrogen. (Table 4.2)

In addition to the melting endotherms, T_1, compounds (7d, n=4) and (7e, n=5) produced broad endotherms, T_2, when heated under hydrogen. These endotherms appeared to be comprised of ca. four overlapping endotherms with T_{max} at 180°C and 171°C for n=4 and n=5 respectively. This would suggest that this process involves the four CO ligands and could possibly be explained by successive dissociation of CO from $[CpRu(CO)_2]_2[\mu\text{-}(CH_2)_n]$. This could be established by Thermal Gravimetric Analysis of the samples. These results are in contrast to the thermal behaviour exhibited by the di-iron analogues, $[CpFe(CO)_2]_2[\mu\text{-}(CH_2)_n]$, where several sharp exothermic peaks were observed in the DSC traces for the decomposition under H_2, (Table 4.2). These exotherms were explained by the reduction of a cluster species formed during decomposition of $[CpFe(CO)_2]_2[\mu\text{-}(CH_2)_n]$, (Section 4.2.2).

TABLE 2.6 DSC results for $[CpRu(CO)_2]_2[\mu\text{-}(CH_2)_n]$, n=4 and 5 decomposed in open pans under hydrogen

COMPOUND No.	n	Melting Range (°C)	T_1 (endo) (°C) Tonset[c]	Tmax[d]	T_2 (endo) (°C) Tonset	Tmax
7d	4	131 - 132[a]	138	139	176	180[e]
7e	5	77 - 84[b]	85	86	162	171[e]

a Reference [25]

b This work

c Temperature corresponding to onset of peak

d Temperature corresponding to peak maximum

e Broad peak comprised of four overlapping endotherms

TABLE 2.7 DSC results for $[CpRu(CO)_2]_2[\mu\text{-}(CH_2)_n]$, n=4 and 5 decomposed in hermetically sealed pans in air

COMPOUND No	n	Melting Range °C	T_1 (endo) (°C) Tonset[c]	Tmax[d]	T_2 (exo) (°C) Tonset	Tmax	T_3 (endo) (°C) Tonset	Tmax
7d	4	131 - 132[a]	136	138	161	177	246	248[e]
7e	5	77 - 84[b]	85	86	133	156	283	284[e]

a Reference [25]

b This work

c Temperature corresponding to onset of peak

d Temperature corresponding to peak maximum

e Very weak, sharp endotherm

2.2.5 X-Ray structural analysis of the compound $[CpRu(CO)_2]_2[\mu-(CH_2)_5]$.

To date relatively few crystal structures of polymethylene bridged complexes without a metal-metal bond have been determined. Amongst those that have, the crystal structures of the compounds $[CpFe(CO)_2]_2[\mu-(CH_2)_n]$ (where n=3,4) [20] and the methylene bridged compound $[CpRu(CO)_2]_2[\mu-(CH_2)]$ [27] are of particular relevance to this study.

In the case of the di-iron compounds, $[CpFe(CO)_2]_2[\mu-(CH_2)_n]$ (n=3,4), the crystal structures confirmed that each iron atom is σ-bonded to one end of an alkyl chain (see Figure 2.17). No unusual bond lengths or angles, which were found to be similar in the two complexes, were observed. The cyclopentadienyl ligands were located on opposite sides of the Fe-Fe axis. This trans arrangement of the Cp rings is probably the energetically more favourable conformation resulting from minimal steric interaction of the bulky ligands. The carbon-carbon bond distances (1.55 Å) within the chain were consistent with C-C single bonds.

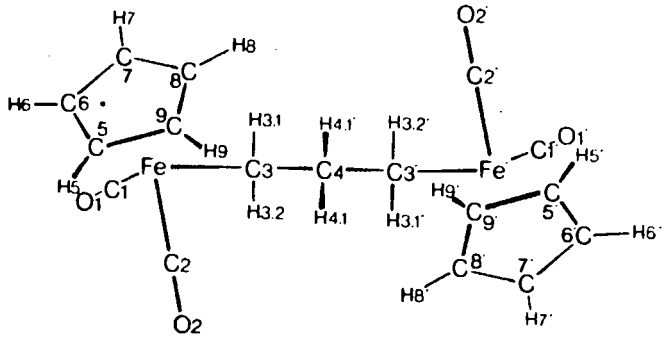

a

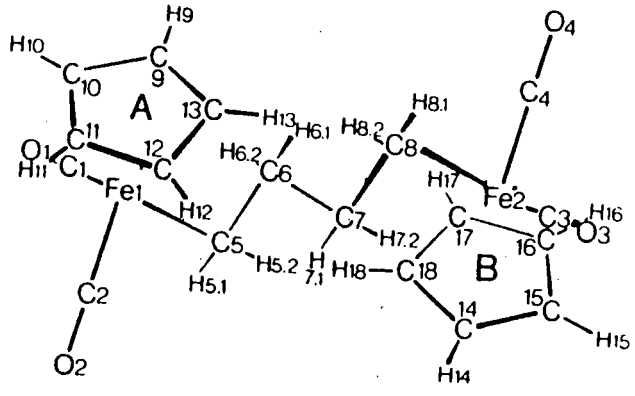

b

FIGURE 2.17 X-ray crystal structure of $[CpFe(CO)_2]_2[\mu\text{-}(CH_2)_n]$:
(a) n=3 (b) n=4

The crystal structures of $[CpFe(CO)_2]_2[\mu\text{-}(CH_2)_n]$ also revealed that one carbon of the cyclopentadienyl ring is in fairly close contact with the β-methylene group of the alkyl chain. The slightly larger than usual $Fe\text{-}C_\alpha\text{-}C_\beta$ angles of 113° and 114° (n=4) and 115° (n=3) (cf. the $C_\alpha\text{-}C_\beta\text{-}C_\gamma$ angle of 111°) was thought to be a direct result of an interaction between the $\beta\text{-}CH_2$ and the Cp ring carbon, [20].

The alternation of melting point between compounds with n_{even} and n_{odd} in the $-(CH_2)_n-$ chain was explained in terms of the difference in packing density of the complexes of $[CpFe(CO)_2]_2[\mu\text{-}(CH_2)n]$ (5) with varying chain length, n. It was thought that the molecules of the butanediyl compound (5d, n=4), with symmetry 1, are closer packed in the crystal than those of the propanediyl complex (5c, n=3) with a 2-fold centrosymmetric structure, [20].

The crystal data obtained for the di-iron complexes proved conclusively that the α and β methylene groups are non-equivalent, as was apparent from the two methylene resonances observed in the ^1H NMR spectra (recorded at 270 MHz) of (5c, n=3) and (5d, n=4). The ^{13}C NMR spectra showed two different environments for the α and β carbon atoms confirming that at ambient temperature and on the NMR time scale, no scrambling of the α and β $-CH_2-$ groups is observed, [20].

The crystal structure of the related cationic complex $\{[CpFe(CO)_2]_2[\mu\text{-}(C_3H_5)]\}^+PF_6^-$ has also been determined, [77]. From these data, there is evidence to suggest that the positive charge

is located on the β-carbon and is stabilised by weak Fe-CH interactions. The Fe-CH_2-CH bond angles of 91° and 98°, as well as the Fe-CH separations of 2.59 Å and 2.72 Å, imply that the cation is almost symmetric.

In 1983, Lin et.al. [27] reported that they had isolated the first dinuclear μ-methylene complex $[CpRu(CO)_2]_2[\mu\text{-}(CH_2)]$ (7a) without either a metal-metal bond or other bridging groups to stabilise it. In addition, they also reported the crystal structure of this novel compound. (See Figure 2.18). The structural data revealed that the two ruthenium atoms are symmetrical about the $\mu\text{-}(CH_2)$ group.

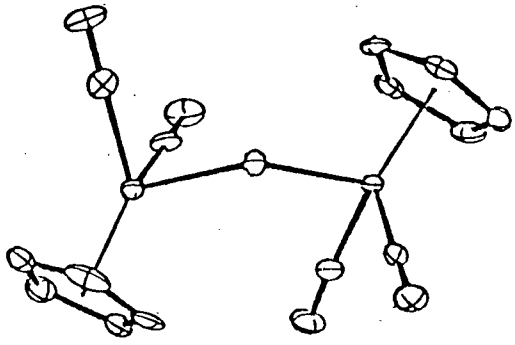

FIGURE 2.18 X-ray crystal structure of $[CpRu(CO)_2]_2[\mu\text{-}(CH_2)]$

A slightly longer Ru-C distance of 2.18 Å was observed in comparison to the Ru-C distance of 2.08 Å and 2.11 Å found in the complexes $[CpRu(CO)]_2[\mu\text{-}CO][\mu\text{-}CHCH_3]$ and $[CpRu(CO)]_2[\mu\text{-}C(CH_3)_2][\mu\text{-}C(CH_3)_2]$ respectively, [29]. These two compounds show a Ru-Ru bond distance of 2.7 Å. The Ru-Ru distance in the μ-methylene complex (7a) of 3.8 Å confirmed that the metal atoms were non-bonded in this compound.

The large Ru-C-Ru bond angle of 123° in complex (7a) (cf. 80° in the metal-metal bonded compounds) implies a large degree of steric crowding around the μ-CH_2 group, which would explain the greater reactivity of this complex. For example, (7a) has been found to readily insert CO [27] while other ruthenium alkyls are known to react extremely slowly to form the acyl derivatives, [CpRu(CO)(L)(COR)], [34,35].

In this thesis, the crystal structure of one of the new polymethylene bridged complexes, $[CpRu(CO)_2]_2[\mu\text{-}(CH_2)_5]$, has been determined. This is the first structure of a polymethylene bridged compound with more than four $-CH_2-$ groups, either with or without a metal-metal bond, ever to be determined. The crystal structure of the analogous iron compound $[CpFe(CO)_2]_2[\mu\text{-}(CH_2)_5]$ (5c) is currently being determined in order to make comparisons with the ruthenium complex (7e). The crystal structure of (7e) is reported and discussed.

Single crystals suitable for X-ray analysis were prepared by slow crystallisation of $[CpRu(CO)_2]_2[\mu\text{-}(CH_2)_5]$ from a dilute solution in hexane at 0°C (under N_2). Initially, thin plate-like crystals crystallised from solution overnight. The mother liquor was removed, refiltered and returned to the fridge for further crystallisation. After about 8 days, a few chunky prisms had formed and a suitable single prism was selected for X-ray structural determination.

The complex $[CpRu(CO)_2]_2[\mu\text{-}(CH_2)_5]$ crystallises in the space group $P\bar{1}$ with a= 7.792 Å, b= 10.691 Å, and c= 12.316 Å, α= 106.76°,

β= 95.58° and γ=90.94°. Tables reporting the fractional atomic coordinates, bond lengths, bond angles and torsion angles can be found in Chapter 6. A few relevant bond distances and bond angles are reported in Tables 2.8 and 2.9 respectively.

TABLE 2.8 Some relevant bond lengths (Å) with e.s.d. s in parenthesis for $[CpRu(CO)_2]_2[\mu\text{-}(CH_2)_5]$

Ru(1) - C(1)	2.180	(9)
Ru(1) - C(111)	1.861	(8)
Ru(1) - C(112)	1.871	(8)
Ru(2) - C(5)	2.164	(7)
Ru(2) - C(211)	1.868	(7)
Ru(2) - C(212)	1.889	(10)
C(1) - C(2)	1.503	(11)
C(2) - C(3)	1.546	(13)
C(3) - C(4)	1.538	(10)
C(4) - C(5)	1.509	(12)
Ru(1) - X	1.935	(8)
Ru(1) - Y	1.942	(8)

a X and Y represent the centroids of the cyclopentadienyl rings C(11) - C(15) and C(21) - C(25) respectively (Figure 2.19)

Figure 2.19 shows the crystal stucture of (7e) while Figure 2.20 shows a projection down the Ru-Ru axis. The crystal structure of $[CpRu(CO)_2]_2[\mu\text{-}(CH_2)_5]$ confirms that the two ruthenium atoms are linked to the terminal carbon atoms of a linear pentyl chain. The two cyclopentadienyl rings, surprisingly, lie on the same side of the Ru-Ru axis in a gauche (cis) orientation. As expected, both rings are planar with the dihedral angle between their least squares planes 79.5 (4)°. The Ru-C_1 (alkyl) bond distance of 2.17 Å (average) is comparable to that observed in the μ-methylene complex (7a) of 2.18 Å (average) [27], while the Ru-Ru distance of 8.81 Å confirms that the two metal atoms are non-bonded. (Table 2.8).

TABLE 2.9 Some relevant bond angles (degrees) with e.s.d. s in parenthesis for $[CpRu(CO)_2]_2[\mu\text{-}(CH_2)_5]$ [a]

C (111) - Ru (1) - C(112)	90.2	(4)
C (1) - Ru (1) - C(112)	88.4	(4)
C (1) - Ru (1) - C(111)	86.1	(3)
C (1) - Ru (1) - X	121.0	
C (111) - Ru (1) - X	129.6	
C (112) - Ru (1) - X	128.3	
C (211) - Ru (2) - C(212)	89.3	(4)
C (5) - Ru (2) - C(212)	85.2	(4)
C (5) - Ru (2) - C(211)	88.2	(3)
C (5) - Ru (2) - Y	123.5	
C (211) - Ru (2) - Y	127.3	
C (212) - Ru (2) - Y	129.8	

a X and Y represent the centroids of the cyclopentadienyl rings C(11) - C(15) and C(21) - C(25) respectively (Figure 2.19).

The bond angle between any of the directly bonded atoms of any two non- cyclopentadienyl ligands (ie. the CO ligands and the alkyl chain) and the metal is close to 90°. (See Table 2.9). In addition, the bond angle between the centroid of the cyclopentadienyl ligand, the metal and any other ligand is ca. 126.5°. This is consistent with an octahedral metal centre in which the cyclopentadienyl ligand effectively occupies the remaining three coordination sites. These features have been observed for several transition metal complexes containing the cyclopentadienyl ligand of type [CpM(CO)LR] and provide evidence that such complexes are octahedral [98] and not tetrahedral as was originally believed. A tetrahedral structure would require the bond angles between any two ligands and the metal atom to be ca. 109.5°.

The slightly larger Ru-C_1-C_2 bond angles of 113.5° and 116.5° compared to the C_1-C_2-C_3 bond angles of 112°, may be a result of the interaction of the protons on C_2 and C_4 with the cyclopentadienyl rings which lie in close proximity to the β-CH_2 groups.

The most interesting feature of the crystal data for $[CpRu(CO)_2]_2[\mu\text{-}(CH_2)_5]$, was the shorter C_1-C_2 (C_4-C_5) bond distance of 1.50 Å in comparison to the C_2-C_3 (C_3-C_4) distance of 1.54 Å in the alkyl chain. This shortening of the C_α-C_β bond length was not observed in the di-iron analogues, [20]. It was thought that this could possibly be due to an agostic C-H-→Ru type interaction. However, no evidence for such a three centre, two electron system could be found in either the proton-coupled ^{13}C or

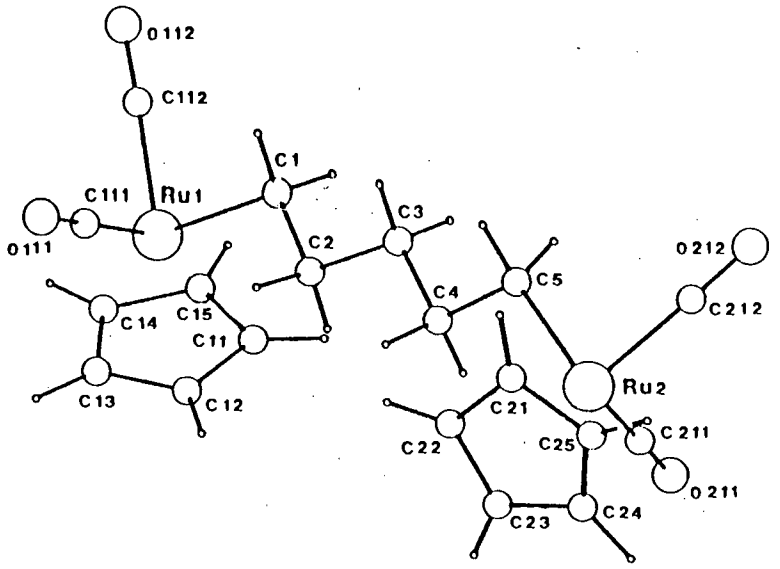

FIGURE 2.19 X-ray crystal structure of $[CpRu(CO)_2]_2[\mu\text{-}(CH_2)_5]$

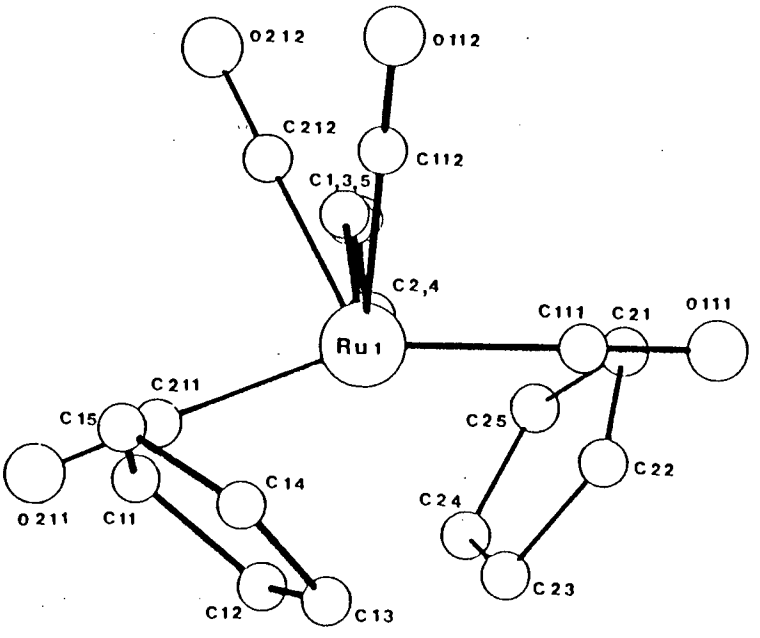

FIGURE 2.20 X-ray crystal structure of $[CpRu(CO)_2]_2[\mu\text{-}(CH_2)_5]$: Projection down the Ru-Ru axis

the ^1H NMR spectra of (7e). (See Section 2.2.2). Furthermore, the Ru-C_α bond distance of 2.18 Å is the same as that observed in the μ-methylene complex (7a), [27]. It is possible that this shorter C_α-C_β bond distance is due to some contribution from a structure having diene character, ie. M-(η^2-CH_2-CH_2).

As mentioned briefly above, the cyclopentadienyl rings in $[CpRu(CO)_2]_2[\mu\text{-}(CH_2)_5]$ are in a gauche orientation, ie. on the same side of the Ru-Ru axis. (Figures 2.19 and 2.20). In both the di-iron complexes (5a) and (5b) these Cp rings were found on the opposite sides of the metal-metal axis, ie. in a trans conformation. There are two possible explanations for these observations. Either the compound $[CpRu(CO)_2]_2[\mu\text{-}(CH_2)_5]$ exists in two stable conformations (ie. cis and trans with respect to the Cp rings) or different conformations of the compounds of type $[CpM(CO)_2]_2[\mu\text{-}(CH_2)_n]$ exist for n_{even} and n_{odd}, (n=3 being an exception due to steric crowding in the short alkyl chain). (See Figure 2.21).

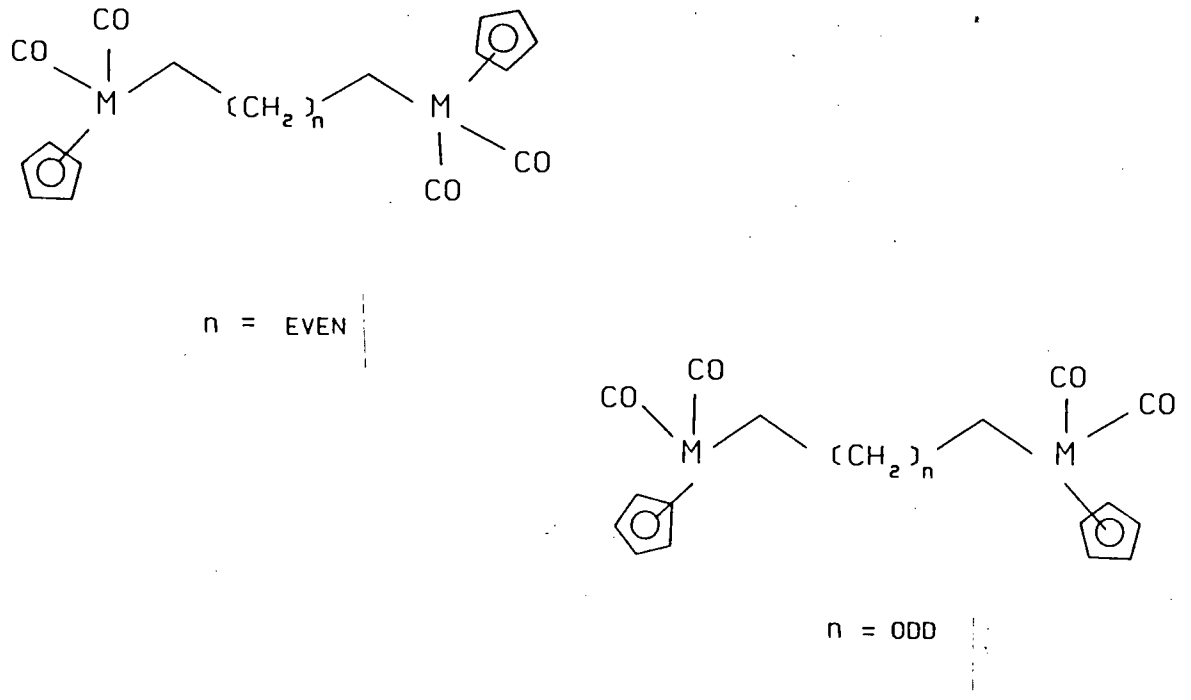

FIGURE 2.21 Possible conformers (cis and trans with respect to the cyclopentadienyl rings) for n_{even} and n_{odd}

The fact that $[CpRu(CO)_2]_2[\mu\text{-}(CH_2)_5]$ was isolated in two different crystalline forms (initially as plates and only after slow crystallisation as prisms) suggests that two different structural forms (cis and trans with respect to the Cp rings) may indeed exist for this complex, the most stable of which preferentially crystallises from solution.

A spacial model of the complex suggests that the cis isomer would produce the least interaction of the carbonyl ligands with the alkyl chain, while the cis cyclopentadienyl ligands are sufficiently isolated from each other to avoid steric repulsions. To investigate this possibility, melting point determinations were carried out on the flaky crystals and the prisms obtained for

(7e). The melting points of 78-79°C for the prisms and 86-88°Cfor the plates would suggest that two different structural forms do exist where the plate form, which crystallises initially, is the most favourable conformation (probably the trans isomer). The broad melting point range generally obtained for $[CpRu(CO)_2]_2[\mu-(CH_2)_5]$ would appear to be due to a mixture of these two crystalline forms, but could also be a result of impurities or decomposition. However, in order to establish conclusively whether or not the plates and prisms represent two different isomers of $[CpRu(CO)_2]_2[\mu-(CH_2)_5]$, a crystal structure determinaton of the plate form is necessary. The space group of the plate-like crystals is initially being determined as it is believed that, in the event of these having a different conformation to that of the prisms, the space group is most likely to be different.

The possibility of two different crystalline forms for n_{even} and n_{odd} can be verified by consideration of the spacial models for the complexes of (7) where n=4 and n=5. For n=4, the least steric interaction of the CO groups with the alkyl chain occurs when the Cp rings are trans to each other. However, for n=5, this steric interacton appears to be minimal when the Cp rings are in the cis configuration. The fact that $[CpFe(CO)_2]_2[\mu-(CH_2)_3]$ (n=odd number) exists in the trans conformation may be a result of steric repulsion of two cis CO and two cis Cp groups in the short chain complexes. In order to examine this hypothesis, a crystal structure determination of the analogous di-iron complex $[CpFe(CO)_2]_2[\mu-(CH_2)_5]$ is currently in progress.

2.2.6. Synthesis and Characterisation of the Heterodinuclear complex, $[Cp(CO)_2Fe(CH_2)_4Ru(CO)_2Cp]$.

Interest in the chemistry of heterodinuclear compounds arises from the realisation that such systems could limit reactivity at a particular metal centre and thus allow optimization of catalytic or stoichiometric transformations by di- or multi-nuclear transition metal complexes, [57-61,78]. Although much information regarding the synthesis of mixed-metal complexes is available [79] little is known about the site selectivity of these systems. Recently, it was shown that the mixed-metal cluster $[H_2FeRu_3(CO)_{13}]$ undergoes CO substitution by a variety of phosphorous donor ligands only at the ruthenium atom, [80]. Similarly, $[(CO)_4Ru(\mu\text{-}PPh_2)Co(CO)_3]$ also undergoes substitution of CO by PPh_3 only at ruthenium, [81]. Substitution studies of the mixed-metal dinuclear complexes $[Cp(CO)_2Fe\text{-}M(CO)_5]$ (M = Mn,Re) [82] and $[(CO)_5Mn\text{-}Re(CO)_5]$ [83] with donor ligands have also shown preferential substitution at one metal centre.

Furthermore, the importance of bimetallic catalysts in controlling product selectivities in industrial processes has already been discussed in Section 1.3. It is therefore clear that the study of such heterodinuclear complexes and their reactivity is of immense significance.

The synthesis of the new mixed-metal compound, $[Cp(CO)_2Fe(CH_2)_4Ru(CO)_2Cp]$ (8b), was achieved in low yield (7%) following the method of Knox [25] and using a 1:1 molar ratio of $[CpFe(CO)_2(CH_2)_4I]$ to $Na[CpRu(CO)_2]$. This yield was improved to

give a 41% crude yield of compound (8b) using an adaptation of Knox's method, (Equation 9).

$$[Cp\,Fe(CO)_2(CH_2)_4I] \;+\; Na[Cp\,Ru(CO)_2] \xrightarrow[-78^\circ C \text{ WARMING TO R.T. } 24 \text{ HRS}]{THF/N_2} [Cp(CO)_2Fe(CH_2)_4Ru(CO)_2Cp] \quad (8b) \qquad 9$$

Thus, a solution of $Na[CpRu(CO)_2]$ in THF was added dropwise to a solution of $[CpFe(CO)_2(CH_2)_4I]$ (prepared as in reference [17]) in THF at -78°C and the mixture allowed to warm to room temperature over 24 hours. The product was isolated by extraction with hexane followed by chromatography on Florisil (eluting with hexane). $[CpFe(CO)_2]_2$, $[CpRu(CO)_2]_2$ and $[CpRu(CO)_2I]$ were also isolated as by-products of this reaction and identified by their infrared spectra in the $\nu(CO)$ region. $[Cp(CO)_2Fe(CH_2)_4Ru(CO)_2Cp]$ was recrystallised from hexane at -78°C as a yellow crystalline solid. The product is relatively air stable when pure, decomposing slowly in air in the dark only after several months.

The new mixed-metal alkanediyl compound (8b), has been fully characterised by IR, ^1H NMR and ^{13}C NMR spectroscopy, mass spectrometry and elemental analysis. The infrared, ^1H and ^{13}C NMR data are represented in Tables 2.10 and 2.11 respectively, along with the data for other members of the series $[Cp(CO)_2Fe(CH_2)_nRu(CO)_2Cp]$, n=3 [25] and n=5 (prepared by H.B.Friedrich of this laboratory [73]).

TABLE 2.10 Melting point, IR and ^1H NMR data (in $CDCl_3$) for $[Cp(CO)_2Fe(CH_2)_nRu(CO)_2Cp]$

COMPOUND No.	n	Melting range (°C)	ν(CO) (cm^{-1})[a]	^1H NMR (ppm)[b] δ Cp(Ru)	δCp(Fe)	$\delta(CH_2)$
8a *	3	85 - 86	2021 (vs) 2010 (vs) 1957 (vs)	5.30(5H)	4.70 (5H)	1.22 - 1.72 (6H)
8b	4	131 - 132	2018 (s) 2008 (s) 1959 (s)	5.22(5H)	4.71 (5H)	1.66 - 1.48 (8H)
8c	5	75 - 77	2018 (s) 2008 (s) 1958 (vs)	5.26(5H)	4.73 (5H)	1.58 (4H), 1,43 (4H), 1.28 (2H)

a Hexane solution ; s = strong , vs = very strong

b $CDCl_3$ solution ; Cp resonances occur as sharp singlets, (CH_2) resonances occur as overlapping multiplets

* Data from Reference [25]

TABLE 2.11 ^{13}C NMR (decoupled) data for $[Cp(CO)_2Fe(CH_2)_nRu(CO)_2Cp]$, n=4 and 5 (in $CDCl_3$)

COMPOUND No.	n	δ (ppm) [a] Fe - CO	Ru - CO	Cp - Ru	Cp - Fe	Fe - (CH_2)	Ru - (CH_2)	$-(CH_2)-$
8b	4	217.5	202.2	88.5	85.2	3.7	-3.2	45.2, 43.7
8c	5	217.3	202.1	88.3	85.1	3.9	-3.2	40.0, 39,6, 38,0

a. $CDCl_3$ solution with $Cr(acac)_3$

The infrared spectra of (8b) and (8c) in hexane both show three stong terminal CO absorptions at 2018 (Ru-CO), 2008 (Fe-CO) and 1959 (both Ru-CO and Fe-CO) cm^{-1}. (cf. (8a, n=3): 2012(vs), 2010(vs) and 1957(vs) cm^{-1} [25].)

The ^1H NMR spectra also compare well with the ^1H NMR data reported for $[Cp(CO)_2Fe(CH_2)_3Ru(CO)_2Cp]$ [25], and confirm the dinuclear mixed-metal nature of these compounds by the appearance of two separate signals for the two C_5H_5 rings. Whereas Knox et. al. reported a single broad multiplet for the methylene protons of the three $-(CH_2)-$ groups in (8a), two separate signals at δ 1.66 and δ 1.48 ppm are observed for the methylene protons of (8b) and (8c).

It is interesting that the melting points of the compounds (8b) and (8c) (Table 2.10) lie closer to those of $[CpRu(CO)]_2[\mu-(CH_2)_n]$, where n=4 (131-132 °C, [25]) and n=5 (see Table 2.1) respectively, rather than midway between those of the di-iron and the diruthenium compounds as might be expected. This trend may be rationalised by consideration of the mass spectrum of $[Cp(CO)_2Fe(CH_2)_4Ru(CO)_2Cp]$, which reveals $[CpFe]^+$ as the most abundant ion. It is possible that during heating, the heterodinuclear complex (8b) initially rearranges to the more stable diruthenium complex (7d) with loss of the $[CpFe(CO)_2]$ fragment. (See Route C, Figure 2.16).

It is also important to note that the melting points of the compounds $[Cp(CO)_2Fe(CH_2)_nRu(CO)_2Cp]$ (n=3-5) exhibit the same trends as the series of compounds (5) and (7) ie. (i) a decrease in melting point as the chain length increases and (ii) melting point of n_{even} is higher than melting point of n_{odd}.

2.2.7 Synthesis and Characterisation of the Mononuclear Haloalkyl Ruthenium complexes, $[CpRu(CO)_2(CH_2)_nX]$.

The compounds $[Cp^*Ru(CO)_2(CH_2)X]$ (where $Cp^* = \eta^5\text{-}C_5Me_5$, X= H, CH_3, CH_2OCH_3) [84], as well as the complexes $[CpRu(CO)_2CH_2X]$ (where X= Cl, OCH_3) [85] have previously been reported. However, it appears that no attempts have been made to synthesise the mononuclear haloalkyl ruthenium analogues of $[CpFe(CO)_2(CH_2)_nX]$ (where X=Br, n=3-5), viz. $[CpRu(CO)_2(CH_2)_nX]$, (where X=Cl, Br, I; n=3,4,5...).

In this study, several attempts were made to prepare the complex $[CpRu(CO)_2(CH_2)_4Br]$ (15) following the route used by Moss [17] to prepare the iron compounds $[CpFe(CO)_2(CH_2)_nBr]$. (Equation 10).

$$Na[Cp\,Fe(CO)_2] + 1.25\ Br(CH_2)_nBr \xrightarrow[-20^\circ C]{THF} [Cp\,Fe(CO)_2(CH_2)_n\,Br] + NaBr \qquad 10$$

However, the reaction of $Na[CpRu(CO)_2]$ with a 1.25 molar excess of the dibromobutane at -20°C yielded a mixture of the desired product (15) and $[CpRu(CO)_2]_2[\mu\text{-}(CH_2)_4]$ (7d), which was identified by infrared and ^1H NMR spectroscopy. Other minor products such as $[CpRu(CO)_2Br]$ and $[CpRu(CO)_2]_2$ were also isolated from the reaction mixture and identified by infrared spectroscopy. This suggests that the mono-haloalkyl complex is formed initially and reacts rapidly with further $Na[CpRu(CO)_2]$ to form the dinuclear product, (7d).

The ^{13}C NMR data of $[Cp(CO)_2Fe(CH_2)_nRu(CO)_2Cp]$ (n=4,5) are reported in Table 2.11. As in the diruthenium complexes $[CpRu(CO)]_2[\mu\text{-}(CH_2)_n]$, Knox assigned the high field carbon-13 resonance at δ 6.7 ppm to the β-CH_2 carbon in $[Cp(CO)_2Fe(CH_2)_nRu(CO)_2Cp]$, [25]. (See Section 2.2.2).

In the present study the mixed-metal complexes $[Cp(CO)_2Fe(CH_2)_nRu(CO)_2Cp]$ (n=4,5) exhibit two high field signals at δ 3.7 and δ -3.2 ppm which are assigned to the α-CH_2 carbons adjacent to the iron and ruthenium atoms respectively on the basis of observations in other mixed metal systems (see Section 2.2.2). In the complex (8c) (n=5), three signals at δ 40.0, δ 39.6 and δ 38.0 ppm are assigned to the carbon atoms β to iron and ruthenium, and to the γ-carbon atom respectively.

As yet, no reactivity studies have been performed on the complex $[Cp(CO)_2Fe(CH_2)_4Ru(CO)_2Cp]$. However, future studies will investigate the substitution and CO migratory insertion reactions with donor ligands (such as PR_3, CNR etc.) to determine site selectivity. From the lack of reactivity of the homodinuclear complexes of ruthenium $[CpRu(CO)_2]_2[\mu\text{-}(CH_2)_n]$ observed in this study, (see Section 3), substitution is expected to occur preferentially at the iron centre.

The reaction of $Na[CpRu(CO)_2]$ with $Br(CH_2)_4Br$ was therefore repeated at -78°C in an attempt to inhibit the formation of $[CpRu(CO)_2]_2[\mu\text{-}(CH_2)_4]$. A colourless oily residue was isolated by chromatography on Florisil and recrystallised from hexane at -78°C. The resulting white crystals melt slowly to give a very pale yellow oil on warming to room temperature. This product was identified as $[CpRu(CO)_2(CH_2)_4Br]$ (59% crude yield) by infrared and ^1H NMR spectroscopy.

The mononuclear chloropropyl derivative $[CpRu(CO)_2(CH_2)_3Cl]$ (16) was prepared in a similar manner by the addition of $Na[CpRu(CO)_2]$ to a 1.17 molar excess of $Cl(CH_2)_3Cl$ at -78°C. Monitoring by infrared spectroscopy revealed no reaction after 35 minutes, so the cold bath was removed and the reaction vessel allowed to warm gradually to room temperature. After 2 hours, the infrared spectrum showed complete reaction.

The product was isolated in the same manner as the bromoalkyl complex, yielding a pale yellow oil at room temperature. This oil was again analysed by ^1H NMR and infrared spectroscopy which are in agreement with the product being the mononuclear chloropropyl compound, $[CpRu(CO)_2(CH_2)_3Cl]$. The oil, obtained in 30% yield, appears to be hygroscopic.

These complexes, $[CpRu(CO)_2(CH_2)_nX]$, (X=Cl, n=3 ; X=Br, n=4) are the first examples of mononuclear haloalkyl ruthenium compounds. Such functionalised alkyl transition metal compounds are important as useful precursors to many new organometallic complexes; for

example the complexes $[CpFe(CO)_2(CH_2)_nX]$ are useful precursors for the dinuclear polymethylene bridged compounds $[CpFe(CO)_2]_2[\mu\text{-}(CH_2)_n]$ (5) [17] and the heterobimetallic complexes $[Cp(CO)_2Fe(CH_2)_nM(CO)_xCp]$ (M=Mo or W, x=3; M=Ru, x=2), [17,25].

Similarly, complexes of the type $[CpRu(CO)_2(CH_2)_nX]$ could serve as precursors to the dinuclear alkanediyls, $[CpRu(CO)_2]_2[\mu\text{-}(CH_2)_n]$.

3. REACTIONS OF μ(α,ω)-ALKANEDIYL COMPLEXES OF RUTHENIUM AND IRON

3.1 Introduction

The observations of Coffield et.al. in 1957 [86] that methylmanganese pentacarbonyl, $[(CO)_5Mn(CH_3)]$, readily and reversibly absorbs carbon monoxide to produce the acetyl derivative, $[(CO)_5Mn(COCH_3)]$, induced widespread interest in the so-called carbonyl insertion (or alkyl migration) reaction. (Equation 11)

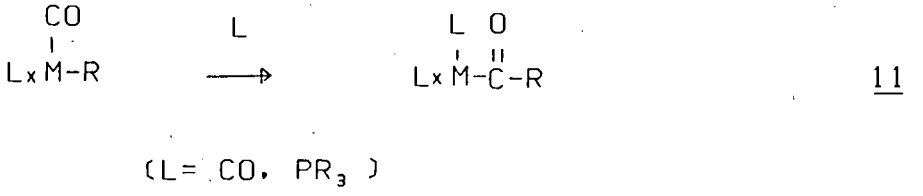

11

This migratory CO insertion reaction functions as a key step in several catalytic transformations. Examples are the hydroformylation reaction in which an olefin is converted to an aldehyde, the carbonylation of methanol to form acetic acid and the hydrogenation of carbon monoxide in the Fischer-Tropsch process, to mention but a few, [87].

In 1966, Bibler and Wojcicki [88], reported that the reaction of $[CpFe(CO)_2CH_3]$ (17) with triphenylphosphine in refluxing THF (or diethyl ether) afforded the acetyl derivative, $[Cp(CO)(PPh_3)Fe(COCH_3)]$ (18). This reaction was subsequently investigated in other, particularly non-polar, solvents over a range of temperatures, [89]. The products of this reaction were

consistent with a mechanism involving initial carbonyl insertion to produce the acetyl product (18). (Scheme 6).

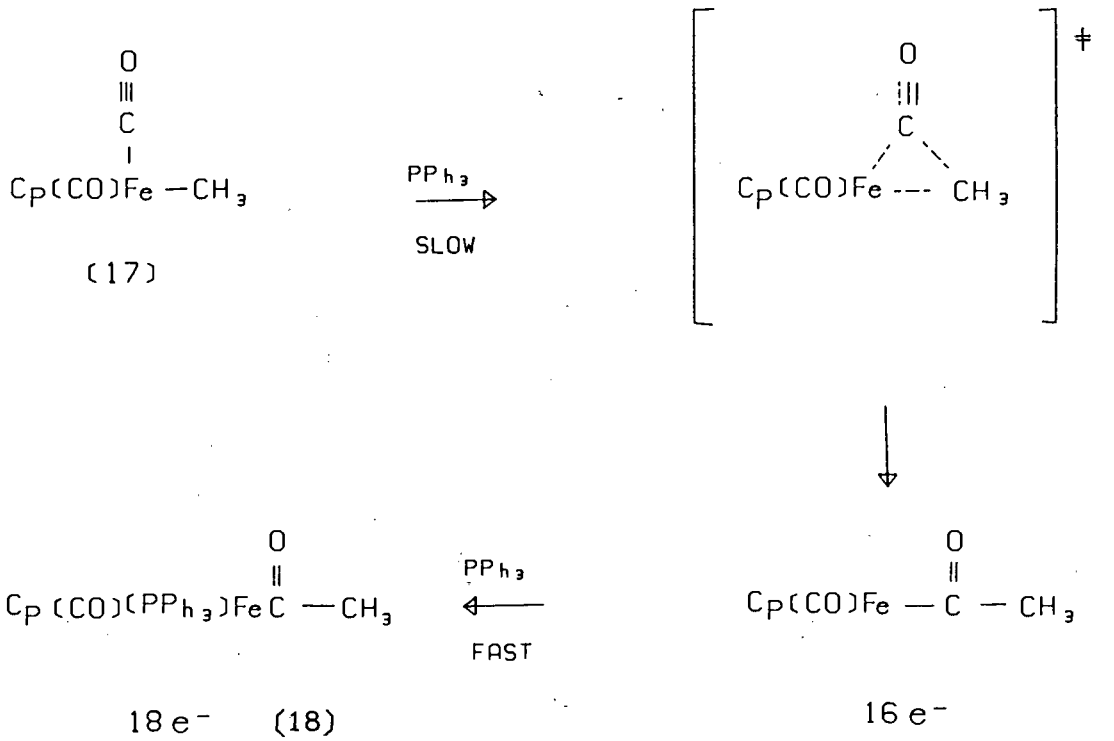

SCHEME 6

Although small quantities of the decarbonylated species $[Cp(CO)(PPh_3)Fe(CH_3)]$ (19) were also isolated when the reaction was performed in ether solvents (THF, diethyl ether or dioxane), subsequent investigations have shown that (19) is formed directly by substitution of CO and not by decarbonylation of (18), [89]. Similar CO insertion was observed in the reaction of $[Cp(CO)_2Fe(C_2H_5)]$ with PPh_3, [89]. In the same publication, Wojcicki and Su also demonstrated that an analogous insertion of SO_2 into the iron-alkyl bond of $[Cp\{P(OR)_3\}(CO)Fe(CH_3)]$ yields the S-sulphinates, $[Cp\{P(OR)_3\}(CO)Fe(SO_2CH_3)]$, [89].

μ(α,ω)-Alkanediyl complexes have been shown to undergo similar carbonyl migratory insertion reactions. The thermally induced reactions of $[CpFe(CO)_2]_2[\mu\text{-}(CH_2)_n]$ (n=3,4) with carbon monoxide were reported to yield the diacyl insertion products $[CpFe(CO)_2]_2[\mu\text{-}C(O)(CH_2)_nC(O)]$, [18]. In a similar reaction of $[CpFe(CO)_2]_2[\mu\text{-}(CH_2)_3]$ with sulphur dioxide, the mono- (20) and di-sulphinato (21) species were obtained, [90].

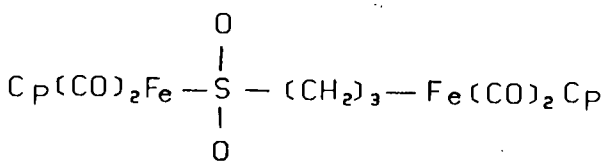

(20)

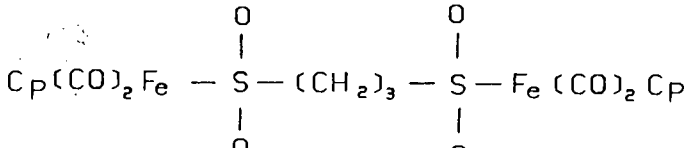

(21)

Moss and Scott [23] recently investigated the thermally induced reactions of $[CpFe(CO)_2]_2[\mu\text{-}(CH_2)_n]$, where n=3-7, with tertiary phosphines. These compounds were found to undergo CO insertion reactions to yield either the mono- or di-acyl substituted products, $[Cp(CO)_2Fe(CH_2)_nC(O)Fe(CO)(PR_3)Cp]$ (22) and $[CpFe(CO)(PR_3)]_2[\mu\text{-}C(O)(CH_2)_nC(O)]$ (23) respectively, depending on the molar ratio of phosphine employed. (Equation 12).

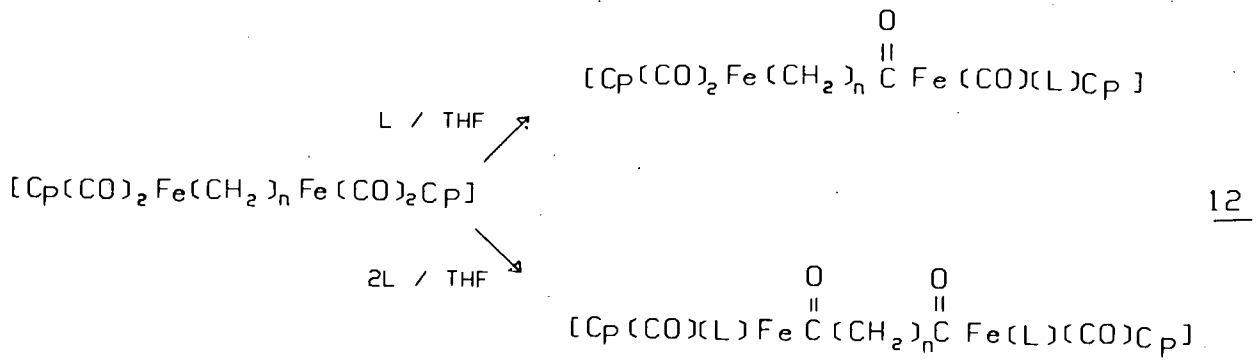

12

L = PPh_3, n = 3-7

L = PPh_2Me, n = 3-4

L = $PPhMe_2$, n = 3

Traces of the monoacyl derivatives (22) were also detected in the reactions of $[CpFe(CO)_2]_2[\mu\text{-}(CH_2)_n]$ with a two molar equivalent of L, (L = PR_3).

These reactions of compounds of the type $[CpFe(CO)_2]_2[\mu\text{-}(CH_2)_n]$ (5) with tertiary phosphines were relatively slow even under fairly vigorous reaction conditions. For example, the diacyl di-substituted derivative, $[CpFe(CO)(PPh_3)]_2[\mu\text{-}C(O)(CH_2)_nC(O)]$, where n=3, formed after ca. 66 hours refluxing in THF while the compounds where n=4-7 were formed more rapidly (36-48 hours), possibly due to relief of steric crowding in the longer chain complexes.

A study of the rates of reaction for the various phosphines [23] revealed an initial relatively rapid reaction of the substrate to form the monoacyl species (22). This monoacyl, mono-substituted product was observed to react more slowly with a second equivalent of phosphine to produce the diacyl, di-substituted product (23). An increase in the rate of reaction was observed with increasing chain length which was indicative of a decrease in steric hindrance in the longer alkyl chain compounds, [23].

In addition to the carbonyl insertion reactions, other important reactions of transition metal complexes include the cleavage of the metal-carbon sigma bonds by electrophiles. The reactions of the mononuclear iron-alkyls, $[CpFe(CO)_2(R)]$ (24), with

electrophilic reagents [91], as well as the analogous reactions of the dinuclear alkanediyl complexes, $[CpFe(CO)_2]_2[\mu\text{-}(CH_2)_n]$ [23], have been studied previously.

Scott and Moss [23] have investigated the reactions of $[CpFe(CO)_2]_2[\mu\text{-}(CH_2)_n]$ (where n=3,4) with halogens and isolated the cleavage products shown in Equation 13.

$$[Cp(CO)_2Fe(CH_2)_nFe(CO)_2Cp] \xrightarrow[RT\ /\ THF]{2X_2} \underset{(25)}{2CpFe(CO)_2X} + \underset{(26)}{X(CH_2)_nX} \qquad 13$$

In addition to the expected products (25) and (26), a cationic species $[Cp_2Fe_2(CO)_4(CH_2)_4]^+$ (27) was also obtained from the reactions of $[CpFe(CO)_2]_2[\mu\text{-}(CH_2)_4]$ with iodine and bromine and isolated as the tetraphenylborate salt, $[Cp_2Fe_2(CO)_4(CH_2)_4]^+BPh_4^-$, [23].

In the present work, the reactions of the $\mu(\alpha,\omega)$-alkanediyl complexes of ruthenium with a range of tertiary phosphines (PPh_3, PPh_2Me and $PPhMe_2$), with halogens (Br_2 and I_2) and with tertiary butylisocyanide (t-BuNC) have been investigated.

3.2 Results and Discussion: Reactions of $[CpRu(CO)_2]_2[\mu\text{-}(CH_2)_n]$ with Tertiary Phosphines.

3.2.1 Reactions of $[CpRu(CO)_2]_2[\mu\text{-}(CH_2)_5]$ with tertiary phosphines, PPh_3, PPh_2Me and $PPhMe_2$.

The iron alkanediyl complexes $[CpFe(CO)_2]_2[\mu\text{-}(CH_2)_n]$ (5) have been shown to undergo carbonyl migratory insertion reactions in the presence of a ligand, $L=PR_3$, in refluxing THF within 25 to 48 hours, [23]. It was therefore assumed that the diruthenium analogues (7) might show similar reactivity towards donor ligands such as tertiary phosphines.

Thus, $[CpRu(CO)_2]_2[\mu\text{-}(CH_2)_5]$ (7e) was refluxed with PPh_3 in THF in an attempt to produce the mono- and diacyl substituted products, $[Cp(CO)_2Ru(CH_2)_5C(O)Ru(CO)(PPh_3)Cp]$ (28) and $[CpRu(CO)(PPh_3)]_2[\mu\text{-}C(O)(CH_2)_5C(O)]$ (29) respectively. However, an infrared spectrum of the reaction mixture after 25 hours refluxing revealed that no reaction had occurred. This initial observation suggested that the diruthenium complexes (7) are more resistant to CO insertion and substitution than their iron polymethylene bridged analogues (5).

The substitution reactions of $[CpRu(CO)_2I]$ with group V donor ligands, L, to yield $[CpRu(CO)LI]$ and $[CpRu(CO)L_2]I$, have been shown to proceed rapidly in the presence of a catalytic amount of $[CpFe(CO)_2]_2$ or $[CpRu(CO)_2]_2$, [92]. In the absence of these catalysts, this reaction is reported to be extremely slow even in high boiling solvents such as xylene, [93, 94].

It was thought that repetition of the reaction of $[CpRu(CO)_2]_2[\mu\text{-}(CH_2)_5]$ (7e) with PPh_3 in the presence of a catalytic amount of $[CpRu(CO)_2]_2$ might induce a similar substitution reaction or even a carbonyl insertion reaction to give the acyl products (28) and (29). However, after 71 hours refluxing in THF in the presence of $[CpRu(CO)_2]_2$, only $\nu(CO)$ absorption bands due to (7e) and $[CpRu(CO)_2]_2$ were detected in the infrared spectrum of the mixture. In order to investigate further the use of these metal carbonyl dimers as substitution catalysts, the reaction of the dinuclear iron compound $[CpFe(CO)_2]_2[\mu\text{-}(CH_2)_5]$ with PPh_3 was carried out in the presence of $[CpFe(CO)_2]_2$. A duplicate reaction was carried out simultaneously, in the absence of added catalyst, under identical conditions for purposes of comparison. The infrared spectra of the reaction mixtures, monitored after the same periods of time, revealed no rate enhancement due to the addition of $[CpFe(CO)_2]_2$. (See Table 6.8).

Even the addition of PdO, as a catalyst, or trimethylamine-N-oxide (Me_3NO) (which is known to assist in the removal of coordinated carbonyl groups) and the substitution of THF with toluene (boiling point 111°C), could not induce a reaction between (7e) and PPh_3 after 48 hours.

It therefore appeared that a higher boiling, preferably coordinating, solvent was required in order for the reaction of $[CpRu(CO)_2]_2[\mu\text{-}(CH_2)_5]$ with PR_3 to occur. The reaction was thus carried out in refluxing acetonitrile (CH_3CN, boiling point 82°C) using a two molar equivalent of PPh_3. The progress of this reaction was monitored at intervals by infrared spectroscopy. After ca. 13 hours, a very slight shoulder at ca. 1920 cm^{-1} was

observed on the strong ν(CO) band at 1942 cm^{-1} (due to (7e)) in the infrared spectrum of the mixture. An extremely slow growth of this shoulder band was observed. After ca. 87 hours refluxing, this band had increased in intensity to approximately half that of the bands produced by the substrate (7e). A broad, weak acyl ν(CO) band could also be detected at 1600 cm^{-1} after ca. 137 hours. This reaction in CH_3CN was monitored for a total of 234 hours (9.7 days!). At this stage the infrared spectrum revealed three strong terminal ν(CO) bands at 2008, 1942 and 1919 cm^{-1} of nearly equal intensity and an acyl ν(CO) band at 1605 cm^{-1} of medium intensity. Separation of the components by column chromatography yielded mainly unreacted starting material (7e) (52%), as well as small amounts of $[Cp(CO)_2Ru(CH_2)_5C(O)Ru(CO)(PPh_3)Cp]$ (28) (31%) and $[CpRu(CO)(PPh_3)]_2[\mu\text{-}C(O)(CH_2)_5C(O)]$ (29) (14%). The monoacyl, mono-substituted product (28), which was obtained as a yellow oil from this reaction, was characterised by infrared only. Since this product (28) required a more polar solvent mixture than (7e) and a less polar solvent than (29) to elute it from the column, it was assumed that the bands observed in the infrared spectrum were <u>not</u> due to a mixture of the three compounds (7e), (28) and (29). Infrared, ^1H NMR and ^{13}C NMR spectroscopy confirmed the diacyl, di-substituted nature of the yellow crystalline solid (29).

The extremely slow reaction of $[CpRu(CO)_2]_2[\mu\text{-}(CH_2)_5]$ with PR_3 in refluxing CH_3CN made further reactivity studies in this solvent particularly unattractive. An alternate solvent system was therefore sought.

As mentioned previously, the substitution reactions of $[CpRu(CO)_2X]$ (X = Cl, I) are extremely slow even in refluxing xylene, [92,93,94]. Little information regarding the reactivity of the mononuclear ruthenium alkyl complexes, $[CpRu(CO)_2(R)]$, has been reported. Howell and Rowan have, however, investigated the substitution reactions of the metal dimer, $[CpRu(CO)_2]_2$, with isonitriles [95, 96] and with phosphines and phosphites, [34, 35]. $[CpRu(CO)_2]_2$ undergoes substitution with CNR slowly in refluxing xylene and only the mono-substituted product, $[Cp_2Ru_2(CO)_3CNR]$ is obtained, [95, 96]. The reactions of $[CpRu(CO)_2]_2$ with $P(OR)_3$ were reported to yield the mononuclear alkyl complexes $[CpRu(CO)_2(R)]$ as by-products, [34, 35]. These latter volatile products, being difficult to separate, were characterised by further reaction with PPh_3, in refluxing xylene, to produce the CO insertion products $[Cp(CO)(PPh_3)Ru(COR)]$. These insertion reactions were found to be extremely slow, even in refluxing xylene and using a large excess of phosphine (5:1). For example, for R = Et or Bu, the reaction was judged to be only ca. 50% complete by infrared spectroscopy after 48 hours, [34, 35]. Thus the mononuclear ruthenium alkyls also show extreme reluctance to undergo CO insertion and substitution reactions.

In the light of the preceding discussion, subsequent reactions of $[CpRu(CO)_2]_2[\mu\text{-}(CH_2)_5]$ with tertiary phosphines were performed in refluxing xylene. Even so, these reactions proceed extremely slowly in comparison to those of their di-iron analogues with PR_3 in refluxing THF, [23].

The reaction of $[CpRu(CO)_2]_2[\mu\text{-}(CH_2)_5]$ with either a one or two molar equivalent of PPh_3 in refluxing xylene thus yielded the

substituted mono- or diacyl insertion products, $[Cp(CO)_2Ru(CH_2)_5C(O)Ru(CO)(PPh_3)Cp]$ (28) and $[CpRu(CO)(PPh_3)]_2[\mu\text{-}C(O)(CH_2)_5C(O)]$ (29) respectively, as yellow, air stable, crystalline solids. (Equation 14)

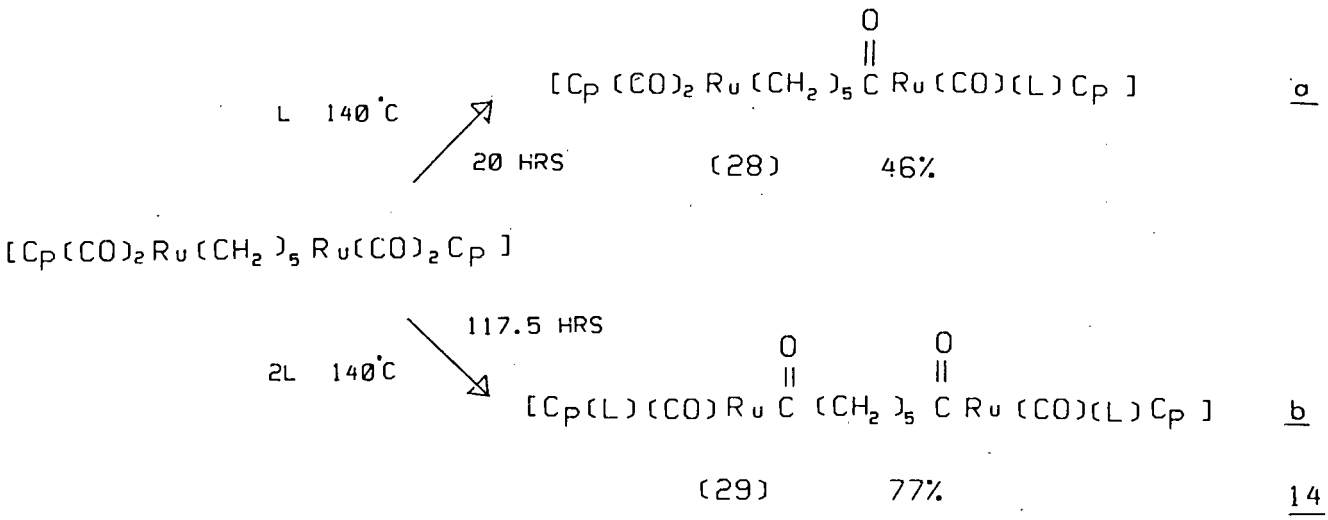

In the reaction of (7e) with a two molar ratio of PPh_3, a small amount (23%) of the monoacyl product (28) was also isolated. Compound (29) has been fully characterised by infrared, ^1H and ^{13}C NMR spectroscopy (Tables 3.1 and 3.2 respectively), as well as by microanalysis and melting point, (Table 6.7). Compound (28) has been characterised by infrared , microanalysis and melting point and partially characterised by ^1H and ^{13}C NMR spectroscopy, although the integration in the proton spectrum and an extra signal at δ 33.9 ppm in the ^{13}C NMR spectrum suggest that impurities are present (possibly $[CpRu(CO)_2]_2[\mu\text{-}(CH_2)_5]$).

Similarly, the products $[Cp(CO)_2Ru(CH_2)_5C(O)Ru(CO)(PPh_2Me)Cp]$ (30) (7%) and $[CpRu(CO)(PPh_2Me)]_2[\mu\text{-}C(O)(CH_2)_5C(O)]$ (31) (67%) were isolated from the reaction of (7e) with PPh_2Me (1:2 molar ratio) in refluxing xylene after 72.5 hours. Compound (30), an orange

coloured oil at room temperature, was characterised only by infrared due to the low yields of this product obtained in all cases. However, complex (31), which exists as a yellow, air stable, crystalline solid at room temperature, has been fully characterised by infrared, ^{1}H and ^{13}C NMR spectroscopy (Tables 3.1 and 3.2 respectively), melting point and microanalysis (Table 6.7).

The reaction of $[CpRu(CO)_2]_2[\mu\text{-}(CH_2)_5]$ with a two molar equivalent of $PPhMe_2$ proceeds relatively rapidly in comparison to those with PPh_3 and PPh_2Me. The diacyl, di-substituted species $[CpRu(CO)(PPhMe_2)]_2[\mu\text{-}C(O)(CH_2)_5C(O)]$ (32) was isolated in 90% yield as the only reaction product after ca. 21 hours. Complex (32) exists as an orange oil at ambient temperature and has been fully characterised by infrared, ^{1}H and ^{13}C NMR spectroscopy (Tables 3.1 and 3.2 respectively) and by microanalysis (Table 6.7).

TABLE 3.1 ^{1}H NMR data for the compounds $[CpRu(CO)(PR_3)]_2[\mu\text{-}C(O)(CH_2)_5C(O)]$, ($PR_3$ = PPh_3, PPh_2Me, $PPhMe_2$) in $CDCl_3$

COMPOUND No.	PR_3	PR_3[b]	C_5H_5	H_A[c]	$H_{A'}$[c]	H_B	$H_{B'}$	H_C	CH_3
				δ (ppm)[a]					
29	PPh_3	7.43 (30H)	4.94 (10H)	2.44(2H)	2.10(2H)	1.09(2H)	0.75(2H)	0.67(2H)	-
31	PPh_2Me	7.36(20H)	4.94(10H)	2.29(2H)	1.95(2H)	1.15(2H)	0.98(2H)	0.69(2H)	2.00(6H)
32	$PPhMe_2$	7.52(10H)	4.93(10H)	2.65(2H)	2.48(2H)	1.36(4H)	-	1.07(2H)	1.55(6H) 1.77(6H)

a In $CDCl_3$

b Value represents centres of broad multiplets

c. $H_A/H_{A'}$, $H_B/H_{B'}$ H_C represent the geminal methylene protons of the alkyl chain as shown in Figure 3.1, Resonances occur as broad multiplets.

d. Resonances occur as doublets due to ^{31}P coupling.

TABLE 3.2 ^{13}C NMR (decoupled) data for the compounds $[CpRu(CO)(PR_3)]_2[\mu\text{-}C(O)(CH_2)_5C(O)]$, ($PR_3$ = PPh_3, PPh_2Me, $PPhMe_2$) in $CDCl_3$

COMPOUND No	PR_3	CO[a]	CO[b]	PR_3[c]	δ (ppm) C_5H_5	C_α	C_β	C_γ	CH_3
29	PPh_3	255.78(d)	205.60(d)	135.77(d) 132.91(d) 129.39(s) 127.54(d)	88.30	65.46	24.53	28.29	-
31	PPh_2Me	257.23(d)	204.92(d)	138.25(d)/137.28(d) 131.94(d)/130.98(d) 129.50(s)/129.06(s) 127.75(d)/127.55(d)	87.58	65.13	24.72	28.42	17.49(d)
32	$PPhMe_2$	258.10(d)	205.17(d)	139.80(d) 129.39(d) 128.37(s) 127.95(d)	87.14	65.89	24.85	28.64	19.20(d) 18.15(d)

a Acyl CO
b Terminal CO
c Signals occur as doublets due to ^{31}P coupling.

It is interesting to note the increase in rate of reaction as the phosphine ligand becomes less bulky and more nucleophilic. The σ-donor nature of a phosphine is largely determined by the substituents on phosphorus, which also affect the ability of the phosphorus atom to act as a π acceptor ligand, [97]. However, the fact that the terminal ν(CO) band does not vary much in the complexes of $[CpRu(CO)(PR_3)]_2[\mu\text{-}C(O)(CH_2)_5C(O)]$ (see Table 6.7, PR_3 = PPh_3, PPh_2Me and $PPhMe_2$), suggests that the observed rate enhancement is a consequence of steric rather than electronic factors. The increase in rate is seen in the decreasing total reaction time (afterwhich no further reaction could be detected by infrared spectroscopy) required to produce compounds (29) (120 hours), (31) (72.5 hours) and (32) (21 hours) respectively.

The rate of reaction was also found to be dependent on the concentration of phosphine. Using a 3:1 molar ratio of PPh_3 to $[CpRu(CO)_2]_2[\mu\text{-}(CH_2)_5]$, the reaction was essentially "complete" (ie. no further reaction detectable) after 90 hours.

In comparison to the mononuclear ruthenium alkyls, $[CpRu(CO)_2(R)]$, these dinuclear alkanediyl complexes, $[CpRu(CO)_2]_2[\mu\text{-}(CH_2)_n]$, appear to undergo CO insertion more "readily". The compounds $[CpRu(CO)_2(R)]$ were reported to react with a large excess of PPh_3 (typically a 5:1 molar ratio) in refluxing xylene to give only 50% reaction, affording $[Cp(CO)(PPh_3)Ru(COR)]$ after 48 hours, [34, 35]. The diruthenium complexes, on the other hand, undergo an analogous CO insertion reaction with an equimolar quantity of PPh_3 to give the monoacyl mono-substituted product $[Cp(CO)_2Ru(CH_2)_5C(O)Ru(CO)(PPh_3)Cp]$ in ca. 46% yield within 20 hours.

However, in comparison to the μ-methylene complex $[CpRu(CO)_2]_2[\mu-(CH_2)]$, the polymethylene bridged diruthenium complexes react extremely slowly with PR_3. The greater reactivity of the former complex has been ascribed to the relief of steric crowding in the product, $[Cp_2Ru_2(CO)_3(PPh_3)]$ $[\mu-C(O)(CH_2)]$, [27].

3.2.2 Chirality of $[CpRu(CO)(PR_3)]_2[\mu-C(O)(CH_2)_5C(O)]$: Effects on ^1H and ^{13}C NMR chemical shifts.

The new mono- and diacyl products (28)-(32) are of interest as they contain either one or two chiral ruthenium centres respectively. Recently, there has been considerable interest in the stereospecificity of organic transformations at such chiral transition metal centres. Of particular relevance to this study are the observations that reactions of the organic ligands bound to the $[CpFe(CO)(PPh_3)]$ fragment are highly stereoselective, [98-100]. Similar stereoselectivity has been observed in the reactions of the analogous chiral rhenium fragment, $[CpRe(NO)(PPh_3)]$, [98]. Such chiral metal centres are potentially useful as mechanistic probes for investigating the reactions occurring at the metal-carbon σ bonds of the organic moiety, LxM-R.

The chirality of the molecules $[CpRu(CO)(PR_3)]_2[\mu\text{-}C(O)(CH_2)_5C(O)]$ is reflected in their ^1H and ^{13}C NMR spectra, (Tables 3.1 and 3.2 respectively). In the ^1H NMR spectra of compounds (29) and (31), five separate resonances, each integrating for two protons, are observed for the polymethylene chain protons (Figure 3.1). In compound (32), two of these signals overlap but are nevertheless recognisable as two distinct resonances. This phenomenon was also observed in the ^1H NMR spectra of $[CpFe(CO)(PR_3)]_2[\mu\text{-}C(O)(CH_2)_5C(O)]$ and attributed to diastereomeric shielding of the methylene protons by the asymmetric $[CpFe(CO)(PR_3)]$ fragments, [23].

Lately, there has been some debate as to whether such chiral transition metal fragments are tetrahedral or octahedral at the metal centre. An early conformational analysis for $[CpFe(CO)(PPh_3)(CH_2R)]$, proposed by Baird et.al. [101], was based on a tetrahedral model. (Scheme 7a). This model was subsequently extended by Gladysz et.al. [102] to a corresponding pseudooctahedral model with approximately the same order of stability of the three possible conformers. (Scheme 7b). However, Davies et.al. have recently and convincingly demonstrated, by means of X-ray crystallographic data for complexes of $[CpFe(CO)(PPh_3)(R)]$ and $[CpRe(NO)(PPh_3)(R)]$, that compounds of this type are clearly octahedral, [98]. (Scheme 7c). This new model predicted a different order of stability of the three conformers (A, B and C) of $[CpFe(CO)(PPh_3)(R)]$ to that predicted by the former models.

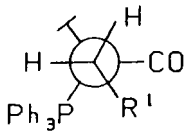

(A) > 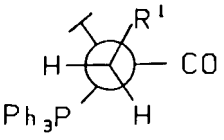

(B) > 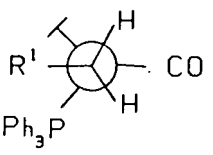

(C) a

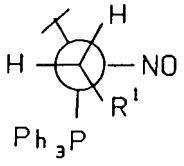

(A) ≃ 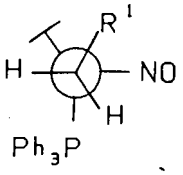

(B) > 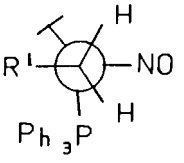

(C) b

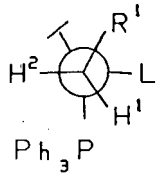

(B) > 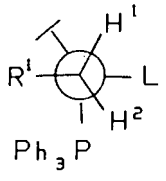

(C) >> 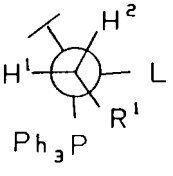

(A) c

(L = CO, NO)

SCHEME 7

Experimental evidence for complexes of this type $[CpFe(CO)(PPh_3)(CH_2R)]$ (where R = alkyl), based on the ^1H NMR chemical shifts of H^1 and H^2 and J_{PH} coupling constants, indicates that only a single conformation (B, Scheme 7c) is populated in the octahedral model. H^1 is found to resonate upfield relative to H^2 since H^1 is shielded by the proximity of the phenyl group, [99].

Applying this octahedral model to the dinuclear ruthenium complexes, $[CpRu(CO)(PR_3)]_2[\mu\text{-}C(O)(CH_2)_5C(O)]$, which is reasonable considering the angles at Ru in $[CpRu(CO)_2]_2[\mu\text{-}(CH_2)_5]$ (see Section 2.2.5), similar non-equivalence of the geminal methylene protons of the alkyl chain (Figure 3.1, H_A / $H_{A'}$) would be expected. Thus, two different chemical shifts would be anticipated in the ^1H NMR spectrum for H_A and $H_{A'}$.

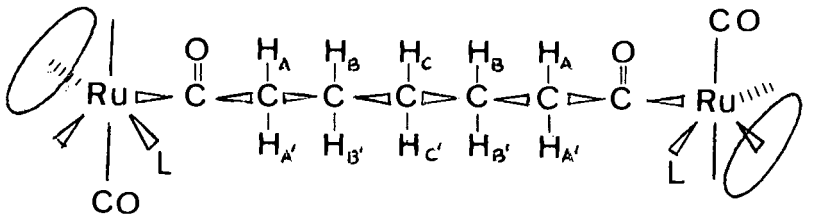

FIGURE 3.1 Diagram depicting the pseudooctahedral structure of the chiral compound, $[CpRu(CO)(L)]_2[\mu\text{-}C(O)(CH_2)_5C(O)]$, and the non-equivalence of the geminal methylene protons

Since five separate resonances, each integrating for two protons are observed in the ^1H NMR spectra of $[CpRu(CO)(PR_3)]_2[\mu\text{-}C(O)(CH_2)_5C(O)]$, it is assumed that the geminal methylene protons, H_A and $H_{A'}$, H_B and $H_{B'}$, are non-equivalent due to chirality of the $[CpRu(CO)(PR_3)]$ fragment. Furthermore, it is assumed that the H_A protons of C_1 and C_5 (Figure 3.1) would be equivalent giving rise to a single resonance. This would explain the observed integration.

This non-equivalence of the geminal methylene protons due to chirality appears to extend only to the C_2 protons. The appearance of only five proton resonances for the alkyl chain protons, implies that H_C and $H_{C'}$ are sufficiently removed from the chiral

centre as to be unaffected by it, and hence give rise to a single resonance.
This phenomenon of chemical shift non-equivalence in chiral and prochiral molecules has also been discussed in detail by Jennings, [103].

The chemical shift non-equivalence of the geminal methylene protons on carbons C_1 and C_2 (and C_4 and C_5) is largest for the PPh_3 derivative (29) where the H_A / H_A, and H_B / H_B, chemical shifts each differ by ca. 0.34 ppm. For the PPh_2Me compound (31), the H_A / H_A, resonances differ by 0.34 ppm while the H_B / H_B, chemical shift separation is only 0.17 ppm. In compound (32) (L = $PPhMe_2$), the H_A / H_A, separation is 0.17 ppm, half that observed for the H_A / H_A, system in compounds (29) and (31). The H_B / H_B, resonances actually overlap in the former complex (32) preventing measurement of this difference.

This trend would suggest that the triphenylphosphine ligand exerts the greatest effect on the chemical shift non-equivalence ("anisochronicity") of the geminal methylene protons. This anisochronicity decreases as the phenyl ligands in PPh_3 are successively replaced by CH_3 in PPh_2Me and $PPhMe_2$. This is presumably due to decreasing shielding of the proton close to the phenyl group (conformation B, Scheme 7c) in PR_3 as the cone angle decreases. Furthermore, PPh_3 being the most bulky ligand would tend to lock the molecule in the most stable conformation (ie. conformation B). With the less bulky phosphines, population of the less favourable conformations A and C may also be possible.

However, in order to verify such statements variable temperature NMR studies, as well as measurement of the J_{PH} coupling constants, is necessary [98].

It is important to note the significant changes in the chemical shifts of the methylene protons and the phenyl substituents as the phenyl groups in PPh_3 are progressively replaced by CH_3. These chemical shifts are observed to decrease in compound (31) (L = PPh_2Me) and increase again in compound (32) (L = $PPhMe_2$) (See Table 3.1). The decrease observed on substitution of one phenyl group in PPh_3 may be due to a decrease in steric interactions in the less bulky phosphine, PPh_2Me. The reason for the subsequent increase in chemical shifts of the methylene protons in the $PPhMe_2$ compound is as yet unknown.

It is interesting that compound (32) (L = $PPhMe_2$) shows two doublets for the methyl proton resonances in the ^1H NMR spectrum. This can be explained by analogy with the organometallic compound $[Cp(CO)(PPhMe_2)Fe(COCH_3)]$ (33), where the geminal methyl groups in the phosphine ligand are reported to be non-equivalent by 0.36 ppm due to the effects of the prochiral phosphorus and chiral iron centres, [104]. This is probably because the time averaged environments of the two methyl groups on the same $PPhMe_2$ ligand are different. (A prochiral centre contains two identical ligands and is so named [105] because if one of these ligands is replaced by a different ligand, a chiral centre is obtained.) Similarly then, the geminal methyl groups in the compound $[CpRu(CO)(PPhMe_2)]_2[\mu\text{-}C(O)(CH_2)_5C(O)]$ (32) are also found to be non-equivalent (by 0.22 ppm) and give rise to two different chemical shifts. Due to coupling of the methyl protons with the

^{31}P nucleus (relative abundance 100%, I=½), each of these signals is split into a doublet.

In the light of the above discussion, one would expect the phenyl groups in the PPh_2Me derivative (31) to be anisochronous due to the prochiral nature of the phosphorus atom and the chiral ruthenium centre. However, such chemical shift non-equivalence is not easily detected in the ^1H NMR spectrum of (31) because of the complexity of the signals arising from the phenyl rings, which is compounded by ^{31}P coupling.

On the other hand, the ^{13}C NMR spectrum of $[CpRu(CO)(PPh_2Me)]_2[\mu\text{-}C(O)(CH_2)_5C(O)]$ clearly reveals that the phenyl rings are indeed non-equivalent in this compound. The ^{13}C NMR spectral data for the compounds (29), (31) and (32) are reported in Table 3.2. Whereas only three doublets and a singlet are observed for the phenyl carbons in both the PPh_3 (29) and $PPhMe_2$ (32) derivatives, six doublets and two singlets are observed in the ^{13}C NMR spectrum of (31). (The signals are doublets due to ^{31}P coupling.) This non-equivalence of two identical ligands at a prochiral centre (PR_2XY) is also reflected in the ^{13}C NMR spectrum of the $PPhMe_2$ derivative (32) where two doublets are observed for the methyl carbon atoms.

These spectral results are thus consistent with the $[CpRu(CO)(PR_2X)]$ fragment being chiral with respect to the ruthenium centre in the compounds (29), (31) and (32) and prochiral with respect to the phosphorus centre in the compounds of $[CpRu(CO)(PR_2X)]_2[\mu\text{-}C(O)(CH_2)_5C(O)]$, (31) and (32).

3.2.3 Possible mechanisms of CO insertion.

Mechanistic studies of the insertion of CO into the metal-carbon sigma bonds of transition metal alkyl complexes have mainly involved $[(CO)_5MnCH_3]$ or related compounds, [106-109]. $[(CO)_5MnCH_3]$ readily inserts carbon monoxide affording the acetyl derivative $[(CO)_5Mn(COCH_3)]$, [86]. Using ^{14}C as a tracer, it has been conclusively proved that the acyl CO is derived from a coordinated CO group and not from the incoming ligand. This CO insertion is more appropriately termed a 1,2-alkyl migration, which probably proceeds via a three centre transition state, [87,110]. (Scheme 8)

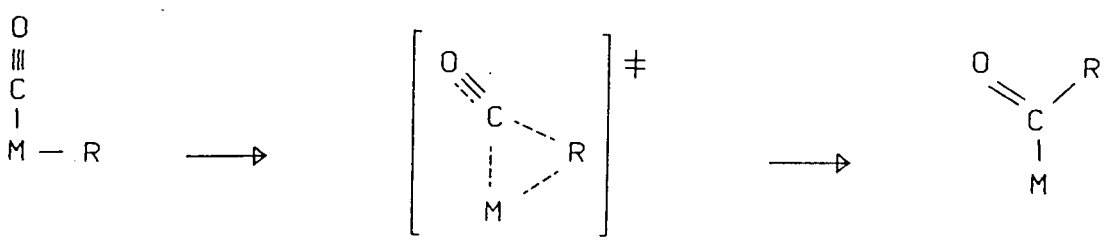

SCHEME 8

The vacant coordination site resulting from such an inter-ligand migration can be occupied by either a coordinating solvent (such as ether) or a suitable donor ligand, L (such as CO, PPh_3 etc.).

Several mechanisms to explain the formation of the observed acyl substitution products, LxM(COR)L, are possible. One of the most widely recognised mechanisms is the (organometallic equivalent of an) S_N1 reaction pathway, where the rate of reaction is dependent

only on the substrate and is therefore independent of the concentration of incoming ligand. Thus, a two step, first order reaction involving only the substrate in the first rate determining step, can be envisaged. (Scheme 9).

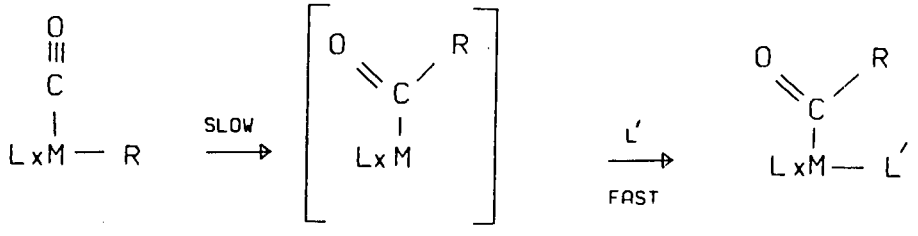

SCHEME 9

Evidence for such an S_N1 mechanism in an organometallic system has recently been observed for the reaction of $[CpFe(CO)_2(t\text{-}Bu)]$ with PPh_3, [111]. A kinetic analysis of this reaction revealed a first order dependence with respect to the iron complex and a zero order dependence with respect to the phosphine ligand over the concentration range of PPh_3 employed. Similar kinetic observations have been reported for the insertion reactions of $[CpFe(CO)_2CH_3]$ induced by PPh_3, [112, 113].

An analogous reaction pathway (Scheme 10) could explain the extremely slow rate of reaction of $[CpRu(CO)_2]_2[\mu\text{-}(CH_2)_5]$ with PR_3 ligands. The isolation of the monoacyl products $[Cp(CO)_2Ru(CH_2)_5C(O)Ru(CO)(PR_3)Cp]$ from the reaction of (7e) with 2 PR_3 (where PR_3 = PPh_3, PPh_2Me), suggests that the reaction occurs in a stepwise manner, in which two S_N1 type insertion

reactions could be seen to occur consecutively as shown in Scheme 10.

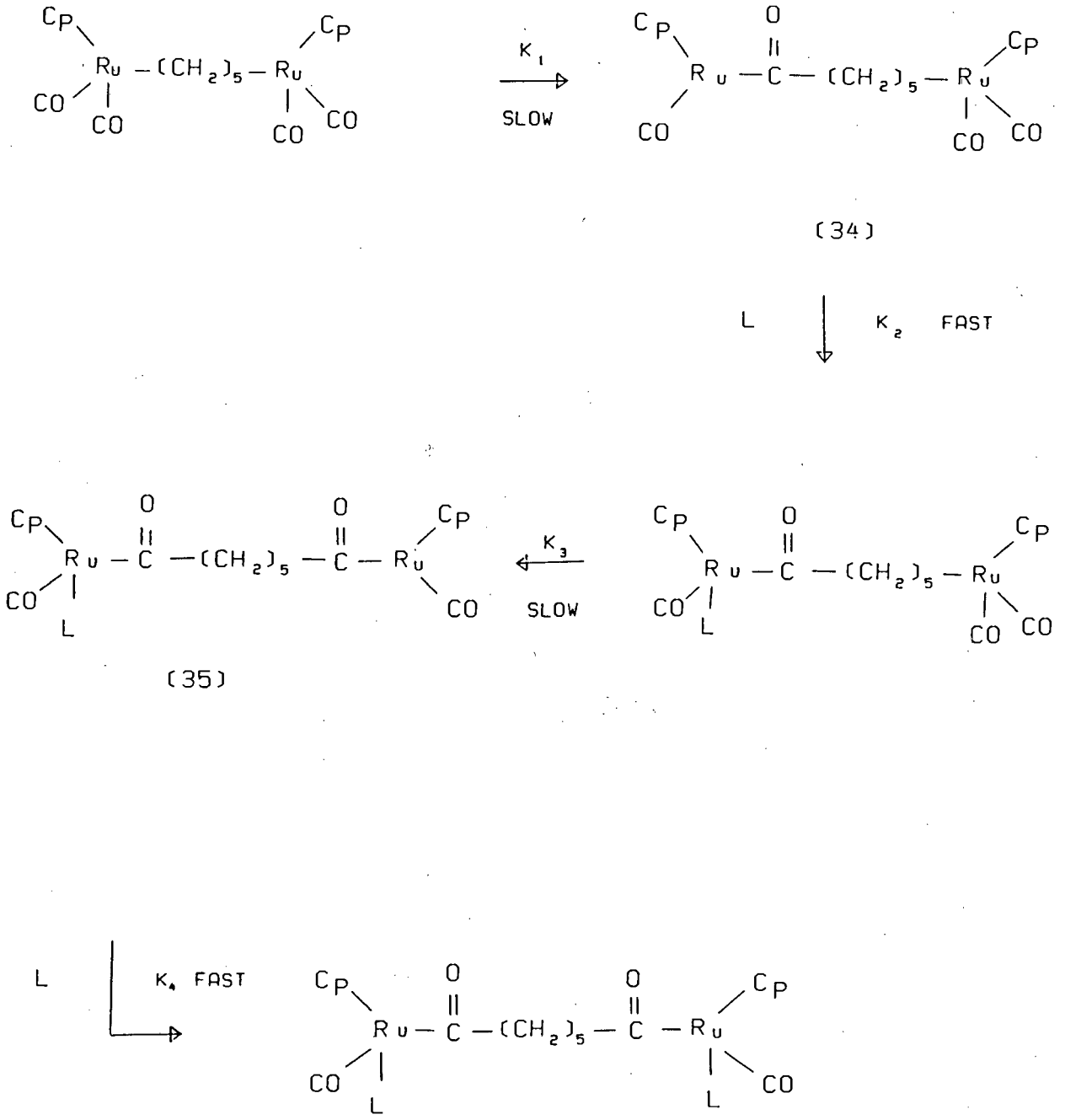

SCHEME 10

Although it is reasonable to assume that $k_1 << k_2$ and $k_3 << k_4$, it is not possible to predict whether k_1 is less than or greater than k_3 from the results available from this study. Further reactivity studies involving actual kinetic measurements of the relative reaction rates k_1 and k_3 are necessary.

It has been suggested that the coordinatively unsaturated intermediates of the type (34) and (35) (Scheme 10) may be stabilised by the formation of a bridging CO coordinated to the second metal atom as in (36) [114] or by the coordination of a nucleophilic solvent (S) [115, 116] as in (37). However, the formation of an intermediate containing a bridging CO ligand would be dependent on the value of n in the alkyl chain. The longer the chain the less stable such an intermediate is expected to be.

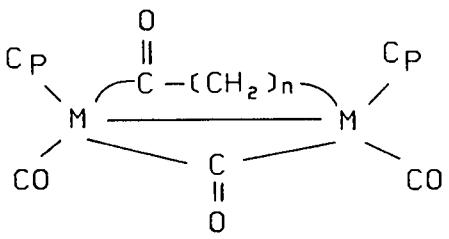

(36)

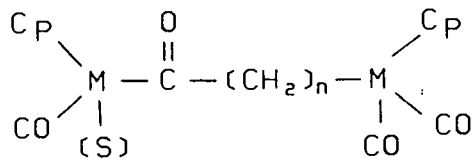

(37)

In a recent report, Halpern et.al. [117] concluded that the rôle of such nucleophilic solvents is not so much to stabilise these

coordinatively unsaturated intermediates but rather to catalyse their formation. In this present study of the CO insertion reactions of $[CpRu(CO)_2]_2[\mu\text{-}(CH_2)_5]$, the effect of a coordinating solvent as either a stabilising or catalysing influence appears to be negligable and temperature plays the major rôle in determining the rate of reaction.

The observation that an increase in the ratio of PPh_3 to substrate, $[CpRu(CO)_2]_2[\mu\text{-}(CH_2)_5]$, results in a significant rate enhancement would suggest, however, that an S_N1 mechanism is <u>not</u> strictly viable here. Furthermore, the fact that the nature and nucleophilicity of the entering PR_3 ligand is observed to have a pronounced effect on the rate of reaction suggests that the ligand <u>is</u> involved in the rate determining step. An alternative associative or S_N2 type mechanism involving the formation of a 19 electron intermediate (38) could account for these observations. (Scheme 11)

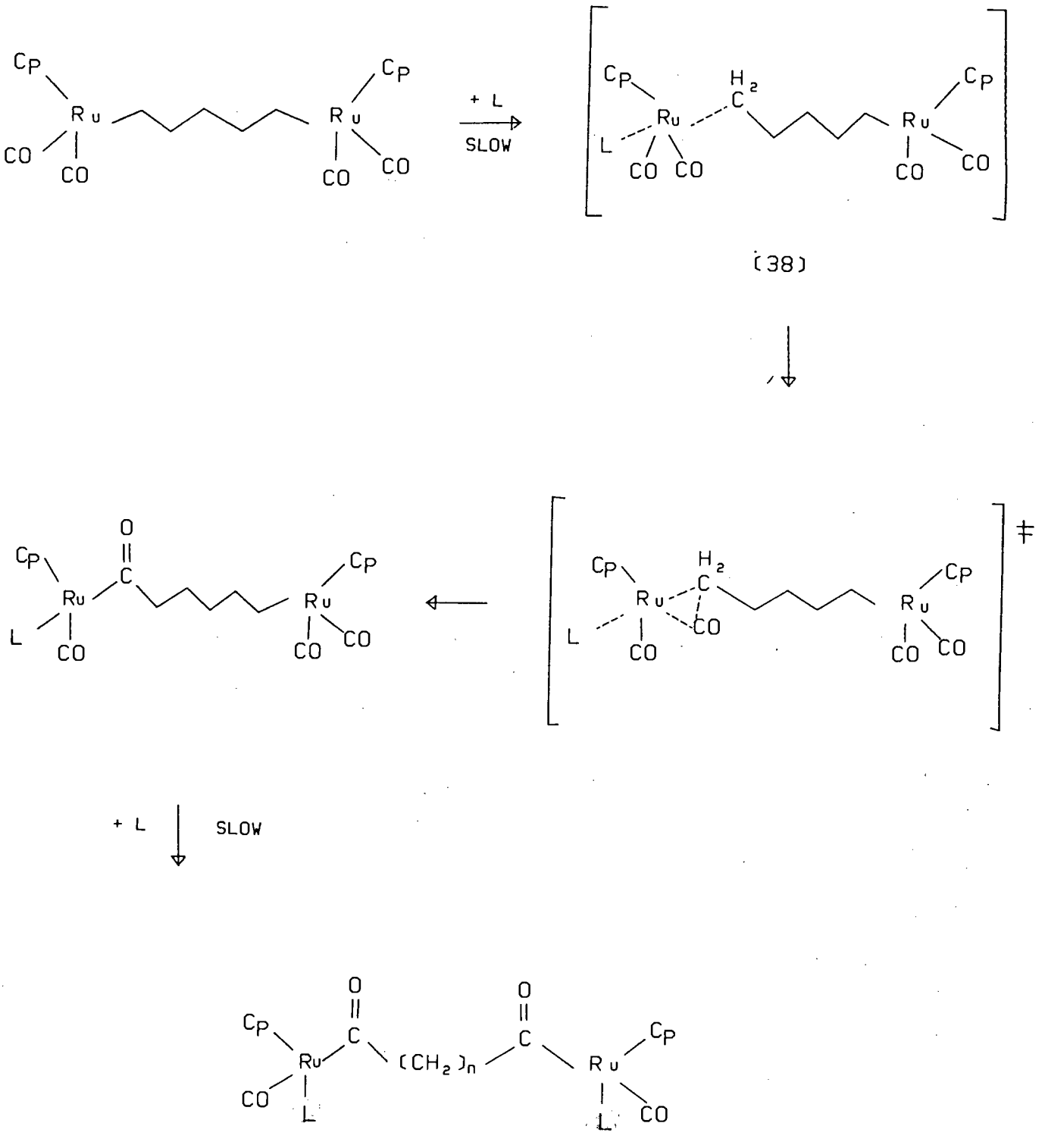

SCHEME 11

Electrochemical and spectroscopic evidence for such a mechanism involving a 19 electron intermediate of type (39) has recently been reported for the oxidatively induced CO insertion reaction of $[CpFe(CO)(PPh_3)CH_3]$ with pyridine, [118]. The data support a mechanism for migratory insertion shown in Scheme 12 and rule out a mechanism where insertion occurs first to give a 15 electron intermediate $[CpFe(PPh_3)(COCH_3)]$ before coordination of the nucleophile.

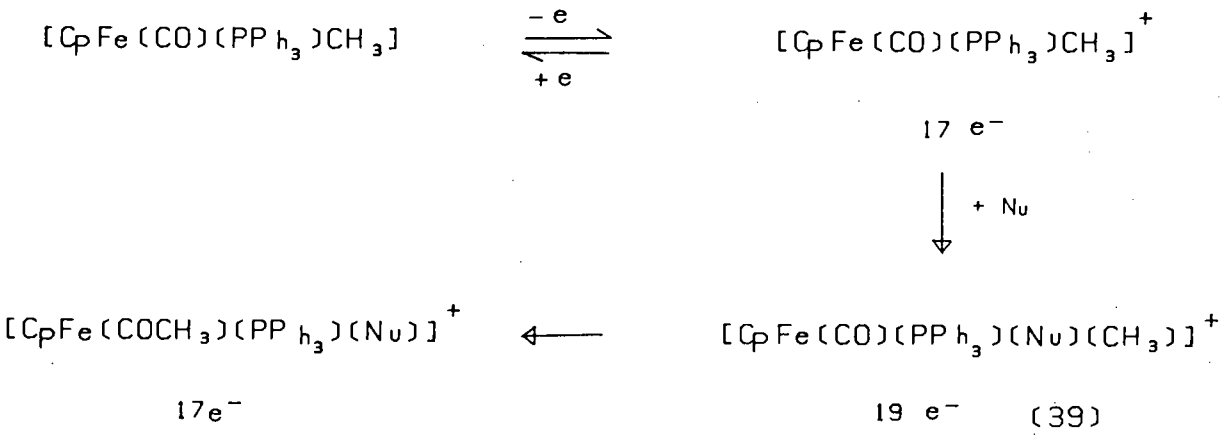

SCHEME 12

Finally, a dissociative mechanism in which CO is dissociated from the ruthenium centre to create a coordinatively unsaturated intermediate of type (40), followed by attack of the nucleophile, L, is unlikely. Such a mechanism would produce the non-acyl substitution products (41) and (42) respectively which are not likely to undergo subsequent CO insertion. (Scheme 13).

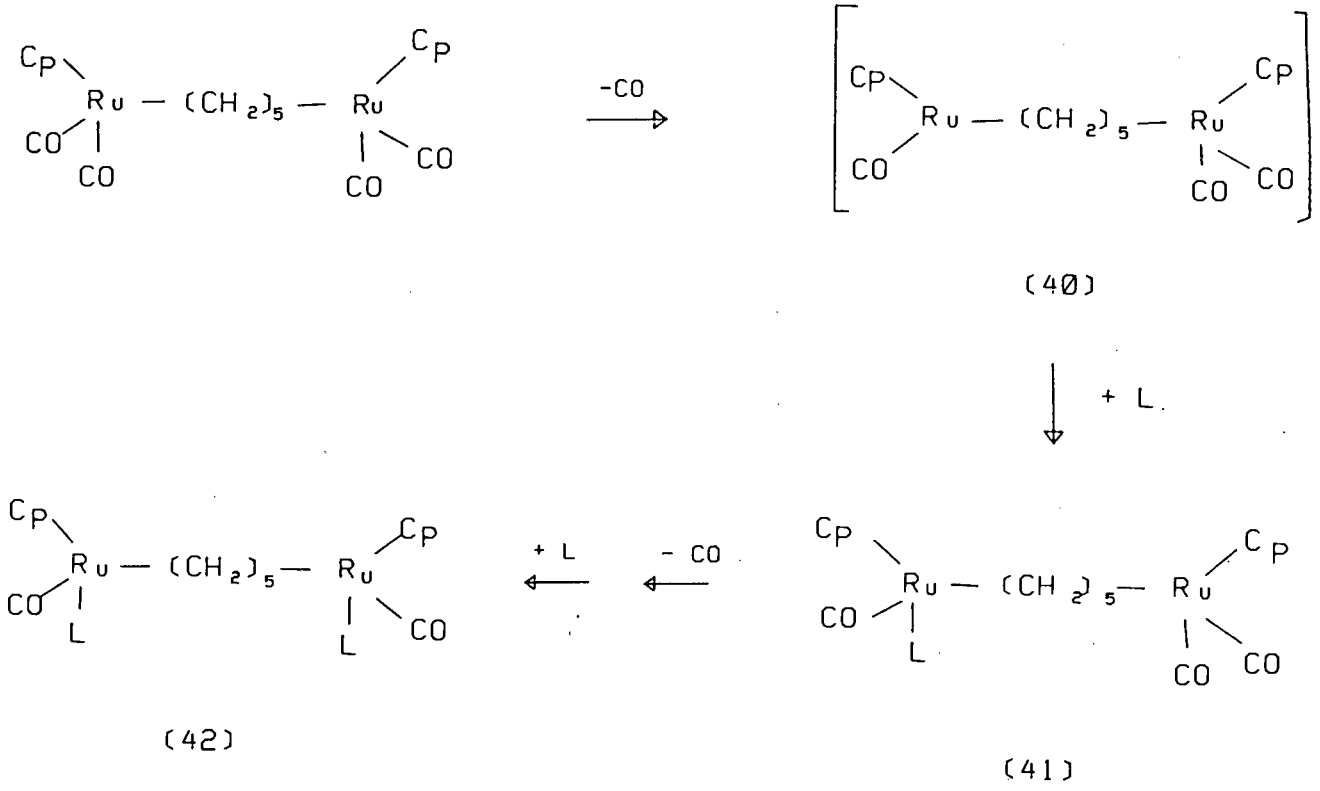

(40)

(42)

(41)

SCHEME 13

However, studies have indicated that the photolysis of the mononuclear ruthenium alkyls, [$CpRu(CO)_2R$], involves dissociative loss of CO as the primary photolysis pathway, [119, 120]. Since the present study is concerned only with thermally induced CO insertion, these results are not directly comparable. Furthermore, the work of Howell et.al. [34, 35] regarding the reactions of

$[CpRu(CO)_2R]$ with tertiary phosphines, did not investigate either the dependence on the concentration of PPh_3 or any other kinetic measurements which allow one to assign either an S_N1, S_N2 or dissociative mechanism to the mononuclear insertion reactions.

In conclusion, the most likely of the mechanisms proposed here is that involving an associative or S_N2 pathway as indicated in Scheme 11. An S_N1 mechanism has been ruled out due to the rate dependence of the insertion reaction on the nature and concentration of phosphine. This is further supported by the formation of the cleavage product $X(CH_2)_nX$ in the reaction of $[CpRu(CO)_2]_2[\mu\text{-}(CH_2)_5]$ with halogens. For systems where the insertion of CO into metal alkyl bonds proceeds readily, for example $[Mn(CO)_5]_2[\mu\text{-}(CH_2)_n]$, the reactions with halogens in a coordinating solvent (THF) have been observed to yield the acid products $HOOC(CH_2)_nCOOH$ on work-up, [121]. Similarly, the mononuclear species $[CpMo(CO)_3CH_3]$ produces CH_3COI on reaction with iodine, [122]. These results imply an S_N1 mechanism where the acyl intermediate is stabilised by the coordinating solvent. For systems of the type studied here, ie. $[CpM(CO)_2]_2[\mu\text{-}(CH_2)_n]$ (M = Fe or Ru), only $X(CH_2)_nX$ is obtained in the reactions with halogens as CO insertion is not assisted by coordination of the solvent in an S_N1 type pathway.

3.3 Results and Discussion: Reactions of $[CpRu(CO)_2]_2[\mu\text{-}(CH_2)_5]$ with Electrophiles.

3.3.1 Reactions with halogens.

The reactions of the dinuclear iron complexes, $[CpFe(CO)_2]_2[\mu\text{-}(CH_2)_n]$ with halogens [23] have already been described in Section 3.1. In this work, the reactions of the analogous diruthenium compounds $[CpRu(CO)_2]_2[\mu\text{-}(CH_2)_5]$ (7e) with bromine and iodine have been investigated. In both cases compound (7e) reacted rapidly with a two molar equivalent of halogen at room temperature to produce the expected cleavage products in high yields. (Equation 15).

$$[Cp(CO)_2Ru(CH_2)_5Ru(CO)_2Cp] \xrightarrow[\text{THF / RT}]{2X_2} 2Cp Ru(CO)_2X + X(CH_2)_5X \qquad 15$$

$$\text{15 mins} \qquad 90\% \qquad (X = Br, I)$$

The ruthenium halide products, $[CpRu(CO)_2X]$ (X = Br or I), were identified by a comparison of their infrared and ^1H NMR spectral data and melting points with reported data for authentic samples [71,123,124], as well as by elemental analysis. The dihalopentanes were identified by their ^1H NMR spectra.

In contrast to the iron compounds (see Section 3.1), no evidence for a cationic species of the type $[Cp_2Ru_2(CO)_4(CH_2)_5]^+$ was observed in the infrared spectra of the reaction mixtures, nor was a product of this type isolated. The cationic species

$[Cp_2Fe_2(CO)_4(CH_2)_4]^+$ was isolated as a cleavage product of the reaction of $[CpFe(CO)_2]_2[\mu\text{-}(CH_2)_4]$ with I_2, [23]. The lack of evidence for a similar diruthenium cation in the reactions of $[CpRu(CO)_2]_2[\mu\text{-}(CH_2)_5]$ with halogens would suggest that, if such a species is formed, it is highly reactive and accumulation of this species is thus negligable. As discussed in Section 3.2.3, the observed cleavage products are consistent with a mechanistic system in which the solvent does not play a stabilising rôle.

3.3.2 Reaction with a trityl salt, $Ph_3C^+PF_6^-$.

The reactions of $[CpFe(CO)_2]_2[\mu\text{-}(CH_2)_n]$ with $Ph_3C^+PF_6^-$ are known to yield the cationic di-iron complexes $\{[CpFe(CO)_2]_2[\mu\text{-}(C_nH_{2n-1})]\}^+$ (where n=3-6), [16,125]. These cationic compounds are apparently formed as a result of β-hydride abstraction from the β carbon atom of $[CpFe(CO)_2]_2[\mu\text{-}(CH_2)_n]$. Few such dinuclear metal stabilised carbonium ions are known, [125]. It was therefore of interest to attempt the preparation of the analogous diruthenium cationic complexes $\{[CpRu(CO)_2]_2[\mu\text{-}(C_nH_{2n-1})]\}^+$ by reaction of $[CpRu(CO)_2]_2[\mu\text{-}(CH_2)_n]$ with $Ph_3C^+PF_6^-$.

However, no reaction of $[CpRu(CO)_2]_2[\mu\text{-}(CH_2)_5]$ (7e) with an equimolar amount of $Ph_3C^+PF_6^-$ in CH_2Cl_2 at room temperature was observed after 23 hours. Only ν(CO) bands due to (7e) at 2009 and 1944 cm^{-1} were detected in the infrared spectrum of the reaction mixture in CH_2Cl_2. This result again reflects the much greater stability and unreactivity of the diruthenium alkanediyls in

comparison to their di-iron analogues. It is likely that the above reaction would proceed either by refluxing in CH_2Cl_2 or in a higher boiling solvent, as was required for the reactions of (7e) with phosphines.

3.4 Results and Discussion: Reactions of $[CpM(CO)_2]_2[\mu\text{-}(CH_2)_5]$ (M = Fe, Ru) with t-Butylisocyanide.

3.4.1 Reaction of $[CpFe(CO)_2]_2[\mu\text{-}(CH_2)_5]$ with t-BuNC.

As far as it is known, no isocyanide (RNC) derivatives of any polymethylene bridged complexes of the type $[CpM(CO)_2]_2[\mu\text{-}(CH_2)_n]$ have previously been prepared. However, numerous studies have been reported on the substitution of carbonyl groups in metal dimers by isocyanide ligands, [82,83,95,96]. In addition, the mononuclear compounds $[CpRu(CO)_2X]$ undergo carbonyl substitution of one or both carbonyl groups by isonitriles (in the presence of substitution catalysts) to afford $[CpRu(CNR)(CO)X]$, $[CpRu(CNR)_2X]$ and $[CpRu(CNR)_3]$, [92b].

It is interesting that studies of the CNR substitution reactions of complexes of the type $[CpM(CO)_2]_2$ have revealed disubstitution in the case of M = Fe, and only mono substitution in the case of M = Ru. It was further found that the osmium dimer, $[CpOs(CO)_2]_2$ did not undergo substitution of CO at all, [96]. These isocyanide substituted metal carbonyl dimers $[Cp_2M_2(CO)_3(CNR)]$ are observed to be fluxional in solution, with rapid exchange of the isocyanide between terminal and bridging positions occurring. This gives rise to a mixture of isomers in solution, [95,96].

Since no other isocyanide derivatives of dinuclear alkanediyl compounds are known, it was of interest to carry out the reactions of $[CpM(CO)_2]_2[\mu\text{-}(CH_2)_5]$ (M = Fe, Ru) with an isocyanide in order to investigate the products.

Thus, $[CpFe(CO)_2]_2[\mu\text{-}(CH_2)_5]$ (5c) was reacted with t-BuNC (t-Bu = $(CH_3)_3C$) in a 1:2 molar ratio in refluxing THF and the reaction monitored by infrared spectroscopy. A gradual disappearance of the strong terminal ν(CO) band at 1998 cm^{-1} and a broadening of the terminal ν(CO) band at 1939 cm^{-1} (both due to (5c)) was observed. The gradual shift of the latter broad band throughout the reaction to the final position at 1935 cm^{-1} suggested a superimposition of the new product ν(CO) band with the reactant ν(CO) band at 1939 cm^{-1}. In addition to the above, a strong ν(CN) band at 2133 cm^{-1} and a new acyl ν(CO) band at 1630 cm^{-1} were also present in the infrared spectra. The reaction was judged to be complete after ca. 22 hours by the total absence of the ν(CO) band at 1998 cm^{-1} due to (5c).

An orange oil (91% crude yield) was extracted and recrystallised from hexane to yield a yellow crystalline solid at -78°C. On warming to ambient temperature, this product melted slowly to give a clear orange-yellow oil. The oil was characterised by microanalysis, infrared, and ^1H and ^{13}C NMR spectroscopy. These results are consistent with the product being the disubstituted, diacyl derivative $[CpFe(CO)(t\text{-}BuNC)]_2[\mu\text{-}C(O)(CH_2)_5C(O)]$ (45). Compound (45) was found to be relatively air and light stable, decomposing slowly - as the pure oil or as a solution in

hydrocarbon solvents - over a period of ca. 48 hours on exposure to air and light. If kept under an inert atmosphere at 0°C, the compound is stable for at least several weeks.

The ^1H NMR data (Table 3.3) for this complex (45) are interesting. As for the chiral molecules, $[CpRu(CO)(PR_3)]_2[\mu\text{-}C(O)(CH_2)_5C(O)]$ (Section 3.2.2), one would expect the chiral complex $[CpFe(CO)(t\text{-}BuNC)]_2[\mu\text{-}C(O)(CH_2)_5C(O)]$ (45) to exhibit a similar non-equivalence of the geminal methylene protons of the alkyl chain. However, this chemical shift anisochronicity is not observed in the ^1H NMR spectrum of compound (45). Instead, a triplet at δ 2.78 ppm (4H) due to the protons in CH_2CO and two multiplets at δ 1.40 ppm and δ 1.14 ppm (2H) for the remaining methylene protons are observed. The signal at δ 1.40 ppm overlaps with the singlet at δ 1.46 ppm for the methyl protons of the t-BuNC group. Together these integrate for 22 protons. The multiplets at δ 1.40 ppm and δ 1.14 ppm have thus been assigned to the protons in $\underline{CH_2}\text{-}CH_2CO$ and the remaining $-CH_2-$ group on the basis of this integration.

The lack of evidence in the ^1H NMR spectrum of (45) for non-equivalence of the methylene protons is probably a result of the small cone angle of the isocyanide ligand in comparison with, for example, the PPh_3 ligand. This assumption is supported by the steady decrease in chemical shift non-equivalence of the geminal methylene protons in $[CpRu(CO)(PR_3)]_2[\mu\text{-}C(O)(CH_2)_5C(O)]$ as the cone angle of the bulky PR_3 ligand decreases. (See Section 3.2.2).

The methylene protons of the compound (45) appear to be slightly more deshielded than in the analogous PR_3 derivatives $[CpFe(CO)(PPh_3)]_2[\mu\text{-}C(O)(CH_2)_3C(O)]$ (46) where the ^1H NMR signals occur at ca. δ 2.60, 1.25 and 0.90 ppm respectively, [23]. Furthermore, the cyclopentadienyl protons of (45) resonate at slightly lower field (δ 4.59 ppm) than those of complexes of type (46) (δ 4.40 ppm). This is probably due to a greater degree of iron-to-carbon π-back bonding in the isocyanide ligand of complex (45) since RNC is known to be a stronger π-acceptor ligand than PR_3, [110]. This is borne out by a comparison of the terminal (CO) stretching frequencies in the infrared spectra of (45) and (46) at 1935 cm^{-1} and 1912 cm^{-1} (both in THF) respectively. The weaker π-acceptor properties of the PR_3 ligand in compounds of type (46) result in greater π-back donation from the metal d orbitals to the π^* orbital of the remaining terminal CO group, thus weakening the CO bond. The lower electron density on the metal atom in (45) therefore, would result in a deshielding of the alkyl chain protons.

The ^{13}C NMR spectrum (Table 3.4) does not reveal any unusual features. The carbons of the alkyl chain were easily assigned by comparison to the ^{13}C NMR spectrum for the compound $[CpRu(CO)(PPh_3)]_2[\mu\text{-}C(O)(CH_2)_5C(O)]$. The terminal CO carbon atom was assigned to the signal at δ 218.65 ppm by comparison to the mixed-metal compound $[Cp(CO)_2Fe(CH_2)_3Ru(CO)_2Cp]$ [25], while the acyl CO carbon was observed at δ 269.6 ppm. The methyl carbons of the tertiary butyl group were assigned to the most intense signal at δ 30.9 ppm (other than the Cp carbon signal). This assignment is in close agreement with the value of δ 28.6 ppm for the CH_3 carbons in $[Cp_2Fe_2(CO)_3(t\text{-}BuNC)]$ [96] and

also falls just outside the range predicted by Leyden and Cox [126] for a CH_3-CR_3 group (ca. 5-30 ppm). The quaternary R_3C-N carbon was assigned to the signal of fairly low intensity at δ 57.43 ppm by comparison to the predicted range of ca. δ 58-73 ppm for R_3C-NR_2', [126]. A resonance of very low intensity was also observed at δ 166.4 ppm. This was assigned to the C=NR carbon atom by analogy with the compound [$Cp_2Fe_2(CO)_3$(t-BuNC)], where the C=N chemical shift for the terminal t-BuNC group is found at δ 157.8 ppm, [96]. This confirms that the t-BuNC group is coordinated in a terminal position in compound (45) and not in a bridging position ($\delta\ CN_{bridging}$ = 239.7 ppm [96]).

TABLE 3.3 ^{1}H NMR data for $[CpFe(CO)(t\text{-}BuNC)]_2[\mu\text{-}C(O)(CH_2)_5C(O)]$ in $CDCl_3$

		δ (ppm)		
C_5H_5	$(CH_2\text{-}CO)$	CH_3	$\underline{CH_2}(CH_2CO)$	$(-CH_2-)$
4.59 (s,5H	2.78 (t,4H)	1.46 (s,18H)	1.40 (m, 4H)	1.14 (m,2H)

TABLE 3.4 ^{13}C NMR (decoupled) data for $[CpFe(CO)(t\text{-}BuNC)]_2[\mu\text{-}C(O)(CH_2)_5C(O)]$ in $CDCl_3$

				δ (ppm)				
CO^a	CO^b	FeC = N	C_5H_5	$(CO\text{-}\underline{CH_2})$	$\underline{C}(CH_3)_3$	CH_3	$\underline{CH_2}CH_2CO$	$(-CH_2-)$
269.6	218.6	166.4	84.6	64.9	57.4	30.9	25.1	28.9

a Terminal carbonyl

b Acyl carbonyl:
s - singlet
t - triplet
m - multiplet

3.4.2 Reaction of $[CpRu(CO)_2]_2[\mu\text{-}(CH_2)_5]$ with t-BuNC.

The reaction of $[CpRu(CO)_2]_2[\mu\text{-}(CH_2)_5]$ (7e) with a two molar equivalent of t-BuNC was carried out in an analogous manner to that of the related iron compound (5c) except that xylene was used as the refluxing solvent. The reaction was monitored by infrared spectroscopy. As in the case of the reaction of the iron complex (5c) with t-BuNC, a gradual decrease in the intensity of the strong ν(CO) band at 2010 cm^{-1} with concomitant broadening of the ν(CO) band at 1946 cm^{-1} (both due to (7e)) was observed. The shifting of the latter band during the course of the reaction to 1944 cm^{-1} suggested a similar superimposition of product and reactant ν(CO) bands as was observed previously in the iron complex. In addition, a new weak acyl ν(CO) absorption at 1628 cm^{-1} and a broad band at ca. 2133 cm^{-1} due to ν(CN) were also present. A large proportion of reactant (7e) was still present after 5 hours so refluxing was continued overnight.

However, an infrared spectrum of the reaction mixture after 21 hours revealed a dramatic change in the products. Besides the broad bands at 2121 and 1944 cm^{-1}, a strong band at 1760 cm^{-1} and two very weak bands at 1734 and 1704 cm^{-1} were also present in the infrared spectrum. The weak acyl absorption band detected earlier in the reaction at 1628 cm^{-1} was no longer present. These new infrared bands are in the region characteristic of both bridging CN (ca. 1730 cm^{-1}) and CO (ca. 1770 cm^{-1}) groups, [96]. It was noted further that the reaction mixture had changed from a pale yellow to an orange coloured solution over the course of the reaction.

From a comparison of the infrared spectrum of the crude product in hexane [2121 (broad, vw), 1974 (mw), 1953 (broad, mw), 1942 (mw) and 1772 (mw)] with the infrared spectrum of $[Cp_2Ru_2(CO)_3(t\text{-BuNC})]$ in hexane [96] [2120, 2075, 1999, 1973, 1955, 1804, and 1775 cm^{-1}], it was initially thought that the crude product was possibly a mixture of $[Cp_2Ru_2(CO)_3(t\text{-BuNC})]$ and the decarbonylated product $[CpRu(CO)(t\text{-BuNC})]_2[\mu\text{-}(CH_2)_5]$. The formation of $[Cp_2Ru_2(CO)_3(t\text{-BuNC})]$ (47) under the conditions of this reaction is quite feasible, since $[CpRu(CO)_2]_2$ undergoes substitution with t-BuNC in refluxing xylene to yield (47) within 24 hours, [96].

On work-up, two products were separated by chromatography. An infrared spectrum of the first orange coloured product (48) in hexane revealed bands at 1974, 1958, 1945 and 1793 cm^{-1} which are characteristic of the unsubstituted ruthenium carbonyl dimer, $[CpRu(CO)_2]_2$, [123].

The second product (49), also a sticky orange residue, showed two broad absorption bands at 2156 (shoulder at 2117 cm^{-1}) and 1969 cm^{-1} in the infrared spectrum in CH_2Cl_2. From the above data, it would seem that (49) is in fact the disubstituted, decarbonylated derivative $[CpRu(CO)(t\text{-BuNC})]_2[\mu\text{-}(CH_2)_5]$. However, further characterisation of both of these products (48) and (49) (isolated in low yields) is necessary to conclusively establish their identity. It would be interesting to see if it is possible to isolate the disubstituted, diacyl product $[CpRu(CO)(t\text{-BuNC})]_2[\mu\text{-}C(O)(CH_2)_5C(O)]$ by allowing a shorter reaction time, as this appears to be the initial (and presumably the kinetically favourable) product of the reaction.

4. CARBON MONOXIDE HYDROGENATION WITH DINUCLEAR ORGANOMETALLIC COMPOUNDS.

4.1 Introduction.

The use of iron and ruthenium as CO hydrogenation catalysts has been discussed in Section 1.3. Binuclear compounds where a hydrocarbon or a CO ligand bridges two metal atoms (either with or without a metal-metal bond) have been proposed as models for the intermediates in several catalytic processes, and in particular the Fischer-Tropsch synthesis, [12,13,127]. Iron compounds are of particular significance, since the only commercial Fischer-Tropsch plants, SASOL I, II and III, use iron-based catalysts.

The mononuclear cyclopentadienyl iron complexes of type $[CpFe(CO)_2R]$ and derivatives of ferrocene $[Cp_2Fe]$ have received considerable research attention in the past, [128]. It has lately become apparent that binuclear (and in particular, heterobinuclear) compounds show novel reactivity and behaviour that is not exhibited by their mononuclear analogues, [57-61, 78-83]. Numerous studies of the chemistry of binuclear cyclopentadienyl iron complexes have been undertaken. For example, the ligand substitution reactions of $[CpFe(CO)_2]_2$ [34,35,95,96], as well as reactions of the hydrocarbon bridged complexes $[Cp_2Fe_2(CO)_2(\mu\text{-}CO)(\mu\text{-}\overline{C\text{-}CH_2CH_2})]$ [129], $[Cp_2Fe_2(CO)_2(\mu\text{-}CO)(\mu\text{-}CHOCH_3)]$ [130], and $[Cp_2Fe_2(CO)_2(\mu\text{-}CO)(\mu\text{-}CH)]^+PF_6^-$ [131] have been investigated.

However, the above complexes all contain metal-metal bonds and far less work has been reported on complexes of the type $[CpFe(CO)_2]_2[\mu\text{-}(CH_2)_n]$ (5), in which the iron atoms are not bonded to each other. An extensive series of the latter compounds where n= 3-12 has been prepared and some of their reaction chemistry (eg. with tertiary phosphines and halogens [23]), has been investigated.

No attempts have, however, been previously made to investigate the CO hydrogenation activity of catalysts prepared from compounds of the type $[CpM(CO)_2]_2[\mu\text{-}(CH_2)_n]$. The object of this study was therefore to investigate the CO hydrogenation activity of supported compounds of $[CpFe(CO)_2]_2$ (5k), $[CpFe(CO)_2]_2[\mu\text{-}(CH_2)_3]$ (5a) and $[CpFe(CO)_2]_2[\mu\text{-}(CH_2)_5]$ (5c). See Figure 4.1.

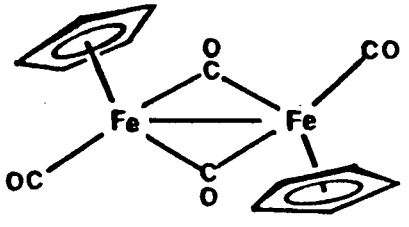

(5k) n=0

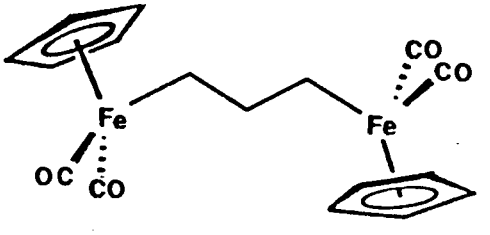

(5a) n=3

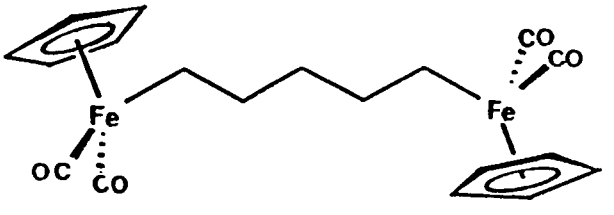

(5c) n=5

FIGURE 4.1 Complexes of $[Cp(CO)_2Fe(CH_2)_nFe(CO)_2Cp]$ (n=0, 3 & 5) used to study the effect of Fe-Fe separation on CO hydrogenation activity

The Fe-Fe separations in these three unsupported catalyst precursors are 2.53 Å (5k) [132], 6.14 Å (5a) [133] and 8.6 Å (5c) [134] respectively. We were interested to see what effect, if any, this range of Fe-Fe separations in the catalyst precursors might have on the CO hydrogenation activity and product selectivity of the supported compounds (5k'), (5a') and (5c') after decomposition.

The three catalyst precursors were thus supported on γ-alumina and decomposed at 250°C to produce the catalytic materials. In order to ascertain the decomposition temperatures and thermal behaviour of the samples, the three unsupported compounds were investigated by Differential Scanning Calorimetry. In appropriate cases, the volatile products of some of the thermal decompositions were analysed by G.C. and G.C-M.S techniques. In addition, the behaviour of the compounds supported on γ-alumina was studied by Diffuse Reflectance FT-Infrared Spectroscopy.

4.2 Results and Discussion

4.2.1 Diffuse Reflectance Fourier-Transform Infrared Studies

Samples of compounds (5k), (5a) and (5c) were supported on γ-alumina and the diffuse reflectance FT-IR spectra of these supported materials recorded in the ν(CO) region (2500 -1600cm^{-1}). The FT-IR spectra of the unsupported compounds, as KBr powders, were also recorded and compared to those of the supported samples.

In the case of compound (5k), the infrared spectrum of the unsupported material as a KBr powder revealed two very strong carbonyl absorption bands centred at 1950 and 1760cm^{-1}. Both these absorptions appeared as double bands. However, in the infrared spectrum of the Al_2O_3 supported compound (5k'), the highest frequency carbonyl absorption occurs at about 1970cm^{-1}. This shift in the carbonyl absorption frequency suggests that compound (5k), $[CpFe(CO)_2]_2$, interacts with the Al_2O_3 support.

Similar shifts in the carbonyl stretching frequencies were observed when either compound (5a) or (5c) was supported on γ-alumina.

Supported samples of compounds (5k) and (5c) were then decomposed under various conditions of temperature and pressure (i.e. under N_2 or vacuum) and the infrared spectra of these decomposed materials recorded. The infrared spectra of samples heated at 145°C for 1 hour showed no change in the carbonyl region when compared to the spectra of the unheated compounds. However, after heating at 180°C for 0.25 hour, no carbonyl bands were observed in the infrared spectra of either of the supported compounds (5k') and (5c') in the region 2200-1600cm^{-1}. It was concluded that either both terminal carbonyl groups had been removed on heating at temperatures between 150° and 180°C or that an interaction with the Al_2O_3 support (e.g. Fe-C-O-Al) lowers the ν(CO) absorption below 1600cm^{-1}. It was decided that all the supported catalysts should be decomposed at 200°C, or above, before the CO-hydrogenation reaction was started. It should also be noted that during decomposition of the supported samples (5k'), (5a') and (5c'), ferrocene crystals (identity confirmed by mass

spectrometry) sublimed onto the necks of the flasks. This suggests that, during decomposition, a decarbonylated species of the type [(η^5-C_5H_5)Fe] could be formed on the alumina surface. It is pertinent to note that ferrocene is also observed as a product of the thermal decomposition of (5a) and (5c) as pure solids, [19].

4.2.2. Thermal Decomposition Studies of (5k), (5a) and (5c) by Differential Scanning Calorimetry (DSC)

The thermal decomposition of unsupported samples of (5k), (5a) and (5c) was studied by Differential Scanning Calorimetry. Samples of (5) were heated from ambient temperature (20°C) to 350°C at a rate of 5°C/min in pans sealed hermetically in air or in open pans under hydrogen. The DSC traces of Heat Flow (mW) versus Temperature (°C) show a vast difference in behaviour of the samples heated in air to that of the samples heated under hydrogen.

The DSC traces for the samples of (5k), (5a) and (5c), heated in pans sealed in air, all show the following features:

(i) the melting point of the particular compound as a sharp endotherm (T_1) and

(ii) a broad strong endotherm with T_{max} at ca. 285°C (T_3).

In addition to these peaks, the samples of (5a) and (5c) also exhibit broad exothermic peaks (T_2) with T_{max} at 143°C (shoulder at 178°C) and T_{max} 158°C (shoulder ca. 181°C) respectively. See Table 4.1.

Both the endothermic peak (T_1) (melting point) and the exothermic peak, (T_2), correspond well to those reported for the thermolysis of $[CpFe(CO)_2]_2[\mu\text{-}(CH_2)_n]$ under N_2 studied by DSC, [19]. The exotherm was reported [19] to be due to decomposition of the polymethylene bridged compounds. As these compounds were only heated to 230°C (500K), the high temperature endotherms (T_3) observed in the present study at 285°C were not observed previously, [19]. We propose that the exotherms, (T_2), are due to the decomposition of $[CpFe(CO)_2]_2[\mu\text{-}(CH_2)_n]$ by loss of the alkyl chain first to form $[CpFe(CO)_2]_2$, followed by loss of terminal CO groups (shoulders on T_2).

$[CpFe(CO)_2]_2$ is a known decomposition product of the complexes of $[CpFe(CO)_2]_2[\mu\text{-}(CH_2)_n]$, [19]. This would also be consistent with the G.C. decomposition studies (Section 4.2.3) where heating of (5a) or (5c) at 120°C resulted in loss of the alkyl chain and also with the FT-IR decomposition studies where the terminal ν(CO) bands disappeared on heating samples of (5a) and (5c) above 150°C. Furthermore, an infrared spectrum (in hexane) of $[CpFe(CO)_2]_2[\mu\text{-}(CH_2)_n]/Al_2O_3$ (decomposed at 120°C) revealed three strong bands at 2007, 1954 and 1793cm^{-1}, confirming the formation of $[CpFe(CO)_2]_2$ as an initial decomposition product in the thermolysis of $[CpFe(CO)_2]_2[\mu\text{-}(CH_2)_n]$.

The broad endotherm, (T_3), observed in the DSC traces of (5k), (5a) and (5c) at ca. 285°C was initially thought to be due to decomposition of the tetramer $[CpFe(CO)]_4$, which could be formed during the loss of terminal CO groups from $[CpFe(CO)_2]_2$.

$[CpFe(CO)]_4$ has been prepared by refluxing $[CpFe(CO)_2]_2$ in xylene for 12 days [136] and by the photolysis of $[CpFe(CO)_2]_2$ in refluxing xylene (7 days), [137]. This reaction was found to proceed rapidly (7 hours) in the presence of a small amount of PPh_3 at 140°C, [138]. According to King [136], $[CpFe(CO)]_4$ forms dark green/black air stable crystals which decompose above 220°C without melting. The X-ray structure of $[CpFe(CO)]_4$ shows a tetrahedral arrangement of iron atoms and a three-way bridging carbonyl in each of the four faces of the iron tetrahedron, [139].

To test this hypothesis, i.e. that on heating samples (5k), (5a) and (5c) to ca. 280°C a tetrameric species $[CpFe(CO)]_4$ is formed, a sample of pure (5c) was heated to 270°C and a mass spectrum of the dark black residue recorded.

These mass spectral results show the highest mass at m/e 740 and several peaks at m/e values reported in the mass spectrum of the tetramer [140] and of $[CpFe(CO)_2]_2$, [76]. On this basis, we propose that a pentameric species $[CpFe(CO)]_5$ (M^+ = 745) may be formed during high temperature decomposition of samples (5a) and (5c) giving rise to the endotherm, (T_3).

Decomposition of (5k) under an H_2 flow gave a broad exothermic peak with T_{max} at 163°C followed by a broad endotherm at ca. 185°C (See Table 4.2). The former exothermic peak (T_2) may be due to the formation of the iron hydride $[CpFe(CO)_2H]$, which is a known product of the thermolysis of $[CpFe(CO)_2]_2$ in hydrogen, [141]. The endotherm (T_3) could then be assigned to the decomposition of this iron hydride species.

When samples (5a) and (5c) were heated under a hydrogen flow, the same endothermic melting points (T_1) as those observed in air were seen in the DSC traces as well as the broad exothermic peaks (T_2) with T_{max} at ca. 155°C and ca. 160°C for (5a) and (5c) respectively (See Table 4.2). However, instead of the broad endotherm observed in air at ca. 285°C, several sharp exothermic peaks occur in the DSC traces of the samples decomposed under H_2 with T_{onset} at 206°C for $[CpFe(CO)_2]_2[\mu\text{-}(CH_2)_3]$ and 217°C for $[CpFe(CO)_2]_2[\mu\text{-}(CH_2)_5]$. These exothermic peaks may be due to reduction of a cluster species, such as the tetramer $[CpFe(CO)]_4$ postulated as a decomposition product of $[CpFe(CO)_2]_2$ as above.

TABLE 4.1 DSC results for the compounds $[CpFe(CO)_2]_2[\mu\text{-}(CH_2)_n]$ (n=0, 3 and 5) decomposed in hermetically sealed pans in air

Compound	Melting Range (°C)	T_1(endo) (°C)		T_2(exo)(°C)		T_3(endo)(°C)	
		Tonset[c]	Tmax[d]	Tonset	Tmax[e]	Tonset	Tmax
5k	194 dec[a]	194	197	-	-	275	285
5a	104-105[b]	103	105	116	143(178)	274	283
5c	83-85[b]	83	85	134	158(181)	283	290

a Reference [135]

b Reference [19]

c Temperature corresponding to onset of peak

d Temperature corresponding to peak maximum

e Values in parenthesis represent Tmax of shoulders on the main peak

TABLE 4.2 DSC results for the compounds $[CpFe(CO)_2]_2[\mu\text{-}(CH_2)_n]$ (n=0, 3 and 5) decomposed in open pans under hydrogen

Compound	Melting ranges °C	T_1(endo)(°C) Tonset[c]	Tmax[d]	T_2(exo)(°C) Tonset	Tmax	T_3(exo)(°C) Tonset
5k	194 dec[a]	-	-	146	164	ca. 182[e]
5a	104-105[b]	103	104	ca.130	153	206[f]
5c	83-85[b]	83	84	ca.130	157	218[f]

a Reference [135]

b Reference [19]

c Temperature corresponding to onset of peak

d Temperature corresponding to peak maximum

e Temperature thought to be due to decomposition of $[CpFe(CO)_2H]$

f Temperature corresponds to onset of a series of sharp exothermic peaks

4.2.3. Thermal decomposition of Al_2O_3 - supported complexes (5a) and (5c) under CO/H_2 (50:50) : Gas chromatography

Polymethylene bridged complexes of the type $LxM-(CH_2)_n-M^1Ly$ have been proposed as models for the polymerisation of methylene groups on a metal surface. With this in mind, supported samples of $[CpFe(CO)_2]_2[\mu-(CH_2)_n]$ (n=3 or 5) were reacted with CO/H_2 (50:50) at atmospheric pressure and elevated temperatures. Under these conditions, no evidence for CO insertion with these systems was found. However, the related complex $[Mn(CO)_5]_2[\mu-(CH_2)_4]$ has been found to react with CO/H_2 in solution to yield $HOCH_2(CH_2)_4CH_2OH$ which can be formed by two CO insertions followed by reduction, [142].

A small glass reactor (shown in Figure 4.2) was prepared such that CO/H_2 gas (or N_2 gas) could pass through the undecomposed, supported catalyst whilst heating. Gas samples were collected at intervals of three minutes in sealed bottles (filled with N_2) by means of two syringes attached to the base of the reactor (one inlet, one outlet syringe).

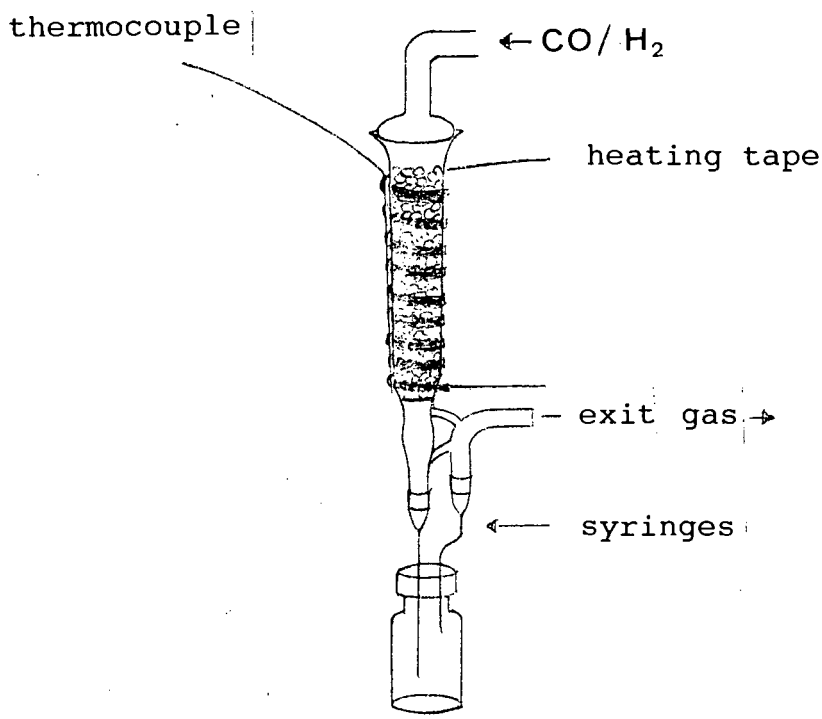

FIGURE 4.2 Microreactor used to study the thermal decomposition of $[CpFe(CO)_2]_2[\mu\text{-}(CH_2)_n]$ (n=3 and 5) under CO/H_2

Gas chromatography revealed that only C_5 products in the case of $[CpFe(CO)_2]_2[\mu\text{-}(CH_2)_5]/Al_2O_3$ and C_3 products in the case of $[CpFe(CO)_2]_2[\mu\text{-}(CH_2)_3]/Al_2O_3$, as well as an unknown component (X) in the C_6 region (the same in both cases), were formed when the

catalysts were heated at 120°C under a CO/H_2 flow. This is consistent with the loss of the $-(CH_2)_n-$ bridge. The same gas products were observed when the catalysts were heated under nitrogen, indicating that the observed products were derived from the decomposition of the supported catalysts and not from a reaction of the catalyst with CO/H_2. For $[CpFe(CO)_2]_2[\mu-(CH_2)_5]/Al_2O_3$, the major organic decomposition product was identified as pentene, while $[CpFe(CO)_2]_2[\mu-(CH_2)_3]/Al_2O_3$ produced both propene and cyclopropane. These products are consistent with those reported previously for the thermal decomposition of the pure solid compounds (5a) and (5c), [19].

In order to identify the unknown component (X), supported samples of (5a) and (5c) were decomposed at 120°C and the volatile organic products analysed by GC-MS. The mass spectra of the gaseous products showed identical peaks for both (5a) and (5c), the most intense peaks being at m/e 91, 92 and 65. In both cases, the highest mass observed was at m/e 354 (of very low intensity) which can be explained by the decomposition of (5a) or (5c) to $[CpFe(CO)_2]_2$ (M = 354) by loss of the alkyl bridge. $[CpFe(CO)_2]_2$ is a known product of the thermolysis of the unsupported complexes of $[CpFe(CO)_2]_2[\mu-(CH_2)_n]$, [19]. This assignment is confirmed by the presence of two other peaks of very low intensity at m/e 177 and m/e 149, which are assigned as $[CpFe(CO)_2]^+$ and $[CpFe(CO)]^+$ respectively on the basis of the reported mass spectrum of $[CpFe(CO)_2]_2$, [76].

The peaks at m/e 92 and m/e 91 can be assigned to the ions $[C_5H_4CO]^+$ and $[C_5H_3CO]^+$ respectively which could be formed by the migration of a CO group to the cyclopentadienyl ring.

It is therefore proposed that the unknown component (X) in the gas chromatogram of the volatile decomposition products could be $[(C_5H_5)CHO]$ which is formed by migration of a CO group to the Cp ring during decomposition of the samples $[CpFe(CO)_2]_2[\mu\text{-}(CH_2)_n]$. The identification of the ions at m/e 91 and 92 could be confirmed by high resolution mass spectrometry.

4.2.4. Preliminary Catalytic Studies: CO hydrogenation using decomposed samples of $[CpFe(CO)_2]_2[\mu\text{-}(CH_2)_n]$ (n=0, 3 and 5) supported on γ-alumina.

The complexes (5k), (5a) and (5c) were supported on calcined and pelleted γ- alumina using the incipient wetness technique [143,144] to give a 5% metal loading in each case. These samples were then decomposed under a strong nitrogen flow at 200°C for 2-3 hours, and the resulting materials used as catalysts for the hydrogenation of carbon monoxide. Each catalyst was tested for Fischer-Tropsch activity at 250°C / 1 atm (in a glass reactor) and at 250°C / 5atm (in a stainless steel reactor) by treatment with a premixed 50:50 CO/H_2 mixture. For the atmospheric pressure runs, the decomposed catalysts were further reduced under hydrogen (10 ml/min) for 2-3 hours before treatment with CO/H_2. In the high pressure catalytic runs, the catalysts were reduced under H_2

(10ml/min) for 16 hours at 200°C and then treated with the CO/H_2 mixture at 250°C. The gas products obtained were analysed by gas chromatography.

The results of these preliminary studies showed a significant difference in the catalytic behaviour of the compounds of $[CpFe(CO)_2]_2[\mu\text{-}(CH_2)_n]$, where n=0, 3 or 5, supported on γ-alumina. Whereas compound (5k) on alumina behaves as a Fischer-Tropsch catalyst at 250°C / 1atm (CO/H_2) producing methane and light hydrocarbons, the supported compounds (5a') and (5c') are virtually inactive under the same conditions. Compound (5c') showed little activity even at 250°C / 5atm (CO/H_2).

Furthermore, the early GC traces of the atmospheric pressure runs using $[CpFe(CO)_2]_2[\mu\text{-}(CH_2)_n]/Al_2O_3$ (n=4,5) showed a large peak in the C_5 region which was not observed in the early GC traces for the identical runs carried out with $[CpFe(CO)_2]_2/Al_2O_3$, (5k'). This peak, which decreased in area and finally disappeared over several hours on-line, was thought to be due to degradation of the cyclopentadienyl ring and implied that the supported complexes $[CpFe(CO)_2]_2[\mu\text{-}(CH_2)_n]/Al_2O_3$ decompose in an entirely different manner to supported iron dimer, (5k'). The supported catalysts, $[CpFe(CO)_2]_2[\mu\text{-}(CH_2)_n]$, behaved as conventional iron catalysts, such as $[Fe(NO_3)_3]/Al_2O_3$ [145], thereafter.

4.2.5 Catalytic Studies: CO hydrogenation using decomposed samples of $[CpFe(CO)_2]_2[\mu\text{-}(CH_2)_n]$ (n=0, 3 and 5) supported on γ-alumina.

Due to the very low CO hydrogenation activity exhibited by the supported hydrocarbon bridged complexes, $[CpFe(CO)_2]_2[\mu\text{-}(CH_2)_n]/Al_2O_3$, at 250°C / 1 atm CO/H_2, subsequent catalytic runs were conducted at 250°C / 5 atm only. The method of decomposition and reduction of the supported materials was also modified and the catalyst precursors prepared immediately prior to use, whenever possible.

Samples of the three compounds (5k), (5a) and (5c) were thus supported on calcined, pelleted $\gamma\text{-}Al_2O_3$ using the incipient wetness technique [143,144], to give a 5% metal loading. The supported materials were then loaded to fixed-bed microreactors and reduced at 250°C under hydrogen (gas hourly space velocity, GHSV = 300 h^{-1}) for ca. 25 hours to give the final catalyst. (See Experimental for full details). Premixed CO/H_2 (1:1 v/v) was reacted over the catalyst at a constant flow rate (GHSV = 300 h^{-1}) and pressure of 500 kPa. The resulting volatile gas products were analysed by on-line gas chromatography. The reactor effluent was cooled to trap liquid products which are currently being analysed by chromatography. Each catalytic run was performed in duplicate to ensure reproducibility of results.

Comparison of the activities of the three different supported systems revealed the catalyst prepared from $[CpFe(CO)_2]_2[\mu\text{-}(CH_2)_3]/Al_2O_3$ (5a') to be the most active, producing the highest conversion of CO (estimated at 15% on the

basis of hydrocarbon area counts). The non-bridged system, $[CpFe(CO)_2]_2/Al_2O_3$ (5k') was slightly less active producing ca. 10-12% conversion. On the other hand, the catalyst prepared from $[CpFe(CO)_2]_2[\mu\text{-}(CH_2)_5]/Al_2O_3$ (5c') exhibited little activity (ca. 3% conversion) under identical conditions (250°C / 5 atm).

These preliminary results suggest that the increasing Fe-Fe separations in the catalyst precursors (5k), (5a) and (5c) may indeed be the cause of the differences in observed activity for the three systems. It would thus appear that the dispersion of the catalytically active metal compound on the support is an important factor in determining CO hydrogenation activity. The Fe-Fe separation produced by the catalyst precursor (5a) seems to provide the optimum dispersion of iron atoms on the alumina support in the three systems studied. However, other factors, as yet unknown, may also be affecting the catalytic activities.

The state of dispersion of the catalytically active metal is also considered to be an important factor in controlling hydrocarbon chain length, [146]. However, comparison of the gaseous product distribution of the three catalyst systems shows little difference in product selectivity. In all cases, methane and light C_2-C_3 hydrocarbons were produced as the major products of the CO hydrogenation. Both (5k') and (5a') gave aqueous and organic liquid products, while (5c') produced only small quantities of organic products as a result of the much lower activity of the latter. These liquid products are currently being analysed.

Increasing the CO/H_2 flow rate (GSHV = $600h^{-1}$) for the system $[CpFe(CO)_2]_2[\mu-(CH_2)_5]/Al_2O_3$ resulted in diminished activity as would be expected due to the decreased residence time of the gas in the reactor. On the other hand, a decrease in the CO/H_2 flow rate (GSHV = 150 h^{-1}) resulted in significant enhancement of activity to give ca. 15% (estimated) conversion.

These results report the preliminary studies on the use of supported compounds of type $[CpM(CO)_2]_2[\mu-(CH_2)_n]$ as catalyst precursors in the hydrogenation of CO, [147]. Further studies are currently in progress (P. Johnston, N. J. Coville and G. J. Hutchings, Chemistry Department, University of the Witwatersrand) in order to quantify conversions and product percentages and identify the liquid products of the catalysed CO hydrogenation reactions. Future studies on compounds of type $[CpM(CO)_2]_2[\mu-(CH_2)_n]$ containing different transition metals (and in particular heterobimetallic systems) and varying chain lengths, are also to be investigated.

5. SYNTHESIS AND CHARACTERISATION OF μ(α,ω)-ALKANEDIYL COBALOXIMES AND THEIR MONONUCLEAR HALOALKYL PRECURSORS.

5.1 Introduction

The cobalt(III) complexes of dimethylglyoxime, $[Co(DH)_2LR]$ (where L = a base such as pyridine, DH = monoanion of dimethylglyoxime and R = an alkyl group such as (CH_3)), known commonly as the "cobaloximes" (Figure 5.1), have been used extensively as models for the vitamin B_{12} complexes, [148-154].

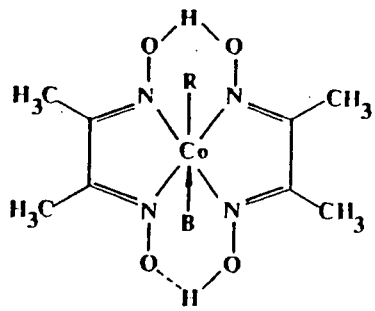

FIGURE 5.1 Structure of a typical cobaloxime compound as a model for vitamin B_{12}

The analogies between the chemical behaviour of vitamin B_{12} and the cobaloximes have been ascribed to the similarities in the coordinating power of the sp^2-hybridized nitrogen atoms surrounding the cobalt atom in both types of compound, [152].

As part of a general study of μ(α,ω)-alkanediyl transition metal complexes, preliminary studies of the synthesis of the dinuclear

cobaloximes $[Co(DH)_2py]_2[\mu\text{-}(CH_2)_n]$ (51) and their mononuclear haloalkyl precursors $[Co(DH)_2py(CH_2)_nX]$ (50), were carried out during an Honours project, [155]. However, only the new complexes of type (50) (where n=3-5, X=Br; n=3, X=I) and (51) (where n=7) were prepared and characterised during this period.

The preparation of dinuclear polymethylene bridged cobaloximes where n=3 and 4 has previously been briefly reported by Schrauzer and Windgassen, [149]. However, these compounds were only partially characterised at the time. Such binuclear cobaloximes may also be considered as models for vitamin B_{12} of type $[Co(DH)_2LR]$ (L = axial base), where R incorporates not only an alkyl group but also a metal atom carrying its own ligand system.

It is interesting to note that Smith and co-workers [156] attempted the preparation of dinuclear polymethylene bridged vitamin B_{12s} complexes. They found that such dimeric coenzyme analogues were only formed if the length of the bridging carbon chain exceeded three ($-CH_2-$) units, as predicted by Crowfoot-Hodgkin and quoted in [156]. This is probably due to steric interference of the bulky ligands in the cobalamin. The dimeric nature of these complexes appears to have been established by analysis of halogen content and by paper chromatography.

Thus, no reaction of 1,2-dibromoethane with vitamin B_{12s} was observed while dibromomethane and 1-chloro,3-bromopropane gave only halogen containing monomers as shown in Equation 16a. However, reaction of vitamin B_{12s} with 1,4-dibromobutane yielded a

"halogen-free" bridged dimer as the major product under all reaction conditions even when a large excess of dibromobutane was used. (See Equation 16b)

$$[Co] + X\text{-}(CH_2)_n\text{-}X \longrightarrow [Co]\text{-}(CH_2)_nX \qquad \underline{16a}$$

(1) X=Br, n=1

(2) X=Br, Cl, n=3

[Co] = vitamin B_{12s}

$$[Co] + X\text{-}(CH_2)_4\text{-}X \longrightarrow [Co]\text{-}(CH_2)_4\text{-}[Co] + [Co](CH_2)_4\text{-}X \qquad \underline{16b}$$

(3) X=Br

The minor product, the bromobutyl B_{12s} monomer, could be extracted and reacted further with B_{12s} to form the dimer, [156]. This reaction was observed to occur even more rapidly than that with the dihaloalkane.

With the exception of the dinuclear polymethylene bridged cobaloximes prepared by Schrauzer (with n=3 or 4) [149] and the vitamin B_{12s} dimer (n=4) prepared by Smith et al. [156], no other binuclear complexes of cobalt without a metal-metal bond are known. However, dicobalt methylene and polymethylene bridged complexes containing cobalt-cobalt bonds and ligands such as cyclopentadienyl and carbon monoxide and bis(diphenylphosphino)methane are known. These have been covered in two recent reviews by Moss et.al [12] and Casey et.al. [13]. Some examples are shown in Figure 5.2.

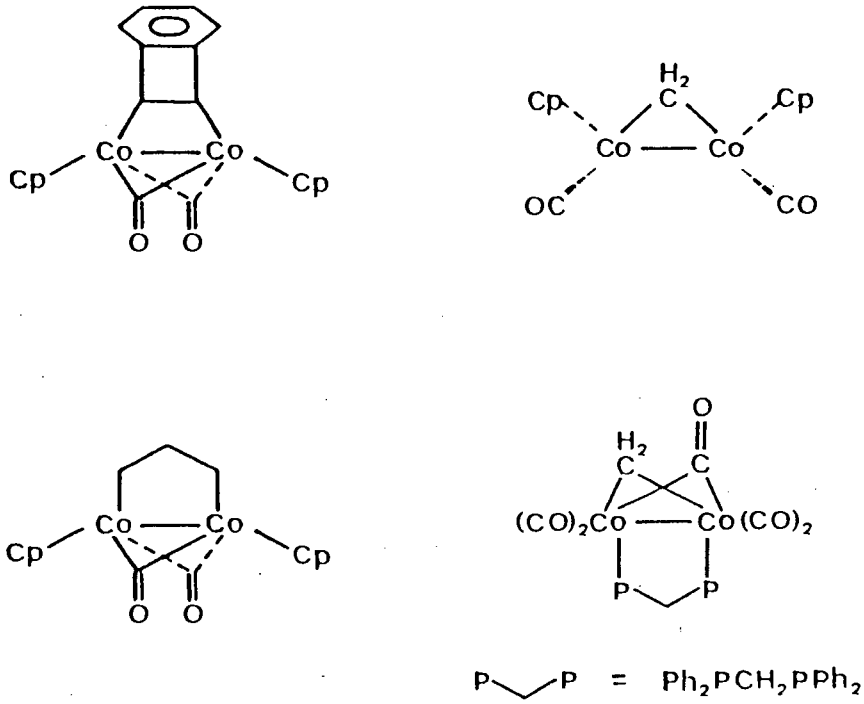

FIGURE 5.2 Examples of some dinuclear cobalt compounds containing bridging units and metal-metal bonds

In this present study, the syntheses of the mononuclear haloalkyl cobalt complexes $[Co(DH)_2py(CH_2)_nX]$, [where X=Br, n=3-7 (50a-e) and X=I, n=3 (50a')] and the subsequent conversion of some of these products to the dinuclear complexes $[Co(DH)_2py]_2[\mu\text{-}(CH_2)_n]$ (where n=4-6, 51b-d) are reported. The compounds of type (51) (where n=4-8, 51b-f) have also been prepared from $[Co(DH)_2pyCl]$ and dihaloalkane in the presence of $NaBH_4$.

5.2 Results and Discussion.

5.2.1 Synthesis of $[Co(DH)_2py(CH_2)_nX]$ and $[Co(DH)_2py]_2[\mu\text{-}(CH_2)_n]$

The reactions of $[Co(DH)_2pyCl]$ with (α,ω)-dihaloalkanes in the presence of sodium borohydride have been investigated. Using a 1 : 1.5 molar ratio of chloro(pyridine)cobaloxime to dibromo- or diiodoalkane, the mononuclear haloalkyl complexes (50) could be isolated as orange, air stable crystalline solids in generally good yield (40-80%).

$$[Co(DH)_2pyCl] + 3/2\ X(CH_2)_nX \xrightarrow[NaBH_4]{MeOH} [Co(DH)_2py(CH_2)_nX] \quad 17$$

(50)

X = Br, (50a) n = 3
(50b) n = 4
(50c) n = 5
(50d) n = 6
(50e) n = 7

X = I , (50a') n = 3

The mononuclear haloalkyl cobaloximes (50) have now been prepared by the route shown in Equation 17 for X=Br, n=3-7 (50a-e) and X=I, n=3 (50a'). These complexes have been fully characterised by melting point, microanalysis (Table 6.9) and ^1H NMR (Table 5.1) and ^{13}C NMR (Table 5.3) spectroscopy. In addition, molecular weight measurements have confirmed the mononuclear nature of the compounds in certain representative samples (See Table 6.11). All the characterisation data are consistent with these complexes being members of a new series of mononuclear haloalkyl cobaloximes of type (50).

The reactions of these haloalkyl compounds, $[Co(DH)_2py(CH_2)_nBr]$, with $[Co(DH)_2pyCl]$ in the presence of sodium borohydride were also investigated. This reaction was found to yield the dinuclear polymethylene bridged cobaloximes (51) shown in Equation 18.

$$[Co(DH)_2py(CH_2)_nX] + [Co(DH)_2pyCl] \xrightarrow[MeOH\ /\ NaBH_4]{} [py(DH)_2Co(CH_2)_nCo(DH)_2py] \quad \underline{18}$$

(51)

(51b) n = 4

(51c) n = 5

(51d) n = 6

This reaction is similar to the reaction of $[CpFe(CO)_2(CH_2)_nX]$ with $Na[CpFe(CO)_2]$ (where Cp $=\eta^5$-C_5H_5), [17]. Although Schrauzer and Windgassen [149] reported a "one-pot" synthesis of the dinuclear cobaloximes, $[Co(DH)_2py]_2[\mu$-$(CH_2)_n]$ (where n=3 and 4), using a 1:1 molar ratio of $CoCl_2.6H_2O$ to $Br(CH_2)_nBr$, only scant characterisation data for these complexes were reported. In particular, no mention was made of molecular weight measurements. Repetition of this "one-pot" synthesis proposed by Schrauzer and Windgassen [149] gave only the mononuclear bromoalkyl complex, (50a), on reaction of $CoCl_2.6H_2O$ with $Br(CH_2)_3Br$. Following a similar procedure with $Br(CH_2)_5Br$, a mixture of the mononuclear bromopentyl complex, (50c), and the dinuclear pentanediyl complex, (51c) was isolated.

On the other hand, the dinuclear alkanediyl cobaloximes (51), can be prepared directly using a 2 : 1 molar ratio of $[Co(DH)_2pyCl]$ to $Br(CH_2)_nBr$ in the presence of sodium borohydride. Using this

stoichiometry, the complexes $[Co(DH)_2py]_2[\mu\text{-}(CH_2)_n]$ (51b-f, where n=4-8) have been prepared as the major reaction products. (See Equation 19). Yields of these dinuclear cobaloximes (51), which were isolated as orange, air stable crystalline solids, are given in Table 6.10.

$$2[Co(DH)_2pyCl] + Br(CH_2)_nBr \xrightarrow[NaBH_4]{MeOH} [py(DH)_2Co(CH_2)_nCo(DH)_2py] \quad (51) \qquad 19$$

(51b) n = 4
(51c) n = 5
(51d) n = 6
(51e) n = 7
(51f) n = 8

In contrast to Schrauzer and Windgassen [149], who state that the dinuclear propanediyl complex $[Co(DH)_2py]_2[\mu\text{-}(CH_2)_3]$ was obtained "with difficulty", this complex was not isolated in any of the present attempts to prepare it. Schrauzer and Windgassen also reported that the 1,4-butanediyl complex was formed "with ease". The fact that the 1,3-propanediyl compound is difficult to prepare may be attributed to steric factors as was the case in the vitamin B_{12s} dimers.

This new series of dinuclear cobaloximes (51b-f) has been characterised by microanalysis (Table 6.10) and ^1H NMR (Table 5.2) and ^{13}C NMR (Table 5.4) spectroscopy.

In addition, the molecular weights of two representative samples have been measured by two different methods (Vaporimetric determination in dichloromethane and fast atom bombardment (FAB)

mass spectrometry). (Table 6.11). All these results are in agreement with these complexes being the binuclear alkanediyl cobaloximes (51).

Since both series of complexes, (50) and (51), exist as orange crystalline solids, distinction on a visual basis is not possible. However, in addition to microanalysis, NMR and molecular weight data, it is also possible to differentiate between (50) and (51) by their thermal behaviour. Whereas all the mononuclear cobaloximes (50) melt below 180°C (See Table 6.9), the dinuclear cobaloximes (51) decompose without melting above 190°C (See Table 6.10). It is interesting to note that, for both species, the melting or decomposition temperatures decrease with increasing alkyl chain length. This general trend has been observed for the complexes $[CpFe(CO)_2]_2[\mu\text{-}(CH_2)_n]$, [19].

Although minor differences do occur in the infrared spectra of compounds of type (50) and (51), they are very similar. The infrared spectrum of chloro(pyridine)cobaloxime provides a reference for determining the presence of new Co-C bonds. On reaction of the latter with a dihaloalkane, the fairly strong, sharp band at 380 cm^{-1}, due to ν(Co-Cl), disappears and a new weak band appears at about 321 cm^{-1}. Schrauzer and Windgasen [149] assigned this band to ν(Co-C). A weak band at 650 cm^{-1} in the spectra of mononuclear cobaloximes (50) may be ν(C-Br). By comparison with the infrared data of the alkylcobaloximes [149], the band at 1560 cm^{-1} was assigned to the C=N stretch of (DH), while the bands at 512, 455 and 420 cm^{-1} have been assigned as the stretching vibrations of the Co-N(DH) and Co-N(py) bonds.

5.2.2 ^{1}H NMR Spectra of $[Co(DH)_2py(CH_2)_nX]$ and $[Co(DH)_2py]_2[\mu\text{-}(CH_2)_n]$.

Together with melting point and microanalysis, ^{1}H NMR spectroscopy provides a very useful method of distinction between the mononuclear and dinuclear cobaloximes. Complexes of the type $[Co(DH)_2py(CH_2)_nX]$ (50) show a characteristic triplet in the region of δ 3.2 ppm (X=Br) or δ 2.9 ppm (X=I) assigned to the protons of the terminal methylene unit attached to the halogen atom. This triplet is thus absent in the spectra of the dinuclear cobaloximes, $[Co(DH)_2py]_2][\mu\text{-}(CH_2)_n]$ (51). Figures 5.3 and 5.4 show typical spectra obtained for compounds of series (50) and (51) respectively. The proton resonances of the dimethylglyoxime and pyridine ligands are presented together with their assignments in Tables 5.1 and 5.2; there are no significant differences in these resonances for compounds (50) and (51).

The signals of the protons of the polymethylene chain for series (50) were assigned on the basis of selective proton decoupling experiments. Assignments are given in Table 5.1. In contrast to the complexes $[CpFe(CO)_2(CH_2)_nX]$ where the methylene protons on the α-carbon atom resonate at the highest field [17], the protons on the carbon atom β to the cobalt atom resonate at the highest field in the spectra of the cobaloximes. The α-CH_2 protons were found to resonate further downfield at approximately δ 1.5 ppm. This difference may be due to the strongly electron withdrawing nature of the axial (py) and equatorial (DH) nitrogen atoms, reducing the electron density at the cobalt atom.

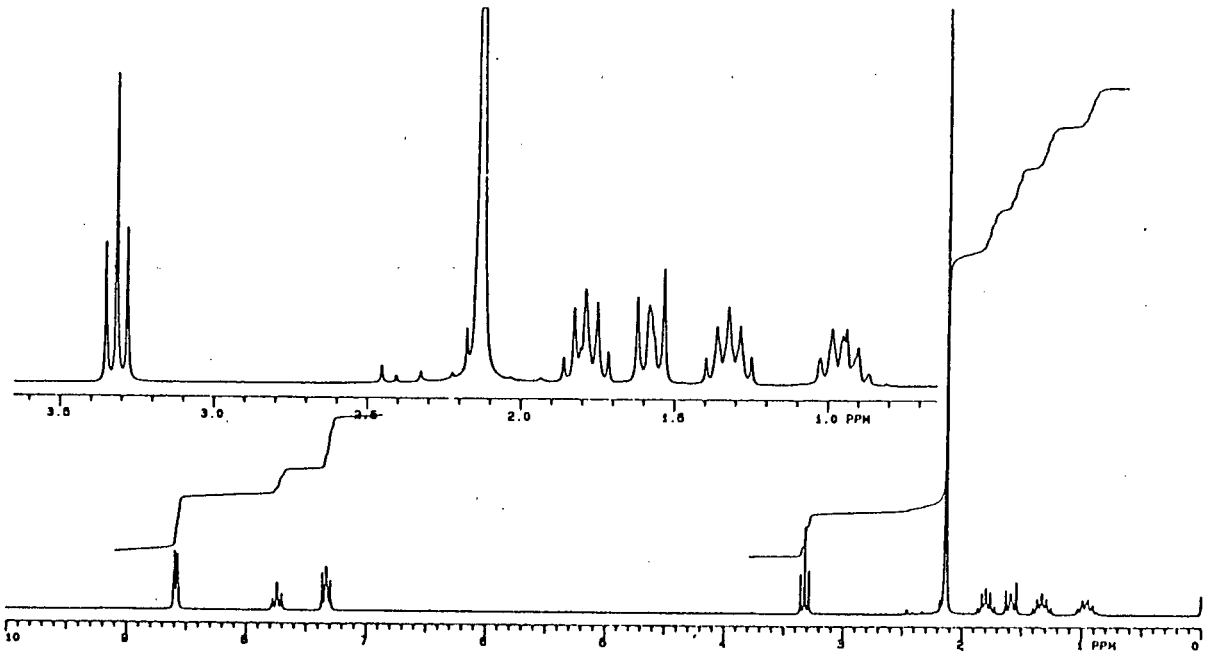

FIGURE 5.3 ^{1}H NMR spectrum of $[Co(DH)_2py(CH_2)_5Br]$ (50c) in $CDCl_3$

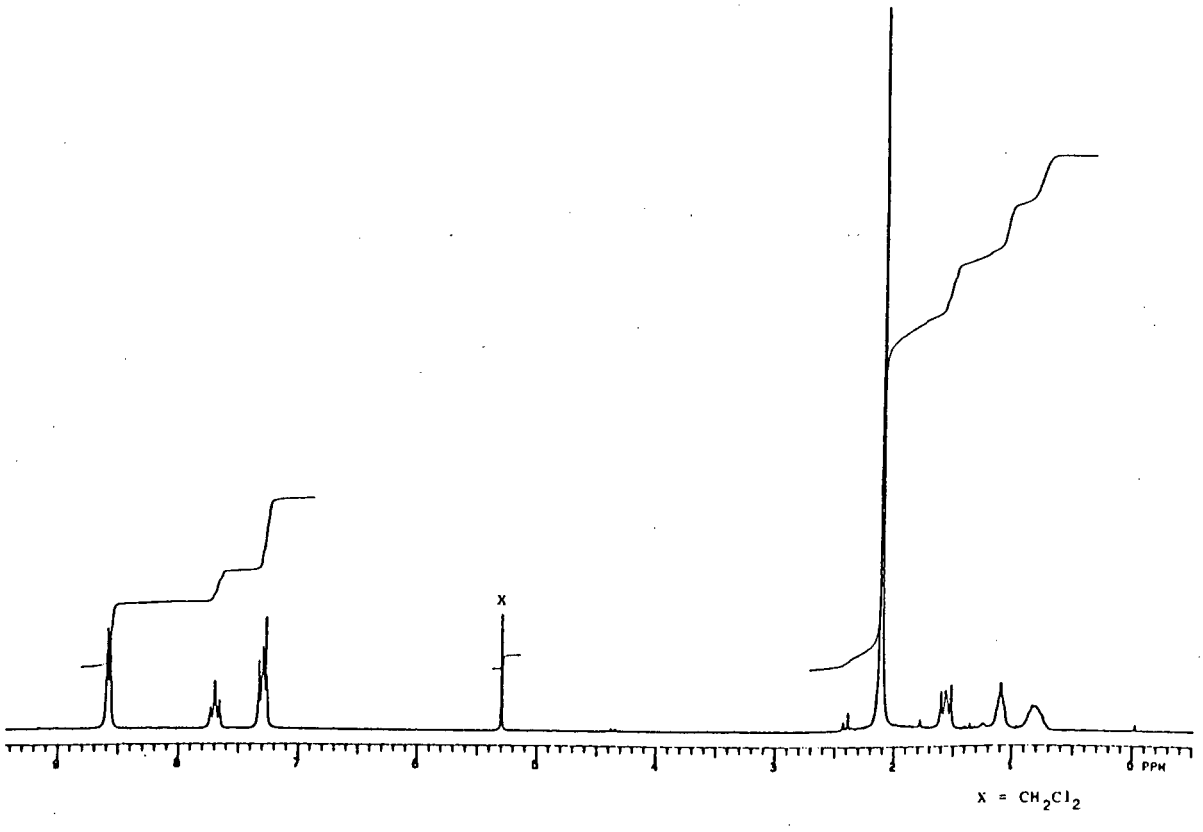

FIGURE 5.4 ^{1}H NMR spectrum of $[Co(DH)_2py]_2[\mu\text{-}(CH_2)_6]$ (51d) in $CDCl_3$

TABLE 5.1 ^{1}H NMR spectral data for $[Co(DH)_2py(CH_2)_nX]$; X=Br, n=3-7 (50a-e); X=I, n=3 (50a') in $CDCl_3$

COMPOUND		PYRIDINE			DIMETHYL-GLYOXIME		POLYMETHYLENE CHAIN				
No	n	o-H	m-H	p-H	O-H--O	CH_3	Co-(CH_2)	Co-CH_2-$\underline{CH_2}$	Other	-$\underline{CH_2}$-CH_2X	CH_2-X
		d(2H)	t(2H)	t(1H)	bs(2H)	s(12H)	t	q	-	q(2H)	t(2H)
50a	3	8.52	7.28	7.70	18.18	2.12	1.37(m,4H)				3.17
50a'	3	8.49	7.27	7.68	18.19	2.07	1.32(m,4H)				2.92
50b	4	8.56	7.31	7.72	18.26	2.12	1.52(t,2H)	1.02(q,2H)		1.73	3.32
50c	5	8.56	7.26	7.68	18.19	2.10	1.51(t,2H)	0.89(q,2H)	1.26(q,2H)	1.72	3.27
50d	6	8.53	7.27	7.65	18.18	2.04	1.51(t,2H)	0.84(q,2H)	1.21(m,4H)	1.68	3.28
50e	7	8.52	7.25	7.67	18.20	2.08	1.55(t,2H)	0.85(q,2H)	1.18(m6H)	1.74	3.33

bs broad singlet
s singlet
d doublet
t triplet
m multiplet

It is interesting to note that the β-(CH_2) proton resonances for the compounds of the series, [$Co(DH)_2py(CH_2)_nX$] (50) show a steady decrease in chemical shift, δ, with increasing chain length (See Table 5.1). This is presumably due to the increasing number of bonds beween the β-(CH_2) group and the electron withdrawing bromine atom as n increases.

The methylene resonances of the series of compounds (51) are broader. While the Co-(CH_2) protons still occur as triplets at about δ 1.55 ppm, the protons on the carbons β to the cobalt appear as broad multiplets centred at about δ 0.85 ppm. The remaining protons in the chain appear as broad resonances at about δ 1.08 ppm. Assignments are shown in Table 5.2.

TABLE 5.2 ^{1}H NMR data for $[Co(DH)_2py]_2[\mu-(CH_2)_n]$; n=4-8 (51b-f) in $CDCl_3$

COMPOUND		PYRIDINE			DIMETHYL-GLYOXIME		POLYMETHYLENE CHAIN		
No	n	o-H	m-H	p-H	O-H--O	CH_3	$Co-(CH_2)$	$Co-CH_2-\underline{CH_2}$	Other CH_2 groups
		d(4H)	t(4H)	t(2H)	bs(4H)	s(24H)	t(4H)	bm(4H)	
51b	4	8.54	7.28	7.67	18.15	2.11	1.55	0.86	
51c	5	8.57	7.28	7.68	18.17	2.10	1.54	0.84	1.08(bm,2H)
51d	6	8.57	7.29	7.69	18.19	2.10	1.57	0.81	1.09(bs,4H)
51e	7	8.53	7.27	7.67	18.19	2.07	1.56	0.83	1.07(bs,6H)
51f	8	8.55	7.27	7.67	18.19	2.08	1.57	0.81	1.05(bm,8H)

bs broad singlet
s singlet
d doublet
t triplet
bm broad multiplet

5.2.3 ^{13}C NMR Spectra of $[Co(DH)_2py(CH_2)_nX]$ and $[Co(DH)_2py]_2[\mu-(CH_2)_n]$.

The ^{13}C of the pyridine and dimethylglyoxime ligands in both series (50) and (51) were assigned by reference to reported values for the free ligands [157] and other cobaloximes, [158]. Selective proton decoupling of the ^{13}C resonances of the $-CH_2-$ units in $[Co(DH)_2py(CH_2)_4Br]$ (50b) allowed assignment of the ^{13}C chemical shifts to particular carbon atoms as shown in Table 5.3. The spectra of other compounds of series (50) were subsequently assigned by comparison with the assignments made for (50b). Distinction between the pyridine α-carbon atom and the dimethylglyoxime C=N carbon, which occur very close together, was achieved by recording the proton coupled ^{13}C spectrum of $[Co(DH)_2py(CH_2)_4Br]$. Only the C=N carbon still occurs as a singlet.

The ^{13}C chemical shifts of the chain carbons (C_α - C_η) occur between δ 27 and δ 34 ppm for series (50), the carbon adjacent to the halogen atom being at the highest value. For (50a'), a dramatic shift to δ 5.2 ppm is observed for the carbon atom of the CH_2-I group. Similarly the carbon bonded to iodine in $CH_3CH_2CH_2I$ resonates at δ 9.2 ppm, [157]. Similar shifts are observed for the series $[CpFe(CO)_2(CH_2)_nX]$ on changing from X=Br to X=I [73] as a result of the lower electronegativity of iodine relative to bromine.

For the compounds of series (50) with shorter methylene chains (n=3-5, X=Br), the carbon atom β to the metal is found at the

lowest chemical shift (ca. δ 28.8 ppm). However, for n=6 and n=7, the γ-carbon shift becomes the lowest. Only six signals are observed for (50e) (n=7); the signals of C_β and C_ϵ are believed to be coincident.

The ^{13}C chemical shift of the carbon atom bonded to cobalt (C_α) shows an increase along the series $[Co(DH)_2py(CH_2)_nBr]$ as n increases (see Table 5.3). This increase becomes smaller as the number of carbons in the chain increases but the reasons for this trend are as yet unknown.

For compounds of series (51), fewer ^{13}C signals are observed due to the equivalence of various carbon units in the chain. Thus, for (51b) two resonances are observed for the polymethylene chain and for (51c), three signals are observed as would be expected. These ^{13}C chemical shifts and assignments are given in Table 5.4.

Finally, it must be mentioned that in the proton decoupled ^{13}C NMR spectra of both series (50) and (51) the carbon bonded to cobalt (C_α) does not produce a sharp, singlet but rather a broad resonance of low intensity. This is believed to be due to coupling of C_α to ^{59}Co, which has a spin of $^7/_2$ and a natural abundance of 100%. Similar broadening of the alkyl C_α resonance has recently been observed in certain permethyl-scandocene derivatives of type $[Cp^*_2Sc\text{-}CH_2R]$ and $[Cp^*_2Sc(CH_2)_nScCp^*_2]$ (where $Cp^* = \eta^5\text{-}C_5Me_5$) and attributed to the ^{45}Sc nucleus which also has a spin of $^7/_2$, [159,160].

TABLE 5.3 ^{13}C NMR spectral data for $[Co(DH)_2py(CH_2)_nX]$; X=Br, n=3-7 (50a-e); X=I, n=3 (50a') in $CDCl_3$

COMPOUND		PYRIDINE			DIMETHYL-GLYOXIME		POLYMETHYLENE CHAIN						
No	n	α-C	ß-C	γ-C	CH_3	C=N	$Co-CH_2$	C_β	C_γ	C_δ	C_ε	C_ζ	CH_2-X
a	3	149.7	125.1	137.4	12.1	149.3	25.8	31.7					34.1
a'	3	149.7	125.1	137.4	12.2	149.3	28.3	35.2					5.2
b	4	149.8	125.2	137.4	12.1	149.0	29.3	28.9	33.3				33.9
c	5	149.7	125.1	137.2	12.0	149.1	31.0	28.8	29.9	32.4			34.2
d	6	150.7	125.8	137.9	12.2	149.6	31.5	29.5	27.8	30.2	32.6		34.1
e	7*	150.1	124.6	137.2	12.1	148.8	31.8	30.3	27.9	28.2	30.3	32.8	34.1

* Only six signals observed for polymethylene chain; C_β and C_ε thought to be superimposed at 30.3 ppm.

TABLE 5.4 ^{13}C NMR data for $[Co(DH)_2py]_2[\mu\text{-}(CH_2)_n]$; n=4-8 (51b-f) in $CDCl_3$

COMPOUND		PYRIDINE			DIMETHYL-GLYOXIME		POLYMETHYLENE CHAIN			
No	n	α-C	ß-C	γ-C	CH_3	C=N	C_α	C_β	C_γ	C_δ
51b	4[a]	150.0	125.2	137.5	12.1	149.2	31.4	32.8		
51c	5	149.8	125.0	137.2	12.1	149.0	32.7	31.4	30.4	
51d	6	149.8	125.0	137.2	12.1	148.9	32.4	30.7	30.5	
51e	7	149.7	125.0	137.2	12.1	148.9	32.8	30.9	30.7	29.3
51f	8	149.7	125.0	137.2	12.0	148.9	32.3	30.8	30.7	29.5

a spectrum recorded in CD_2Cl_2

6. EXPERIMENTAL

6.1 General

All reactions were carried out in Schlenk tubes under an atmosphere of nitrogen, using nitrogen-saturated analytical grade solvents. THF was routinely distilled over Na wire / benzophenone. Xylene (mixture of isomers) and heptane were dried by distillation over Na wire before use. CH_3CN was dried over P_2O_5.

^1H and ^{13}C NMR spectra were recorded in $CDCl_3$ (unless otherwise stated) on a Varian VXR 200 NMR instrument or a Bruker WH 90 NMR instrument. Chemical shifts are reported relative to Tetramethylsilane (δ 0.00 ppm) as an external (VXR 200) or internal (WH 90) reference standard. $[Cr(acac)_3]$ (where acac = acetylacetonato) was used as a paramagnetic relaxation agent to observe the acyl carbonyl resonances in the ^{13}C NMR spectra of $[CpRu(CO)(PR_3)]_2[\mu\text{-}C(O)(CH_2)_5C(O)]$.

Infrared spectra were recorded on a Perkin-Elmer 983 infrared spectrometer, in solution cells using NaCl windows or as Nujol mulls between CsI plates. In the description of infrared spectra the following abbreviations have been used: weak (w), medium to weak (mw), medium (m), medium to strong (ms), strong (s), very strong (vs) and shoulder (sh).

Differential Scanning Calorimetry was carried out on a Du Pont 910 DSC instrument and a Du Pont 9900 Thermal Analyser.

The low resolution electron impact (EI) mass spectra were recorded by Miss. B. Williamson or Mrs. H. von der Stratten on a VG Micromass 16 F spectrometer, operating at 70 eV with an accelerating voltage of 4 kV and the data analysed on a VG 2000 Digital data system. G.C.-M.S. runs were carried out using a Carlo-Erba Fractovap 4200 G.C. instrument with a Carbowax 25 m capilliary column, coupled to the V.G. Micromass 16F spectrometer.

Microanalyses were performed by Mr. W. T. Hemsted or Mr. G. P. Benin-Casa of the microanalytical laboratory at the University of Cape Town.

Melting point ranges were determined using a Kofler Hotstage Microscope (Reichert Thermovar) and are uncorrected.

X-Ray crystal structure determinations were performed by Dr. M. L. Niven of the Crystallography Unit at the University of Cape Town. Reflections were measured using an Enraf Nonius CAD4 Diffractometer.

$[CpFe(CO)_2]_2$ and $Ru_3(CO)_{12}$ were purchased from Strem Chemicals Inc, $RuCl_3.nH_2O$ was obtained on loan from Johnson Matthey (Pty) Ltd. Tertiary phosphines were obtained from Merck or Strem Chemicals Inc. and t-BuNC from Fluka AG Chemicals. $I(CH_2)_nI$, $Br(CH_2)_nBr$ and $Cl(CH_2)_3Cl$ were obtained from Aldrich Chemical Corporation, Ventron, or Ega Chemie.

$[CpFe(CO)_2]_2[\mu\text{-}(CH_2)_n]$, (n=3,4,5) were synthesised from $Na[CpFe(CO)_2]$ and the corresponding dibromoalkane following a reported method, [19].

[$CoCl_2.6H_2O$] and dimethylglyoxime were obtained from Saarchem (Pty) Ltd. [$Co(DH)_2pyCl$] was synthesised by the method of Schrauzer, [150].

Vaporimetric molecular weight determinations in CH_2Cl_2 were carried out by Pascher Mikroanalytisches Laboratorium. Fast Atom Bombardment (FAB) mass spectra were recorded by R McQueen at the University of Cambridge England.

Column Chromatography was carried out on Florisil (0.150-0.250 mm, 60-100 mesh ASTM) obtained from Merck.

6.2 Synthesis of μ-(α,ω)-Alkanediyl Complexes of Ruthenium and their Haloalkyl Precursors.

6.2.1 General

$[CpFe(CO)_2]_2$ was obtained from Strem Chemicals Inc. and used without further purification. $[CpRu(CO)_2]_2$ was prepared from $Ru_3(CO)_{12}$ or from $RuCl_3.nH_2O$ following reported methods, [69-71]. The sodium salts of the anions $[CpFe(CO)_2]^-$ and $[CpRu(CO)_2]^-$ were prepared by stirring a solution of the corresponding dimer for 2-3 hours at room temperature.

$[CpFe(CO)_2(CH_2)_4I]$ was pepared by the method of Moss [17]. The dihaloalkanes, $Br(CH_2)_nBr$ (n=4) and $I(CH_2)_nI$ (n=3-6, 8-10) were obtained from Aldrich Chemical Corporation, Ventron or EGA Chemie respectively. $I(CH_2)_7I$ was prepared by the reaction of $Br(CH_2)_7Br$

with excess NaI in refluxing acetone (distilled over $CaCl_2$) for three days.

6.2.2 General Synthetic route to $\mu(\alpha,\omega)$-alkanediyl complexes of ruthenium, $[CpRu(CO)_2]_2[\mu\text{-}(CH_2)_n]$, n=5-10 (7e-j).

$I(CH_2)_nI$ (1.05 mmol) in THF (1 cm^3) was added dropwise over 5 minutes to a stirred solution of $Na[CpRu(CO)_2]$ (2.29 mmol) in THF (10 cm^3). The red-brown mixture was stirred for 1.25 hours in the dark at room temperature and then the solvent was removed under reduced pressure. The dark brown residue was extracted with hexane (ca. 5 x 30 cm^3) and the extractions filtered and concentrated to give an orange solution. This solution was chromatographed on a Florisil column (ca. 6 cm high by 3 cm diameter). A colourless band was eluted initially with hexane. Removal of the solvent under reduced pressure yielded the cream coloured crystals of $[CpRu(CO)_2]_2[\mu\text{-}(CH_2)_n]$ which were recrystallised from hexane at -78°C. Melting point and infrared data are reported in Table 2.1; ^1H NMR and ^{13}C NMR data in Tables 2.2 and 2.3 repectively. (Mass spectra are reported and discussed in Section 2.2.3.). Yields and microanalytical results are recorded in Table 6.1. In addition, small quantities of $[CpRu(CO)_2I]$ (ca. 5%) and $[CpRu(CO)_2]_2$ (ca. 10%) were eluted from the column using hexane/ether solutions in the ratio of (80:20) and (50:50) respectively. These products were identified by their infrared spectra in the $\nu(CO)$ region.

TABLE 6.1 Yields and microanalysis for $[CpRu(CO)_2]_2[\mu\text{-}(CH_2)_n]$, n=5-10 (7e-j)

COMPOUND No.	n	Yield[a] (%)	Analysis[b] % C	% H
7e	5	61(39)	44.40 (44.35)	4.10 (3.93)
7f	6	60(30)	45.50 (45.44)	4.30 (4.20)
7g	7	55(18)	46.50 (46.48)	4.50 (4.47)
7h	8	75(44)	47.50 (47.47)	4.70 (4.72)
7i	9	64(32)	48.20 (48.41)	5.00 (4.96)
7j	10	66(24)	49.30 (49.30)	5.20 (5.18)

a Yields after recrystallisation in parenthesis

b Calculated values in parenthesis

6.2.3 Synthesis of the Heterodinuclear compound, $[Cp(CO)_2Fe(CH_2)_4Ru(CO)_2Cp]$ (8b).

$Na[CpRu(CO)_2]$ (1.134 mmol) in THF ($6cm^3$) was added dropwise over 2 minutes to a stirred solution of $[CpFe(CO)_2(CH_2)_4I]$ (0.405 g, 1.14 mmol) in THF (4 cm^3) at -78°C. The mixture was allowed to warm gradually to room temperature and stirring continued for 24 hours. The solvent was then removed under reduced pressure yielding a yellow-brown solid residue. This residue was extracted with hexane (ca. 5 x 25 cm^3) and the extraction combined, filtered and concentrated. The resulting orange solution was chromatographed on a Florisil column eluting with hexane only. A yellow fraction was collected and the solvent removed under reduced pressure. The resulting yellow solid (0.130 g, 41% crude yield) was recrystallised from hexane at -78°C to give $[Cp(CO)_2Fe(CH_2)_4Ru(CO)_2Cp]$ as a yellow crystalline solid in a 20% yield. Melting range, infrared and ^1H NMR data are reported in Table 2.10, ^{13}C NMR data reported in Table 2.11. In addition, a mass spectrum of the compound was recorded. Compound (8b) requires M^+ of 456; observed M^+ at m/e 456 as well as M^++2 ion at m/e 458. The correct isotope pattern for this compound was also observed. Analysis: $C_{18}H_{18}O_4FeRu$ requires 47.48 %C, 3.99 %H; Found 48.00 %C, 4.10 %H.

Small amounts of $[CpRu(CO)_2I]$ and $[CpRu(CO)_2]_2$ were also eluted from the column with (80:20) and (50:50) mixtures of hexane/ether respectively. These products were identified by their infrared spectra (in hexane) in the $\nu(CO)$ region.

6.2.4 Synthesis of 4-bromobutyl cyclopentadienylruthenium dicarbonyl, $[CpRu(CO)_2(CH_2)_4Br]$ (15).

$Na[CpRu(CO)_2]$ (1.13 mmol) in THF (10 cm^3) was added dropwise over 12 minutes to a stirred solution of $Br(CH_2)_4Br$ (0.321 g, 1.49 mmol) in THF (6 cm^3) at -78°C. The mixture was stirred at -78°C for a further 25 minutes and then the solvent was removed under reduced pressure. The crude brown residue was extracted with hexane (ca. 4 x 50 cm^3), the extractions filtered and the orange solution concentrated. The solution was chromatographed on a Florisil column (5 cm high by 3 cm diameter) and a colourless fraction eluted with hexane. Removal of the solvent under reduced pressure yielded $[CpRu(CO)_2(CH_2)_4Br]$ (0.240 g, 59%) as a very pale yellow, almost colourless, oil. Further elution from the column with hexane/ether (50:50) gave a pale yellow fraction which yielded $[CpRu(CO)_2]_2$ (0.070 g, 28%) (identified by infrared spectroscopy) on removal of the solvent.

$[CpRu(CO)_2(CH_2)_4Br]$ was recrystallised from hexane at -78°C to give white crystals which melt slowly on warming to room temperature. This product was characterised by infrared and ^1H NMR spectroscopy. IR in hexane: ν(CO): 2020 (vs), 1961 (vs), 1931 (vw) cm^{-1}. ^1H NMR in $CDCl_3$: δ 5.20 ppm (singlet, 5H, C_5H_5); δ 3.41 ppm (triplet, 2H, CH_2Br); δ 1.84 ppm (multiplet, 2H, $\underline{CH_2}CH_2Br$); δ 1.64 ppm (multiplet, 4H, $Ru\text{-}CH_2CH_2\text{-}$). (Note, signals at δ 1.84 ppm and δ 1.64 overlap slightly.) Microanalysis was not performed on this complex.

6.2.5 Synthesis of 3-chloropropyl cyclopentadienylruthenium dicarbonyl, $[CpRu(CO)_2(CH_2)_3Cl]$ (16).

$Na[CpRu(CO)_2]$ (1.38 mmol) in THF (12 cm^3) was added dropwise to a stirred solution of $Cl(CH_2)_3Cl$ (0.182 g, 1.61 mmol) in THF (5 cm^3) at -78°C over 15 minutes and stirring continued for a further 10 minutes at -78°C. The infrared spectrum of the reaction mixture at this stage revealed two strong bands at 2022 and 1957 cm^{-1} (the latter broad), as well as bands at 1998 (ms), 1906 (s) and 1822 (m) cm^{-1} due to $Na[CpRu(CO)_2]$. The cold bath was therefore removed and the reaction mixture allowed to warm gradually to room temperature while stirring. The reaction was monitored after 0.83, 1.25 , 1.75 , 2.5 and 6.0 hours. A new band at 2012 cm^{-1} present in the infrared spectrum after 1.25 hours was observed to grow in intensity, while the broad band at 1957 cm^{-1} shifted gradually to 1949 cm^{-1} during the course of the reaction. No change in the infrared spectrum was observed between 2.5 and 6.0 hours so the reaction was assumed to be complete after 2.5 hours. The infrared spectrum after 2.5 hours showed ν(CO) bands at 2011 (vs), 1998 (m), 1949 (vs), 1909 (m) and 1649 (w) cm^{-1}. A colour change from an orange-red to a red solution was also noted during the course of the reaction. The solvent was removed under reduced pressure and the crude residue extracted with hexane (4 x 30 cm^3), the extractions filtered and the pale orange-yellow solution concentrated. This solution was chromatographed on a Florisil column (5 cm high by 3 cm diameter) and a colourless fraction eluted with hexane. This gave a colourless oil (0.120 g, 29%) on removal of the solvent. A second bright yellow fraction was eluted with hexane/ether (9:1). An infrared of the yellow residue in hexane revealed $[CpRu(CO)_2]_2$ (0.090 g, 29%). The oil was

recrystallised from hexane to give white crystals at -78°C which melt slowly on warming to room temperature to afford a very pale yellow oil. The oil was characterised by infrared and ^{1}H NMR as $[CpRu(CO)_2(CH_2)_3Cl]$. IR in hexane: ν(CO): 2022 (vs), 1965 (vs), 1935 (vw) cm^{-1}. ^{1}H NMR in $CDCl_3$: δ 5.25 ppm (singlet, 5H, C_5H_5); δ 3.42 (triplet, 2H, CH_2Cl); δ 1.98 ppm (multiplet, 2H, CH_2CH_2Cl); δ 1.57 ppm (multiplet, 2H, Ru-CH_2); in addition two singlets of very low intensity at δ 1.78 ppm (0.8 H) and δ 1.25 ppm (0.5 H) were observed as minor impurities. This product appeared to be hygroscopic and, although a microanalysis was performed, the results were not particularly reliable.

6.3 Experimental Details of the X-Ray Structural Determination

6.3.1 Growing crystals of $[CpRu(CO)_2]_2[\mu$-$(CH_2)_5]$.

$[CpRu(CO)_2]_2[\mu$-$(CH_2)_5]$ (0.080 g) was dissolved in a minimum of hexane and filtered under N_2. The volume of hexane was doubled and the solution stored under N_2 at 0°C for a few days. Thin plates of $[CpRu(CO)_2]_2[\mu$-$(CH_2)_5]$ crystallised from solution. The mother liquor was syringed off, re-filtered under N_2 and returned to the fridge at 0°C for further crystal growth. After ca. 8 days, several large chunky white prisms had grown from solution. The solvent was syringed off and the crystals dried under a nitrogen flow. A suitable chunky prism was selected for X-Ray analysis. Melting points: plates 86-88°C; prisms 78-79°C.

6.3.2 Experimental details of X-ray data collection.

X-ray crystal stucture determinations were performed by Dr Margaret Niven of the Crystallography Unit at the University of Cape Town. A suitable single crystal was selected and irradiated with MoK_{α} (λ= 0.7107 Å) radiation using an Enraf-Nonius CAD4 diffractometer. Cell parameters were obtained by least squares analysis of the setting angles of 24 reflections in the range $16 \leq \theta \leq 17°$. Intensities of three standard reference reflections were monitored every hour and recentring checked every hundred measured reflections during the data collection. Intensities were corrected for Lorentz polarisation effects and for absorption. The structure was solved by location of the two heavy metal atoms in a Patterson map and the remaining non-hydrogen atoms located by subsequent difference Fouriers. In the final refinements all non hydrogen atoms were treated anisotropically. The methylene hydrogens were placed in calculated positions with a single isotropic temperature factor. The maximum parameter shift/ e.s.d. was less than 0.005. Structure solution and refinement was carried out using SHELX-76 [161], molecular parameters obtained from PARST [162] and drawings obtained with PLUTO [163]. All computations were carried out on a Sperry 1100 computer. Crystal data, fractional atomic coordinates, bond lengths, bond angles and torsion angles are presented in Tables 6.2 - 6.6.

TABLE 6.2 Crystal data, experimental details of data collection and structure refinement for $[CpRu(CO)_2]_2[\mu\text{-}(CH_2)_5]$

Molecular formula	$C_{19}H_{20}O_4Ru_2$
Mr / g mol^{-1}	514.51
Space Group	$P\bar{1}$
a / Å	7.792(1)
b / Å	10.691(3)
c / Å	12.316(2)
α / °	106.76(2)
β / °	95.58(1)
γ / °	90.94(2)
V / $Å^3$	976.7(4)
Dc for Z = 2 / g cm^{-3}	1.75
F(000)	508
μ (MoKα) / cm^{-1}	15.36
Dimensions of crystal / mm	0.28 x 0.28 x 0.30
Crystal decay / %	0.4
Scan mode	ω - 2θ
Scan width / °ω	(1.00 + 0.35 tan θ)
Aperture width / mm	(1.20 + 1.05 tanθ)
θ range /°	1-25
% Transmission on absorption correction	
Min/Max/Average	91/100/97
Total no. of reflections collected	3278
No. of reflections observed, N (with I rel > 2σ I rel)	3092
No. of parameters, NP	227
$R = \Sigma \lvert\Delta\rvert / \Sigma \lvert Fo\rvert$	0.037
$S = (\Sigma \lvert\Delta\rvert^2 / N\text{-}NP)^{\frac{1}{2}}$	1.71

TABLE 6.3 Fractional atomic coordinates (x 10**4)
and thermal parameters (Å**2 x 10**3)
with e.s.d s in parenthesis for the compound $[CpRu(CO)_2]_2[\mu\text{-}(CH_2)_5]$

Atom	x/a	y/b	z/c	Uequiv
Ru(1)	-452(1)	9244(1)	2824(0)	38(0)
Ru(2)	5741(1)	6001(1)	-2872(0)	39(0)
C(1)	1052(11)	9543(8)	1510(7)	53(3)
C(2)	1863(10)	8325(8)	856(7)	52(3)
C(3)	2862(10)	8561(8)	-97(7)	52(3)
C(4)	3612(10)	7318(7)	-835(6)	49(3)
C(5)	4693(10)	7638(7)	-1680(7)	49(3)
C(11)	-2370(12)	7968(11)	1435(9)	75(4)
C(12)	-1536(12)	7170(9)	2017(10)	75(5)
C(13)	-1941(13)	7556(10)	3154(10)	78(5)
C(14)	-3022(12)	8581(11)	3310(9)	73(4)
C(15)	-3317(11)	8857(10)	2248(11)	83(5)
C(111)	1659(10)	9167(7)	3643(7)	47(3)
O(111)	2952(8)	9111(6)	4131(6)	71(3)
C(112)	-391(10)	11060(8)	3465(8)	55(3)
O(112)	-394(10)	12148(6)	3872(7)	95(4)
C(21)	8382(14)	5812(13)	-2038(17)	122(9)
C(22)	7175(14)	5357(11)	-1436(8)	75(4)
C(23)	6413(15)	4270(12)	-2227(15)	97(6)
C(24)	7072(25)	4090(13)	-3244(14)	125(8)
C(25)	8232(19)	4961(22)	-3148(13)	125(8)
C(211)	3495(10)	5500(7)	-3561(7)	48(3)
O(211)	2146(7)	5168(6)	-3980(6)	73(3)
C(212)	5913(11)	7145(8)	-3777(7)	57(3)
O(212)	6002(10)	7832(7)	-4301(6)	92(3)

Anisotropic atoms have thermal parameters (Å**2 x 10**3) of the form :

EXP(-2*PI**2(U11*H**2*(A*)**2+...+2*U12*H*K*(A*)*(B*)+...)

Atom	U11	U22	U33	U23	U13	U12
Ru(1)	35(0)	40(0)	39(0)	11(0)	9(0)	2(0)
Ru(2)	36(0)	38(0)	43(0)	11(0)	10(0)	3(0)
C(1)	61(5)	61(5)	50(5)	28(4)	27(4)	20(4)
C(2)	53(5)	55(5)	52(5)	18(4)	22(4)	8(4)
C(3)	56(5)	58(5)	48(5)	21(4)	22(4)	20(4)
C(4)	50(4)	51(4)	48(5)	15(4)	20(4)	6(4)
C(5)	60(5)	39(4)	51(5)	12(3)	24(4)	8(3)
C(11)	60(6)	93(8)	61(6)	7(5)	-4(5)	-26(5)
C(12)	58(6)	46(5)	105(9)	0(5)	7(6)	-10(4)
C(13)	68(6)	79(7)	99(8)	52(6)	-10(6)	-36(6)
C(14)	50(5)	93(7)	67(6)	6(5)	21(5)	-26(5)
C(15)	34(5)	66(6)	137(11)	21(7)	-18(5)	-6(4)
C(111)	45(4)	43(4)	51(5)	12(4)	5(4)	0(3)
O(111)	50(4)	73(4)	81(5)	14(3)	-10(3)	7(3)
C(112)	44(4)	51(5)	72(6)	16(4)	16(4)	5(4)
O(112)	98(6)	41(4)	138(7)	9(4)	24(5)	10(4)
C(21)	49(6)	94(9)	229(18)	83(11)	-62(9)	-18(6)
C(22)	80(7)	90(7)	56(6)	25(5)	0(5)	35(6)
C(23)	75(7)	68(7)	162(13)	71(9)	-31(8)	0(6)
C(24)	142(14)	78(9)	110(12)	-21(8)	-56(11)	70(9)
C(25)	77(9)	225(21)	84(10)	50(12)	31(8)	91(11)
C(211)	46(4)	44(4)	60(5)	21(4)	8(4)	4(3)
O(211)	43(3)	77(4)	96(5)	27(4)	-6(3)	-8(3)
C(212)	58(5)	59(5)	56(5)	16(4)	17(4)	-2(4)
O(212)	114(6)	95(5)	89(5)	60(5)	20(4)	-11(4)

TABLE 6.4 (a) Bond lengths (Å) with e.s.d s in parenthesis for the compound $[CpRu(CO)_2]_2[\mu\text{-}(CH_2)_5]$

Ru(1)	- C(1)	2.180(9)	C(2)	- C(3)	1.546(13)
Ru(1)	- C(11)	2.260(9)	C(3)	- C(4)	1.538(10)
Ru(1)	- C(12)	2.263(9)	C(4)	- C(5)	1.509(12)
Ru(1)	- C(13)	2.283(12)	C(11)	- C(12)	1.395(17)
Ru(1)	- C(14)	2.301(11)	C(11)	- C(15)	1.439(14)
Ru(1)	- C(15)	2.269(9)	C(12)	- C(13)	1.411(17)
Ru(1)	- C(111)	1.861(8)	C(13)	- C(14)	1.373(15)
Ru(1)	- C(112)	1.871(8)	C(14)	- C(15)	1.419(19)
Ru(2)	- C(5)	2.164(7)	C(111)	- O(111)	1.133(10)
Ru(2)	- C(21)	2.247(13)	C(112)	- O(112)	1.126(10)
Ru(2)	- C(22)	2.279(11)	C(21)	- C(22)	1.414(21)
Ru(2)	- C(23)	2.264(16)	C(21)	- C(25)	1.400(23)
Ru(2)	- C(24)	2.255(15)	C(22)	- C(23)	1.365(15)
Ru(2)	- C(25)	2.258(17)	C(23)	- C(24)	1.364(26)
Ru(2)	- C(211)	1.868(7)	C(24)	- C(25)	1.259(26)
Ru(2)	- C(212)	1.889(10)	C(211)	- O(211)	1.130(9)
C(1)	- C(2)	1.503(11)	C(212)	- O(212)	1.113(13)

TABLE 6.4 (b) Non-bonded distances (Å) involving the centroids X and Y of the cyclopentadienyl rings C_{11}-C_{15} and C_{21}-C_{25} respectively

Ru(1) ....Ru(2)	8.811(4)		
Ru(1) X	1.935(8)	Ru(2).....Y	1.942(8)
Ru(1).....C(2)	3.103(8)	Ru(2).....C(4)	3.142(7)
Ru(1).....H(211)	3.219(8)	Ru(2).....H(411)	3.227(8)
Ru(1).....H(212)	3.181(8)	Ru(2).....H(412)	3.289(7)

TABLE 6.5 (a) Bond angles (degrees) with e.s.d s in parenthesis for the compound $[CpRu(CO)_2]_2[\mu\text{-}(CH_2)_5]$

C(111)	- Ru(1)	- C(112)	90.2(4)
C(15)	- Ru(1)	- C(112)	99.9(4)
C(15)	- Ru(1)	- C(111)	157.9(4)
C(14)	- Ru(1)	- C(112)	102.8(4)
C(14)	- Ru(1)	- C(111)	122.4(4)
C(14)	- Ru(1)	- C(15)	36.2(3)
C(13)	- Ru(1)	- C(112)	133.2(4)
C(13)	- Ru(1)	- C(111)	99.8(4)
C(13)	- Ru(1)	- C(15)	59.1(4)
C(13)	- Ru(1)	- C(14)	34.9(4)
C(12)	- Ru(1)	- C(112)	159.7(4)
C(12)	- Ru(1)	- C(111)	107.8(4)
C(12)	- Ru(1)	- C(15)	59.9(4)
C(12)	- Ru(1)	- C(14)	59.8(4)
C(12)	- Ru(1)	- C(13)	36.2(4)
C(11)	- Ru(1)	- C(112)	128.5(4)
C(11)	- Ru(1)	- C(111)	140.9(4)
C(11)	- Ru(1)	- C(15)	37.0(4)
C(11)	- Ru(1)	- C(14)	61.2(4)
C(11)	- Ru(1)	- C(13)	60.2(4)
C(11)	- Ru(1)	- C(12)	35.9(4)
C(1)	- Ru(1)	- C(112)	88.4(4)
C(1)	- Ru(1)	- C(111)	86.1(3)
C(1)	- Ru(1)	- C(15)	113.6(4)
C(1)	- Ru(1)	- C(14)	148.7(3)
C(1)	- Ru(1)	- C(13)	137.4(4)
C(1)	- Ru(1)	- C(12)	101.8(4)
C(1)	- Ru(1)	- C(11)	88.9(4)
C(211)	- Ru(2)	- C(212)	89.3(4)
C(25)	- Ru(2)	- C(212)	100.6(5)
C(25)	- Ru(2)	- C(211)	130.7(5)
C(24)	- Ru(2)	- C(212)	121.8(5)
C(24)	- Ru(2)	- C(211)	102.9(5)
C(24)	- Ru(2)	- C(25)	32.4(6)
C(23)	- Ru(2)	- C(212)	156.2(4)
C(23)	- Ru(2)	- C(211)	100.9(4)
C(23)	- Ru(2)	- C(25)	56.6(6)
C(23)	- Ru(2)	- C(24)	35.1(5)
C(22)	- Ru(2)	- C(212)	142.9(4)
C(22)	- Ru(2)	- C(211)	127.6(4)
C(22)	- Ru(2)	- C(25)	59.9(5)
C(22)	- Ru(2)	- C(24)	59.3(5)
C(22)	- Ru(2)	- C(23)	35.0(5)
C(21)	- Ru(2)	- C(212)	108.9(5)
C(21)	- Ru(2)	- C(211)	158.2(5)
C(21)	- Ru(2)	- C(25)	36.2(6)
C(21)	- Ru(2)	- C(24)	57.6(6)
C(21)	- Ru(2)	- C(23)	57.8(5)
C(21)	- Ru(2)	- C(22)	36.4(5)
C(5)	- Ru(2)	- C(212)	85.2(4)
C(5)	- Ru(2)	- C(211)	88.2(3)
C(5)	- Ru(2)	- C(25)	140.4(4)
C(5)	- Ru(2)	- C(24)	150.4(5)
C(5)	- Ru(2)	- C(23)	116.3(5)
C(5)	- Ru(2)	- C(22)	92.2(3)
C(5)	- Ru(2)	- C(21)	104.7(5)

TABLE 6.5 (a)

Ru(1)	- C(1)	- C(2)	113.5(6)
C(1)	- C(2)	- C(3)	112.1(7)
C(2)	- C(3)	- C(4)	113.7(7)
C(3)	- C(4)	- C(5)	110.9(6)
Ru(2)	- C(5)	- C(4)	116.5(5)
Ru(1)	- C(11)	- C(15)	71.8(6)
Ru(1)	- C(11)	- C(12)	72.1(6)
C(12)	- C(11)	- C(15)	106.0(10)
Ru(1)	- C(12)	- C(11)	71.9(7)
C(11)	- C(12)	- C(13)	108.7(9)
Ru(1)	- C(12)	- C(13)	72.7(6)
Ru(1)	- C(13)	- C(12)	71.1(6)
C(12)	- C(13)	- C(14)	109.7(10)
Ru(1)	- C(13)	- C(14)	73.3(7)
Ru(1)	- C(14)	- C(13)	71.8(6)
C(13)	- C(14)	- C(15)	107.0(10)
Ru(1)	- C(14)	- C(15)	70.7(5)
C(11)	- C(15)	- C(14)	108.6(9)
Ru(1)	- C(15)	- C(14)	73.2(5)
Ru(1)	- C(15)	- C(11)	71.1(5)
Ru(1)	- C(111)	- O(111)	179.2(8)
Ru(1)	- C(112)	- O(112)	177.8(8)
Ru(2)	- C(21)	- C(25)	72.3(8)
Ru(2)	- C(21)	- C(22)	73.0(7)
C(22)	- C(21)	- C(25)	107.3(12)
Ru(2)	- C(22)	- C(21)	70.6(8)
C(21)	- C(22)	- C(23)	103.3(12)
Ru(2)	- C(22)	- C(23)	71.9(8)
Ru(2)	- C(23)	- C(22)	73.1(8)
C(22)	- C(23)	- C(24)	110.5(13)
Ru(2)	- C(23)	- C(24)	72.1(9)
Ru(2)	- C(24)	- C(23)	72.8(9)
C(23)	- C(24)	- C(25)	109.6(15)
Ru(2)	- C(24)	- C(25)	73.9(13)
C(21)	- C(25)	- C(24)	109.3(14)
Ru(2)	- C(25)	- C(24)	73.7(12)
Ru(2)	- C(25)	- C(21)	71.5(8)
Ru(2)	- C(211)	- O(211)	178.4(7)
Ru(2)	- C(212)	- O(212)	179.0(8)

TABLE 6.5 (b) Bond angles at ruthenium between various carbon or hydrogen atoms and the centroid, X or Y, of the cyclopentadienyl ring

X - Ru(1) - C(111)	129.64	Y-Ru(2)-C(211)	127.27
X - Ru(1) - C(112)	128.29	Y-Ru(2)-C(212)	129.83
X - Ru(1) - C(1)	120.95	Y-Ru(2)-C(5)	123.51
X - Ru(1) - H(211)	110.73	Y-Ru(2)-H(411)	114.67
X- Ru(1) - H(212)	87.80	Y-Ru(2)-H(412)	92.93
C111-Ru(1)- H(211)	62.44	C211-Ru(2)-H(411)	62.63
C111-Ru(1)- H(212)	91.28	C211-Ru(2)-H(412)	90.85
C112-Ru(1)- H(211)	117.45	C212-Ru(2)-H(411)	112.5
C112-Ru(1)- H(212)	127.96	C212-Ru(2)-H(412)	122.93

TABLE 6.6 Tortion angles (degrees) with e.s.d. s in parenthesis for the compound $[CpRu(CO)_2]_2[\mu\text{-}(CH_2)_5]$

(RIGHT-HAND RULE,KLYNE & PRELOG.(1960).EXPERIENTIA,16,521)
(E.S.D.'S, FOLLOWING STANFORD & WASER,ACTA CRYST.(1972).A28,213)

C(112)	- Ru(1)	- C(15)	- C(11)	144.7(6)
C(111)	- Ru(1)	- C(15)	- C(11)	-99.2(11)
C(14)	- Ru(1)	- C(15)	- C(11)	-117.1(9)
C(13)	- Ru(1)	- C(15)	- C(11)	-80.4(7)
C(12)	- Ru(1)	- C(15)	- C(11)	-38.2(6)
C(1)	- Ru(1)	- C(15)	- C(11)	52.1(7)
C(112)	- Ru(1)	- C(15)	- C(14)	-98.2(7)
C(111)	- Ru(1)	- C(15)	- C(14)	17.8(13)
C(13)	- Ru(1)	- C(15)	- C(14)	36.7(6)
C(12)	- Ru(1)	- C(15)	- C(14)	78.9(7)
C(11)	- Ru(1)	- C(15)	- C(14)	117.1(9)
C(1)	- Ru(1)	- C(15)	- C(14)	169.1(6)
C(13)	- Ru(1)	- C(14)	- C(15)	-116.2(9)
C(12)	- Ru(1)	- C(14)	- C(15)	-79.3(7)
C(11)	- Ru(1)	- C(14)	- C(15)	-37.8(6)
C(1)	- Ru(1)	- C(14)	- C(15)	-19.4(10)
C(112)	- Ru(1)	- C(14)	- C(13)	-154.5(6)
C(111)	- Ru(1)	- C(14)	- C(13)	-55.9(8)
C(15)	- Ru(1)	- C(14)	- C(13)	116.2(9)
C(12)	- Ru(1)	- C(14)	- C(13)	36.9(6)
C(11)	- Ru(1)	- C(14)	- C(13)	78.4(7)
C(1)	- Ru(1)	- C(14)	- C(13)	96.8(9)
C(12)	- Ru(1)	- C(13)	- C(14)	-118.3(9)
C(11)	- Ru(1)	- C(13)	- C(14)	-81.3(7)
C(1)	- Ru(1)	- C(13)	- C(14)	-130.4(7)
C(112)	- Ru(1)	- C(13)	- C(12)	153.5(6)
C(111)	- Ru(1)	- C(13)	- C(12)	-106.9(6)
C(15)	- Ru(1)	- C(13)	- C(12)	80.2(7)
C(14)	- Ru(1)	- C(13)	- C(12)	118.3(9)
C(11)	- Ru(1)	- C(13)	- C(12)	37.0(6)
C(1)	- Ru(1)	- C(13)	- C(12)	-12.1(9)
C(11)	- Ru(1)	- C(12)	- C(13)	-117.0(9)
C(1)	- Ru(1)	- C(12)	- C(13)	171.7(6)
C(112)	- Ru(1)	- C(12)	- C(11)	47.6(14)
C(111)	- Ru(1)	- C(12)	- C(11)	-160.9(6)
C(15)	- Ru(1)	- C(12)	- C(11)	39.4(6)
C(14)	- Ru(1)	- C(12)	- C(11)	81.4(7)
C(13)	- Ru(1)	- C(12)	- C(11)	117.0(9)
C(1)	- Ru(1)	- C(12)	- C(11)	-71.3(6)
C(1)	- Ru(1)	- C(11)	- C(12)	112.0(6)
C(1)	- Ru(1)	- C(11)	- C(15)	-133.7(6)
C(11)	- Ru(1)	- C(1)	- C(2)	-67.5(6)
C(12)	- Ru(1)	- C(1)	- C(2)	-33.7(7)
C(13)	- Ru(1)	- C(1)	- C(2)	-26.5(9)
C(14)	- Ru(1)	- C(1)	- C(2)	-83.5(9)
C(15)	- Ru(1)	- C(1)	- C(2)	-95.9(6)
C(111)	- Ru(1)	- C(1)	- C(2)	73.7(6)
C(112)	- Ru(1)	- C(1)	- C(2)	164.0(6)
C(12)	- Ru(1)	- C(11)	- C(15)	114.3(9)
C(13)	- Ru(1)	- C(11)	- C(15)	77.0(7)
C(13)	- Ru(1)	- C(11)	- C(12)	-37.3(6)
C(14)	- Ru(1)	- C(11)	- C(15)	36.9(6)
C(14)	- Ru(1)	- C(11)	- C(12)	-77.4(7)

TABLE 6.6 (contd.)

C(15)	- Ru(1)	- C(11)	- C(12)	-114.3(9)
C(111)	- Ru(1)	- C(11)	- C(15)	143.9(6)
C(111)	- Ru(1)	- C(11)	- C(12)	29.6(9)
C(112)	- Ru(1)	- C(11)	- C(15)	-46.6(8)
C(112)	- Ru(1)	- C(11)	- C(12)	-160.9(6)
C(14)	- Ru(1)	- C(12)	- C(13)	-35.6(6)
C(15)	- Ru(1)	- C(12)	- C(13)	-77.7(7)
C(111)	- Ru(1)	- C(12)	- C(13)	82.1(7)
C(112)	- Ru(1)	- C(12)	- C(13)	-69.4(13)
C(15)	- Ru(1)	- C(13)	- C(14)	-38.1(6)
C(111)	- Ru(1)	- C(13)	- C(14)	134.8(6)
C(112)	- Ru(1)	- C(13)	- C(14)	35.2(9)
C(111)	- Ru(1)	- C(14)	- C(15)	-172.1(6)
C(112)	- Ru(1)	- C(14)	- C(15)	89.3(7)
C(212)	- Ru(2)	- C(25)	- C(21)	107.7(10)
C(211)	- Ru(2)	- C(25)	- C(21)	-154.0(8)
C(24)	- Ru(2)	- C(25)	- C(21)	-117.5(16)
C(23)	- Ru(2)	- C(25)	- C(21)	-79.6(10)
C(22)	- Ru(2)	- C(25)	- C(21)	-38.4(9)
C(5)	- Ru(2)	- C(25)	- C(21)	12.5(14)
C(212)	- Ru(2)	- C(25)	- C(24)	-134.9(11)
C(211)	- Ru(2)	- C(25)	- C(24)	-36.6(14)
C(23)	- Ru(2)	- C(25)	- C(24)	37.8(11)
C(22)	- Ru(2)	- C(25)	- C(24)	79.1(11)
C(21)	- Ru(2)	- C(25)	- C(24)	117.5(16)
C(5)	- Ru(2)	- C(25)	- C(24)	129.9(10)
C(23)	- Ru(2)	- C(24)	- C(25)	-117.1(15)
C(22)	- Ru(2)	- C(24)	- C(25)	-81.3(12)
C(21)	- Ru(2)	- C(24)	- C(25)	-38.4(11)
C(5)	- Ru(2)	- C(24)	- C(25)	-97.8(14)
C(212)	- Ru(2)	- C(24)	- C(23)	172.1(8)
C(211)	- Ru(2)	- C(24)	- C(23)	-90.6(9)
C(25)	- Ru(2)	- C(24)	- C(23)	117.1(15)
C(22)	- Ru(2)	- C(24)	- C(23)	35.7(8)
C(21)	- Ru(2)	- C(24)	- C(23)	78.7(10)
C(5)	- Ru(2)	- C(24)	- C(23)	19.3(16)
C(22)	- Ru(2)	- C(23)	- C(24)	-118.9(13)
C(21)	- Ru(2)	- C(23)	- C(24)	-78.2(10)
C(5)	- Ru(2)	- C(23)	- C(24)	-169.5(9)
C(212)	- Ru(2)	- C(23)	- C(22)	102.0(12)
C(211)	- Ru(2)	- C(23)	- C(22)	-144.1(7)
C(25)	- Ru(2)	- C(23)	- C(22)	84.0(9)
C(24)	- Ru(2)	- C(23)	- C(22)	118.9(13)
C(21)	- Ru(2)	- C(23)	- C(22)	40.7(8)
C(5)	- Ru(2)	- C(23)	- C(22)	-50.7(9)
C(21)	- Ru(2)	- C(22)	- C(23)	-111.8(11)
C(5)	- Ru(2)	- C(22)	- C(23)	136.1(8)
C(212)	- Ru(2)	- C(22)	- C(21)	-27.3(11)
C(211)	- Ru(2)	- C(22)	- C(21)	158.5(8)
C(25)	- Ru(2)	- C(22)	- C(21)	38.2(9)
C(24)	- Ru(2)	- C(22)	- C(21)	75.9(9)
C(23)	- Ru(2)	- C(22)	- C(21)	111.8(11)
C(5)	- Ru(2)	- C(22)	- C(21)	-112.1(8)
C(5)	- Ru(2)	- C(21)	- C(22)	73.1(8)
C(5)	- Ru(2)	- C(21)	- C(25)	-171.8(9)
C(212)	- Ru(2)	- C(5)	- C(4)	158.5(6)
C(211)	- Ru(2)	- C(5)	- C(4)	69.0(6)
C(25)	- Ru(2)	- C(5)	- C(4)	-100.8(9)
C(24)	- Ru(2)	- C(5)	- C(4)	-44.5(12)

TABLE 6.6 (contd.)

C(23)	- Ru(2)	- C(5)	- C(4)	-32.2(8)
C(22)	- Ru(2)	- C(5)	- C(4)	-58.6(6)
C(21)	- Ru(2)	- C(5)	- C(4)	-93.2(7)
C(22)	- Ru(2)	- C(21)	- C(25)	115.1(13)
C(23)	- Ru(2)	- C(21)	- C(25)	76.1(11)
C(23)	- Ru(2)	- C(21)	- C(22)	-39.0(7)
C(24)	- Ru(2)	- C(21)	- C(25)	34.3(10)
C(24)	- Ru(2)	- C(21)	- C(22)	-80.8(9)
C(25)	- Ru(2)	- C(21)	- C(22)	-115.1(13)
C(211)	- Ru(2)	- C(21)	- C(25)	63.5(17)
C(211)	- Ru(2)	- C(21)	- C(22)	-51.5(16)
C(212)	- Ru(2)	- C(21)	- C(25)	-81.9(10)
C(212)	- Ru(2)	- C(21)	- C(22)	163.0(7)
C(24)	- Ru(2)	- C(22)	- C(23)	-35.9(9)
C(25)	- Ru(2)	- C(22)	- C(23)	-73.6(9)
C(211)	- Ru(2)	- C(22)	- C(23)	46.7(9)
C(212)	- Ru(2)	- C(22)	- C(23)	-139.1(8)
C(25)	- Ru(2)	- C(23)	- C(24)	-34.8(10)
C(211)	- Ru(2)	- C(23)	- C(24)	97.1(10)
C(212)	- Ru(2)	- C(23)	- C(24)	-16.8(17)
C(211)	- Ru(2)	- C(24)	- C(25)	152.4(11)
C(212)	- Ru(2)	- C(24)	- C(25)	55.0(13)
Ru(1)	- C(1)	- C(2)	- C(3)	177.8(5)
C(1)	- C(2)	- C(3)	- C(4)	-176.3(7)
C(2)	- C(3)	- C(4)	- C(5)	-175.2(7)
C(3)	- C(4)	- C(5)	- Ru(2)	-176.4(5)
C(12)	- C(11)	- C(15)	- Ru(1)	64.5(7)
Ru(1)	- C(11)	- C(15)	- C(14)	-64.0(8)
Ru(1)	- C(11)	- C(12)	- C(13)	63.8(8)
C(15)	- C(11)	- C(12)	- Ru(1)	-64.3(7)
C(12)	- C(11)	- C(15)	- C(14)	.5(12)
C(15)	- C(11)	- C(12)	- C(13)	-.4(12)
C(11)	- C(12)	- C(13)	- Ru(1)	-63.4(8)
C(11)	- C(12)	- C(13)	- C(14)	.3(13)
Ru(1)	- C(12)	- C(13)	- C(14)	63.6(8)
C(12)	- C(13)	- C(14)	- Ru(1)	-62.3(8)
C(12)	- C(13)	- C(14)	- C(15)	.1(13)
Ru(1)	- C(13)	- C(14)	- C(15)	62.3(8)
Ru(1)	- C(14)	- C(15)	- C(11)	62.7(8)
C(13)	- C(14)	- C(15)	- C(11)	-.3(13)
C(13)	- C(14)	- C(15)	- Ru(1)	-63.1(8)
C(22)	- C(21)	- C(25)	- Ru(2)	65.2(10)
Ru(2)	- C(21)	- C(25)	- C(24)	-64.4(14)
Ru(2)	- C(21)	- C(22)	- C(23)	65.1(9)
C(25)	- C(21)	- C(22)	- Ru(2)	-64.7(12)
C(22)	- C(21)	- C(25)	- C(24)	.7(20)
C(25)	- C(21)	- C(22)	- C(23)	.4(16)
C(21)	- C(22)	- C(23)	- Ru(2)	-64.1(9)
C(21)	- C(22)	- C(23)	- C(24)	-1.3(16)
Ru(2)	- C(22)	- C(23)	- C(24)	62.8(12)
C(22)	- C(23)	- C(24)	- Ru(2)	-63.5(10)
C(22)	- C(23)	- C(24)	- C(25)	1.8(20)
Ru(2)	- C(23)	- C(24)	- C(25)	65.3(14)
Ru(2)	- C(24)	- C(25)	- C(21)	63.0(13)
C(23)	- C(24)	- C(25)	- C(21)	-1.5(21)
C(23)	- C(24)	- C(25)	- Ru(2)	-64.6(13)

6.4 Reactions of $[CpRu(CO)_2]_2[\mu\text{-}(CH_2)_5]$ with Tertiary Phosphines.

6.4.1 Reaction of $[CpRu(CO)_2]_2[\mu\text{-}(CH_2)_5]$ with PPh_3

$[CpRu(CO)_2]_2[\mu\text{-}(CH_2)_5]$ (0.171 g, 0.332 mmol) and PPh_3 (0.088 g, 0.335 mmol) were refluxed under N_2 in xylene (15 cm^3) and the reaction monitored by observing the gradual disappearance of the reactant ν(CO) bands at 2010 and 1947 cm^{-1} and the growth of two new bands at 1923 and 1602 cm^{-1} in the infrared spectrum. No change was detected in the infrared spectrum after 17 hours. At this point, the new terminal ν(CO) band at 1923 cm^{-1} had grown to half the intensity of the bands due to the reactant implying that a large proportion of starting material was still present. During the course of the reaction, the solution changed from very pale yellow to a bright yellow-orange colour. The solvent was removed under reduced pressure and hexane added to the residue. The cloudy yellow solution was stored overnight at 0°C resulting in the precipitation of a pale yellow solid. The hexane solution was syringed off and the product dried under vacuum to yield $[Cp(CO)_2Ru(CH_2)_5C(O)Ru(CO)(PPh_3)Cp]$ (28) (0.120 g, 45%) as a yellow micro-crystalline solid. This product was identified by its infrared spectrum in hexane which showed ν(CO) bands of equal intensity at 2018, 1959 and 1932 cm^{-1} and a weak acyl ν(CO) band at 1602 cm^{-1}. This compound was later isolated from the reaction of $[CpRu(CO)_2]_2[\mu\text{-}(CH_2)_5]$ with $2PPh_3$ and further characterised by melting point, microanalysis, ^1H and ^{13}C NMR spectroscopy.(Section 6.4.2).

6.4.2. Reaction of $[CpRu(CO)_2]_2[\mu\text{-}(CH_2)_5]$ with 2 PPh_3 in Xylene.

$[CpRu(CO)_2]_2[\mu\text{-}(CH_2)_5]$ (0.170 g, 0.330 mmol) and PPh_3 (0.173 g, 0.660 mmol) were refluxed under N_2 in xylene (20 cm^3). The reaction was monitored at intervals by observing the gradual decrease in intensity of the reactant ν(CO) bands at 2010 and 1943 cm^{-1} and the concomitant growth of a new terminal band at 1923 cm^{-1} and a new weak acyl CO band at 1602 cm^{-1} in the infrared spectrum. After 20.75 hours, the new ν(CO) band at 1923 cm^{-1} was of the same intensity as the ν(CO) band at 2010 cm^{-1}. After 32 hours, this band at 1923 cm^{-1} was the strongest of the three terminal CO bands. The reaction was monitored for a total of 165.25 hours, however, little change in the infrared spectrum was detected after 117.25 hours, indicating that the reaction was essentially "complete".

At this point, the new ν(CO) band at 1923 cm^{-1} was twice the intensity of the stongest ν(CO) band at 1943 cm^{-1}. The solvent was removed under reduced pressure and the residue taken up in CH_2Cl_2 (3 cm^3) and chromatographed on a Florisil column. A pale yellow band was eluted with a CH_2Cl_2/hexane (50:50) mixture followed by an (80:20) mixture and yielded an orange coloured residue (0.070 g, 23%) on removal of the solvent. This product was recrystallised from hexane at -78°C to give orange crystals of $[Cp(CO)_2Ru(CH_2)_5C(O)Ru(CO)(PPh_3)Cp]$. Infrared data, melting range and microanalysis for this compound (28) are reported in Table 6.7. (Partial characterisation by NMR although integration reveals presence of impurities; ^1H NMR in $CDCl_3$: δ 7.47 ppm (5H, PPh_3), δ 5.14 and δ 4.90 ppm (3H each, C_5H_5), δ 2.43 ppm (1H), δ 2.16 ppm (1H), δ 1.19 ppm (7H), δ 0.82 ppm (6H); ^{13}C NMR in $CDCl_3$:

δ 256.2 ppm (d, acyl CO), δ 205.6 ppm (d, terminal CO), δ 135.3 (d), 133.0 (d), 129.4 (s) and 127.5 (d) ppm (PPh_3), δ 88.5 and 88.3 ppm (2x C_5H_5), δ 65.6 ppm (CH_2CO), δ 39.4 ppm (Ru-$CH_2\underline{CH_2}$), δ 33.9 ppm (impurity), δ 29.4 ppm ($\underline{CH_2}CH_2CO$), δ 24.3 ppm (-CH_2-) and δ -3.5 ppm (Ru-CH_2)).

A second bright yellow fraction was eluted from the column with methanol and gave $[CpRu(CO)(PPh_3)]_2[\mu\text{-}C(O)(CH_2)_5C(O)]$ (29) (0.312 g, 77%) as a yellow solid on removal of the solvent. The product was recrystallised from methanol at -78°C to give pale yellow crystals. Melting point ranges, microanalysis and infrared data are reported in Table 6.7. ^1H and ^{13}C NMR data are reported in Table 3.1 and 3.2 respectively (Section 3).

6.4.3. Reaction of $[CpRu(CO)_2]_2[\mu\text{-}(CH_2)_5]$ with $2PPh_3$ in CH_3CN.

$[CpRu(CO)_2]_2[\mu\text{-}(CH_2)_5]$ (0.174 g, 0.336 mmol) and PPh_3 (0.173 g, 0.660 mmol) were refluxed under N_2 in CH_3CN (20 cm^3) and the reaction monitored by infrared spectroscopy. After 13.45 hours a very slight shoulder at ca 1920 cm^{-1} could be detected on the strong ν(CO) band, due to reactant, at 1942 cm^{-1}. The intensities of the ν(CO) bands at 1942 and 2008 cm^{-1} due to reactant were practically unchanged. After 87 hours refluxing, the shoulder at 1920 cm^{-1} was observed as a separate band of half the intensity of the band at 1942 cm^{-1}. After 138 hours, a new acyl ν(CO) band could be detected at 1604 cm^{-1} while the band at 1920 cm^{-1} had grown to two-thirds the intensity of the band at 1942 cm^{-1}. The reaction was monitored for 233.5 hours (9.7 days) at which stage the new band at 1919 cm^{-1} was of equal intensity to the band at

1942 cm^{-1}. The reaction was stopped and the solvent removed under reduced pressure. The yellow residue was taken up in CH_2Cl_2 (3 cm^3) and chromatographed on a Florisil column. A colourless fraction was eluted with hexane. Removal of the solvent yielded $[CpRu(CO)_2]_2[\mu\text{-}(CH_2)_5]$ (0.090 g, 52%) identified by infrared spectroscopy. A pale yellow fraction, eluted with CH_2Cl_2/hexane (80:20), followed by CH_2Cl_2 (100%), gave $[Cp(CO)_2Ru(CH_2)_5C(O)Ru(CO)(PPh_3)Cp]$ (28) (0.080 g, 31%) as a yellow oil which was identified by infrared spectroscopy only. (IR in hexane, ν(CO): 2017 (s), 1958 (s), 1932 (ms), 1600 (m,broad) cm^{-1}). A third pale yellow fraction was eluted with methanol and gave a pale yellow solid which was identified as $[CpRu(CO)(PPh_3)]_2[\mu\text{-}C(O)(CH_2)_5C(O)]$ (29) (0.050 g, 14%) from the infrared spectrum in CH_2Cl_2 (ν(CO): 1922 (m) 1603 (mw) cm^{-1}).

$[CpRu(CO)(PPh_3)]_2[\mu\text{-}C(O)(CH_2)_5C(O)]$ was recrystallised from methanol at -78°C as a pale yellow microcrystalline solid with a melting point range 98-105°C. This product was further identified by its ^1H and ^{13}C NMR spectra which were in agreement with previous data for this compound (Section 3, Tables 3.1 and 3.2).

6.4.4. Reaction of $[CpRu(CO)_2]_2[\mu\text{-}(CH_2)_5]$ with 3 PPh_3.

$[CpRu(CO)_2]_2[\mu\text{-}(CH_2)_5]$ (0.250 g, 0.486 mmol) and PPh_3 (0.382 g, 1.456 mmol) were refluxed under N_2 in xylene (20 cm^3) and the reaction monitored at intervals by infrared spectroscopy. After 15 hours, the infrared spectrum revealed that the new band at 1923 cm^{-1} was of slightly greater intensity than the ν(CO) band at 2010 cm^{-1} due to reactant. Thus, the reaction of $[CpRu(CO)_2]_2[\mu\text{-}(CH_2)_5]$

with a 3 molar equivalent of PPh_3 appears to proceed more rapidly than with a 2 molar equivalent of PPh_3 (See Section 6.4.2 where the band at 1923 cm^{-1} was of slightly lower intensity than that at 2010 cm^{-1} after 20.75 hours refluxing.). This would imply that the rate of reaction is dependant on the concentration of phosphine present. The reaction was monitored for a total of 111.75 hours. However, no change was detected in the infrared spectrum between 89.25 and 111.75 hours. The solvent was removed under reduced pressure and the orange residue taken up in CH_2Cl_2 (3 cm^3) and chromatographed on a Florisil column (8 cm high by 2 cm diameter). Elution with hexane gave a colourless fraction which yielded $[CpRu(CO)_2]_2[\mu\text{-}(CH_2)_5]$ (0.100 g, 40%) identified by infrared spectroscopy. A pale yellow fraction, eluted with CH_2Cl_2/hexane (50:50) mixture followed by an (80:20) mixture, gave $[Cp(CO)_2Ru(CH_2)_5C(O)Ru(CO)(PPh_3)Cp]$ (28) (0.070 g, 18.5%) as an orange oil. $[CpRu(CO)(PPh_3)]_2[\mu\text{-}C(O)(CH_2)_5C(O)]$ (29) (0.200 g, 40%) was eluted from the column with methanol.

These compounds were again characterised by microanalysis, melting point and infrared, which were in agreement with previous characterisation data (Section 6.4.2) for (28) and (29) . Compound (29) was characterised further by ^1H and ^{13}C NMR spectroscopy (Tables 3.1 and 3.2).

6.4.5 Reaction of $[CpRu(CO)_2]_2[\mu\text{-}(CH_2)_5]$ with 2 PPh_2Me.

$[CpRu(CO)_2]_2[\mu\text{-}(CH_2)_5]$ (0.251 g, 0.488 mmol) and PPh_2Me (0.198 g, 0.989 mmol) were refluxed under N_2 in xylene (20 cm^3) and the reaction monitored at intervals by infrared spectroscopy by observing the gradual decrease in intensity of the ν(CO) bands at 2010 and 1948 cm^{-1} due to reactant and the concomitant growth of two new ν(CO) bands at 1923 (terminal CO) and 1600 cm^{-1} (acyl CO).

After 17.75 hours, the new band at 1923 cm^{-1} was of equal intensity to the band at 2010 cm^{-1} (and of comparable intensity to the corresponding band observed after 20.75 hours with 2 PPh_3 - section 6.4.2). After 72.5 hours this new band had grown to twice the intensity of the band at 1947 cm^{-1}. The reaction was monitored for a total of 91.75 hours but no further change in the infrared spectrum was observed after 72.5 hours. The solvent was removed under reduced pressure, the residue dissolved in CH_2Cl_2 (2 cm^3) and the solution chromatographed on a Florisil column (7 cm high by 2 cm diameter). A colourless fraction eluted with hexane yielded $[CpRu(CO)_2]_2[\mu\text{-}(CH_2)_5]$ (0.060 g, 24%) on removal of the solvent, which was identified by an infrared spectrum in hexane. A pale yellow fraction was eluted with CH_2Cl_2/hexane (50:50) mixture followed by an (80:20) mixture and gave an orange residue identified as $[Cp(CO)_2Ru(CH_2)_5C(O)Ru(CO)(PPh_2Me)Cp]$ (30) (0.030 g, 9%) by its infrared spectrum in hexane, ν(CO): 2017 (m), 1959 (ms), 1933 (m) and 1600 (m) cm^{-1}.

A third bright yellow fraction, eluted with methanol gave $[CpRu(CO)(PPh_2Me)]_2[\mu\text{-}C(O)(CH_2)_5C(O)]$ (31) (0.300g, 67%) which was

recrystallised from methanol at -78°C to give a pale yellow microcrystalline solid. This product has been characterised by melting point, microanalysis and infrared spectroscopy (Table 6.7), as well as by ^{1}H and ^{13}C NMR spectroscopy (Tables 3.1 and 3.2 respectively).

6.4.6 Reaction of $[CpRu(CO)_2]_2[\mu\text{-}(CH_2)_5]$ with 2 $PPhMe_2$.

$[CpRu(CO)_2]_2[\mu\text{-}(CH_2)_5]$ (0.166 g, 0.323 mmol) and $PPhMe_2$ (0.097 g, 0.702 mmol) were refluxed under N_2 in xylene (15 cm^3). The reaction was monitored by infrared spectroscopy in the ν(CO) region after 20.5 hours, 68.25 hours and 91.25 hours, which revealed the reaction to be essentially complete after 20.5 hours. The infrared spectrum at 20.5 hours showed only one strong terminal ν(CO) band at 1918 cm^{-1} (with a slight shoulder at ca. 1945 cm^{-1}) and a strong acyl ν(CO) band at 1602 cm^{-1}. The solvent was removed under reduced pressure and the product taken up in a minimum of CH_2Cl_2 (2 cm^3). Chromatography on a Florisil column (6 cm high by 3 cm diameter) separated two products. The first colourless product eluted with hexane, was identified by its infrared spectrum as $[CpRu(CO)_2]_2[\mu\text{-}(CH_2)_5]$ (0.010 g, 6%). The second pale yellow fraction was eluted with methanol and yielded $[CpRu(CO)(PPhMe_2)]_2[\mu\text{-}C(O)(CH_2)_5C(O)]$ (32) (0.230 g, 90%) as an oily yellow liquid, on removal of the solvent under reduced pressure. Recrystallisation of compound (32) was attempted from methanol at -78°C, however, no crystals formed. The product was thus isolated as an orange oil at room temperature and characterised by microanalysis, infrared (Table 6.7) and ^{1}H and ^{13}C NMR spectroscopy (Tables 3.1 and 3.2 respectively).

TABLE 6.7 Yields, melting point, IR and microanalytical data for $[Cp(CO)_2Ru(CH_2)_5C(O)Ru(CO)(PR_3)Cp]$ and $[CpRu(CO)(PR_3)]_2[\mu\text{-}C(O)(CH_2)_5C(O)]$ (PR_3 = PPh_3, PPh_2Me and $PPhMe_2$)

COMPOUND No.	PR_3	Yield (%)	Melting Range (°C)	ν(CO) in cm^{-1} [a]	Analysis[b] %C	%H
28	PPh_3	46	42 - 48	2010(m), 1943(m), 1922(m), 1600(m)	57.10(57.20)	4.60 (4.55)
29	PPh_3	77	95 - 102	1922(s), 1603(ms)	63.00(63.57)	4.80 (4.86)
31	PPh_2Me	67	50 - 56	1920(vs), 1592(broad,s)	58.90(59.07)	5.10 (5.08)
32	$PPhMe_2$	90	oil at R.T.	1922(s) , 1605(ms)	53.70(53.5)	5.60 (5.36)

a In CH_2Cl_2

b. Calculated values in parenthesis

6.4.7 Reaction of $[CpFe(CO)_2]_2[\mu\text{-}(CH_2)_5]$ with 2 PPh_3.

$[CpFe(CO)_2]_2[\mu\text{-}(CH_2)_5]$ (0.252 g, 0.594 mmol) (prepared as in [19]) and PPh_3 (0.310 g, 1.182 mmol) were refluxed under N_2 in THF (20 cm^3). The reaction was monitored by infrared spectroscopy by observing the growth of a terminal ν(CO) band at 1912 cm^{-1} and the decrease in reactant ν(CO) bands at 1998 and 1939 cm^{-1}. The reaction was monitored at 0.5, 2.25, 4.25, 7.25, 23.5, 31.25 and 47.5 hours and the intensity of the respective bands compared to those observed for the corresponding reaction in the presence of $[CpFe(CO)_2]_2$ (as catalyst) at identical time intervals (See Table 6.8).

6.4.8 Reaction of $[CpFe(CO)_2]_2[\mu\text{-}(CH_2)_5]$ with 2 PPh_3 in the presence of $[CpFe(CO)_2]_2$ as catalyst.

$[CpFe(CO)_2]_2[\mu\text{-}(CH_2)_5]$ (0.251 g, 0.592 mmol) (prepared as in [19]) and PPh_3 (0.311 g, 1.186 mmol) were refluxed under N_2 in THF (20 cm^3) in the presence of a catalytic amount of $[CpFe(CO)_2]_2$ (recrystallised from hexane prior to use). The reaction was monitored by infrared spectroscopy by observing the growth of a new terminal ν(CO) band at 1912 cm^{-1} and the decrease in intensity of the reactant bands at 1998 and 1939 cm^{-1}. The reaction was monitored at 0.5, 2.25, 4.25, 7.25, 23.5, 31.25 and 47.5 hours and the intensities of the bands compared to those for the corresponding reaction in the absence of $[CpFe(CO)_2]_2$ at identical time intervals. No rate enhancement due to the addition of $[CpFe(CO)_2]_2$ was observed. (See Table 6.8).

TABLE 6.8 Intensities of ν(CO) bands observed during the reaction of $[CpFe(CO)_2]_2[\mu\text{-}(CH_2)_n]$ with 2 PPh_3

Reaction Time hr.	% T							
	Without $[CpFe(CO)_2]_2$				With $[CpFe(CO)_2]_2$			
	cm^{-1} 1998	1939	1912	1613	cm^{-1} 1998	1939	1912	1613
0.5	3.05	2.24	66.51	-	2.94	2.09	65.97	-
2.25	5.44	3.85	45.65	79.56	5.07	3.66	45.95	79.86
4.25	8.65	6.39	32.73	74.45	7.38	5.44	32.52	74.73
7.25	10.53	7.79	20.67	67.34	9.62	7.25	21.79	67.67
23.5	27.16	21.56	10.42	59.60	26.02	20.75	11.55	60.63
31.25	34.79	28.53	11.04	60.33	31.17	25.21	10.74	59.84
47.5	36.15	29.32	7.67	55.06	35.69	28.87	8.98	57.10

6.5 Experimental Details of the Reaction of $[CpRu(CO)_2]_2[\mu-(CH_2)_5]$ with Electrophiles.

6.5.1 Reaction of $[CpRu(CO)_2]_2[\mu-(CH_2)_5]$ with Bromine.

A solution of bromine (0.065 g, 0.407 mmol) in THF (1 cm^3) was added to a stirred solution of $[CpRu(CO)_2]_2[\mu-(CH_2)_5]$ (0.103 g, 0.200 mmol) in THF (5 cm^3) under N_2. Within a few minutes the originally pale yellow solution became a clear, light green colour. After 10 minutes an infrared spectrum revealed two new strong $\nu(CO)$ bands at 2046 and 1994 cm^{-1} (and a very weak band at 1946 cm^{-1} due to $[CpRu(CO)_2]_2[\mu-(CH_2)_5]$).
The reaction mixture was stirred for a further 20 minutes and the solvent removed under reduced pressure. The green oily residue was taken up in diethyl ether and chromatographed on a Florisil column (ca.3 cm high by 3 cm diameter). A pale yellow band was eluted with hexane first. Removal of the solvent afforded a yellow coloured oil (0.045 g, 98%) which smelled strongly of $Br(CH_2)_5Br$. A ^1H NMR spectrum of this product revealed mainly $Br(CH_2)_5Br$ with traces of $[CpRu(CO)_2]_2[\mu-(CH_2)_5]$ and $[CpRu(CO)_2Br]$ (detectable by the presence of singlets of low intensity at δ 5.21 ppm and δ 5.43 ppm for the Cp protons).

A second bright yellow fraction was eluted with a hexane/ether (19:1) mixture followed by a (40:60) mixture. Removal of the solvent afforded $[CpRu(CO)_2Br]$ (0.110 g, 91%) as yellow needles. The yellow needles were recrystallised from hexane at -78°C and identified by comparision of the melting point, infrared and ^1H

NMR data with that of authentic samples [71,123,124] as well as by microanalysis.

Infrared spectroscopy in hexane, ν(CO): 2055 (s) and 2008 (s) cm^{-1}. Melting point range: sublimes 75-80°C; melt 89-92°C (cf 88.5-88.8°C, [71]). ^1H NMR in $CDCl_3$: δ 5.42 ppm (singlet, 5H, C_5H_5). Analysis: $C_7H_5O_2RuBr$ requires 27.83 %C, 1.67 %H; found 28.3 %C, 1.70 %H.

6.5.2 Reaction of $[CpRu(CO)_2]_2[\mu\text{-}(CH_2)_5]$ with Iodine.

A solution of iodine (0.103 g, 0.410 mmol) in THF (1 cm^3) was added to a stirred solution of $[CpRu(CO)_2]_2[\mu\text{-}(CH_2)_5]$ (0.103 g, 0.200 mmol) in THF (5 cm^3) under N_2. The reaction mixture immediately turned from a pale yellow to a clear red brown colour. After 15 minutes an infrared spectrum in THF revealed two strong ν(CO) bands at 2042 and 1991 cm^{-1}. The reaction mixture was stirred for a further 20 minutes and the solvent removed under reduced pressure. The residue was taken up in hexane/ether (60:40) and chromatographed on a Florisil column (3 cm high by 3 cm diameter). Elution initially with hexane/ether (19:1) gave a yellow oil (0.060 g, 93%) identified as $I(CH_2)_5I$ by ^1H NMR. Subsequent elution with a hexane/ether (50:50) mixture and finally a (40:60) mixture gave a bright orange solution. Removal of the solvent under reduced pressure afforded $[CpRu(CO)_2I]$ (0.120 g, 86%) as an orange crystalline solid which was identified by comparision of the melting point and infrared data with that of authentic samples [123,124] as well as by microanalysis and ^1H NMR spectroscopy.

Melting point: 114-123°C (cf. 121-122°C [107]); Infrared spectroscopy in hexane, ν(CO): 2050 (s) and 2005 (s) cm^{-1} (cf. ν(CO) in CS_2: 2055 (vs) and 2007 (vs) cm^{-1} [108]); Analysis: $C_7H_5O_2RuI$ requires 24.08 %C, 1.45 %H; found 24.5 %C, 1.5 %H; ^1H NMR in $CDCl_3$: δ 5.46 ppm (singlet, 5H, C_5H_5). No acyl organic products such as $IC(O)(CH_2)_5C(O)I$ were detected.

6.5.3 Reaction of $[CpRu(CO)_2]_2[\mu\text{-}(CH_2)_5]$ with $Ph_3C^+PF_6^-$.

To a stirred solution of $[CpRu(CO)_2]_2[\mu\text{-}(CH_2)_5]$ (0.048 g, 0.093 mmol) in CH_2Cl_2 (2 cm^3) a solution of $Ph_3C^+PF_6^-$ (0.036 g, 0.093 mmol) in CH_2Cl_2 (2 cm^3) was added dropwise. The reaction was monitored at intervals by infrared spectroscopy. After 23 hours the infrared spectrum revealed only the carbonyl bands at 2009 (vs) and 1944 (vs) cm^{-1} due to $[CpRu(CO)_2]_2[\mu\text{-}(CH_2)_5]$ indicating that no reaction had occurred with $Ph_3C^+PF_6^-$.

6.6 Reaction of $[CpM(CO)_2]_2[\mu\text{-}(CH_2)_5]$ with t-BuNC.

6.6.1 Reaction of $[CpFe(CO)_2]_2[\mu\text{-}(CH_2)_5]$ with 2t-BuNC in THF

$[CpFe(CO)_2]_2[\mu\text{-}(CH_2)_5]$ (0.189 g, 0.445 mmol) (prepared as in [19]) and t-BuNC (0.10 cm^3, 0.074 g, 0.890 mmol) were refluxed under N_2 in THF (20 cm^3) and the reaction monitored by observing the disappearance of the ν(CO) reactant band at 1998 cm^{-1} and the broadening of the ν(CO) reactant band at 1939 cm^{-1} in the infrared spectrum.

A new acyl ν(CO) band at 1630 cm^{-1} was also observed, in addition to a band at 2133 cm^{-1} due to ν(CN). After 7.0 hours, the broad band at 1939 cm^{-1} had shifted to 1937 cm^{-1} and the new acyl band at 1630 cm^{-1} was of greater intensity than the band at 1998 cm^{-1} due to starting material. After 21.75 hours, the band at 1998 cm^{-1}, due to starting material, had completely disappeared and only bands at 2133 (vs), 1935 (vs) and 1629 (m) cm^{-1} were present in the infrared spectrum. The reaction was thus assumed to be complete and the solvent was removed under reduced pressure. The residue was taken up in CH_2Cl_2 (2 cm^3) and chromatographed on a Florisil column. A colourless fraction was eluted with CH_2Cl_2/hexane (50:50) mixture followed by CH_2Cl_2 (100%). This gave a colourless residue (0.050 g) which revealed one strong band at 1732 cm^{-1} in the infrared spectrum in hexane. This residue was not characterised further, but the strong band is believed to be due to contamination by acetone, probably present in the glass sinter of the column. A second bright yellow fraction was eluted from the column with methanol and gave an orange oily residue (0.240 g, 91%) on removal of the solvent. This residue was recrystallised from hexane at -78°C to give a yellow crystalline solid which melts slowly on warming to room temperature to an orange-yellow oil. The oil was identified as $[CpFe(CO)(t\text{-}BuNC)]_2[\mu\text{-}C(O)(CH_2)_5C(O)]$. Analysis: $C_{29}H_{38}N_2O_4Fe_2$ requires 58.99 %C, 6.50 %H and 4.75 %N; found 59.00 %C, 6.10 %H and 4.70 %N. Infrared spectroscopy in hexane: ν(CN) 2114 (broad, m) and 2080 (sh) cm^{-1}; ν(CO) 1945 (s) and 1636 (m) cm^{-1}. ^1H and ^{13}C NMR data are reported in Tables 3.3 and 3.4 respectively.

6.6.2 Reaction of $[CpRu(CO)_2]_2[\mu\text{-}(CH_2)_5]$ with 2 t-BuNC in Xylene.

$[CpRu(CO)_2]_2[\mu\text{-}(CH_2)_5]$ (0.230 g, 0.447 mmol) and t-BuNC (0.10 cm^3, 0.074 g, 0.890 mmol) were refluxed under N_2 in xylene (20 cm^3) and the reaction monitored by infrared spectroscopy at intervals. A gradual decrease in the intensity of the strong ν(CO) band at 2010 cm^{-1} with the concomitant broadening of the band at 1946 cm^{-1} (both due to starting material) was observed. This band at 1946 cm^{-1} shifted during the reaction to 1944 cm^{-1}. In addition a new acyl ν(CO) band at 1628 cm^{-1} and a broad ν(CN) band at 2133 cm^{-1} were also observed after 5 hours. The reaction was left to reflux overnight. After 21 hours, the infrared spectrum showed that a change had occurred in the reaction products. Besides the broad bands at 2121 and 1944 cm^{-1}, a strong band at 1760 cm^{-1} was also observed. In addition, the weak ν(CO) band at 1628 cm^{-1} had disappeared. The solvent was removed under reduced pressure and the product dissolved in CH_2Cl_2 (2 cm^3) and chromatographed on a Florisil column. A pale yellow fraction, eluted with CH_2Cl_2/hexane (50:50) followed by CH_2Cl_2 (100%) gave an orange residue which was identified by its infrared spectrum in hexane as $[CpRu(CO)_2]_2$ (0.060 g, 30%). A second yellow fraction was eluted with methanol to give $[CpRu(CO)(t\text{-}BuNC)]_2[\mu\text{-}(CH_2)_5]$ (0.060 g , 20%) identified only by infrared spectroscopy in CH_2Cl_2: ν(CN) 2156 (m) and 2117 (m) cm^{-1}; ν(CO) 1969 (m) cm^{-1}.

6.7 Experimental Details of Catalysis with γ-Al_2O_3 Supported $[CpFe(CO)_2]_2[\mu\text{-}(CH_2)_n]$.

6.7.1 General

γ -Al_2O_3 was obtained from Strem Chemicals (Lot No 14068-5) and calcined at 470°C in air prior to pelletting. The calcined Al_2O_3 was then compressed into pellets and sieved to give a particle size of 1180μm - 500μm. THF was routinely distilled from Na wire/benzophenone. Catalysts containing 5 % by mass Fe were prepared by supporting compounds of $[CpFe(CO)_2]_2[\mu\text{-}(CH_2)_n]$ (n=0, 3 and 5) on γ-Al_2O_3, prepared as above, using the incipient wetness technique [143,144] and the resulting materials dried in vacuo for 1 - 2 hours before use. Prior to testing, the supported materials (2 g) were loaded into a fixed-bed microreactor and were reduced under hydrogen (gas hourly space velocity, GHSV = 300 h^{-1}) at 100°C for 0hr20, 150°C for 4hr40 and at 250°C for 20hr00 (Total reduction time 25hr00) to give the final catalyst.

6.7.2 Catalytic Run: 250°C / 5 atm.

Premixed CO/H_2 (1:1 v/v) was reacted over the catalyst at 250°C at a constant flow rate (GHSV = 300 h^{-1}). The pressure was maintained at 500 kPa. The reactor effluent was cooled to 20°C to trap liquid products and the resulting gas was analysed using on-line gas chromatography on a 2 m, $^1/_8$ inch stainless steel Porapak Q column. A Varian 3300 GC instrument and a Varian 4270 integrator were used.

6.7.3 Thermal Decomposition studied by FT-IR Spectroscopy.

Al_2O_3 - supported samples of $[CpFe(CO)_2]_2[\mu-(CH_2)_n]$ where n=0 (5k) and n=5 (5c) (containing 2.5 % by mass Fe) were prepared by the incipient wetness technique [143,144] , and dried in vacuo for ca. 1 hour. The supported materials were then divided into 300 mg portions and the various samples heated under vacuum in an oil bath as follows.

(i) for 1.0 hour at 145°C

(ii) for 0.25 hour at 180°C

(iii) for 0.5 hour at 180°C

(iv) for 1.0 hour at 180°C

(v) for 2.0 hours at 180°C

(vi) for 1.0 hour at 200°C

The diffuse reflectance FT-infrared spectra of all the above samples, as well as of the pure solids (5k) and (5c) as KBr powders, were recorded in the region 2200-1600 cm^{-1} using a Bruker FT-IR Spectrometer having a diffuse reflectance attachment.

6.7.4 Differential Scanning Calorimetry of $[CpFe(CO)_2]_2[\mu\text{-}(CH_2)_n]$.

Thermal decomposition of the pure solid compounds (5) (n= 0,3,5) was studied by Differential Scanning Calorimetry (DSC) on a Du Pont 910 DSC instrument and a Du Pont 9900 Computer/Thermal Analyser. Samples of ca. 1.0 - 1.5 mg were heated from ambient temperature (ca. 20°C) to 350°C at a rate of 5°C / minute in open pans under hydrogen and in pans sealed hermetically in air. Results are reported in Tables 4.1 and 4.2.

6.7.5 Thermal Decomposition of $[CpFe(CO)_2]_2[\mu\text{-}(CH_2)_n]$, (n= 3,5) under CO/H_2: Analysis by Gas Chromatography.

A small glass reactor (shown in Figure 4.2) equipped with an inlet and exit for gas, two small syringes attached to the base, a heating tape and thermocouple was constructed. The reactor was insulated by wrapping in fibreglass. 200 mg of supported catalyst $[CpFe(CO)_2]_2[\mu\text{-}(CH_2)_n]$ / Al_2O_3 (n = 3 or 5),(prepared by the incipient wetness technique [143,144]), containing 20 % by mass Fe, was loaded to the minireactor and the system flushed well with nitrogen. Premixed CO/H_2 (1:1 v/v) was reacted over the catalyst (GHSV = $600h^{-1}$) at 120°C; (these runs were repeated under nitrogen). Gas samples were collected in N_2 - filled, sealed sample bottles (5 cm^3) by flushing each bottle with gas from the reactor for 3 minutes (by means of the two syringes attached to the base of the reactor). The samples were analysed by FID gas chromatography on a Varian 3300 G.C. instrument and a Varian 4290

integrator. Column: $^{1}/_{8}$ inch stainless steel column packed with Porapak Q. G.C temperature programme : 80°C for 5 minutes, heat at 20°C/minute to 200°C, held at 200°C for 100 minutes.

6.7.6 Thermal Decomposition of $[CpFe(CO)_2]_2[\mu\text{-}CH_2)_n]/Al_2O_3$ (n=3 or 5): GC-MS analysis.

Supported samples of $[CpFe(CO)_2]_2[\mu\text{-}(CH_2)_n]$ (n=3, 5) containing ca. 20% by mass Fe were prepared by the incipient wetness method, [143,144]. These supported materials were decomposed under vacuum at 120°C (in an oil bath) and the volatile products condensed at -196°C. The volatile products were subsequently injected into a GC-MS. using a V.G. Micromass 16F spectrometer (at 70eV with an accelerating voltage of 4 kV) coupled to a Carlo-Erba Fractovap 4200 GC Instrument using a Carbowax 25m capilliary column.

6.8 Preparation of Haloalkyl Cobaloximes, $[Co(DH)_2py(CH_2)_nX]$ (50a-e)

6.8.1 General

^{1}H NMR and ^{13}C NMR data are reported in Tables 5.1 and 5.3 respectively . All other characterisation data are reported in Tables 6.9 and 6.11.

6.8.2 Preparation of $[Co(DH)_2py(CH_2)_3Br]$ (50a)

$[Co(DH)_2pyCl]$ (0.500 g, 1.24 mmol) was added to 10cm^3 of nitrogen saturated methanol and the slurry stirred for 5 minutes. To this was added $Br(CH_2)_3Br$ (0.19 cm^3, 1.86 mmol), followed after 5 minutes by $NaBH_4$ (0.252 g, 6.66 mmol). The reaction mixture was stirred for a further 5 minutes after the final addition and the resulting orange solution cooled to 0°C. The solution was allowed to crystallise at -15°C and the bright orange crystals filtered off and washed with 3 cm^3 methanol to give 0.382 g (55%) of (50a). The product was recrystallised from CH_2Cl_2 / hexane.

6.8.3 Preparation of $[Co(DH)_2py(CH_2)_4Br]$ (50b)

(50b) was prepared using the method described above for (50a) with the following quantities of reagents and a reaction time of 6 minutes after the final addition. $[Co(DH)_2pyCl]$, (0.502 g, 1.24 mmol); $Br(CH_2)_4Br$, (0.22 cm^3, 0.401 g, 1.86 mmol); $NaBH_4$, (0.251 g, 6.64 mmol). A yield of 0.351 g (54%) of orange crystals of (50b) were recovered before recrystallisation from CH_2Cl_2/hexane.

6.8.4 Preparation of $[Co(DH)_2py(CH_2)_5Br]$ (50c)

$[Co(DH)_2pyCl]$ (0.500 g, 1.24 mmol) was added to 10 cm^3 of nitrogen saturated methanol and the slurry stirred for 5 minutes. $Br(CH_2)_5Br$ (0.25 cm^3, 1.86 mmol) was added followed by $NaBH_4$ (0.252 g, 6.66 mmol) after 5 minutes. The reaction mixture was allowed to stir for a further 8 minutes after the final addition. The solution was cooled to 0°C and an insoluble brown-grey precipitate filtered off. The filtrate was diluted with 10-20 cm^3 of distilled water and the solution cooled to -15°C. The resulting orange crystals were collected by filtration to give 0.266 g (41%) of (50c). The product was further purified by recrystallisation from CH_2Cl_2/hexane.

6.8.5 Preparation of $[Co(DH)_2py(CH_2)_6Br]$ (50d)

(50d) was prepared using the method described for (50c) above with the following quantities of reagents and a reaction time of 17 minutes after the final addition. $[Co(DH)_2pyCl]$, (0.500 g, 1.24 mmol); $Br(CH_2)_6Br$, (0.28 cm^3, 0.453 g, 1.86 mmol); $NaBH_4$, (0.250 g, 6.55 mmol). After filtering off the brown-grey solid residue, the filtrate was diluted with about 25 cm^3 of distilled water and allowed to crystallise at -15°C. The resulting orange crystals were filtered off to give 0.486 g (74%) of (50d). The product was further purified by recrystallisation from CH_2Cl_2/hexane.

6.8.6 Preparation of $[Co(DH)_2py(CH_2)_7Br]$ (50e)

(50e) was prepared using the method described for (50c) with the following quantities of reagents and a reaction time of 20 minutes after the final addition. $[Co(DH)_2pyCl]$, (0.496 g, 1.23 mmol); $Br(CH_2)_7Br$, (0.31 cm^3, 0.475 g, 1.84 mmol); $NaBH_4$, (0.248 g, 6.55 mmol). The solution was cooled to 0°C and an insoluble grey solid filtered off. The filtrate was diluted with 25 cm^3 distilled water and the product allowed to crystallise at -15°C. The orange crystals were recrystallised from CH_2Cl_2/hexane to give 0.387 g (58%) of (50e).

6.8.7 Preparation of $[Co(DH)_2py(CH_2)_3I]$ (50a')

$[Co(DH)_2pyCl]$ (0.676 g, 1.67 mmol) was added to 22 cm^3 of nitrogen saturated methanol and the slurry stirred for 10 minutes. $I(CH_2)_3I$ (0.08 cm^3, 0.67 mmol) was added, followed by $NaBH_4$ (0.331 g, 8.45 mmol). The solution immediately turned dark green in colour and then rapidly became bright orange. Stirring under N_2 was continued for 10 minutes and the bright orange crystals filtered off to give 0.596 g (78%) of (50a').

The product was recrystallised from CH_2Cl_2/ hexane.

Note: The mononuclear $[Co(DH)_2py(CH_2)_3I]$ formed even though a 2.5 : 1 molar ratio of $[Co(DH)_2pyCl]$ to $I(CH_2)_3$ I was used.

TABLE 6.9 Microanalysis, yield and melting point data for $[Co(DH)_2py(CH_2)_nX]$

Compound Number	n	X	Melting Point °C	Yield %	Analysis [a] %C	%H	%N	%Br
50a	3	Br	173-180	55	(39.19)	(5.15)	(14.29)	(16.30)
					39.10	5.10	14.20	19.43
50a'	3	I	175-177	78	(35.76)	(4.70)	(13.04)	(23.62)*
					35.80	4.60	13.00	25.10
50b	4	Br	160-165	51	(40.48)	(5.41)	(13.89)	(15.84)
					40.60	5.40	13.80	17.85
50c	5	Br	162-173	41	(41.71)	(5.61)	(13.51)	(15.41)
					41.50	5.50	13.50	17.11
50d	6	Br	155-166	74	(42.86)	(5.88)	(13.16)	(15.01)
					42.90	5.80	13.30	16.36
50e	7	Br	145-153	58	(43.96)	(6.10)	(12.82)	(14.62)
					44.10	6.00	12.80	14.65

[a] Calculated values in parenthesis

* % I

6.9 Preparation of μ(α,ω)-Alkanediyl Cobaloximes (51b-d, n=4-6) from their Mononuclear Haloalkyl Precursors (50b-d)

6.9.1 General

^{1}H NMR and ^{13}C NMR data are reported in Tables 5.2 and 5.4 respectively. All other characterisation data are reported in Tables 6.10 and 6.11.

6.9.2 Preparation of $[Co(DH)_2py]_2[\mu-(CH_2)_4]$ (51b)

$[Co(DH)_2pyCl]$ (0.081 g, 0.20 mmol) was added to 10 cm^3 of nitrogen saturated methanol and the slurry stirred for 5 minutes. $[Co(DH)_2py(CH_2)_4Br]$ (0.101 g, 0.20 mmol) was then added followed by $NaBH_4$ (0.067 g, 1.78 mmol) after 5 minutes. The brown solution immediately turned dark green. Stirring was continued for a further 30 minutes during which time the solution became bright orange in colour. The resulting orange crystals were precipitated by the addition of about 2 cm^3 of water and the solution allowed to crystallise further at 0°C. Orange crystals of (51b) (0.150 g, 95%) were filtered off and recrystallised from CH_2Cl_2/hexane.

6.9.3 Preparation of $[Co(DH)_2py]_2[\mu\text{-}(CH_2)_5]$ (51c)

(51c) was prepared using the method described above for (51b) using the following quantities of reagents and a reaction time of 30 minutes after the final addition. $[Co(DH)_2pyCl]$, (0.081 g, 0.20 mmol) ; $[Co(DH)_2py(CH_2)_5Br]$, (0.104 g, 0.20 mmol); $NaBH_4$, (0.068 g, 1.8 mmol). About 20 cm^3 of distilled water were added to crystallise the orange product and the solution cooled to 0°C. A yield of 0.102 g (63%) of (51c) was obtained. The product was further purified by recrystallisation from CH_2Cl_2/hexane.

6.9.4 Preparation of $[Co(DH)_2py]_2[\mu\text{-}(CH_2)_6]$ (51d)

(51d) was prepared using the method described above for (51b) with the following quantities of reagents and a reaction time of 1.5 hours after the final addition. $[Co(DH)_2pyCl]$, (0.081 g, 0.20 mmol) ; $[Co(DH)_2py(CH_2)_6Br]$, (0.107 g, 0.20 mmol); $NaBH_4$, (0.072 g, 1.90 mmol). About 25 cm^3 of distilled water were added to crystallise the orange product and the solution cooled at 0°C overnight. 0.105 g (65%) of orange crystals of (51d) were isolated by filtration and the product recrystallised from CH_2Cl_2/hexane.

6.10 Preparation of μ(α,ω)-Alkanediyl Cobaloximes (51b-f, n=4-8) from [Co(DH)$_2$pyCl] and the Dibromoalkanes.

6.10.1 General

^{1}H NMR and ^{13}C NMR data are reported in Tables 5.2 and 5.4 respectively. All other characterisation data are reported in Tables 6.10 and 6.11.

6.10.2 Preparation of [Co(DH)$_2$py]$_2$[μ-(CH$_2$)$_4$] (51b)

[Co(DH)$_2$pyCl] (1.002 g, 2.48 mmol) were added to 15 cm^3 of nitrogen saturated methanol and the brown slurry stirred for 5 minutes. Br(CH$_2$)$_4$Br (0.15 cm^3, 1.28 mmol) were then added followed after 5 minutes by NaBH$_4$ (0.500 g, 13.2 mmol). The solution immediately turned dark and gradually became bright orange as stirring was continued. The mixture was stirred for 20 minutes after the final addition of NaBH$_4$. A few cm^3 of distilled water were added to initiate crystallisation and the orange solution cooled overnight at 0°C. The resulting orange product was filtered off and washed with petroleum ether (bp 30-60°C). to give 0.884 g (90%) of (51b) as orange prisms. The product was recrystallised from absolute ethanol.

6.10.3 Preparation of $[Co(DH)_2py]_2[\mu\text{-}(CH_2)_5]$ (51c)

(51c) was prepared using the method described above for (51b) but using the following quantities of reagents. $[Co(DH)_2pyCl]$, (0.874 g, 2.16 mmol); $Br(CH_2)_5Br$, (0.15 cm^3, 0.255 g, 1.11 mmol) ; $NaBH_4$, (0.474 g, 12.5 mmol). This gave 0.781 g (90%) of (51c) as orange crystals which were recrystallised three times from CH_2Cl_2/hexane.

The crystals were dried under vacuum at 70°C for 4 hours in order to remove CH_2Cl_2 of crystallisation shown to be present in the ^1H NMR spectrum of (51c).

6.10.4 Preparation of $[Co(DH)_2py]_2[\mu\text{-}(CH_2)_6]$ (51d)

(51d) was prepared using the method described above for (51b) but with the following quantities of reagents. $[Co(DH)_2pyCl]$, (0.901 g, 2.23 mmol); $Br(CH_2)_6Br$, (0.17 cm^3, 0.271 g, 1.11 mmol); $NaBH_4$, (0.504 g, 13.3 mmol). This gave 0.709 g (77%) of (51d) as fine orange crystals which were recrystallised three times from CH_2Cl_2 /hexane and dried under vacuum at 70°C for 4 hours. The ^1H NMR spectrum of (51d) showed a singlet at δ 5.38 ppm indicative of CH_2Cl_2 of crystallisation. Microanalytical results confirm that about 0.5 mol CH_2Cl_2 is present as solvent of crystallisation.

6.10.5 Preparation of $[Co(DH)_2py]_2[\mu\text{-}(CH_2)_7]$ (51e)

(51e) was prepared using the method described above for (51b) but with the following quantities of reagents. $[Co(DH)_2pyCl]$, (0.965 g, 2.39 mmol); $Br(CH_2)_7Br$, (0.20 cm^3, 0.306 g, 1.19 mmol); $NaBH_4$, (0.503 g, 13.3 mmol). This gave 0.853 g (86%) of (51e) as orange plates. The product was recrystallised from absolute ethanol and dried under vacuum.

6.10.6 Preparation of $[Co(DH)_2py]_2[\mu\text{-}(CH_2)_8]$ (51f)

(51f) was prepared using the method described above for (51b) but with the following quantities of reagents. $[Co(DH)_2pyCl]$, (0.972 g, 2.41 mmol); $Br(CH_2)_8Br$, (0.20 cm^3, 0.292 g, 1.07 mmol); $NaBH_4$, (0.478 g, 12.6 mmol). This gave 0.766 g (75%) of mustard-coloured crystalline (51f). The product was recrystallised three times from CH_2Cl_2/ hexane and dried under vacuum.

TABLE 6.10 Microanalysis, yield and decomposition points of $[Co(DH)_2py]_2[\mu\text{-}(CH_2)_n]$

Compound Number	n	% Yield	Decomposition Point, °C	Analysis [b] % C	%H	%N
51b	4[d]	95	215-227	(45.45)	(5.85)	(17.67)
				45.15	5.80	17.50
	4[e]	90	202-210	(45.45)	(5.86)	(17.67)
				45.10	5.75	17.45
51c	5[d]	63	185-215	(46.15)	(6.01)	(17.37)
				45.40	6.00	16.90
	5[e]	90	>195	(46.15)	(6.01)	(17.37)
				45.80	6.00	17.00
51d	6[d]	64	>175	(46.82)	(6.15)	(17.07)
				46.40	6.00	16.50
	6[c,e]	77	>195	(45.91)	(6.08)	(16.23)
				45.70	6.00	16.40
51e	7[e]	86	194-202	(47.48)	(6.29)	(16.78)
				47.30	6.30	16.50
51f	8[c,e]	75	190-197	(47.16)	(6.35)	(15.72)
				47.15	6.40	15.90

a All compounds decompose without melting
b Calculated values are in parentheses
c Calculated values with 0.5 mol CH_2Cl_2
d Prepared by Method A, see experimental, 6.9
e Prepared by Method B, see experimental, 6.10

TABLE 6.11 Molecular weights of some representative mononuclear and dinuclear cobaloximes.

Compound		Molecular Weight Calculated	Found
$[Co(DH)_2py(CH_2)_3Br]$	50a	490	490[a]
$[Co(DH)_2py(CH_2)_5Br]$	50c	518	518[a]
$[Co(DH)_2py]_2[\mu\text{-}(CH_2)_4]$	51b	793	793[b]
$[Co(DH)_2py]_2[\mu\text{-}(CH_2)_7]$	51e	835	830[a]

a. Determined by Fast Atom Bombardment Mass Spectrometry at Cambridge, England.

b. Vaporimetric Molecular Weight Determination in CH_2Cl_2.

REFERENCES

1. F. Fischer and H. Tropsch, Brennst.Chem., 7 (1926) 97.

2a. R.R. Schrock, J. Amer. Chem. Soc., 97 (1975) 6577.

b. L.J. Guggenberger and R.R. Schrock, J. Amer. Chem. Soc., 97 (1975) 6578.

3. R.R. Schrock, Acc. Chem. Research, 12 (1979) 98.

4. W.A. Herrmann, B. Reiter and H. Biersack, J. Organomet. Chem., 97 (1975) 245.

5. W.A. Herrmann, Angew. Chem., 90 (1978) 855.

6. J.C. Hayes, G.D.N. Pearson and N.J. Cooper, J. Amer. Chem. Soc., 103 (1981) 4648.

7. E.R. Evitt and R. Bergman, J. Amer. Chem. Soc., 101 (1979) 3973.

8. F. Garnier, P. Krausz, J.E. Dubois, J. Organomet. Chem., 170 (1979) 195.

9. P. Pertici and G. Vitulli, Tetr. Lett., 21 (1979) 1897.

10. W.A. Herrmann, Pure and Appl. Chem., 54 (1982) 65.

11. W.A. Herrmann, Adv. Organomet. Chem., 20 (1982) 159.

12. J.R. Moss and L.G. Scott, Coord. Chem. Rev., 60 (1984) 171.

13. C.P. Casey and J.D. Audett, Chem. Rev., 86 (1986) 339.

14. J. Holton, M.F. Lappert, R. Pearce and P.I.W. Yarrow, Chem Rev., 83 (1983) 135.

15. R.B. King, Inorg. Chem., 85 (1963) 531.

16. R.B. King and M.B. Bisnette, J. Organomet. Chem., 7 (1967) 311.

17. J.R. Moss, J. Organomet. Chem., 231 (1982) 229.

18. S.C. Kao, C.H. Thiel and R. Pettit, Organomet., 2 (1983) 914.

19. L.G. Scott, J.R. Moss, M.E. Brown and K.J. Hindson, J. Organomet. Chem., 282 (1985) 255.

20. L. Pope, P. Sommerville, M. Laing, K.J. Hindson and J.R. Moss, J. Organomet. Chem., 112 (1976) 309.

21. J.J. Bennet, R. Mathieu, R. Poilblanc and J.A. Ibers, J. Amer. Chem. Soc., 101 (1979) 7487.

22. W.A. Herrmann, G. Kriechbaum, preliminary results quoted in W.A. Herrmann, Adv. Organomet. Chem., 20 (1982) 159.

23. J.R. Moss and L.G. Scott, manuscript in preparation.

24. M. Cooke, N.J. Forrow and S.A.R. Knox, J. Organomet. Chem., 222 (1981) C21.

25. M. Cooke, N.J. Forrow and S.A.R. Knox, J.C.S. Dalton Trans., (1983) 2435.

26. P.A. Wegner and G.P. Sterling, J. Organomet. Chem., 167 (1978) C31.

27. Y.C. Lin, J.C. Calabrese and S.S. Wreford, J. Amer. Chem. Soc., 105 (1983) 1679.

28. D.L. Davies, A.F. Dyke, S.A.R. Knox and M.J. Morris, J. Organomet. Chem., 215 (1981) C30.

29a. A.F. Dyke, S.A.R. Knox, K.A. Mead and P. Woodward, J.C.S. Chem. Commun., (1981) 861.

29b. M. Cooke, J.E. Davies, S.A.R. Knox, K.A. Mead, J. Roue and P. Woodward, J.C.S. Chem. Commun., (1981) 862.

30. C.E. Sumner, Jr., P.E. Riley, R.E. Davis and R. Pettit, J. Amer. Chem. Soc., 102 (1980) 1752.

31. S.F. Mapolie and J.R. Moss, S. Afr. J. Chem., 40 (1987) 12.

32. C. Hsu, M.A. Thesis, California State University, Fullerton, (1982).

33. T. Blackmore, M.I. Bruce and F.G.A. Stone, J.C.S. (A), Inorg. Phys. Theor., (1968) 2158.

34. J.A.S. Howell and A.J. Rowan, J.C.S. Chem. Commun., (1979) 482.

35. J.A.S. Howell and A.J. Rowan, J.C.S. Dalton Trans., (1980) 1845.

36. P.Q. Adams, D.L. Davies, A.F. Dyke, S.A.R. Knox, K.A. Mead and P. Woodward, J.C.S. Chem. Commun., (1983) 222.

37. D.L. Davies, S.A.R. Knox, K.A. Mead, M.J. Morris and P. Woodward, J.C.S. Dalton Trans., (1984) 2293.

38. J.R. Norton, K.M. Motyl, C.K. Schauer and C.P. Anderson, J. Amer. Chem. Soc., 104 (1982) 7325.

39. M.R. Burke, J. Takats, F.W. Grevels and J.G.A. Reuvers, J. Amer. Chem. Soc., 105 (1983) 4092.

40. G.J. Hutchings, S. Afr. J. Chem., 39 (1986) 65 (and references therein).

41. S.T. Tauster, S.C. Fung and R.L. Garten, J. Amer. Chem. Soc., 100 (1978) 170.

42. G.J. Hutchings and J.C.A. Boeyens, J. Catal., 100 (1986) 507.

43. K.B. Jensen and F.E. Massoth, J. Catal., 92 (1985) 98.

44. K.B. Jensen and F.E. Massoth, J. Catal., 92 (1985) 109.

45. C.N. Satterfield and G.A. Huff, J. Catal., 85 (1984) 370.

46. J. Barrault, C. Renard, L.T. Yu and J. Gal, Proc. 8th Int. Conf. Catal., Berlin, 2 (1984) 101.

47. J. Barrault, "Metal Support and Metal Additive Effects in Catalysis", in Stud. Surf. Sci. Catal., 11 (1982) 225.

48. M.A. Vannice, J. Catal., 37 (1975) 449.

49. R.C. Everson, E.T Woodburn and A.R.M. Kirk, J. Catal., 53 (1978) 186.

50. J.R. Anderson, P.S. Elmes, R.F. Howe and D.E. Mainwaring, J. Catal., 50 (1977) 508.

51. D. Commereuc, Y. Chauvin, F. Hugues, J.M. Basset and D. Olivier, J.C.S. Chem. Commun., (1980) 154.

52. H.E. Ferkul, D.J. Stanton, J.D. McCowan and M.C. Baird, J.C.S. Chem. Commun., (1982) 955.

53. F. Hugues, B. Besson, P. Bussiere, J.A. Dalmon, M. Leconte, J.M. Basset, Y. Chauvin and D. Commereuc, A.C.S. Symp. Ser., 192 (1982) 255.

54. Y. Doi, H. Miyake, A. Yokota and K.Soga, J. Catal., 95 (1985) 293.

55. A.K. Smith, A. Theolier, J.M. Basset, R. Ugo, D. Commereuc and Y. Chauvin, J. Amer. Chem. Soc., 100 (1978) 2590.

56. V.D. Alexiev, N. Binsted, J. Evans, G.N. Greaves and R.J. Price, J.C.S. Chem. Commun., (1987) 395.

57. M.A. Vannice and R.L. Garten, J. Mol. Catal, 1 (1975/6) 201.

58. M.A. Vannice, Y. Lam and R.L. Garten, "Hydrocarbon Synthesis" Adv. Chem. Ser., 178 (1979) 26. (Amer. Chem. Soc.).

59. G.L. Ott, T. Fleisch and W.N. Delgass, J. Catal., 60 (1979) 394.

60. J.R. Anderson and D.E. Mainwaring, J. Catal., 35 (1974) 162.

61. M. Kaminsky, K.J. Loon, G.L. Geoffroy and M.A. Vannice, J. Catal., 91 (1985) 338.

62. J. Venter, M. Kaminsky, G.L. Geoffroy and M.A. Vannice, J. Catal., 103 (1987) 450.

63. W.R. Pretzer, T.P. Kobylinski and J.E. Bozik, U.S. Patent 4 239 924 (1980).

64. H. Kheradmand, G. Jenner, A. Kiennemann and A. Deluzarche, Chem. Lett., (1982) 395.

65. H. Kheradmand, A. Kiennemann and G. Jenner, J. Organomet. Chem., 251 (1983) 339.

66. G. Doyle, J. Mol. Catal., 18 (1983) 251.

67. G. Jenner and P. Andrianary, J. Catal., 88 (1984) 535.

68. M. Tanaka, Y. Kiso and K. Saeki, J. Organomet. Chem., 329 (1987) 99.

69. A.P. Humphries and S.A.R. Knox, J.C.S. Dalton Trans., (1975) 1710.

70. N.M. Doherty and S.A.R. Knox, Inorg. Synth. - paper in press.

71. D.H. Gibson, W.L. Hsu, B.V. Johnson and A.L. Steinmetz, J. Organomet. Chem., 208 (1981) 89.

72. R.E. Dessey, R.L Pohl and R.B. King, J. Amer. Chem. Soc., 88 (1966) 5121.

73. H.B. Friedrich and J.R. Moss, unpublished results.

74. M. Brookhart and M.L.H. Green, J. Organomet. Chem., 250 (1983) 395.

75. R.B. King, J. Amer. Chem. Soc., 90 (1968) 1417.

76. J. Lewis, A.R. Manning, J.R. Miller and J.M. Wilson, J.C.S. (A), (1966) 1663.

77. M. Laing, J.R. Moss and J. Johnston, J.C.S. Chem. Commun., (1971) 656.

78. K.R. Pope and M.S. Wrighton, J. Amer. Chem. Soc., 109 (1987) 4545.

79. G. Wilkinson, F.G.A. Stone and E.W. Abel, "Comprehensive Organometallic Chemistry", Vol. 6 (Ch.40), Pergamon Press, Oxford (1982).

80. J.R. Fox, W.L. Gladfelter, T.G. Wood, J.A. Smegal, T.K. Foreman, G.L. Geoffroy, I. Tavaniepour, V.W. Day and C.S. Day, Inorg. Chem., 20 (1981) 3214.

81. R. Regregui, P.H Dixneuf, N.J. Taylor and A.J. Carty, Organomet., 5 (1986) 1.

82. P. Johnston, G.J. Hutchings, N.J. Coville, L. Denner and J.C.A. Boeyens, Organomet., 6 (1987) 1292.

83. D.J. Robinson, E.A. Darling and N.J. Coville, J. Organomet. Chem., 310 (1986) 203.

84. A. Stasunik, D.R. Wilson and W. Malisch, J. Organomet. Chem., 270 (1984) C18.

85a. C. Botha, J.R. Moss and S. Pelling, J. Organomet. Chem., 220 (1981) C21.

85b. J.R. Moss and S. Pelling, J. Organomet. Chem., 236 (1982) 221.

86. T.H.Coffield, J. Kozikowski and R.D. Closson, J. Org. Chem., 22 (1957) 598.

87. C. Masters, "Homogeneous Transition Metal Catalysis - A Gentle Art" , Chapman Hall (London) (1981).

88. J.P. Bibler and A. Wojcicki, Inorg. Chem., 5 (1966) 889.

89. S.R. Su and A. Wojcicki, J. Organomet. Chem., 27 (1971) 231.

90. J.P. Bibler and A. Wojcicki, J. Amer. Chem. Soc., 88 (1966) 4862.

91. M.D. Johnson, Acc. Chem. Research, 11 (1978) 57.

92a. N.J. Coville and E.A. Darling, J. Organomet. Chem., 277 (1984) 105.

b. J.C.A. Boeyens, N.J. Coville and K. Soldenhoff, S. Afr. J. Chem., 37 (1984) 153.

93. K. Tabatabaian and C. White, Inorg. Chem., 20 (1981) 2020.

94. D.A. Brown, H.J. Lyons and R.T. Sane, Inorg. Chim. Acta., 4 (1970) 621.

95. J.A.S. Howell and A.J. Rowan, J. Organomet. Chem., 165 (1979) C33.

96. J.A.S. Howell and A.J. Rowan, J.C.S. Dalton Trans., (1980) 503.

97. H.C. Clark and M.J. Hampden Smith, Coord. Chem. Rev., 79 (1987) 229.

98. J.I. Seeman and S.G. Davies, J. Amer. Chem. Soc., 107 (1985) 6522 (and references therein).

99. S.G. Davies, I.M. Dordor-Hedgecock, K.H. Sutton and M. Whittaker, J. Amer. Chem. Soc., 109 (1987) 5711 (and references therein).

100. T.C. Flood, F.J. Disanti and D.L. Miles, Inorg. Chem., 15 (1976) 1910.

101. J. Thomson, W. Keeney, M.C. Baird and W.F. Reynolds, J. Organomet. Chem., 40 (1972) 205.

102. W.A. Kiel, W.E. Buhro and J.A. Gladysz, Organomet., 3 (1984) 879.

103. W.B. Jennings, Chem. Rev., 75 (1975) 307.

104. H. Brunner and E. Schmidt, Angew. Chem. Int. Ed. Eng., 8 (1969) 616.

105. K.R. Hanson, J. Amer. Chem. Soc., 88 (1966) 2731.

106. J.P. Collman, R.G. Finke, J.N. Cawse and J.I. Brauman, J. Amer. Chem. Soc., 100 (1978) 4766.

107. F. Calderazzo, Angew. Chem. Int. Ed. Eng., 16 (1977) 299.

108. A. Wojcicki, Adv. Organomet. Chem., 11 (1973) 87.

109. G. Henrici-Olivé and S. Olivé, Trans. Met. Chem., 1 (1976) 77.

110. F.A. Cotton and G. Wilkinson, "Advanced Organometallic Chemistry - A Comprehensive Text", John Wiley and Sons (Wiley Interscience) (4^{th} Ed).

111. K.H. Pannell, T. Giasolli and R.N. Kapoor, J. Organomet. Chem., 316 (1986) 315.

112. I.S. Butler, F. Basolo and R.G. Pearson, Inorg. Chem., 6 (1967) 2074.

113. M. Green and D.J. Westlake, J.C.S.. (A), (1971) 367.

114. M. Wrighton, Inorg. Chem., 26 (1987) 2321.

115. R.J. Mawby, F.Basolo and R.G. Pearson, J. Amer. Chem. Soc., 86 (1964) 3994.

116. M.J. Wax and R.C. Bergman, J. Amer. Chem. Soc., 103 (1981) 7028.

117. S.L. Webb, C.M. Giandomenico and J. Halpern, J. Amer. Chem. Soc., 108 (1986) 345.

118. M.J. Therien and W.C. Trogler, J. Amer. Chem. Soc., 109 (1987) 5127.

119. M.S. Wrighton and R.J. Kazlauskas, Organomet., 1 (1982) 602.
120. K.A. Mahmoud, A.J. Rest and H.G. Alt, J.C.S. Dalton Trans., (1985) 1365.
121. S.F. Mapolie, J.R. Moss and L.G. Scott, J. Organomet. Chem., 297 (1985) C1.
122. S.P. Nolan, R.L. de la Vega and C.D Hoff, J. Organomet. Chem., 315 (1986) 187.
123. R.J. Angelici and A.E. Kruse, J. Organomet. Chem., 24 (1970) 231.
124. A. Davison, J.A. McCleverty and G. Wilkinson, J.Chem. Soc., (1963) 1133.
125. J.W. Johnston and J.R. Moss, Polyhed., 4 (1985) 563 (and references therein).
126. D.E. Leyden and R.H. Cox, "Analytical Applications of NMR", Wiley (New York) (1977).
127. G. Henrici-Olive and S. Olive, "The Chemistry of the Catalyzed Hydrogenation of Carbon Monoxide", Springer-Verlag, Berlin 1984.
128. G. Wilkinson, F.G.A. Stone and E.W. Abel, Eds. "Comprehensive Organometallic Chemistry", Vol. 4, (Ch. 31), Pergamon Press, Oxford (1982).
129. E.L. Hoel, G.B. Ansell and S. Leta. Organomet., 3 (1984) 1633.
130. S. Kao, P.P.Y. Lu and R. Pettit, Organomet., 1 (1982) 911.
131a C.P. Casey, M.W. Meszaros, P.J. Fagan, R.K. Bly, S.R. Marder and E.A. Austin, J. Amer. Chem. Soc., 108 (1986) 4043.
131b C.P. Casey, M.W. Meszaros, P.J. Fagan, R.K. Bly and R.E. Colborn, J. Amer. Chem. Soc., 108 (1986) 4053.
132. R.F. Bryan and P.T. Greene, J. Chem. Soc.,(A), (1970) 3064.
133. Calculated by M.W. Taylor from the atomic coordinates in ref. 20.

134. Estimated on the basis of the Ru-Ru separation of 8.81Å found in the compound $[CpRu(CO)_2]_2[\mu\text{-}(CH_2)_5]$; K.P. Finch, J.R. Moss and M.L. Niven, to be published.

135. Strem Inorganic and Organometallic Research Chemicals Catalogue No. 11.

136. R.B. King, Inorg. Chem., 5 (1966) 2227.

137. D.A. Symon and T.C. Waddington, J.C.S. Dalton Trans., (1973) 1879.

138. A.J. White, J. Organomet.Chem., 168 (1979) 197.

139. M.A. Neuman, J. Toan and L.F.Dahl, J. Amer. Chem. Soc., 94, (1972) 3383.

140. R.B. King, J.C.S. Chem. Comm., (1969) 436.

141. C.U. Pittman, Jr., R.C. Ryan, J. McGee and J.P. O'Connor, J. Organomet. Chem., 178 (1979) C43.

142. S.F. Mapolie and J.R. Moss, unpublished results.

143. M.A. Vannice, J. Catal., 50 (1977) 228.

144. R.L. Varma, L. Dan-Chu, J.F. Matthews and N.N. Baklshi, Can. J. Chem.Eng., 63 (1985) 72.

145. R.G. Copperthwaite, G.J. Hutchings, M. van der Riet and J. Woodhouse, S. Afr. J. Chem., 39 (1986) 251.

146. M.A. Vannice, Catal. Rev. Sci. Eng., 14 (1976) 153.

147. P. Johnston, G.J. Hutchings, N.J. Coville, K.P. Finch and J.R. Moss - unpublished results.

148. G.N.Schrauzer and J. Kohnle, Chem. Ber., 97 (1964) 3056.

149. G.N. Schrauzer and R.J. Windgassen, J. Amer. Chem. Soc., 88 (1966) 3738.

150. G.N. Schrauzer, Inorg. Synth., 11 (1968) 61.

151. G.N. Schrauzer and L.P. Lee, J. Amer. Chem. Soc., 92 (1970) 1551.

152. G.N. Schrauzer, Angew. Chem. Int. Ed. Eng., 15 (1976) 417.

153. E.N. Stadbauer, R.J. Holland, F.P. Lamm and G.N. Schrauzer, Bioinorg. Chem., 4 (1974) 67.

154. L.G. Marzilli, M.F. Summers, J.H. Ramsden, L Randaccio, N. Bresciani-Pahor, E. Zangrando and P. Marzilli, Organomet., 4 (1985) 2086.

155. K.P. Finch, Honours Project, University of Cape Town (1985).

156. E.L. Smith, L. Mervyn, P.E. Huggleton, D.W. Johnson and N. Straw, Annals N.Y. Acac. Sci., 112 (1964) 565.

157. L.F. Johnson and W.C. Jankowski, "Carbon-13 NMR Spectra: A Collection of Assigned, Coded and Indexed Spectra", John Wiley, (New York), (1972).

158. N. Bresciani-Pahor, M. Forcolin, L.G. Marzilli, L. Randaccio, M.F. Summers and P.J. Toscano, Coord. Chem. Rev., 63 (1985) 1.

159. M.E. Thompson, S.M. Baxter, A.R. Bulls, B.J. Burger, M.C. Nolan, B.D. Santarsiero, W.P. Schaefer and J.E. Bercaw, J Amer. Chem. Soc., 109 (1987) 203.

160. J.E.Bercaw, B.J. Burger, E. Bunel and J.R. Moss, unpublished results.

161. G.M. Sheldrick, SHELX, in "Computing in Crystallography", Ed. H. Schenk, R. Olthof-Hazekamp, H. van Koningsveld and G.C. Bassi, 34 (1978), Delft. Univ. Press.

162. M Nardelli, Comput. Chem., 7 (1983) 95.

163. W.D.S. Motherwell, PLUTO; programme for plotting molecular and crystal structures, Cambridge Univ., England (1974) - unpublished.